Estrogen and the innate epithelial defences of the urogenital tract

Anna Maria Stanton (BSc, MRes)

Thesis submitted for the degree of Doctor of Philosophy

September 2016

Institute for Cell and Molecular Biosciences
Faculty of Medical Sciences
Newcastle University

Abstract

Approximately 40% of women will experience at least one urinary tract infection (UTI) in their lifetime and 25% of these women will go on to suffer recurrent UTIs. After the menopause, the risk of developing a recurrent UTI doubles, which is putatively linked to reduced estrogen levels. Topical vaginal estrogen treatment in postmenopausal women has been shown to reduce the incidence of UTIs. However, the mechanism by which vaginal estrogen helps to protect against UTIs is not well understood. Antimicrobial peptides (AMPs), secreted in response to infection and functioning via bacterial cell lysis, are an important component of the host innate immune response to infection. The aim of this project was to investigate the effects of estrogen treatment on vaginal epithelial AMP expression and synthesis.

Immortalised vaginal epithelial cells (VK2 E6/E7), used to model the vaginal epithelium, were treated with 4nM 17β-estradiol for seven days and then challenged with 50ng/ml flagellin (isolated from *Escherichia coli* clinical UTI isolate) for 24 hours. Combined estrogen pretreatment plus flagellin resulted in a 2.3- and 2.1-fold increase in expression of the AMPs human β-defensin 2 (hBD2) and hBD3, respectively, above that observed with flagellin challenge alone (p-values <0.001).

Microarray analyses identified upregulation of the AMPs LCN2, RNase 7, S100A7, S100A12, SLPI, by estrogen pretreatment plus flagellin in addition to hBD2 and hBD3. Furthermore, several genes relating to keratinisation (for example keratin and SPRR genes) and inflammation (for example SERPINB4, S100A8 and S100A9) were also upregulated suggesting that estrogen pretreatment stimulated multiple protective responses in VK2 cells.

A hBD2 luciferase reporter vector containing a 2032bp hBD2 promoter region was used to measure hBD2 expression in response to estrogen and flagellin treatments. Reporter activity in VK2 cells significantly increased 2.1-fold following seven day estrogen pretreatment (4nM) plus flagellin (50ng/ml) challenge compared to flagellin challenge without estrogen pretreatment (p=0.0367). Six estrogen response elements (EREs) were identified in the hBD2 promoter and were mutated by site-directed mutagenesis. Mutation of each of the EREs abolished hBD2 gene expression potentiation by estrogen pretreatment plus flagellin, suggesting that hBD2 is regulated through ER-α or ER-β binding to EREs in the hBD2 promoter.

Pathway analysis of the microarray data identified IL-17A as a potential regulator of AMP expression. Thus, VK2 cells were challenged with exogenous IL-17A in concentrations ranging from 0.1ng/ml to 100ng/ml for 24 hours. The expression of hBD2, LCN2, RNase 7, and S100A7 was significantly increased between 2- and 21- fold in an IL-17A dose dependent manner (p-values <0.001). In addition, estrogen pretreatment of VK2 cells prior to challenge with IL-17A (100ng/ml) plus flagellin (50ng/ml) significantly increased the expression of hBD2, hBD3 and S100A7 by between 1.4- and 1.6-fold compared to IL-17A plus flagellin without estrogen (p-values <0.05). These data indicated an important role for estrogen in AMP expression even in the presence of proinflammatory cytokines, such as IL-17A.

Altogether, these data indicated that estrogen is an important regulator of innate epithelial defences of the urogenital tract. These results suggest that estrogen protects against UTIs by augmenting the vaginal antimicrobial response to infection and by strengthening the epithelial barrier to infections. Hence, loss of estrogen following the menopause leaves postmenopausal women susceptible to repeated UTIs.

Acknowledgements

I am very grateful to have received support from a huge number of kind people throughout my PhD. Firstly, I would like to thank my supervisory team, Dr Judith Hall, Prof Robert Pickard and Mr Ased Ali for all of their advice and encouragement throughout my project. I very much appreciate all the help and guidance from Judith over the last 4 years. I have benefitted enormously from Rob's clinical insight and ability to bring the focus back to the bigger picture. I also thank Ased for undertaking the task of obtaining ethical approval and liaising with doctors and nurses for sample collection.

I would also like to acknowledge the other members of the Hall group. Words are not enough to thank Dr Catherine Mowbray, who has been both a fantastic mentor, with amazing knowledge of so many techniques, and a good friend. I apologise to the others in our office who have had to listen to our daily conversations, scientific and otherwise. I would also like to thank Dr Marcelo Lanz, Dr Kevin Cadwell, Dr Sherko Subhan, and Andrejus Suchenko for their ideas and advice.

I would also like to thank the members of the ERG, many of whom have been a huge help throughout my project, from lending reagents to lending their ears in times of need. A special thank you goes to Maxine Geggie for her invaluable knowledge and expertise in cell culture. I would also like to thank Anthony Moore for his friendship throughout my PhD and for keeping my days in the lab interesting and unpredictable. I am also very grateful to Lauren Drage, who was always ready with wine, whether we were celebrating a long awaited result or drowning our sorrows.

Finally, I would like to thank all of my friends and family outside of the lab who have supported me on this crazy journey. I, of course, thank my Mum and Dad, who will probably never read beyond this page, but will be unbelievably proud of every word of this thesis nevertheless. Thank you both for your constant support and everything you do for me. And lastly Craig, to whom no words could do justice to my gratitude. Thank you for celebrating even the smallest of successes with me and for keeping me laughing on the days I felt dejected. You are a constant source of strength and encouragement and with your support I have achieved all of this…

Table of contents

List of figures

List of tables

Abbreviations

AMP	Antimicrobial peptide
ANOVA	Analysis of variance
AP-1	Activator protein 1
AU	Arbitrary units
BLAST	Basic local alignment search tool
BPE	Bovine pituitary extract
CEBPB	CCAAT/enhancer binding protein beta
CEBP	CCAAT/enhancer binding protein
CASP1	Caspase 1
CCL5	C-C motif
cDNA	Complementary deoxyribonucleic acid
CFU	Colony forming unit
CMV	Cytomegalovirus
CNF1	Cytotoxic necrotising factor 1
CNFN	Cornifelin
CREB	cAMP response element binding protein
CXCL10	C-X-C motif chemokine 10
DMEM	Dulbecco's Modified Eagle Medium
DMSO	Dimethyl sulfoxide
DNA	Deoxyribonucleic acid
dNTP	Deoxynucleotide
EGF	Epidermal growth factor
EHF	ETS homologous factor
ELF3	ETS transcription factor E74-like factor 3
ELISA	Enzyme-linked immunosorbent assay
EP	Estrogen pretreatment
EP/F	Estrogen pretreatment plus flagellin
ER	Estrogen receptor
ERE	Estrogen response element
ERK	Extracellular signal-regulated kinase
ESE	Epithelial specific expression
ETS	E26 transformation-specific
F	Flagellin
F3	Coagulation factor 3
FCS	Fetal calf serum
FOXO1	Forkhead box protein O1
GPER	G protein-coupled estrogen receptor
hBD	Human beta-defensin
HD	Human defensin
HIV	Human immunodeficiency virus
HlyA	Hemolysin A
HNP	Human neutrophil peptide
HRPO	Horseradish peroxidase
IFIT3	Interferon induced protein with tetratricopeptide repeats 3
IFN-γ	Interferon gamma

IPA	Ingenuity pathway analysis
IPTG	Isopropyl beta-D-1-thiogalactopyranoside
IRF	Interferon regulatory factor
ISG	Interferon-stimulated genes
JNK	c-Jun N-terminal kinase
KDAMPS	Keratin-derived antimicrobial peptide
KLF4	Kruppel-like factor 4
KRT	Keratin
LB	Lysogeny broth
LCE	Late cornified envelope protein
LCN2	Lipocalin 2
LGALS	Lectin, galactoside binding soluble
LPS	Lipopolysaccharide
MAP	Mitogen-activated protein
MAPK	Mitogen-activated protein kinase
MMLV	Moloney Murine Leukemia Virus
mRNA	Messenger ribonucleic acid
MYC	V-myc avian myelocytomatosis viral oncogene homolog
N	Biological repeats
n	Technical replicates
NCOA2	Nuclear receptor coactivator 2
NF-κB	Nuclear factor-kappa B
NK	Natural killer
NLR	NOD-like receptors
NOD	Nucleotide-binding oligomerisation domain
ns	Not significant
OAS1	2'-5'-oligoadenylate synthetase 1
OASL	2'-5'-oligoadenylate synthetase-like
PAMP	Pathogen-associated molecular patterns
PBS	Phosphate-buffered saline
PCR	Polymerase chain reaction
PRR	Pattern recognition receptor
PVEC	Primary vaginal epithelial cells
qPCR	Quantitative polymerase chain reaction
RA	Rheumatoid arthritis
RELA	V-rel avian reticuloendotheliosis viral oncogene homolog A
RIN	RNA integrity number
RLR	RIG-I-like receptors
RNA	Ribonucleic acid
rUTI	Recurrent urinary tract infection
SBSN	Suprabasin
SFM	Serum-free medium
SLPI	Secretory leukocyte protease inhibitor
SOX2	SRY-box 2
spp	Species
SPRR	Small proline rich proteins
STAT	Signal transducer and activator of transcription

Th17	T helper 17
TLR	Toll-like receptor
TMP-SMX	Trimethoprim-sulfamethoxasole
TNF-α	Tumor necrosis factor alpha
TP53	Tumour protein p53
UPEC	Uropathogenic Escherichia coli
UTI	Urinary tract infection
WT	Wild type
X-GAL	5-bromo-4-chloro-3-indolyl-beta-D-galactopyranoside
YBX1	Y-box binding protein 1

1 Introduction

1.1 The urogenital tract

The urogenital tract consists of the reproductive and urinary systems. These are grouped together due to their proximity and use of common pathways, for example the male urethra, which carries both urine and semen. The reproductive system consists of the sex organs involved in human reproduction. In females this consists of the ovaries, fallopian tubes, uterus, cervix and vagina, which function in the development and transportation of oocytes. In males the reproductive system consists of the testes, epididymis, vas deferens, seminal vesicles, prostate and urethra, which function in the development and transportation of sperm cells. The urinary tract is the same in both men and women and consists of the kidneys, ureters, bladder, and urethra. The upper urinary tract is responsible for filtering waste products out of the blood to produce urine. Urine is transported from the kidneys to the bladder, via the ureters, where it is stored until excretion from the body via the urethra. Women are more prone to urinary tract infections (UTIs) than men; approximately 50% of women of women experience at least one UTI in their lifetime, compared to only 12% of men[1]. This is largely due to anatomy, as the urethra is shorter in women than in men and is much closer to the anus, the source of bacteria that cause UTIs.

1.2 Infections of the urogenital tract

UTIs occur when bacteria from the gut colonise the urinary tract. Initially the bacteria migrate from the bowel to the periurethral area, where the organisms can multiply and establish a reservoir. In women the vagina also provides an important reservoir for the invading organisms. Nearly 50 years ago Gruneberg (1969) demonstrated that in more than 80% of patients the urinary bacterial strain causing an acute symptomatic UTI could also be recovered from and was the predominant strain in the rectum, vagina, and periurethral area[2]. From the periurethral area and/or vagina bacteria can colonise the urethral opening and ascend the urethra to infect the bladder. In the bladder, the invading bacteria can replicate extracellularly in the bladder lumen, or penetrate the bladder epithelium and replicate intracellularly within the superficial umbrella cells[3]. Bacterial infection of the bladder is termed cystitis and is clinically diagnosed by bacterial numbers in the urine greater than $5x10^5$ colony forming units (CFU) per millilitre. Typical symptoms of cystitis include cloudy urine, urinary urgency and frequency, and pain upon urination. In approximately 1% of cystitis patients the bacteria ascend from the bladder into the ureters and from here infect the kidneys causing pyelonephritis[4]. Once the kidneys are infected, the bacteria can access the bloodstream and cause bacteraemia, which may be fatal[1]. Figure 1.1

shows the progression of bacteria from the bowel to the kidney. UTIs can also be asymptomatic; asymptomatic bacteriuria is the presence of $>5x10^5$ CFU/ml bacteria in the urine but without the patient experiencing any symptoms. It is not well understood what host or bacterial factors contribute to the development of an asymptomatic UTI.

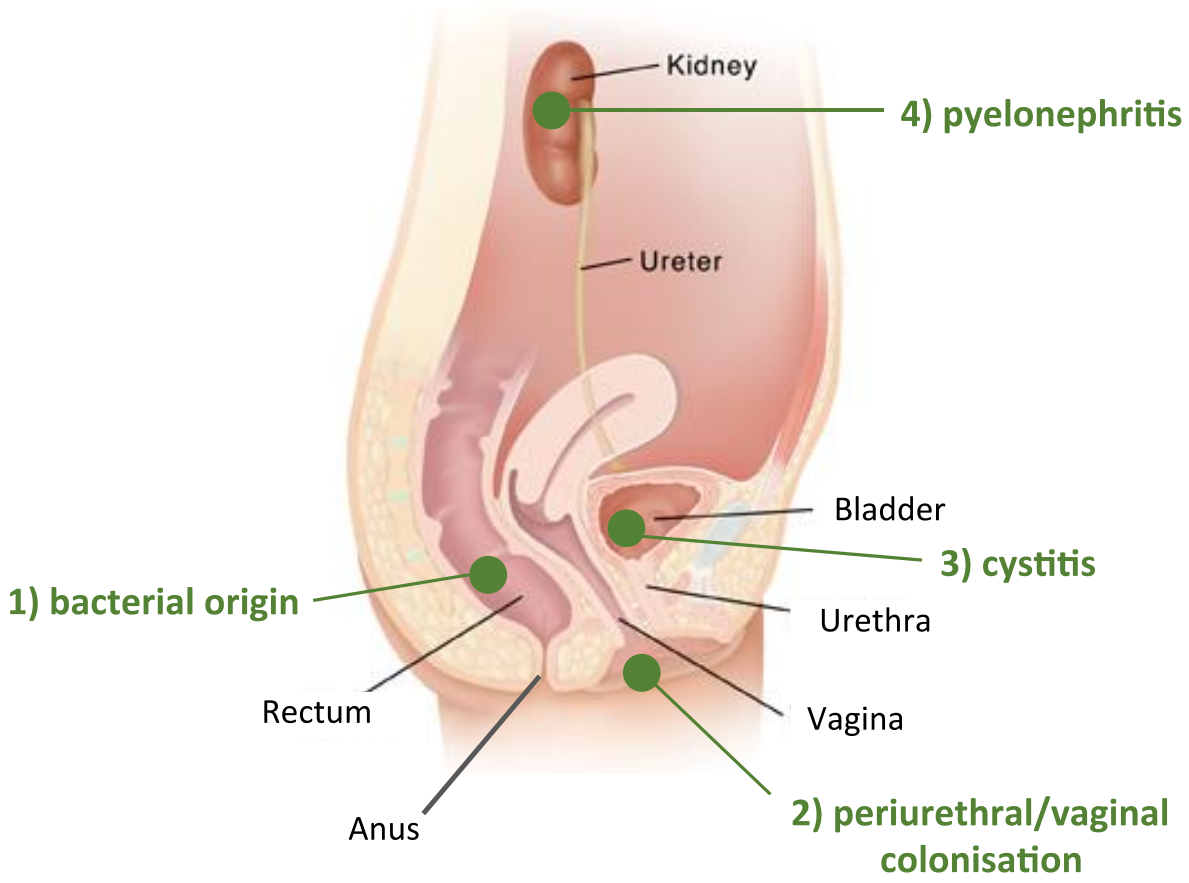

Figure 1.1: Bacterial migration in UTIs. UTIs occur when bacteria from the bowel colonise the periurethral area/vagina and from here ascend the urethra and infect the bladder. From the bladder the bacteria may ascend the ureter to infect the kidney. Diagram adapted from ref 5.

After the initial infection, approximately 25% of cystitis patients will experience a recurrent urinary tract infection (rUTI)[6]. Recurrent UTI is defined as either two episodes of UTI within six months or three episodes within twelve months[7]. A rUTI usually occurs when the bacterial strain that caused the initial infection is not successfully cleared from the urogenital tract and residual bacteria in the vagina or periurethral area can reinfect the bladder. However, less commonly rUTI can occur by reinfection of the urinary tract by a different bacterial strain[8].

1.3 UTI prevalence and risk factors

There are approximately 150 million cases of UTIs worldwide each year and UTIs account for 1-

3% of all GP visits[9]. Cost analyses in 1995 revealed the estimated cost of community-acquired UTIs in the USA was $1.6 billion per annum[10]. Limited figures are available for the UK, but an investigation into hospital-acquired infections in 1995 showed that hospital-acquired UTIs alone cost the NHS £124 million per annum[11]. More recent figures (from 2010) suggest that diagnosis and treatment of an acute UTI costs approximately £33 per patient[12].

In women risk factors associated with increased incidence of UTI differ between pre- and postmenopausal women. Risk factors for premenopausal women include frequent sexual intercourse, use of spermicides as a contraceptive and congenital urinary tract abnormalities[10]. The menopause could be classed as a risk factor in itself, as postmenopausal women are more susceptible to UTIs and are twice as likely to experience a rUTI than premenopausal women[13]. Other risk factors for postmenopausal women include incontinence, post-voiding residual urine volume and abnormal urine flow[14].

1.4 Uropathogenic organisms

Urinary tract infections may be caused by bacteria, fungi or viruses, although fungal and viral UTIs are rare and only seen in immunocompromised or hospitalised patients[15,16]. Approximately 75-95% of bacterial UTIs are caused by the Gram-negative microorganism *Escherichia coli*. Other potential but less common causes of bacterial UTIs include *Staphylococcus saprophyticus*, *Klebsiella pneumoniae*, and *Enterococcus faecalis,* however, these organisms are more frequent in hospital-acquired UTIs[17,18]. As *E. coli* is the primary cause of community-acquired UTIs this will be the focus of discussions in this thesis.

1.4.1 Bacterial virulence factors

E. coli that infect the urinary tract are called uropathogenic *E. coli* (UPEC) and display a variety of virulence factors to facilitate colonisation of the host (Figure 1.2).

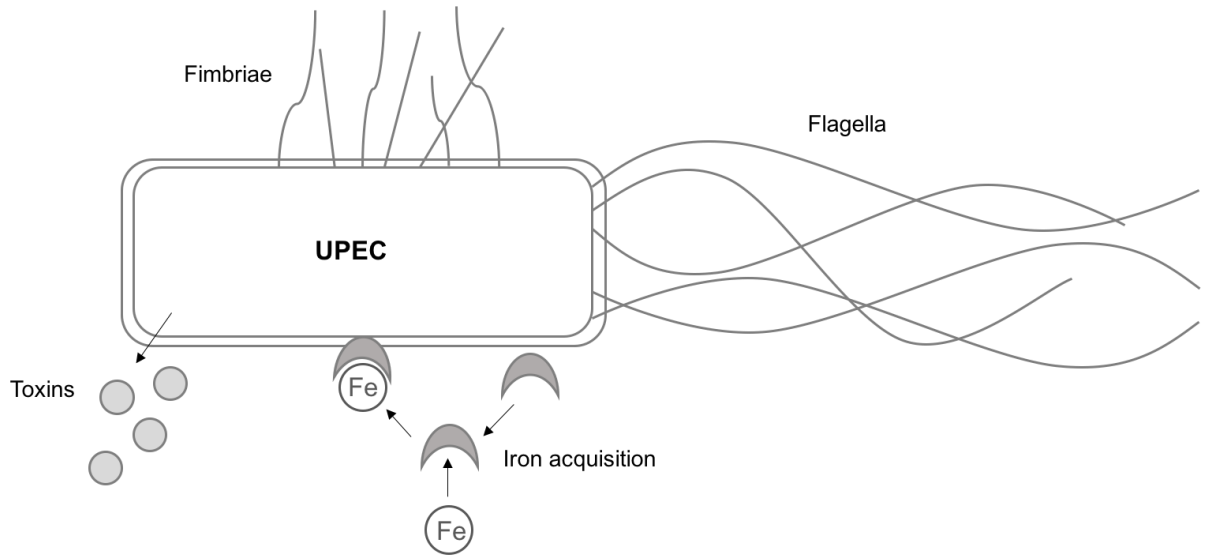

Figure 1.2: Virulence factors of uropathogenic *E. coli* (UPEC). UPEC possess a number of virulence factors to facilitate survival within the host. These include fimbriae, flagella, iron acquisition systems, and toxins.

The first of these virulence factors are fimbriae. Fimbriae, also called pili, are short filamentous organelles on the bacterial surface that are vital for adherence to cell surfaces. UPEC strains carry significantly more fimbrial gene clusters than commensal *E. coli* isolates[19]. Although there are many different types of fimbriae, type I fimbriae and P fimbriae are the most well characterised. Deletion or mutation of the type I fimbrial adhesin *fimH* gene diminishes the ability of UPEC to colonise the urinary tract[20,21]. The FimH adhesin of type I fimbriae binds to the host glycoprotein uroplakin 1a on the bladder epithelium and has an important role in adhesion to and invasion of bladder epithelial cells (Figure 1.3)[22–24]. P fimbriae are unique to UPEC and are associated with pyelonephritic UPEC isolates[25]. The PapG adhesin of P fimbriae recognises and binds to glycoproteins found abundantly within the renal epithelium[26]. However, although some research has shown that P fimbriae are required for renal colonisation by UPEC, others have reported that deletion of P fimbriae genes does not affect the ability of UPEC to infect the kidney[25,27]. The contribution of P fimbriae to UPEC virulence is, therefore, unclear.

In addition to fimbriae, UPEC also possess flagella, which provide the bacteria with motility. Flagella are an important virulence factor with respect to UTIs as ascension of the urinary tract is key to colonisation and maximal flagella expression coincides with bacterial ascension of the urinary tract[28]. UPEC must coordinate the expression of fimbriae and flagella, as these perform opposing functions. Thus, expression of type I fimbriae to allow adhesion downregulates expression of flagellin, the main component of flagella, and hence reduces motility[29].

UPEC also secrete toxins to facilitate invasion of the host. Hemolysin A (HlyA) is the most well characterised toxin and is encoded by approximately 50% of UPEC isolates[30,31]. HlyA is a pore-

forming toxin that has cytolytic activity. Furthermore, expression of HlyA results in shedding of the bladder epithelial cells and is associated with increased UTI severity[32,33]. The HlyA toxin has also been reported to stimulate degradation of host signalling pathway components and thus reduce the inflammatory response to UPEC[34]. The toxin cytotoxic necrotising factor 1 (CNF1) is produced by approximately 30% of UPEC isolates. CNF1 has been reported to exacerbate UTIs by activating Rho family GTPases, which affects many host cell functions. For example, activation of the Rho GTPase Rac stimulates ruffling of the host cell membrane which promotes bacterial uptake into the cell (Figure 1.3)[35]. Similarly to HlyA, CNF1 has also been reported to cause apoptosis and exfoliation of bladder epithelial cells[36]. CNF1 deletion in a mouse model of UTI resulted in reduced bacteria in the urine and bladder compared to UPEC strains producing CNF1, suggesting that CNF1 production confers a survival advantage to UPEC isolates[37].

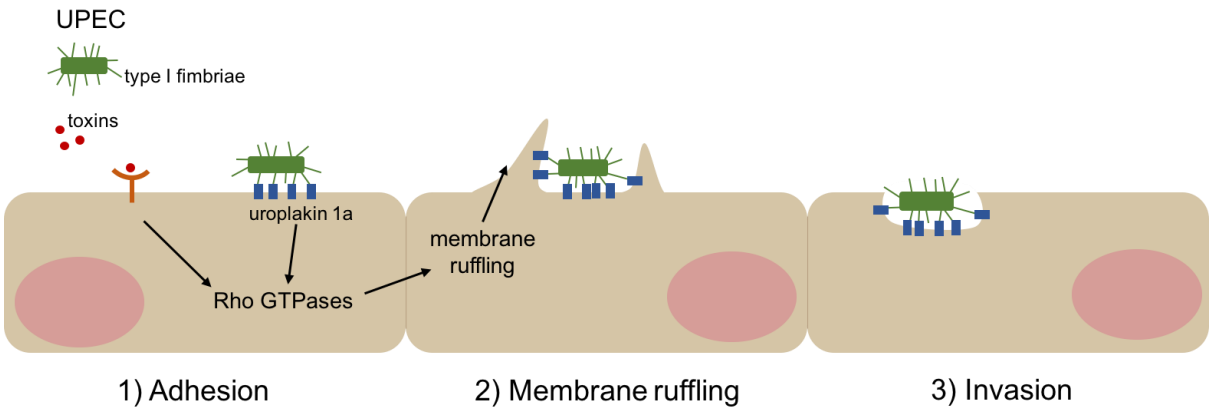

Figure 1.3: Role of type I fimbriae and toxins in bladder cell invasion. Binding of type I fimbriae or toxins to bladder epithelial cells activates Rho GTPases and causes membrane ruffling and uptake of bacteria into the epithelial cell.

Additionally, as iron availability is limited within the host, UPEC require an effective method of acquiring iron. UPEC secrete siderophores, which bind to iron and are transported into the bacterium by active transport. *E. coli* can produce up to four siderophores: enterobactin, salmochelin, aerobactin, and yersiniabactin. Compared to faecal *E. coli* strains UPEC produce more salmochelin and yersiniabactin suggesting these siderophores confer a survival advantage in the urinary tract[38]. However, deletion of the UPEC siderophore receptor genes revealed that iron uptake by aerobactin and yersiniabactin was more important than uptake by enterobactin and salmochelin for successful colonisation of the urinary tract[39]. Thus, UPEC strains regulate siderophore production to facilitate iron acquisition in the urinary tract.

Altogether, UPEC possess a variety of virulence factors that promote bacterial survival within the urogenital tract and encourage bacterial invasion of epithelial cells.

1.5 Host response to infection

The host detects pathogen invasion through pattern recognition receptors (PRRs), which recognise conserved microbial structures called pathogen-associated molecular patterns (PAMPs). There are four types of PRR and these are toll-like receptors (TLRs), c-type lectin receptors (CLRs), retinoic acid-inducible gene (RIG)-I-like receptors (RLRs) and nucleotide-binding oligomerisation domain (NOD)-like receptors (NLRs). These receptors bind to a range of microbial PAMPs and initiate signalling cascades.

1.5.1 Toll-like receptors

There are currently ten TLRs (TLR1-10) identified in humans and these bind to bacterial and viral PAMPS (Figure 1.4). TLR localisation within the cell corresponds to where the ligand for that TLR is likely to be present during an infection. TLR1/2/5/6/10 are localised to the cell membrane and are linked to ligands present on the pathogen surface, whereas TLR3/7/8/9 are found in endosomes in the cytoplasm and are linked to detection of pathogenic molecular material, such as bacterial DNA. TLR4 localises to both the plasma membrane and endosomes. The ligand for each of the TLRs is shown in Table 1.1. The ligand for TLR10 has not yet been identified, however, homology modelling suggests a similar binding pocket to TLR2[40]. In addition, Oosting *et al.* (2014) reported that TLR10 is an anti-inflammatory PRR that acts to inhibit TLR2 mediated responses[41].

Interestingly, TLR11 is present in mice and is associated with protection against UTI[42]. This receptor has not been identified in humans and this, therefore, indicates genetic differences between mice and humans. This should be taken into account when using mouse models of UTI, as the presence of an additional TLR may influence the mouse innate immune response to UPEC.

Table 1.1: Toll-like receptor (TLR) ligands. The ligand for each TLR is shown. TLR2 dimerises with TLR1 and TLR6 to detect bacterial lipopeptides. The ligand for TLR10 remains unknown[43–49].

TLR	Ligand
TLR1-TLR2	Triacyl lipopeptides
TLR2-TLR6	Diacyl lipopeptides
TLR3	dsRNA
TLR4	Lipopolysaccharide
TLR5	Flagellin
TLR7	ssRNA
TLR8	ssRNA
TLR9	Bacterial DNA
TLR10	Unknown

The adapter molecule MyD88 is activated downstream of the TLRs, with the exception of TLR3, and initiates signalling cascades that result in activation of NF-κB, p38 mitogen-activated protein (MAP) kinase, AP-1 and JNK transcription factors[50–53]. These transcription factors upregulate proinflammatory cytokines and chemokines, and produce an innate immune response to the invading pathogen. As a result of ligand binding to TLR3 and TLR4, MyD88-independent signalling pathways can be activated via the adapter protein TRIF, which stimulates the activity of the transcription factor IRF3 and causes transcription of interferon-inducible genes[54–56].

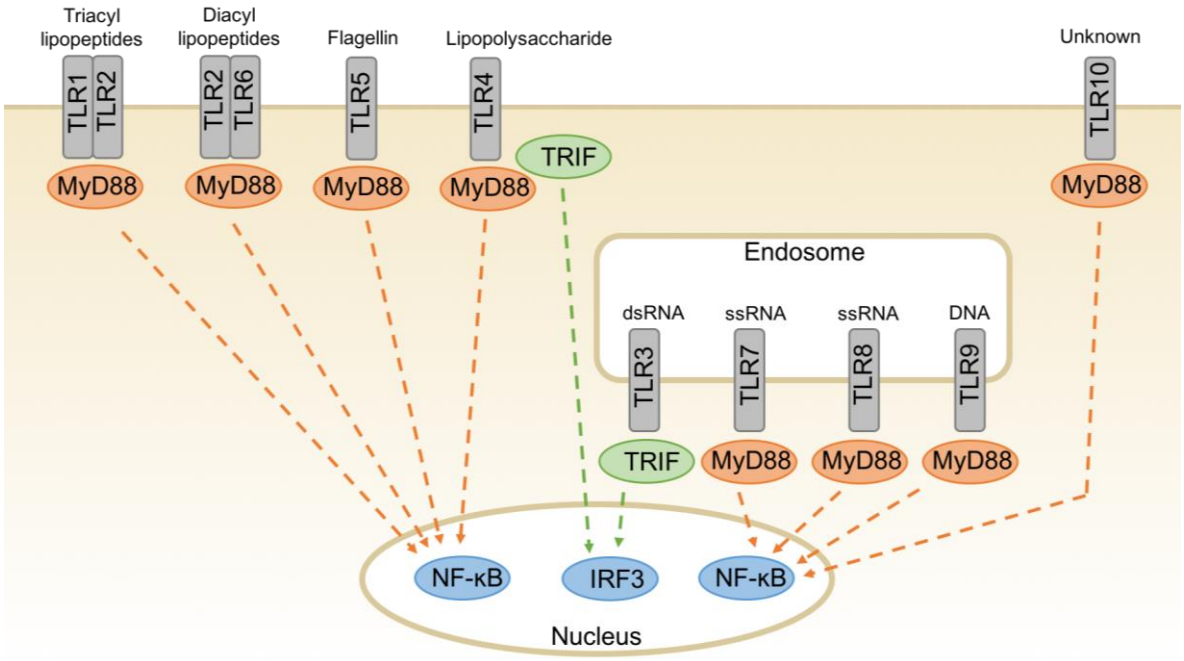

Figure 1.4: Toll-like receptor ligands, localisation, and signalling. The adaptor protein MyD88 is activated downstream of TLR1/2/4/5/6/7/8/9/10 and this leads to activation of NF-κB and other transcription factors such as AP-1. The adapter protein TRIF is activated downstream of TLR3/4 and this activates transcription factor IRF3.

The importance of TLR signalling with respect to UTI susceptibility is not well characterised. Tabel *et al.* (2007) studied 124 Turkish children who suffered at least one UTI and found that the G2258A mutation in the TLR2 gene occurred more frequently in this group than in 116 healthy controls. Furthermore, those carrying the G2258A mutation in the TLR2 gene suffered significantly more UTI episodes than non-carriers[57]. However, a second study by Hawn *et al.* (2009) examining 1261 American adult women did not find any significant difference in UTI frequency between women carrying the TRL2 G2258A mutation and non-carriers[58]. Thus, the importance of TLR2 in protecting against UTIs is not clear. Hawn *et al.* also found that the A896G mutation in TLR4 was protective against rUTI. However, other researchers examining 377 adults (both men and women) reported that this mutation had a higher frequency in patients with a rUTI and was associated with increased susceptibility to UTI[59]. TLR4 expression in monocytes was also reported to be lower in rUTI patients than healthy controls. Thus, the role of TLR4 in UTI protection is also unclear. Hawn *et al.* also identified a C1174T mutation in the TLR5 gene that was linked to increased rUTI susceptibility. This mutation introduces an early stop codon in TLR5 and has since been confirmed to increase susceptibility to UTIs[60]. TLR5 null mice have been shown to have increased susceptibility to UTIs and had significantly more bacteria in the bladder and kidneys following transurethral injection of *E. coli* than wild type mice[61]. Thus, these data demonstrate that flagellin detection by TLR5 is highly important for bacterial clearance from the urogenital tract.

1.5.2 Nod-like receptors (NLRs)

NLRs are cytoplasmic PRRs. The NLRs NOD1 and NOD2 recognise bacterial peptidoglycan. NOD1 recognises peptidoglycan containing γ-D-glutamyl-meso-diaminopimelic acid (iE-DAP), which is present in most common Gram-negative bacteria, such as *E. coli* and *Bacillus subtilis*[62]. Muramyl dipeptide (MDP) is the ligand for NOD2 and this is present in the peptidoglycan of all Gram-positive and Gram-negative species[63]. Activation of NOD1 and NOD2 results in NF-κB activation, which results in proinflammatory cytokine upregulation[64]. In addition, the MAP kinases p38, ERK, and JNK can be activated by ligand binding to NOD1 and NOD2[65,66].

NOD1 null mice showed significantly greater burden of UPEC in the kidney following inoculation than wild type mice, suggesting NOD1 has a protective role against pyelonephritis[67]. Wang *et al.* (2014) showed that transgenic mice lacking the NOD2 gene did not have increased susceptibility to UTI compared to NOD2 competent mice[68]. These data suggest that NLRs do not have a role in protecting the host from UTI, however, following bladder infection NOD1 may reduce the bacterial burden in the kidney.

1.5.3 Rig-I-like receptors (RLRs) and c-type lectin receptors (CLRs)

RLRs are cytoplasmic receptors that detect dsRNA from viral pathogens. This may either be the dsRNA of the viral genome, or may be produced during replication of a ssRNA virus. Three RLRs exist: RIG-I, MDA5, and LGP2[69–71]. RIG-I recognises short dsRNA, up to 1kb in length, whereas, MDA5 recognises long dsRNA strands[72]. It is hypothesised that the third RLR LGP2 may modify viral RNA or act to unwind complex RNA structures to facilitate binding by RIG-I or MDA5. Activation of RLRs results in expression of antiviral interferon-inducible genes. As RLRs are involved in antiviral immunity no role for these in defence against UTIs has been reported.

CLRs recognise carbohydrate motifs on invading pathogens and are primarily involved in recognition of fungal pathogens. Dectin-1 and Dectin-2 are the most well characterised members and recognise β-glucans and mannans, respectively, from fungal cell walls[73,74]. Thus, CLRs are unlikely to be involved in the recognition of UPEC in the urogenital tract.

1.5.4 Innate immunity to UTIs

Pathogen recognition by TLRs activates signalling pathways that trigger an immune response to the invading pathogen. An innate immune response is produced immediately and is not specific to the invading microorganism. TLR activation by microbial ligands results in the production of antimicrobial cytokines and chemokines. Interleukin (IL)-6 and -8 are important for bacterial clearance from the urinary tract. IL-6 promotes an acute phase response, which is an early inflammatory response to infection, and is elevated in patients with a UTI. IL-8 is also elevated in the urogenital tract following infection with UPEC[75,76]. IL-8 is chemotactic for neutrophils through interaction of IL-8 with the IL-8 receptors CXCR1 and CXCR2. Recruitment of neutrophils to the site of infection is vital for clearance of UPEC from the urogenital tract[77–79]. Indeed, mice deficient in the IL-8 receptor showed delayed neutrophil migration, increased UTI susceptibility and increased bacterial loads in the bladder and kidneys compared to wild type mice[80].

In addition to neutrophils, other cellular components of the innate immune system also play a role in UTI clearance. LY6C macrophages reside within the bladder epithelium and following infection secrete cytokines and chemokines that aid in neutrophil recruitment. Natural killer (NK) cells and mast cells are also thought to be important to UPEC clearance. The roles of these cells is less well understood, but the number of mast cells and NK cells in the urine increases during

UTI indicating a role for these cells in bacterial clearance[81]. NK cells facilitate bacterial killing through production of TNF-α, however, UPEC can abrogate this response by secreting the HlyA toxin, which causes NK cell death[82]. Dendritic cells are also recruited to the bladder during a UTI, but were dispensable for bacterial clearance in a mouse model of UTI[83]. Mice depleted of dendritic cells prior to transurethral UPEC infection did not demonstrate a significant difference in the bacterial CFU of the bladder compared to non-depleted control mice[83].

A key part of the host innate immune response to infection is antimicrobial peptide (AMP) synthesis. These molecules are vital to bacterial clearance from the urogenital tract and are discussed in more detail below.

1.5.5 Antimicrobial peptides

AMPs have been identified in bacteria, archaea, protists, fungi, plants and animals, suggesting they play a fundamental role in organism survival. As of July 2016, 2722 AMPs have been identified in total and 2043 of these are in animals, with 113 existing in humans[84]. The underlying principle of AMPs is the ability to form a structure that consists of discrete hydrophilic and hydrophobic areas. This amphipathic structure allows insertion of the peptides into bacterial membranes to cause cell lysis. The peptides are small, up to 100 amino acids in length, and usually carry an overall positive charge. The exact mechanism of action of AMPs is not understood, but disruption of the microbial membrane is the key principle. Several models of how the peptides interact with membranes have been proposed. These include the barrel and stave model, whereby the peptides bore into the bacterial membrane to form a pore through the lipid bilayer, and the carpet model, which suggests that AMPs coat the outer bacterial membrane in peptides which causes membrane disintegration[85].

The positive charge of AMPs ensures preferential binding to microbial membranes over host cell membranes (Figure 1.5). Anionic phospholipid head groups, such as phosphatidylglycerol, in the lipid bilayer give bacterial cell membranes a negative charge. Whereas, the lipid bilayer of mammalian cells consists of neutral phospholipids[86]. Thus, positively charged AMPs preferentially interact with negatively charged microbial membranes. Furthermore, incorporation of cholesterol into mammalian membranes hinders AMP binding[86,87]. Cullen *et al.* (2015) recently reported that commensal bacteria from the gut can survive at higher concentrations of AMPs than pathogenic species[88]. In addition, the authors identified an enzyme, LpxF, present in commensal species that removes the negatively charged phosphate group from LPS. This neutralises the LPS negative charge and interferes with AMP binding to commensal organisms.

Thus, AMP specifically target pathogenic bacterial cell membranes, making AMPs an interesting area for development of alternative therapeutics to antibiotics. In humans several groups of AMPs exist and are outlined below.

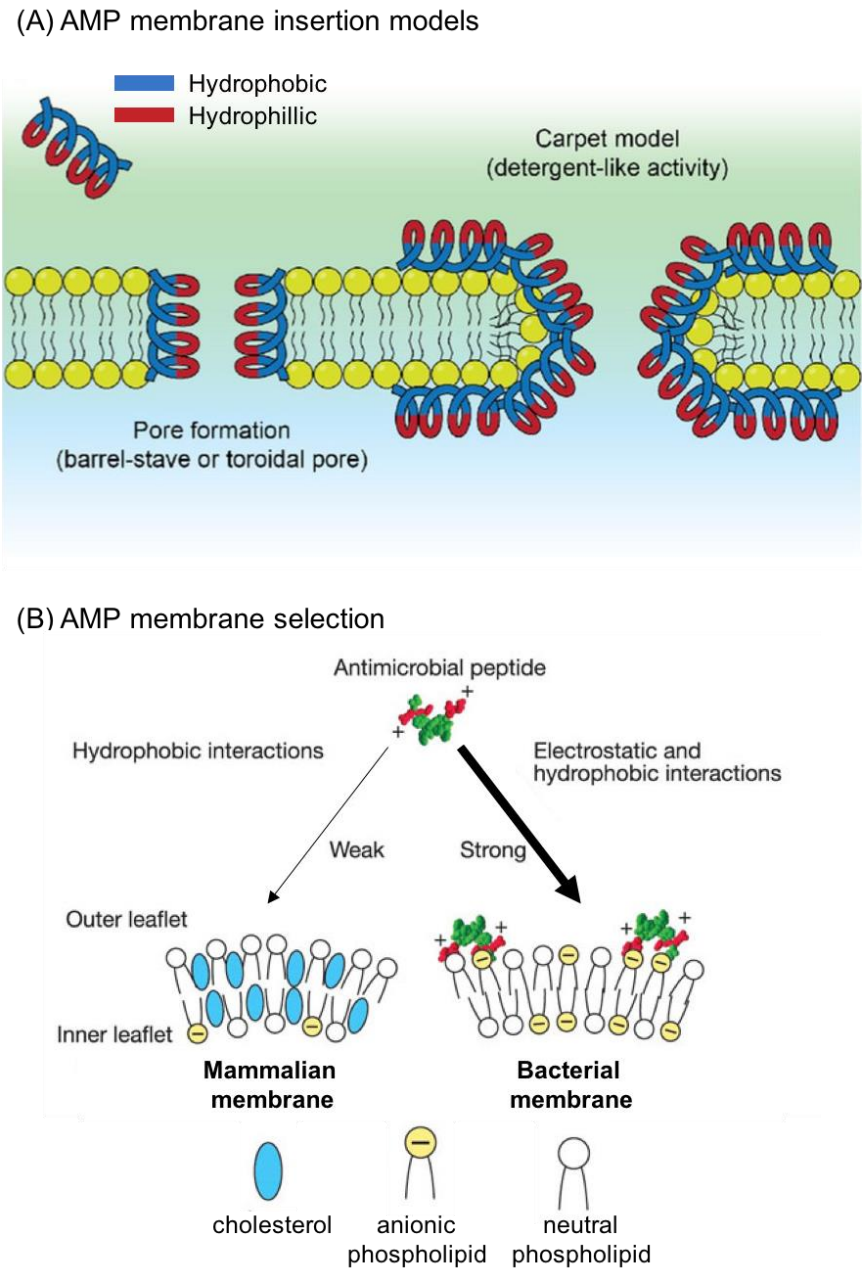

Figure 1.5: Mechanism of AMP membrane selection and insertion. (A) AMPs have distinct hydrophobic (blue) and hydrophilic (red) areas. This allows insertion into bacterial membranes. Several models exist for how AMPs lyse bacteria, and these include the barrel and stave model, where the AMPs form a pore in the membrane, and the carpet model, where AMPs coat the bacterial membrane and cause membrane disintegration. (B) Cationic AMPs preferentially bind to negatively charged phospholipids of microbial membranes. The presence of cholesterol in mammalian membrane also inhibits AMP binding. (A) adapted from ref 89 and (B) adapted from ref 90.

1.5.5.1 Defensins

The defensins are an important group of AMPs that can be further divided into three categories,

α-defensins, β-defensins and θ-defensins, based on the spacing between six cysteine residues and the resultant disulphide bridges[91].

There are six human α-defensins: HNP1-4 are found primarily within granules of neutrophils and HD5 and HD6 are produced in gut Paneth cells[92,93]. HD5 is also expressed in epithelial cells of the respiratory tract, urinary tract and female reproductive tract[94–96]. These six α-defensins are 29-35 amino acids long and disulphide bonds are formed between cysteine residues 1 and 6, 2 and 4, and 3 and 5.

The θ-defensins only exists in non-human primates. The θ-defensin genes have been identified within the human genome; however, these genes encode a premature stop codon. Therefore, functional θ-defensins are not synthesised in humans[97].

Evolutionarily, the α-defensin and θ-defensin genes descended from β-defensins. Human β-defensins (hBDs) are produced by epithelial cells and are a vital component of innate immunity at epithelial surfaces. Although over 30 gene loci for hBDs are thought to exist, mostly clustered on chromosome 8p23, only hBD1-4 have been identified *in vivo* and studied in detail[98]. Zhou *et al.* (2013) have shown that deletion of nine murine β-defensin genes in the cluster on chromosome 8 resulted in reduced sperm motility and infertility in male mice[99]. This suggests that in mammals other β-defensin genes may have alternative functions to AMPs. hBDs are larger than α-defensins, consisting of 36-47 amino acids. They have little primary sequence homology to α-defensins, but due to the disulphide bridges between cysteine residues hBDs and α-defensins share a similar tertiary structure. In hBDs the disulphide bridges form between cysteine residues 1 and 5, 2 and 4, and 3 and 6. hBD1 has antimicrobial activity against the Gram-negative bacteria *E. coli* and *Pseudomonas aeruginosa*, however expression of hBD1 is constitutive and is not induced by bacterial PAMPs[60,100,101]. hBD2 has strong killing activity against Gram-negative bacteria and fungi and is bacteriostatic against Gram-positive pathogens[102]. Similarly, hBD3 has broad-spectrum activity against Gram-negative, Gram-positive and fungal pathogens[103]. Expression of both hBD2 and hBD3 is induced by bacterial PAMPs during infection[60,102–106]. hBD4 has been shown to be induced by bacteria and has antimicrobial activity against Gram-negative bacteria, Gram-positive bacteria, and yeast[107,108]. However, hBD4 is less well studied than hBD1-3.

1.5.5.2 Cathelicidins

Like defensins, cathelicidins are cationic, amphipathic peptides. Cathelicidins vary in size, sequence and structure, but all share a common cathelin domain at the N-terminal of the

precursor protein. The cathelicidin precursor protein is then processed to release the active peptide at the C-terminal. Approximately 30 cathelicidin genes have been identified in mammals. Many animals possess multiple cathelicidin genes, for example, eleven cathelicidin genes have been identified in the bovine genome[109]. However, in humans only one cathelicidin gene exists (CAMP) and this encodes the AMP LL-37[110]. LL-37 begins with two leucine resides at the N-terminus and is 37 amino acids long, hence the name. Expression of LL-37 has been identified in many cell types including neutrophils, myeloid bone marrow cells, and epithelial cells[111–113]. LL-37 has antimicrobial activity against both Gram-positive and Gram-negative bacteria and can be induced by bacterial PAMPs[105,114].

1.5.5.3 Antimicrobial proteins

Antimicrobial proteins are larger than AMPs, typically at 100-200 amino acids in length. As of July 2016 there were 17 human antimicrobial proteins in the antimicrobial peptide database[84]. These include several members of the ribonuclease (RNase) A superfamily. The human genome contains 13 RNase genes, RNase 1-13, which act to degrade RNA. In ruminants these genes are important for digestion of dietary RNA and recovering RNA-nitrogen from the intestinal flora[115]. However, many members of the RNase family have evolved alternative functions, including antimicrobial activity. RNase 2, 3, 5, 7 and 8 appear to function in host defence. RNase 2 is an eosinophil protein and has antiparasitic and antiviral activity[116,117]. RNase 3 has recently been reported to have activity against mycobacteria[118]. The antimicrobial role of RNase 5 is unclear as although it was initially reported to have antimicrobial activity, a later publication showed the antimicrobial activity to be negligable[119,120]. RNase 7 and 8 are produced by epithelial cells and have both been identified as having broad-spectrum antimicrobial activity against Gram-positive and Gram-negative bacteria[121,122]. RNase 7 is an extremely potent AMP and despite being an RNase exerts its antimicrobial activity in the traditional manner for AMPs i.e. through membrane disruption and not through interaction with bacterial RNA[123].

S100A7, also called psoriasin, is an antimicrobial protein from the S100 protein family and is 101 amino acids in length. S100 proteins have multiple functions ranging from cell differentiation to cancer suppression, but are characterised by the presence of two calcium binding EF-hand motifs[124–126]. S100A7, S100A12, and S100A15 are produced by epithelial cells and have antimicrobial activity against *E. coli*[127–129].

Finally, lactoferrin and lipocalin 2 (LCN2) are cationic antimicrobial proteins of 710 and 198 amino acids, respectively, that are produced by epithelial cells and inhibit bacterial growth

through sequestration of iron. Lactoferrin can also interact with bacterial membranes and lyse bacteria through membrane damage. Lactoferrin binds iron and prevents uptake by bacterial pathogens[130,131]. However, a number of Gram-negative pathogens, such as *Neisseria gonorrhoeae*, have been reported to overcome iron sequestration by lactoferrin, by inducing a conformational change in the lactoferrin molecule and causing release of iron[132]. LCN2 binds to siderophores, primarily enterobactin, and prevents uptake of siderophores by bacteria, thus limiting iron intake[133]. However, as discussed previously, some pathogens can alter their siderophore production to favour salmochelin and yersiniabactin, which are not inhibited by LCN2[38].

It is clear that many AMPs exist in humans and are important in the host immunity to pathogens. Expression of many AMPs has been reported in the urogenital tract and the expression pattern of these AMPs is summarised in Figure 1.6.

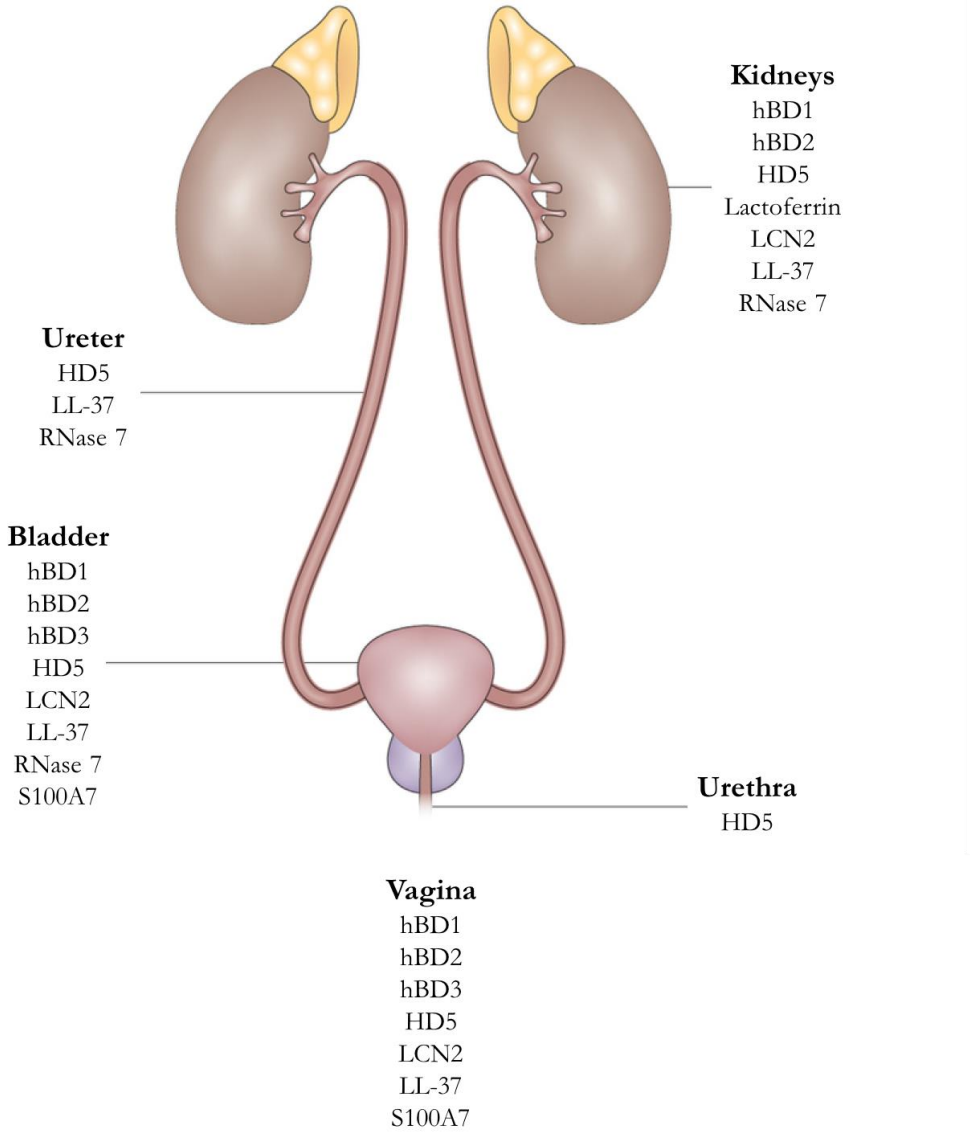

Figure 1.6: Antimicrobial peptide expression in the urogenital tract. The antimicrobial peptides that have been identified in the vagina, urethra, bladder, ureter and kidneys are shown[60,106,129,134,135]. Figure adapted from ref 135.

1.5.6 Adaptive immunity to UTIs

Adaptive immunity is characterised by production of antibodies specific to the infecting organism and provides the host with an immunological memory of the pathogen. Following antigen exposure, T lymphocytes produce cytokines that activate B lymphocytes and stimulate antibody production. The cytokine profile produced by T cells determines the nature of the immune response produced. Thus, cross-talk between T and B cells is crucial for a robust adaptive immune response. The fact that many patients suffer recurrent UTIs caused by the same strain of *E. coli* suggests that an effective adaptive immune response is not mounted. Chan *et al.* (2013) used a mouse model to demonstrate that the kidney produces UPEC-specific antibodies in response to pyelonephritis, but that UPEC-specific antibodies are not produced in the bladder in response to cystitis[136]. The authors identified IL-10, secreted from mast cells, as the cause of bladder tolerance to infection. Deleting the IL-10 gene in mice resulted in antibody production in the bladder following cystitis, which was not seen in IL-10 competent mice. It was demonstrated that IL-10 deficient mice had improved dendritic cell activation compared to IL-10 competent mice, suggesting that IL-10 drives bladder tolerance to UPEC by reducing dendritic cell activation. However, the role of IL-10 in UTI clearance is controversial as Duell *et al.* (2012) have shown that IL-10-depleted mice had higher bacterial loads in the bladder following transurethral UPEC injection than wild type mice[137]. Thus, IL-10 may be important for rapid clearance of bacteria from the bladder, but also be detrimental to the adaptive immune response.

Interestingly, Mora-Bau *et al.* (2015) showed that the adaptive immune response in the bladder is improved following macrophage depletion[138]. In addition, Mora-Bau *et al.* measured cytokine levels following macrophage depletion and demonstrated that the level of IL-10 was not affected, showing that macrophage depletion did not indirectly improve adaptive immunity by reducing the IL-10 concentration. In fact, the authors demonstrated that macrophage depletion resulted in increased phagocytosis of UPEC by dendritic cells. This increased antigen presentation to T and B cells and hence, improved the adaptive immune response. Taken together, these results suggest that dendritic cell activation is a key step in mounting an adaptive immune response to UPEC. However, this does not occur effectively in the bladder in response to UTI and it is not clear whether this is due to the presence of macrophages and/or IL-10 secretion from mast cells.

These data show that the adaptive immune response to UTI is not well understood. However, as it appears that an adaptive immune response is not properly developed in response to UTI, the consensus is that innate immune responses to UTI are key to bacterial clearance.

1.6 Treatment of UTIs

1.6.1 Antibiotic treatment

Although the majority of UTIs are usually successfully cleared by the immune system, a course of antibiotics is usually prescribed to reduce the recovery time. Trimethoprim-sulfamethoxasole (TMP-SMX), fluoroquinolones and nitrofurantoin are the first line agents that are commonly prescribed. The second line agents, β-lactams and fosfomycin, are mainly used in cases such as pregnancy where other antibiotics may not be safe[139]. Treatment duration can vary from three to ten days; five to ten day treatment courses are more effective at eradicating the bacteria than three day courses, but are linked to an increased risk of adverse reactions and non-compliance[140].

Long-term antibiotic treatment is used for women who regularly suffer from rUTIs. The 2008 Cochrane review concluded that antibiotic use significantly reduced UTI recurrence in both pre- and postmenopausal women when compared to placebo treatment[141]. However, extended antibiotic treatment was associated with adverse events including vaginal candidiasis. There is also the major concern that long-term antibiotic use promotes antibiotic resistance. Indeed, UTI resistance to TMP-SMX, the antibiotic most commonly used to treat UTIs, is on the increase. Current estimates show that approximately 20% of UTI cases are linked to TMP-SMX resistant uropathogens[142]. Furthermore, resistance to TMP-SMX is associated with resistance to other antibiotics, including ampicillin and ciprofloxacin, indicating that TMP-SMX resistant strains may also be more difficult to treat with other antibiotics[143]. This emerging resistance demonstrates the need for alternative, non-antibiotic based therapies for UTIs. Specifically, research into treatments that may be taken long-term to treat rUTIs without causing side effects would be extremely valuable.

1.6.2 Vaccination against UTI

Although adaptive immunity is not thought to play a major role in protection against UTIs some vaccination candidates have shown encouraging results. Mouse models of UTI have identified several potential vaccine candidates including fimbriae (FimH), flagellin (FliC) and the bacterial receptors for the siderophores salmochelin, aerobactin and yersiniabactin, which confer protection against UTIs[144–149]. A FimH vaccine has also been shown to confer protection against UTIs in a small group of Cynomolgus monkeys[150]. Clinical trials have also been performed in humans and showed promising results. Bauer *et al.* (2005) performed a double-blind study where women with rUTI were given capsules containing lyophilised *E. coli* or placebo[151]. The capsules were taken daily for three months and then for ten days in months 7, 8 and 9. In the placebo

group 122 patients suffered 276 UTIs in the 12 month follow-up period, whereas, in the treatment group 93 patients suffered 185 UTIs. Overall this represented a significant 34% reduction in UTI occurrence in the vaccine group. Hopkins *et al.* (2007) also demonstrated that vaginal suppositories containing ten human uropathogenic strains (6 *E. coli*, 1 *K. pneumoniae*, 1 *E. faecalis*, 1 *Proteus mirabilis* and 1 *Morganella morganii*) were protective against UTIs; women who received the vaccine plus boosters had a significantly lower incidence of UTIs caused by UPEC than women receiving placebo[152]. It is worth noting that although these vaccines conferred some protection against UTIs, the vaccines were far from 100% effective. The 34% decrease in UTI occurrence reported by Bauer *et al.* is low compared to a near 100% effectiveness for classical vaccines such as the measles, mumps, and rubella vaccine. Thus, even with successful UTI vaccine development a large number of women could remain unprotected and in need of alternative therapeutics.

Only three companies are currently pursuing a UTI vaccine and all three vaccines are in the pre-clinical stages[153]. It is thought that as antibiotic treatment is still effective for many UTI patients development of a UTI vaccine is not profitable for pharmaceutical companies. Although a large number of patients suffer from UTIs and antibiotic resistance is on the increase, it is unlikely that a UTI vaccine would be included in national immunisation programmes and thus is unlikely to generate enough revenue to entice development from pharmaceutical companies. Hence, a UTI vaccine may still be many years from coming to fruition.

1.6.3 Natural agents from the diet

1.6.3.1 Cranberries

For decades it has been thought that cranberries can relieve the symptoms of UTIs. The mechanism is not fully understood, but evidence suggests that cranberries may inhibit adhesion of uropathogens to epithelial cells of the urinary tract, preventing infection[154,155]. However, a review of the published data on this topic by Jepson *et al.* in 2012 concluded that there is no significant reduction in rUTI incidence in women using cranberry products compared to those using a placebo treatment[156].

1.6.3.2 Vitamin C and D

In vitro studies of vitamin C showed that it is bacteriostatic in urine due to acidification of the urine and generation of nitric oxide, which is toxic to UPEC[157]. A clinical trial compared 55 pregnant women receiving vitamin C, along with ferrous sulfate and folic acid, to 55 pregnant

women receiving ferrous sulfate and folic acid without vitamin C[158]. The trial reported that 12.7% of the vitamin C group suffered a UTI, whereas 29.1% of the women not taking vitamin C suffered a UTI. Thus, vitamin C supplementation significantly reduced the incidence of UTIs in pregnant women.

Similarly, low serum vitamin D levels have been associated with increased risk of UTI[159]. One study has compared UTI incidence in patients taking vitamin D to patients taking placebo, however, this trial was primarily observing progression from prediabetes to type 2 diabetes mellitus[160]. Therefore, the patients included in the study were not suffering from rUTI and a relatively low number of UTIs were recorded throughout the follow-up period (18 patients out of 116 receiving vitamin D and 34 patients out of 111 in the placebo group). Nevertheless, the results showed reduced UTI incidence in patients taking vitamin D. However, more robust studies specifically examining pre- and postmenopausal women who regularly suffer UTIs are required to properly assess the benefits of vitamin C and D in these patients.

1.6.4 Hormonal treatment

In certain populations of women estrogen treatment may be effective at reducing the incidence of UTIs. Postmenopausal women have an increased risk of developing a rUTI, which has been linked to reduced estrogen levels. Evidence suggests that estrogen replacement therapy is successful in reducing the incidence of UTIs in postmenopausal women[7].

The function of estrogen and its role in protecting against UTIs will now be discussed in more detail.

1.7 Estrogen

Estrogen is a female steroid hormone that is produced by the ovaries and is responsible for regulating the menstrual cycle in women. Three forms of estrogen naturally occur in women; 17β-estradiol is the predominant form, whilst estrone and estriol circulate at much lower levels[161]. The concentration of estrogen in the blood fluctuates throughout the menstrual cycle; the lowest estrogen levels occur during the luteal and early follicular phase, ranging between 70 and 510pM and the concentration of estrogen peaks before ovulation at a range of 390 to 1480pM[162]. In postmenopausal women estrogen levels drop below 130pM, which is lower than the reported estrogen concentration in men (200pM).

Estrogens exert their actions by binding to estrogen receptors (ERs). There are two types of

estrogen receptor: genomic, consisting of estrogen receptor alpha and beta (ER-α and –β), and non-genomic, consisting of the G protein-coupled estrogen receptor (GPER) also known as G protein-coupled receptor 30 (GPR30).

1.7.1 Genomic ERs

The genomic ERs, ER-α and ER-β, are located in the cytoplasm and are encoded by the ESR1 and ESR2 genes, respectively. ER-α and –β consist of five domains: the ligand binding domain, the dimerisation domain, the nuclear localisation sequence, the N-terminal transactivation domain and the DNA binding domain[161]. Estrogen diffuses through the cell membrane and binds to the receptors intracellularly, causing the receptors to dimerise, forming homodimers (α-α or β-β complexes) or heterodimers (α-β complexes)[163,164]. The receptor dimers recognise and bind to estrogen response elements (EREs) with consensus sequence GGTCAnnnTGACC in the promoter region of estrogen responsive genes resulting in transcription of the gene[165]. The mechanism of action of the genomic ERs is shown in Figure 1.7.

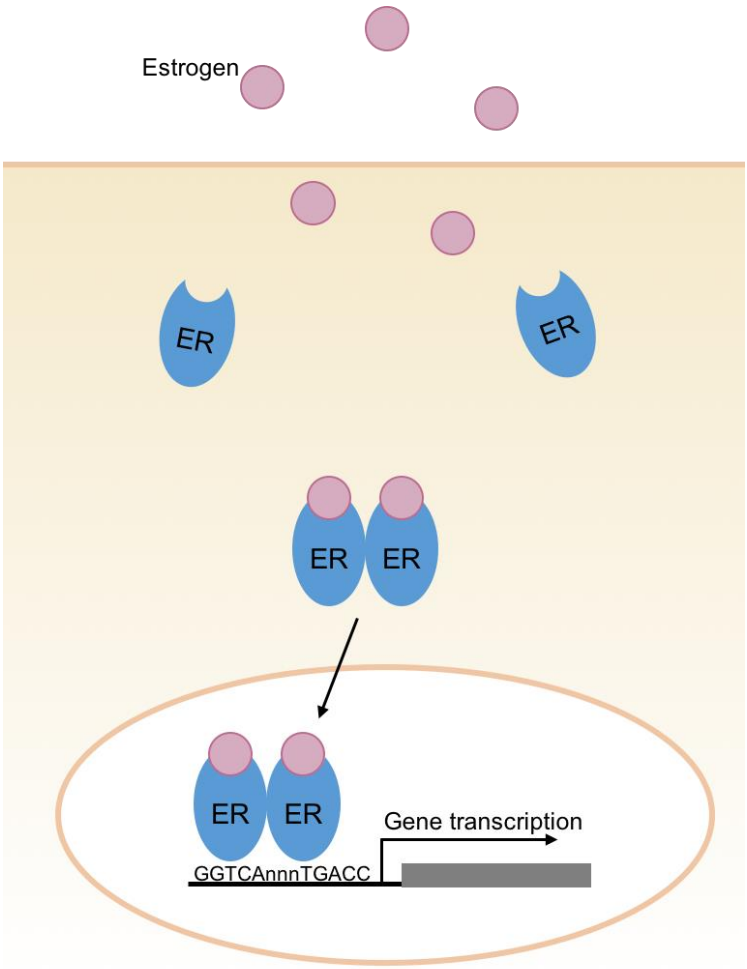

Figure 1.7: Mechanism of action of genomic estrogen receptors. ER-α and ER-β are localised to the cytoplasm. Estrogen diffuses through the cell membrane and binds to the ERs. Upon ligand binding, the ERs dimerise, migrate to the nucleus and bind to estrogen response elements (EREs) with consensus sequence GGTCAnnnTGACC to initiate gene transcription.

Although the DNA binding domains of ER-α and ER-β are nearly identical, there is only 56% amino acid identity in the ligand binding domain[166]. As a result, certain ligands preferentially bind to one receptor over the other. For example, the three naturally occurring estrogens in women (17β-estradiol, estriol and estrone) preferentially bind to ER-α, whilst phytoestrogens genistein and coumestrol have a higher affinity for the ER-β receptor[167]. In addition to this, the two genomic receptors also differ in their transcriptional potencies, with ER-α being a stronger activator of transcription than ER-β[168]. These distinctions between the receptors mean that certain compounds can initiate effects on certain tissues whilst causing a minimal response in others; this is already being exploited for treatment of other estrogen-regulated diseases, such as breast cancer[169].

ER-α and -β are differentially expressed in many cell types and tissues, including the reproductive organs, breast tissue, bones and cardiovascular tissue, and are capable of transcribing a multitude

of genes[170,171]. Microarrays on human tissue support the notion that the number of estrogen responsive genes in human is in the hundreds[172]. Thus, it is clear that estrogen is a powerful regulator of gene transcription, by activity through ER-α and –β, and the ability to harness and manipulate this power may be highly beneficial in development of future therapeutics.

1.7.2 Non-genomic ER

After the discovery of ER-α and –β, papers were published demonstrating that estrogen can also elicit very rapid responses within cells that occur too quickly to be attributed to the transcriptional activity of the genomic ERs[173,174]. As a result, in 2005 a third ER was identified. The G protein-coupled receptor 30 (GPR30), previously an 'orphan' receptor with unknown function, was discovered to bind estrogen and produce non-genomic responses within the cell. These include upregulation of intracellular calcium, nitric oxide and receptor tyrosine kinases[175]. The receptor has now been renamed the G protein-coupled estrogen receptor (GPER). Like all G protein-coupled receptors GPER is made up of an N-terminal receptor, seven transmembrane domains and a C-terminal that activates the associated G protein upon estrogen binding to the receptor. Localisation of GPER within the cell is contentious; the receptor has been reported to localise to the plasma membrane, the endoplasmic reticulum, the cytoplasm and the nucleus[176–179]. Recently Samartzis *et al.* (2014) have reported that whilst the localisation is predominantly cytoplasmic in one immortalised breast carcinoma cell line (T47D), GPER had nuclear localisation in a second immortalised cell line (MCF7)[179]. Thus this inability to reliably determine the subcellular localisation of GPER indicates that the receptor may localise to different places in the cell depending on the cell type, function and possibly even disease state.

1.7.3 Estrogen receptor cross-talk

Although the genomic and non-genomic receptors were identified based on their differing functions, there is evidence for cross-talk between the two signalling pathways. For example, estrogen binding to GPER can result in phosphorylation of the transcription factors CCAAT/enhancer binding protein beta (CEBPB), cAMP response element binding protein (CREB) and activator protein 1 (AP-1) by activation of the MAP kinase signalling pathway[174,180–182]. Activation of these transcription factors initiates transcription of their target genes. Consequently, estrogen interaction with the classical or non-classical estrogen receptors may not produce mutually exclusive outcomes, as estrogen binding to the non-genomic receptor, GPER, can lead to genomic events.

1.7.4 Estrogen protects against UTIs

In premenopausal women estrogen has an important role in protecting the urinary tract from invasion by pathogenic bacteria. In the vagina the presence of estrogen stimulates glycogen production[183]. This promotes the growth of commensal bacteria, such as lactobacilli, that can readily metabolise the glycogen. An abundance of commensal organisms within the vagina is crucial to preventing uropathogens from establishing a reservoir in this environment. Several studies have shown that *Lactobacillus* species are capable of inhibiting the growth of uropathogens, such as *E. coli*, in a number of ways.

First, the metabolism of glycogen by lactobacilli produces lactic acid. This lowers the pH of the vagina so that it is inhospitable to pathogens such as *E. coli*[184]. Second, some *Lactobacillus* species also produce hydrogen peroxide. Hydrogen peroxide oxidises halides, such as chloride, when combined with a peroxidase, to form oxidants that are toxic to many bacterial species[185]. One study revealed that hydrogen peroxide generating lactobacilli were present in the vagina of 96% of premenopausal women[186]. Peroxidase activity has been detected within the vaginal fluid and has been shown to be induced by estrogen in the rat uterus[187,188]. Therefore, hydrogen peroxide production by lactobacilli may be an important system in protecting the vagina from colonisation by uropathogens. Finally, cell extracts of *Lactobacillus* species have been shown to prevent adhesion of uropathogens to the urothelium[189]. These data demonstrate that promotion of lactobacilli growth by estrogen helps in preventing colonisation by pathogenic bacteria.

Given the mechanisms by which estrogen potentially protects the urinary tract from uropathogens, it is discernible that depleted estrogen levels after the menopause may have a knock-on effect on the ability of postmenopausal women to successfully clear a UTI. Lower circulating estrogen levels in postmenopausal women reduce the vaginal *Lactobacillus* population resulting in a higher vaginal pH, hence increasing the vaginal susceptibility to colonisation by uropathogens. Indeed, women who regularly suffer from UTIs typically have a vaginal pH above 4.5[190]. Furthermore, unpublished data from our laboratory has indicated that estrogen may also protect the urinary tract from infection by increasing the expression of the AMP hBD2 in the vagina[60]. Thus, it is possible to speculate that these women may have lower expression of certain AMPs, further increasing their risk of developing a UTI that they are unable to fully eradicate from the urinary tract and surrounding reservoirs.

1.7.5 Efficacy of estrogen treatment of UTIs in postmenopausal women

Many studies have tested the efficacy of estrogen treatment on the incidence of UTIs and rUTIs

in postmenopausal women. Unfortunately, although the beneficial role of estrogen in urinary tract seems clear, clinical studies have failed to fully validate this hypothesis. This ambiguity around the usefulness of estrogen as a therapeutic may arise from differences in the method used to administer estrogen; estrogen can be delivered orally or directly to the vagina using creams, pessaries and rings[7].

Studies investigating the effects of oral estrogen on the prevalence of UTIs in postmenopausal women unanimously concluded that oral estrogen does not reduce the risk of developing a UTI in this population[7,191–193]. One of these trials supplemented postmenopausal women with 3mg of estrogen daily, but no difference in UTI incidence was seen between the estrogen supplemented and the placebo group despite this relatively high dose of estrogen[191].

Vaginal estrogen creams, however, have shown more promising results. A study conducted by Raz & Stamm in 1993 compared the efficacy of estrogen cream versus a placebo cream[190]. The estrogen cream was found to significantly reduce the incidence of UTIs in postmenopausal women compared to the placebo treatment. After four months the cumulative likelihood of being disease free was 0.95 for the women given estrogen cream, compared to 0.30 for those receiving the placebo. Over the course of the study the estrogen treatment group had 12 episodes of bacteriuria, whilst the placebo group suffered from 111 episodes. Furthermore, the estrogen treatment significantly increased the vaginal lactobacilli colonisation and significantly decreased the vaginal pH, compared to the control group. These results are supported by a second study showing that vaginal estrogen cream significantly reduced the incidence of UTIs in postmenopausal women compared to a group receiving oral antibiotics[194].

Other methods of vaginal estrogen application have shown mixed results. One study by Raz *et al.*, found that estrogen application using a vaginal pessary resulted in significantly more UTIs during the study period than a group receiving the antibiotic, oral nitrofurantoin. Furthermore, this method of administering estrogen did not affect the vaginal pH or lactobacilli colonisation[195]. Conversely, a study administering estrogen through a vaginal ring found that estrogen treatment significantly reduced the incidence of UTIs compared to the placebo group[196]. After nine months the cumulative event-free survival was 45% in the estrogen treated group compared to 20% in the control group. This study did not measure the number of women who were positive for lactobacilli in the vagina, but did report a significantly decreased vaginal pH in the estrogen treated group after 12 weeks of treatment. Interestingly, this study also used a lower estrogen dose than the vaginal pessary study, 2mg of estrogen over 12 weeks compared to 0.5mg estrogen given twice weekly. As Raz *et al.* compared estrogen treatment with antibiotic treatment it cannot

be determined whether estrogen, delivered by a vaginal pessary, would have reduced UTI incidence compared to a placebo group.

Taken together, the results from these clinical studies indicate that vaginal, as opposed to oral, estrogen treatment may reduce the occurrence of UTIs in postmenopausal women, with vaginal estrogen creams being particularly promising.

Despite these encouraging findings, two further published papers using ovariectomised mice modelling the menopause have reported contrasting results regarding the effect of estrogen on the susceptibility of mice to UTIs. One study reported that estrogen treatment promoted an ascending UTI, with estrogen treated mice having significantly higher bacterial infection rates in the kidney than non-estrogen treated controls[197]. However, the second study showed that ovariectomised mice had significantly higher quiescent intracellular bacterial reservoirs, which can seed recurrent infections, 14 days after infection than non-ovariectomised controls. This effect, was reversed following estrogen treatment, suggesting that estrogen impairs formation of intracellular bacterial reservoirs[198].

1.8 Hypothesis and aims

Many of the aforementioned studies concentrate on the overall effect of estrogen on UTI incidence in postmenopausal women, focusing particularly on the changes in vaginal pH and lactobacilli colonisation. However, few studies have looked into the effects of estrogen on the innate immune defences in the urinary tract[134,199]. Therefore, the aim of this project was to investigate the roles of estrogen on the innate epithelial immune defences in the vagina in response to *E. coli* infection. Investigations were focused on the vagina as this is a key reservoir of infection. Understanding the mechanisms involved in effective eradication of bacteria from the vagina may prevent progression to UTI. Furthermore, knowledge of the signalling pathways involved in estrogen regulation of innate epithelial immunity may aid in the design of novel therapeutics that exploit this system in postmenopausal women.

Previous work in our laboratory has shown that the AMP hBD2 is increased in vaginal douches of postmenopausal women receiving topical estrogen treatment, compared to postmenopausal women not receiving estrogen treatment[60]. Based on these data, it was hypothesised that estrogen treatment of vaginal epithelial cells will result in increased expression of hBD2 and other AMPs during infection of the urogenital tract.

Therefore, the overarching aim of this project was to investigate the effects of estrogen on the innate epithelial defences of the urogenital tract, with specific focus on AMPs.

More specifically, this project aimed to:

- Investigate the effects of estrogen on the AMPs hBD2 and hBD3, which have been previously studied in the bladder by our group, in vaginal epithelial cells.
- Utilise microarray analyses to identify other components of the innate vaginal epithelial defences that are enhanced by estrogen treatment.
- Examine the signalling pathways involved in estrogen regulation of innate immune defences of vaginal epithelial cells.

2 Materials and methods

2.1 Tissue culture

2.1.1 Vaginal epithelial cell line

The vaginal keratinocyte cell line VK2 E6/E7 was cultured in tissue culture flasks in keratinocyte-SFM (Life Technologies, USA) with 0.1ng/ml epidermal growth factor, 0.05mg/ml bovine pituitary extract and 0.2mM of $CaCl_2$. The cells were incubated at 37°C with 5% CO_2 and passaged once a week when a confluent monolayer was formed. To passage, cells were washed with phosphate-buffered saline (PBS, Sigma, USA) before adding 0.1% trypsin (Sigma, USA) and incubating at 37°C for approximately 10 minutes, or until the cells detached from the flask surface. Trypsin was neutralised by the addition of Dulbecco's Modified Eagle's Medium (DMEM, Life Technologies) containing 10% fetal calf serum (FCS, Life Technologies, USA) at a ratio of 2:1. The cell suspension was centrifuged at 1500rpm for 3 minutes in a MSE Centaur 2 centrifuge, before being resuspended in keratinocyte-SFM and passed through a needle. The Cellometer Auto T4 Cell Viability Counter (Nexcelom, USA) was used to count the cells, before seeding a new T75 cell culture flask (Corning, USA) with $1.5x10^6$ cells. The cells were incubated at 37°C with 5% CO_2 and the medium was replaced every 2-3 days.

2.1.2 Primary vaginal epithelial cell culture

Vaginal biopsy tissue was collected from women undergoing gynaecological surgery at the Royal Victoria Infirmary, Newcastle upon Tyne. Collection and use of biopsy tissue was covered by ethics REC reference number: 2003/11. Tissue was stored in Ham's F12 Nutrient Mix Medium (Life Technologies, USA) with 100U/ml penicillin and 100µg/ml streptomycin (Sigma, USA) and 10% FCS for delivery. Following delivery to the laboratory, the tissue was washed in PBS and any excess connective tissue was removed. The tissue was incubated in PBS with 10% Penicillin/Streptomycin/Amphotericin B (Lonza, USA) and 2mg/ml Dispase II (Sigma-Aldrich, USA) overnight at 4°C to dissociate the epithelial cells from the lamina propria. Epithelial cells were removed using tweezers and the cells were incubated in trypsin for 20 minutes at 37°C with shaking every 5 minutes. The trypsin was neutralised with DMEM containing 10% FCS, and the cell suspension centrifuged at 1200rpm for 5 minutes. The cells were resuspended in EpiLife medium (Life Technologies, USA) or DMEM with 10% FCS, passed through a needle to ensure a single cell suspension and seeded into 6-well plates. The cells were incubated at 37°C with 5% CO_2 and the media was renewed every 2 days.

2.1.3 Cell challenges

Cell challenges with both primary and VK2 cells were performed in either 6- or 12-well plates. VK2 cells were seeded into 6-well plates at densities between $2.5x10^5$ and $3.5x10^5$ cells/well, and 12-well plates at a density of $1x10^5$ cells/well. Primary vaginal epithelial cells were seeded into the wells at the highest density possible from the number of cells harvested. Once the cells reached 80% confluency, the medium was removed, cells were washed with PBS and 1ml of cell culture medium was added to the cells. The cells were incubated at 37°C with 5% CO_2 for 24 hours in this medium.

2.1.3.1 Challenge reagents

The estrogen used for challenges was (2-hydroxypropyl)-β-cyclodextrin encapsulated 17β-estradiol (Sigma, USA) at a final concentration of 4nM. Encapsulation of estrogen in cyclodextrin makes it water-soluble. Initial experiments were carried out using water-treated VK2 cells as the control. However, the effects of cyclodextrin were analysed, and cyclodextrin-treated VK2 cells were used as the control in later experiments. The water-soluble estrogen consisted of 48.3mg 17β-estradiol per gram of solid, thus, 4nM estrogen had a cyclodextrin concentration of 14.8nM. This concentration of cyclodextrin was, therefore, used for experiments where the control was cyclodextrin-treated cells.

The flagellin used was purified by Dr Marcelo Lanz from *E. coli* clinical isolate 3408 from a cystitis patient[106]. Flagellin was resuspended in PBS and cells were challenged with 50ng/ml flagellin (or otherwise stated) or PBS. G-1 and ICI 182,780 were both from Tocris Bioscience, UK, and were resuspended in dimethyl sulfoxide (DMSO) to an initial concentration of 1mM. Human recombinant IL-17A was purchased from Sigma-Aldrich, USA, and was resuspended to an initial concentration of 20μg/ml in 10mM Tris-HCL, pH 7.4 containing 250mM NaCl.

2.1.3.2 Acute estrogen and flagellin challenge

VK2 cells were treated with 4nM 17β-estradiol (Sigma, USA) and 50ng/ml flagellin or PBS. Each of these treatments was performed in triplicate and on three separate occasions. After 0, 8, 12 and 24 hours the medium was removed, the cells washed with PBS and the RNA extracted.

2.1.3.3 Acute estrogen and flagellin dose response challenge

VK2 cells were treated with 4nM 17β-estradiol and flagellin at concentrations of 0.0025, 0.025, 0.25, 2.5, 25 and 50ng/ml, or PBS. Each of these treatments was performed in triplicate and on

two separate occasions. After 24 hours the cells were washed with PBS and the RNA was extracted.

2.1.3.4 Estrogen pretreatment and flagellin challenge

VK2 cells were pretreated with 4nM 17β-estradiol for at least 7 days prior to challenge. The cells were seeded into 6-well plates at a density of $3.5x10^5$ cells/well in keratinocyte-SFM supplemented with 4nM 17β-estradiol and the medium and estrogen were typically replaced every two days. Once the cells reached 80% confluency the cell culture medium was removed, the cells were washed with PBS and 1ml keratinocyte-SFM supplemented with 4nM 17β-estradiol was added to the wells. The cells were incubated in this medium for approximately 24 hours and then challenged with 50ng/ml flagellin, or PBS. After 0, 8, 12 and 24 hours the medium was removed and stored at -80°C for analysis by enzyme-linked immunosorbent assays (ELISA), the cells were washed with PBS and the RNA was extracted. Primary vaginal epithelial cells were pretreated with 4nM 17β-estradiol (4nM) for 5-10 days and then challenged with 50ng/ml flagellin, or PBS. After 24 hours the cells were washed with PBS and the RNA extracted.

2.1.3.5 Cyclodextrin and flagellin challenge

VK2 cells were pretreated with 14.8nM (2-hydroxypropyl)-β-cyclodextrin for 7 days prior to challenge. The cells were seeded into 6-well plates at a density of $3.5x10^5$ cells/well in keratinocyte-SFM supplemented with 14.8nM cyclodextrin and the medium and cyclodextrin were replaced every two days. Once the cells reached 80% confluency the cell culture medium was removed, the cells were washed with PBS and 1ml keratinocyte-SFM supplemented with 14.8nM cyclodextrin was added to the wells. The cells were incubated in this medium for approximately 24 hours before challenge with either 50ng/ml flagellin or PBS. Each of these treatments was performed in triplicate and on two separate occasions. After 24 hours the medium was removed, the cells washed with PBS and the RNA extracted.

2.1.3.6 Fulvestrant and flagellin challenge

VK2 cells were seeded into 12-well plates at a density of $1x10^5$ cells/well in keratinocyte-SFM and were pretreated with either 1μM ICI 182,780 or 0.1% DMSO vehicle, and 4nM 17β-estradiol, or cyclodextrin vehicle, for at least 7 days prior to challenge. The medium, ICI 182,780 and 17β-estradiol were replaced every two days. Once the cells reached 80% confluency the medium was removed, the cells were washed with PBS and 1ml keratinocyte-SFM supplemented with 1μM ICI 182,780 and/or 4nM 17β-estradiol was added to the cells. The cells were incubated

in this medium for approximately 24 hours and then challenged with either 50ng/ml flagellin or PBS. Each of these treatments was performed in triplicate and on three separate occasions. After 24 hours the medium was removed, the cells washed with PBS and the RNA extracted.

2.1.3.7 G1 and flagellin challenge

The cells were seeded into 12-well plates at a density of $1x10^5$ cells/well and were pretreated with either 100nM G1 or 0.01% DMSO vehicle for 1, 5 and 7 days prior to challenge. Once the cells reached 80% confluency the medium was removed, the cells were washed with PBS and 1ml keratinocyte-SFM supplemented with 100nM G1, or 0.01% DMSO, was added to the cells. The cells were incubated in this medium for approximately 24 hours and then challenged with 50ng/ml flagellin, or PBS. Each of these treatments was performed in triplicate and on two separate occasions. After 24 hours the medium was removed, the cells washed with PBS and the RNA extracted.

2.1.3.8 IL-17A dose response challenge

VK2 cells were seeded into 12-well plates at a density of $1x10^5$ cells/well. Once they reached 80% confluency the medium was removed, the cells were washed with PBS and 1ml keratinocyte-SFM medium was added to the cells. The cells were incubated in this medium for 24 hours and then challenged with IL-17A (Sigma, USA) at concentrations of 0.1, 1, 10, 100ng/ml or 100μM Tris-HCL, pH 7.4 with 2.5mM NaCl. Each of these treatments was performed in triplicate and on two separate occasions. After 6 and 24 hours the medium was removed and stored at -80°C, the cells washed with PBS and the RNA extracted.

2.1.3.9 Estrogen and IL-17A challenge

VK2 cells were seeded into 12-well plates at a density of $1x10^5$ cells/well in keratinocyte-SFM and were pretreated with either 4nM 17β-estradiol or 14.8nM cyclodextrin for at least 7 days prior to challenge. The medium, 17β-estradiol and cyclodextrin were replaced every two days. Once the cells reached 80% confluency the medium was removed, the cells were washed with PBS and 1ml keratinocyte-SFM medium was added to the cells. The cells were incubated in this medium for 24 hours and then challenged with 100ng/ml IL-17A (Sigma, USA), or 100μM Tris-HCL, pH 7.4 with 2.5mM NaCl, and 50ng/ml flagellin, or PBS. Each of these treatments was performed in triplicate and on two separate occasions. After 24 hours the medium was removed, the cells washed with PBS and the RNA extracted.

2.1.4 Cell viability assay

To measure the effect of 17β-estradiol, ICI 182,780 and G-1 on the growth rate of VK2 cells the CellTiter-Blue Cell Viability Assay (Promega, USA) was used. CellTiter-Blue Reagent contains highly purified resazurin, which is reduced to resorufin by viable cells. The absorbance maximum of resazurin is at 605nm and that of resorufin is at 573nm, therefore measurement of absorbance at 573 and 605nm determines the amount of reduction of resazurin. The reduction of resazurin to resorufin is directly proportional to the number of viable cells, therefore, the more cells in the well, the larger the absorbance value at 573nm. VK2 cells were seeded into 6- or 12-well plates and were grown under the same conditions as they were for a challenge. Mitomycin C (1μM, Sigma, USA) treated VK2 cells were included as a negative control, as Mitomycin C inhibits DNA replication, preventing cell growth. Medium-only wells (no VK2 cells) were also included to determine background absorbance values. At each time point growth medium was removed from the cells, the cells were washed with PBS, 500 μl keratinocyte-SFM was added to each well and the cells were imaged using the EVOS XL Core Cell Imaging System (ThermoFisher Scientific, UK). 100μl CellTiter-Blue Reagent was added to each well, and the cells were incubated at 37°C for 1 hour. To measure the absorbance, 150μl medium was removed from each well and transferred to a white plastic, clear bottom, Costar Assay Plate, 96 well (Corning, USA) and the absorbance was measured at 573nm and 605nm using the FLUOstar Omega Microplate Reader (BMG Labtech, Germany). To analyse the results the absorbance at 605nm was subtracted from the absorbance at 573nm for each sample. To adjust for the background the results from the medium-only wells was then subtracted.

2.2 RNA extraction

RNA was extracted using the Promega SV Total RNA Extraction Kit (Promega, USA). Lysis buffer was added to each well, the cells were scraped from the well surface and transferred to a microfuge tube. The lysis buffer was passed through a needle and RNA extracted as per the kit instructions. Briefly, the RNA was passed through a Spin Column, washed, DNase treated and eluted into Milli-Q water. The Thermo Scientific Nanodrop 2000 was used to determine the RNA concentration. RNA was stored at -80°C.

2.3 Reverse transcription

RNA was reverse transcribed into cDNA by mixing 1μg of RNA with Milli-Q water to a volume of 25μl. One nanogram of random hexamers (Roche, Switzerland) was added and the reaction

was heated at 65°C for 5 minutes. The RNA was immediately placed on ice for 2 minutes, before adding the following reagents:

10µl	5x Moloney murine leukaemia virus (MMLV) buffer (Promega, UK)
12.5µl	2mM dNTPs (Bioline, UK)
0.5µl	RNase inhibitor (20 units, Promega, UK)
1µl	Reverse transcriptase (100 units, Promega, UK)

The samples were briefly centrifuged, then incubated at 42°C for 2 hours followed by 70°C for 3 minutes. cDNA was stored at -80°C.

2.4 End-point polymerase chain reaction

End-point polymerase chain reaction (PCR) was performed using the following volumes of reagents:

0.4µl	25mM $MgCl_2$ (Bioline, UK)
2µl	10x NH_4 buffer (Bioline, UK)
0.25µl	Taq polymerase (Bioline, UK)
2.5µl	2mM dNTPs (Bioline, UK)
1µl	10µM forward primer
1µl	10µM reverse primer
7.85µl	MQ water
5µl	Sample cDNA
---	---
20µl	Total volume

The samples were briefly centrifuged and PCR was performed under the conditions shown in Table 2.1.

Table 2.1: Cycling conditions used for end-point PCR.

Step	Temperature (°C)	Time (min:sec)	Cycles
Preincubation	95	03:00	1
Denaturation	95	00:30	35
Annealing	Tm	00:30	
Elongation	72	00:30	
Final elongation	72	10:00	1
Final hold	4	∞	

The annealing temperature (Tm) was dependent on the primers used in the reaction and these are detailed in Table 2.2. 18S was used as the housekeeping gene. 18S primers were predesigned by Life Technologies with a product size of 315bp.

Table 2.2: Table of primers used for end-point PCR.

Primer name	Sequence	Accession number	Temperature (Tm, °C)	Product length (bp)
ER Alpha Forward	GGATACGAAAAGACCGAAGAG	NM_001122740.1	58	236
ER Alpha Reverse	GTCTGGTAGGATCATACTCGG			
ER Beta Forward	TAGTGGTCCATCGCCAGTTATCAC	NM_001437.2	55	439
ER Beta Reverse	GCACTTCTCTGTCTCCGCACAA			
GPER Forward	GGCTTTGTGGGCAACATC	NM_001098201.1	58	680
GPER Reverse	CGGAAAGACTGCTTGCAGG			
IL17RA Forward	GTACTGGTTCATCACGGGCA	NM_014339.6	58	132
IL17RA Reverse	AGGCCATCGGTGTATTTGGT			
IL17RC Forward	AAAAACCTGACTGGACCGCA	NM_153461	58	338
IL17RC Reverse	TGGCCTTTCAGCAATGGGAA			
KRT8 Forward	AAGGATGCCAACGCCAAGTT	NM_001256282.1, NM_002273.3, NM_001256293.1	56	190
KRT8 Reverse	TCATGTTCTGCATCCCAGACTC			
KRT18 Forward	CCAGTCTGTGGAGAACGACAT	NM_000224.2, NM_199187.1	56	207
KRT18 Reverse	TCCTGAGATTTGGGGGCATC			

2.5 Gel electrophoresis

To visualise DNA products, the DNA samples were mixed with 10x Loading Buffer (Bioline, UK) in a 9:1 ratio and loaded onto an agarose gel. Agarose gels were prepared using TBE (Tris, Boric acid, EDTA, pH 8) buffer with an agarose content between 1-2%. 5µl of SafeView (NBS Biologicals, UK) was added per 100ml gel. A DNA ladder solution (Bioline, UK or New England Biolabs, USA) was loaded onto the gel and the gel electrophoresed at 60-100V for 60-90 minutes. The gel was viewed using the Bio Rad Gel Doc EZ Imager and Image Lab 4.0 software.

2.6 Gel extraction

To extract DNA products from the gel the bands were excised using a scalpel and the QIAquick Gel Extraction Kit (Qiagen, Germany) was used to isolate the DNA. The kit was used as per the manufacturers protocol. Briefly, the agarose gel was dissolved in binding buffer, the DNA was passed through a Spin Column, washed and eluted in Milli-Q water.

2.7 Quantitative PCR

Quantitative PCR (qPCR) was performed using both probe-based and SYBR-green-based assays. A probe-based assay was initially developed for measuring the expression of hBD2. However, this assay was not sensitive for measuring low level gene expression and thus a SYBR-green-based assay was developed to measure hBD2 expression. The expression of all other genes was measured solely by SYBR-green-based qPCR assay.

2.7.1 Probe-based qPCR assay

Probes-based qPCR involves a DNA probe, consisting of a fluorescent reporter and a quencher, which binds to a specific target sequence of the cDNA during the annealing step of the qPCR reaction (Figure 2.1). During the elongation step the probe is displaced from the target DNA, cleaving the fluorescent reporter from the quencher and resulting in fluorescence being emitted. Thus, fluorescence levels are proportional to the amount of probe-specific target cDNA within a sample. This differs from SYBR-green, which is not target specific and simply detects all double-stranded DNA within a sample.

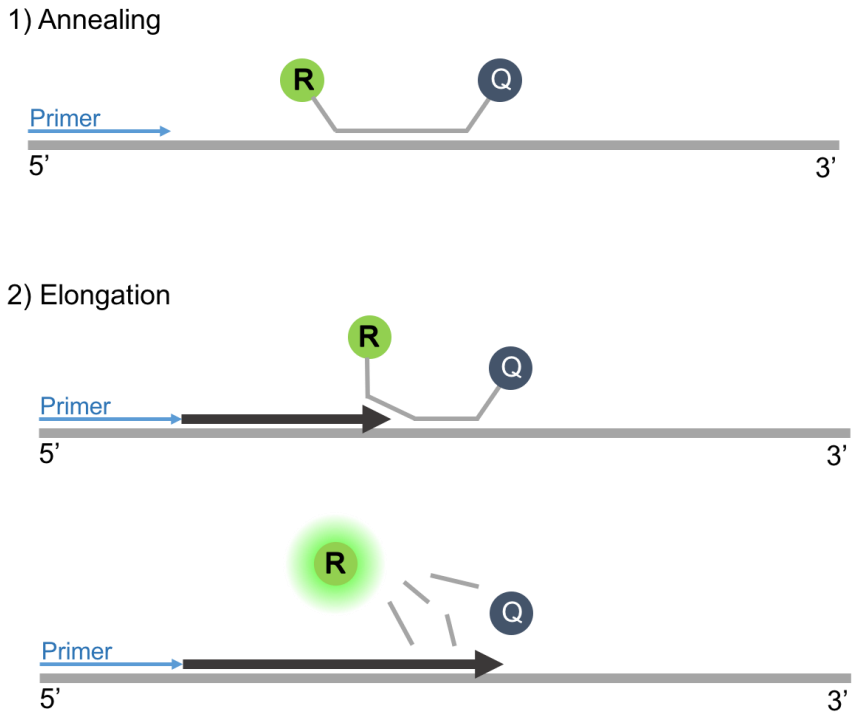

Figure 2.1: Mechanism of probes-based qPCR. During the annealing step a DNA probe, consisting of a fluorescent reporter (R) and a quencher (Q), binds to a specific sequence in the target gene cDNA. During elongation of the PCR product, the probe is displaced and the reporter is cleaved from the quencher. Release of the reporter from the quencher produces a fluorescent signal.

Probe-based qPCR was performed by adding the following volumes of reagents into each well of a white 96-well PCR microplate (Starlab, UK):

5µl	Lightcycler 480 Probes Master (Roche, Switzerland)
0.5µl	5µM primer mix (Integrated DNA Technologies, USA)
2µl	Milli-Q water
2.5µl	Sample cDNA
---	---
10µl	Total volume

The probe-based hBD2 primers for the DEFB4A gene were predesigned by Integrated DNA Technologies and the sequences are shown in Table 2.3.

Table 2.3: Table of probe-based primers.

Gene	Forward primer	Reverse primer	Product length (bp)
DEFB4A	CGCCTATACCACCAAAAACAC	TCCTGGTGAAGCTCCCA	106

After addition of each of the reagents the plate was sealed with StarSeal Advanced Polyolefin Film (Starlab, UK) and the plate was briefly centrifuged in a MPS 1000 Mini PCR Plate Spinner (Labnet, USA). The plate was loaded into the Lightcycler 480 Instrument II (Roche, Switzerland) and qPCR performed as per the cycling conditions shown in Table 2.4.

Table 2.4: Cycling conditions for probe-based qPCR assay.

Step	Temperature (°C)	Time (min:sec)	Cycles
Preincubation	95	05:00	1
Denaturation	95	00:10	45
Annealing	60	00:30	
Elongation	72	00:01	

2.7.2 SYBR-green based qPCR

SYBR-green-based qPCR assays utilise the fluorescent dye SYBR Green I, which binds to all double-stranded DNA and fluoresces. Therefore, the amount of fluorescence emitted is directly proportional to the amount of amplified cDNA in the sample.

SYBR-green based qPCR was prepared by adding the following volumes of reagents into each well of a white 96-well PCR microplate (Starlab, UK):

5µl Lightcycler 480 SYBR Green I Master (Roche, Switzerland)
0.5µl Forward primer
0.5µl Reverse primer
1.5µl Milli-Q water
2.5µl Sample cDNA

10µl Total volume

SYBR-green-based qPCR primers were designed to be approximately 20 base pairs long, have a melting temperature between 55°C and 60°C, have a GC content of roughly 50% and produce a product size of approximately 100 base pairs. Where possible the primers were also designed to span an exon-exon junction to prevent amplification of genomic DNA. The primers used for SYBR-green-based qPCR are detailed in Table 2.5. GAPDH and ATP5B were selected as housekeeping genes following geNorm analysis performed by Dr Ased Ali[60]. The primers for

GAPDH and ATP5B were predesigned by Primerdesign, UK, and the sequences were not provided.

Table 2.5: Table of primers used for qPCR.

Primer name	Sequence	Accession number	Temperature (Tm, °C)	Product length (bp)
hBD2 Forward	CAGCCATCAGCCATGAGGGT	NM_004942.2	58	83
hBD2 Reverse	CCACCAAAAACACCTGGAAGAGG			
hBD3 Forward	GTGAAGCCTAGCAGCTATGAG	NM_018661.4	60	89
hBD3 Reverse	TGATTCCTCCATGACCTGGAA			
LCN2 Forward	CAAAGACCCGCAAAAGATGT	NM_005564.4	58	128
LCN2 Reverse	GGCAACCTGGAAGAAAAGTC			
RNase 7 Forward	TGACAGCCTAGGAGTGCGT	NM_032572.3	56	83
RNase 7 Reverse	CAGGGGTCGCTTTGCG			
S100A7 Forward	ACACCAGACGTGATGACAAG	NM_002963.3	58	114
S100A7 Reverse	CATCGGCGAGGTAATTTGTG			

After addition of each of the reagents the plate was sealed with StarSeal Advanced Polyolefin Film (Starlab, UK) and the plate was briefly centrifuged in a MPS 1000 Mini PCR Plate Spinner (Labnet, USA). The plate was loaded into the Lightcycler 480 Instrument II (Roche, Switzerland) and qPCR performed as per the cycling conditions shown in Table 2.6.

Table 2.6: Cycling conditions for qPCR assays.

Gene	Step	Temperature (°C)	Time (min:sec)	Cycles
GAPDH, ATP5B	Preincubation	95	10:00	1
	Denaturation	95	00:15	45
	Annealing	60	00:30	
	Elongation	72	00:01	
DEFB103A, DEFB4A, RNASE7, S100A7	Preincubation	95	10:00	1
	Denaturation	95	00:20	45
	Annealing	Tm	00:30	
	Elongation	72	00:20	
LCN2	Preincubation	95	10:00	1
	Denaturation	95	00:10	45
	Annealing	Tm	00:20	
	Elongation	72	00:20	

After each run the results were analysed to calculate the concentration of target cDNA in each sample by comparison with a positive control plasmid. The melt curve of each sample was also analysed to confirm amplification of a single DNA product.

2.7.3 Cloning of qPCR positive control plasmids

To determine the relative concentration of cDNA in each sample when using qPCR, positive control plasmids were produced for each qPCR assay. Positive control plasmids had already been made for GAPDH, ATP5B, by Dr Ased Ali, and for hBD2 by Dr Marcelo Lanz[60,106]. To obtain the appropriate PCR product, end-point PCR was performed as outlined in section 2.4 using the qPCR primers shown in Table 2.5. The product was gel electrophoresed and the DNA extracted from the gel as outlined in sections 2.5 and 2.6. The PCR product was cloned into the pGEM-T Easy Vector using the pGEM-T Easy Vector System I (Promega, USA) as per the manufacturer's instructions. Briefly, the PCR product was ligated into the vector, transformed into JM109 competent cells, and plated out onto LB plates containing 100μg/ml ampicillin with 100mM IPTG and 50mg/ml X-GAL for blue/white colony selection. The plates were incubated overnight at 37°C and growth of white colonies indicated successful integration of the PCR product into the vector. White colonies were picked and used to inoculate 5mls LB/ampicillin broth, which was incubated overnight at 37°C with shaking at 200rpm in an Incu-Shake TL6-5R rotary shaker (SciQuip, UK). After overnight incubation the plasmid was isolated from the cultures using the PureYield Plasmid Miniprep System (Promega, USA). The isolation was carried out as per the manufacturer's instructions, and consisted of pelleting the cultures, lysing the bacteria, pelleting the cell debris and proteins, passing the supernatant containing the DNA through a Spin Column, washing, and finally eluting into Milli-Q water. The purified plasmid DNA was serially diluted and qPCR was performed on each dilution to produce a standard curve.

Positive control plasmids and standard curves were produced using such protocols for DEFB4A, LCN2, RNASE7, and S100A7.

2.7.4 qPCR data analysis

The qPCR results for each gene were analysed using the standard curve method, relative to the geometric mean of the two housekeeping genes, GAPDH and ATP5B.

2.8 Protein analysis by enzyme-linked immunosorbent assay

Sandwich ELISAs were used to measure the concentration of peptides secreted into the cell culture medium after challenge. In this type of ELISA a capture antibody was attached to the plastic bottom of a 96-well plate. The wells were blocked, samples were bound and a detection antibody was added, which bound to any protein bound to the capture antibody. Typically, the detection antibody is biotin labelled and binds to streptavidin conjugated to horseradish

peroxidase (HRPO). A substrate was added to the well, which reacted with HRPO to cause a colour change in the well proportional to the amount of protein bound to the capture antibody.

The ELISA for hBD2 was performed using the Human Beta-Defensin-2 (BD-2) ELISA Development Kit (Leinco Technologies, USA). The ELISA for LCN2 was performed using the Human Lipocalin-2/NGAL DuoSet ELISA Kit (R&D Systems, USA). Each of these kits contained capture antibody, detection antibody, standards and HRPO. No ELISA kit for hBD3 was available, therefore, the ELISA method for hBD3 was developed and optimised by Dr Catherine Mowbray. The concentrations of reagents used for each assay is shown in Table 2.7.

Table 2.7: Reagents used for hBD2, hBD3 and LCN2 ELISAs.

	hBD2	**hBD3**	**LCN2**
Kit name	Human Beta-Defensin-2 (BD-2) ELISA Development Kit		Human Lipocalin-2/NGAL DuoSet ELISA Kit
Supplier	Leinco Technologies		R&D Systems
Wash buffer	0.05% Tween 20 in PBS	0.05% Tween 20 in PBS	0.05% Tween 20 in PBS
Blocking buffer	1% BSA in PBS	1% BSA in PBS	1% BSA in PBS
Diluent	0.05% Tween 20, 0.1% BSA in PBS	1% BSA in PBS	1% BSA in PBS
Capture antibody	0.5µg/ml	ab109572 (Abcam) 0.25µg/ml	0.25µg/ml
Standard	7.8125-2000pg/ml	4382-s (Peptide Institute) 7.8125-1000pg/ml	19.5313-5000pg/ml
Detection antibody	0.5µg/ml	ab84234 (Abcam) 1µg/ml	25ng/ml
HRPO	1:2000	Ultra Streptavidin-HRPO (Life Technologies) 1:400	1:200
Substrate solution	ABTS Liquid Substrate Solution (Leinco Technologies)	1-Step Ultra-TMB ELISA Substrate Solution (Life Technologies)	Substrate Reagent (R&D Systems)

To perform the ELISAs the capture antibody was diluted to the required concentration in PBS and 100µl was added to each well of a Nunc-Immuno Microwell 96 well plate (Sigma, USA). The plate was sealed (ELISA Plate Sealers, R&D Systems, USA) and incubated overnight at room temperature. The wells were aspirated to remove the antibody and washed four times with 300µl wash buffer. 300µl blocking buffer was added to each well, the plate sealed and incubated at room temperature for 1 hour. The wells were aspirated and washed 4 times with wash buffer. The standard was serially diluted 1:2 in diluent and 100µl of each standard added to the plate in duplicate. 100µl of each sample was added to the plate in duplicate. 100µl of diluent only was added to two wells of the plate as a blank. The plate was sealed and incubated for 2 hours at room temperature. The wells were aspirated and washed 4 times with wash buffer. The detection antibody was diluted to the specified concentration in diluent and 50µl added to each well of the

plate. The plate was sealed and incubated for 2 hours at room temperature. The wells were then aspirated and washed 4 times with wash buffer. HRPO was diluted to the required concentration in diluent and 100µl added to each well. The plate was sealed and incubated for 30 minutes at room temperature in the dark. The wells were aspirated and washed 4 times with wash buffer. 100µl substrate solution was added to each well and the plate was sealed and incubated for 20 minutes at room temperature in the dark. 50µl of 1M sulphuric acid was added to each well to stop the reaction. Absorbance was measured at 450nm with wavelength correction at 540nm using the FLUOstar Omega Microplate Reader (BMG Labtech, Germany). A standard curve was produced using 4-parameter fit to analyse the data and the concentrations of the samples was determined.

2.9 Whole transcriptome analysis by microarray

Microarray analysis was performed to identify other potential genes regulated by estrogen and to help determine signalling pathways. VK2 cells that were pretreated with 4nM estrogen for seven days followed by 50ng/ml flagellin challenge were analysed by microarray. The 12 and 24 hour samples of control, estrogen pretreatment, flagellin, and estrogen pretreatment plus flagellin challenged VK2 cells were selected for analysis. Three technical replicates of each treatment were analysed, totalling 24 samples. Samples to be analysed were shipped on dry ice to Service XS, The Netherlands, who performed RNA quality analysis and carried out the microarray experiments.

2.9.1 RNA quality analysis

Samples used for microarray analysis must be high quality in order to obtain reliable results. Service XS confirmed that the RNA samples were high quality using the Agilent RNA 6000 Nano Kit and the Agilent 2100 Bioanalyser. The kit analyses the 18S and 28S RNA and calculates an RNA integrity number (RIN) between 0 and 10. A RIN above 7 is considered good quality. All RNA samples analysed by Service XS had a RIN of 10 and thus could proceed to microarray analysis.

2.9.2 Microarray experiments

Microarrays are useful as they allow analysis of global gene expression changes. This type of analysis is not feasible using qPCR. A microarray consists of a chip with thousands of oligonucleotides, known as probes, attached. These probes will have a nucleotide sequence specific for a given gene and are in a known location on the chip. After exposing cells to a specific treatment, the mRNA is extracted and reverse transcribed into cDNA. This cDNA is

then labelled with a fluorescent tag before being added to the chip. During the hybridisation step the labelled cDNA binds to the complementary probes on the chip and any unbound cDNA is subsequently washed off. The fluorescence level of each probe can then be measured to determine the level of mRNA of each gene in the sample; as it is the cDNA that is fluorescently labelled and not the probe, a probe will only emit fluorescence if cDNA has bound. Binding of cDNA to a probe indicates expression of that gene in the sample. Multiple identical probes are grouped into 'spots' on the chip, and each spot represents a single gene (see Figure 2.2). Therefore, increased mRNA of a particular in a sample will result in a higher fluorescent readout for that spot. To ensure accurate detection of the cDNA some genes are represented by more than one set of probes.

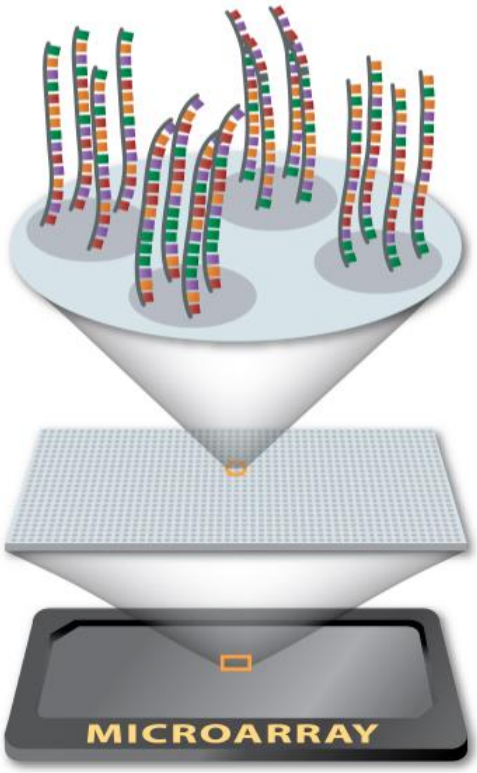

Figure 2.2: Diagram showing multiple identical probes within each spot on a microarray chip[200].

Microarrays were carried out using the Illumina HumanHT-12 v4 Expression Beadchip (Illumina, USA) for each of the 24 samples sent. The HumanHT-12 v4 chip measures the expression of 31,000 genes based upon the NCBI RefSeq Release 38 using 50mer probes bound to silica beads.

2.9.3 Analysis of microarray data

Raw expression data was received from Service XS and analysed in collaboration with the Bioinformatics Support Unit, Newcastle University. The raw data was analysed in R using Bioconductor using lumi (Methods for Illumina Microarrays) and limma (Linear Models for

Microarray Data) packages. The raw data was normalised to the housekeeping genes and converted to fold change relative to the control. A fold change in gene expression was considered significant if it had a fold change or + or -2 and a p-value <0.05. Venn diagrams were produced using the BioVenn software[201]. Lists of differentially expressed genes were uploaded to Ingenuity Pathway Analysis (Qiagen, USA) for pathway analysis.

2.10 Construction of reporter plasmids

To analyse the regulation of hBD2 and hBD3 by ER-α and –β, a hBD2 promoter reporter plasmid was constructed and an attempt was made to construct a hBD3 promoter reporter plasmid.

2.10.1 hBD2 reporter plasmid

The hBD2 promoter reporter plasmid (phBD-2-luc) was constructed by Dr Marcelo Lanz[106]. The plasmid contained the 2000bp hBD2 promoter region upstream of the luciferase gene (Figure 2.3).

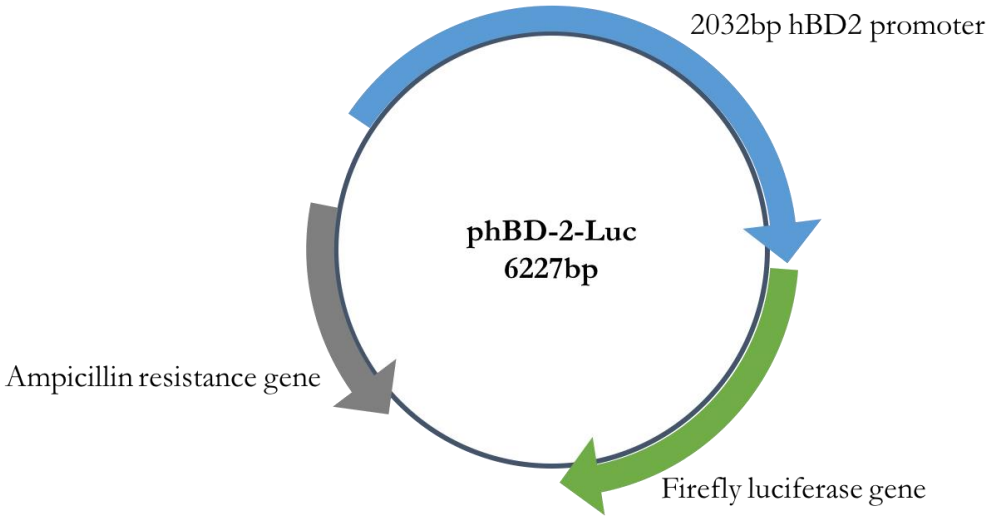

Figure 2.3: Diagram of phBD-2-Luc engineered by Dr Marcelo Lanz[106].

Analysis of the 2000bp promoter region of hBD2 using PROMO revealed six EREs in the promoter, which are transcription factor binding sites for the classical estrogen receptors ER-α and –β. Each of these EREs was mutated, in turn, by site-directed mutagenesis in collaboration with Tom Powell (MRes student, 2014) using the QuikChange II site-directed mutagenesis kit (Agilent, USA) to produce six mutant hBD2 promoter reporter plasmids. Briefly, to perform the site-directed mutagenesis mutant strand synthesis was performed by end-point PCR using the

primers detailed in Table 2.8. The parental DNA was digested using the restriction enzyme DpnI and the mutant DNA was transformed into XL10-Gold Ultracompetent Cells (Agilent, USA) and plated out onto LB/ampicillin agar plates. Colonies were picked and inoculated into 5mls LB/ampicillin broth and incubated overnight at 37°C with shaking at 200rpm in an Incu-Shake TL6-5R rotary shaker (SciQuip, UK). Plasmid DNA was isolated using the PureYield Plasmid Miniprep System (Promega, USA) and sequenced to confirm successful mutagenesis (Genevision, UK).

Table 2.8: Table of primers used for site-directed mutagenesis of hBD2 promoter plasmid. The ERE site mutated at 2 or 3 base pairs is shown in red.

Primer	Sequence	Tm (°C)
ERE1 forward	GACATGTGCATGGTGAGG**CAAATTAT**CAGCAGCAAGTGAGAGCT	78.9
ERE1 reverse	AGCTCTCACTTGCTGCTG**ATAATTTG**CCTCACCATGCACATGTC	
ERE2 forward	TAGCAGTTCTGACAGCAT**CTATCTCA**GCCCTCTCTTTGCATACC	78.9
ERE2 reverse	GGTATGCAAAGAGAGGGC**TGAGATAG**ATGCTGTCAGAACTGCTA	
ERE3 forward	GATAGGAGTGTGAAACTAAT**TTGACCAA**CATGGCAAAACCCC	78.4
ERE3 reverse	GGGGTTTTGCCATG**TTGGTCAA**ATTAGTTTCACACTCCTATC	
ERE4 forward	GTCAAATTGGTCTCACACTC**CTATCTTC**ATGTGATCCACCTGCCT	79
ERE4 reverse	AGGCAGGTGGATCACAT**GAAGATAG**GAGTGTGAGACCAATTTGAC	
ERE5 forward	GGGTTCTTCAGAACCTGACATTTTAAATGAA**GAAATTAG**GCAGGTCATGAGGAA	79.4
ERE5 reverse	TTCCTCATGACCTGC**CTAATTTC**TTCATTTAAAATGTCAGGTTCTGAAGAACCC	
ERE6 forward	ATTTTAAATGAAGAGGTCAGG**CAAATTAT**GAGGAAAGCCTCATTGTCCCC	78.4
ERE6 reverse	GGGGACAATGAGGCTTTCCTC**ATAATTTG**CCTGACCTCTTCATTTAAAAT	

2.10.2 hBD3 reporter plasmid

An attempt was made to construct a hBD3 promoter reporter plasmid in order to examine the role of ER-α and –β in hBD3 expression.

2.10.2.1 End-point PCR using KOD polymerase

End-point PCR was performed on genomic DNA (extracted from vaginal tissue by Dr Catherine Mowbray) using primers detailed in Table 2.9 using KOD polymerase (Merck Millipore, Germany). KOD polymerase is a high fidelity proofreading polymerase that accurately replicates the template DNA without introducing errors. The end-point PCR reaction was set up with the following volumes of reagents:

2.5µl 10x PCR buffer for KOD polymerase

1.5µl 25mM $MgSO_4$

2.5µl 2mM dNTPs

0.5µl KOD polymerase

0.75µl 10µM Forward primer

0.75µl 10µM Reverse primer

14.5µl Milli-Q water

2µl Template DNA

25µl Total volume

The primers were designed to include a restriction enzyme binding site sequence and are detailed in Table 2.9. The reactions were briefly centrifuged and PCR was performed as shown in Table 2.10. The PCR product was gel electrophoresed and the product was extracted from the gel as detailed in sections 2.5 and 2.6.

Table 2.9: Table of hBD3 promoter region cloning primers. The restriction binding site is shown in red.

Primer name	Sequence	Restriction site	Temperature (Tm, °C)	Product length (bp)
Forward primers				
hBD3 promoter 500bp forward	GCGC**GAGCTC**GTAATCATGCCACTGCACTC	SacI	58	513
hBD3 promoter 1KB forward	GCGC**GGTACC**GTCAACCAAATACAACCCATC	KpnI	56	1258
hBD3 promoter 2KB forward	GCGC**GGTACC**CGGATTTTGTGTGTCTGGAG	KpnI	56	2189
Reverse primer				
hBD3 promoter reverse	GCGC**TTCGAA**GAACACACCCACTCACTCAG	HindIII		

Table 2.10: Table of PCR cycling conditions for end-point PCR with KOD polymerase.

Step	Temperature (°C)	Time (min:sec)	Cycles
Preincubation	95	02:00	1
Denaturation	95	00:20	35
Annealing	Tm	00:10	
Elongation	70	01:20	
Final elongation	72	10:00	1
Final hold	4	∞	

2.10.2.2 Restriction digest

To clone the hBD3 promoter region into the pGL4.10[luc2] vector (Promega, USA) restriction digests were performed on the PCR products and pGL4.10. The pGL4.10 vector is shown in

Figure 2.4 and contains the *luc2* luciferase gene downstream of a multiple cloning site and the ampicillin resistance gene.

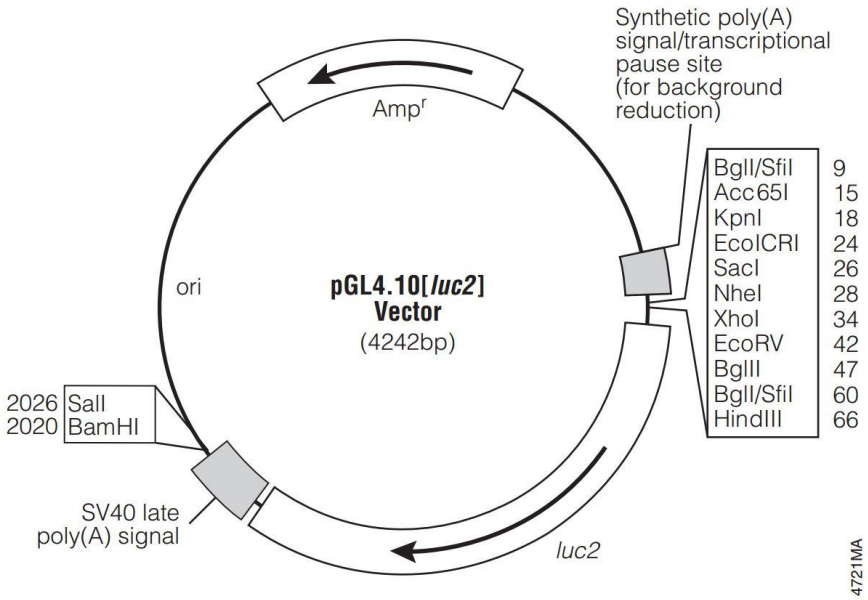

Figure 2.4: Diagram of pGL4.10 Vector (Promega, USA).

Single and double restriction digests were set up with the following volumes of reagents (all from Promega, USA):

pGL4.10 single digest:		pGL4.10 double digest:		Insert double digest:	
3µl	10x Buffer E	3µl	10x Buffer E	3µl	10x Buffer E
3µl	BSA (1µg/µl)	3µl	BSA (1µg/µl)	3µl	BSA (1µg/µl)
1.5µl	SacI	1.5µl	SacI	1.5µl	SacI
1.5µl	pGL4.10 (1µg/µl)	1.5µl	HindIII	1.5µl	HindIII
21µl	Milli-Q water	1.5µl	pGL4.10 (1µg/µl)	10µl	Insert DNA
---	---	19.5µl	Milli-Q water	11µl	Milli-Q water
30µl	Total volume	---	---	---	---
		30µl	Total volume	30µl	Total volume

Digestion reactions were incubated at 37°C for up to 5 hours and then heat inactivated at 65°C for 15 minutes. The reactions were gel electrophoresed and the digested DNA products were extracted from the gel.

2.10.2.3 Ligation reaction

Ligation reactions were performed in order to introduce the hBD3 promoter fragment into the pGL4.10 vector. Ligation reactions, including controls, were set up as shown in Table 2.11.

Table 2.11: Table of ligation reactions and reagents.

Reaction	**Vector + insert + ligase**	**Vector + ligase**	**Vector only**	**Uncut vector**	**Single digest vector + ligase**
Reason	Cloning reaction	Quantifies vector recircularisation	Quantifies undigested vector	Verifies transformation	Verifies ligation reaction
10x Ligase Buffer (Promega, USA)	1µl	1µl	1µl	1µl	1µl
DNA Ligase (Promega, USA)	1µl	1µl			1µl
Double digested vector	1µl	1µl	1µl		
Single digested vector					1µl
Uncut vector				1µl	
Double digested insert	1µl				
Milli-Q water	6µl	7µl	8µl	8µl	7µl
Total volume	10µl	10µl	10µl	10µl	10µl

The ligation reactions were incubated overnight at 4°C and transformed the following day.

2.10.2.4 Transformation

The ligation reactions were transformed into Subcloning Efficiency DH5α Competent Cells (Invitrogen, USA) as per the manufacturers protocol. Briefly, 25µl of DH5α cells were gently mixed with 5µl of ligation reaction and incubated on ice for 30 minutes. The cells were heat shocked at 42°C for 20 seconds, returned to ice for 2 minutes, mixed with 950µl LB medium and incubated for 1.5 hours at 37°C with shaking at 200rpm in an Incu-Shake TL6-5R rotary shaker (SciQuip, UK). The transformation cultures were plated onto LB plates containing 100µg/ml ampicillin and incubated overnight at 37°C to allow colony growth.

2.10.2.5 Colony PCR

Colonies that grew on the LB/ampicillin plates were picked using a pipette tip, streaked onto a fresh LB/ampicillin plate, and then transferred into a PCR tube containing the following reagents:

2.5µl 10x PCR buffer for KOD polymerase

1.5µl 25mM $MgSO_4$

2.5µl 2mM dNTPs

0.5µl KOD polymerase

0.75µl 10µM Forward primer

0.75µl 10µM Reverse primer

16.5µl Milli-Q water

25µl Total volume

PCR was performed using the cycling conditions described in section 2.10.2.1. PCR products were gel electrophoresed, extracted from the gel and sent for sequencing (Genevision, UK) to determine whether the hBD3 promoter region was present in the vector.

2.11 Transient transfection of VK2 cells

To determine the role of each of the EREs in the hBD2 promoter region, the WT hBD2 promoter plasmid and the six mutant plasmids were transiently transfected into VK2 cells. The transfection reaction was optimised for VK2 cells.

2.11.1 Transfection optimisation

The transfection reaction was optimised to establish which conditions resulted in maximum transfection efficiency. For this, the reporter plasmid pGL4.51 (Promega, USA) was used. This reporter plasmid consists of a cytomegalovirus (CMV) promoter upstream of the *luc2* gene. Thus, this plasmid constitutively produced luciferase after transfection. The Attractene transfection reagent (Qiagen, USA) was used to transfect VK2 cells as it exhibits very low cytotoxicity. Attractene is a lipid based transfection reagent, which incorporates DNA into liposomes that then fuse with the cell membrane, introducing the DNA into the cell.

To optimise the transection, 0-0.8µl of Attractene and 150-250ng pGL4.51 DNA was mixed with keratinocyte-SFM without BPE, EGF and $CaCl_2$, to a final volume of 50µl and incubated at room temperature for approximately 30 minutes while the cells were prepared. VK2 cells were trypsinised, centrifuged, counted and seeded into a white plastic, clear bottomed Costar Assay 96 well plate (Corning, USA) at a density of $5x10^4$ cells/well in 150µl keratinocyte-SFM medium. 50µl Attractene/DNA/medium mix was added to each well and the cells were incubated with the

transfection reagents for 18 hours at 37°C. After this time the medium was removed from each well, the cells were washed twice with PBS and 20µl Reporter Lysis 5x Buffer (Promega, USA) was added to each well. Air bubbles in the lysis buffer were removed using a needle and the 96-well plate was incubated at -80°C overnight. Luciferase levels were measured using the Luciferase Assay System (Promega, USA) and the FLUOstar Omega Microplate Reader (BMG Labtech, Germany) as detailed in section 2.11.2.

Transfection optimisation determined 0.5µl of Attractene and 150ng DNA to be the optimum transfection conditions.

2.11.2 Luciferase assay

The Luciferase Assay System (Promega, USA) was used to measure luciferase levels in each well after transfection with a reporter plasmid. The 96-well plate was removed from the -80°C freezer and was defrosted at room temperature for at least one hour. The Luciferase Assay Buffer (Promega, USA) was defrosted and added to the Luciferase Assay Substrate. The 96-well plate and the Luciferase Assay Substrate were placed inside the FLUOstar Omega Microplate Reader (BMG Labtech, Germany), which automatically injected 100µl substrate into each well of the 96-well plate before measuring the luminescence.

2.11.3 Transient transfection of hBD2 reporter plasmid

To determine the effect of estrogen on hBD2 expression, either untreated VK2 cells or VK2 cells pretreated with estrogen for 7 days were transfected with either the hBD-2-luc plasmid or one of the hBD-2-luc ERE mutant plasmids. 0.5µl of Attractene Transfection Reagent was mixed with 150ng plasmid DNA and made up to 50µl total volume with keratinocyte-SFM without BPE, EGF and $CaCl_2$. The Attractene/DNA/medium mixture was incubated for approximately 30 minutes at room temperature to allow complex formation while the VK2 cells were prepared. The VK2 cells were trypsinised, centrifuged, resuspended, counted and seeded into a white plastic, clear bottomed 96-well plate at a density of $5x10^4$ cells/well in 150µl keratinocyte-SFM supplemented with 4nM 17β-estradiol or 14.8nM cyclodextrin. 50µl Attractene/DNA/medium mix was added to each well and the cells were incubated for 18 hours at 37°C to allow the cells to adhere to the bottom of the well and incorporate the plasmid DNA. After 18 hours the medium was removed the cells were washed with PBS and 200µl fresh keratinocyte-SFM supplemented with estrogen or cyclodextrin was added to each well and the cells were incubated for another 24 hours at 37°C. The cells were challenged with either 50ng/ml flagellin (clinical isolate 3408) or PBS for 24 hours. After 24 hours the medium was removed, the cells were washed with PBS and

20µl of Reporter Lysis 5x Buffer (Promega, USA) was added to each well. Air bubbles were removed with a needle and the plate was incubated at -80°C overnight. Luminescence levels were determined using the Luciferase Assay System (Promega, USA) as detailed in section 2.11.2.

2.12 Statistical analysis

Statistical analysis was performed using GraphPad Prism 6 software (GraphPad Software, USA). Following data analysis by one- or two-way ANOVA multiple comparisons were performed using Dunnet's, Sidak's or Tukey's post hoc tests. Dunnett's post hoc test compares each of the treatment means to a single control mean. Sidak's post hoc test performs pairwise comparisons between two treatment means. Tukey's post hoc test compares each treatment mean to every other treatment mean.

3 Effects of estrogen on hBD2 and hBD3 expression

3.1 Introduction

Approximately 50% of postmenopausal women develop a recurrent infection after an initial UTI[13]. This risk is double that of premenopausal women. As circulating estrogen is depleted after the menopause, this suggests a role for estrogen in protecting against UTIs. Topical vaginal estrogen treatment is used to treat vaginal atrophy in postmenopausal women and has also been shown to reduce the incidence of rUTIs in this population[190,194]. The vagina is a key reservoir of UPEC colonisation in women and clearance of pathogenic bacteria from this reservoir helps prevent progression to UTI.

In healthy premenopausal women the vaginal epithelium consists of stratified squamous epithelial cells. This means there are multiple layers of thin, flat cells that sit on top of the lamina propria – a layer of connective tissue. The vaginal epithelium is also keratinised, whereby the outer epithelial cells terminally differentiate into cornified cells that lose their nuclei and other organelles and are filled with keratin filaments, making the cells hardened and resistant to mechanical stress (see Figure 3.1). The outer membrane of these cells is replaced with a cornified envelope covalently cross-linked to the keratin filaments. This keratinised outer layer protects the underlying epithelial cells[202]. The keratinised cells are also known as superficial cells and this layer is termed the *stratum corneum*. It is estimated that the outermost layer of the *stratum corneum* is lost every 4 hours[203]. This sloughing of cells removes any attached pathogens from the vagina, but also releases glycogen into the vaginal lumen, which is utilised by lactobacilli to produce lactic acid and maintain the vaginal pH.

In postmenopausal women vaginal atrophy occurs, which is thinning of the vaginal epithelium due to loss of the superficial epithelial cells. In addition, estrogen depletion results in reduced vaginal glycogen and consequently, reduced lactobacilli colonisation and a higher vaginal pH. These conditions facilitate vaginal colonisation by UPEC. UPEC in the vagina can readily infect the urinary tract, due to the proximity of the urethra to the vagina, and cause repeated UTIs.

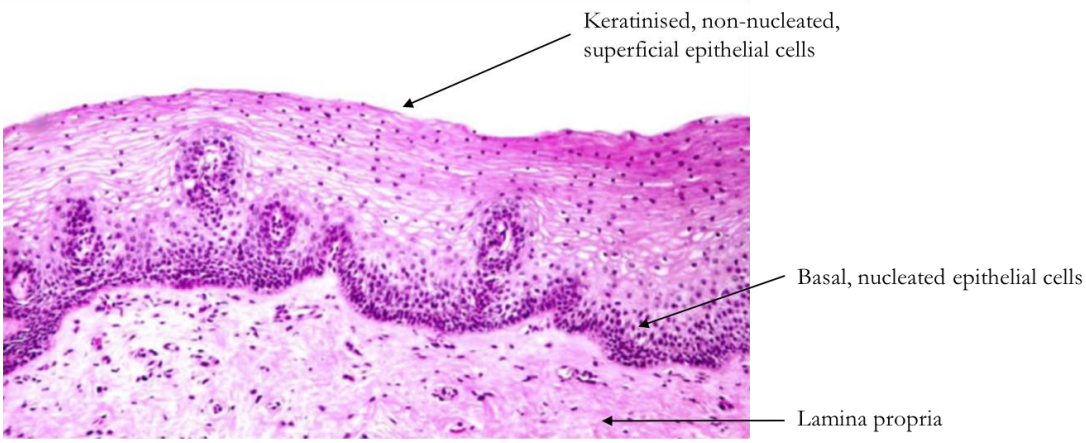

Figure 3.1: Diagram of the stratified squamous vaginal epithelium. Multiple layers of stratified squamous epithelial cells sit on top of the lamina propria – a layer of connective tissue. The outermost epithelial cells lose their nuclei and become filled with keratin, creating a hardened outer layer. Figure adapted from ref 204.

Studies investigating the roles of estrogen in UTIs have predominantly focused on the ability of estrogen to increase vaginal glycogen levels, which promotes growth of *Lactobacillus* spp. and lowers vaginal pH. However, very few studies have examined the effect of estrogen on the innate immune defences of the urogenital tract.

AMPs are a vital component of the innate immune system, especially at epithelial surfaces. AMPs have been demonstrated to be important in protecting the urogenital tract from infection. Previous work from our laboratory has investigated the AMPs hBD2 and hBD3 and has shown that the vaginal concentration of these peptides increases in postmenopausal women receiving topical estrogen treatment, compared with non-estrogen treated postmenopausal women[60]. These data suggest that estrogen may also have roles in enhancing the innate immunity to UPEC. Following on from previous work in our laboratory, the initial investigations of this thesis, which are reported in this chapter, focused on the effect of estrogen on the AMPs hBD2 and hBD3 in the vaginal epithelium.

3.2 VK2 cells express estrogen receptors

It was of interest to study the effects of estrogen on vaginal AMP expression, as effective clearance of UPEC from the vagina is thought to prevent progression to UTI. To model the vaginal epithelium *in vitro* the VK2 E6/E7 (VK2) cell line was used. This is an immortalised human vaginal epithelial cell line. To determine estrogen receptor expression in VK2 cells, end-point PCR was performed for each of the receptors (ER-α, ER-β, and GPER). PCR was performed on cDNA extracted from untreated VK2 cells, and products representing ER-α, ER-β, and GPER were detected at 236bp, 439bp, and 680bp, respectively (Figure 3.2). The PCR

products were confirmed as ER-α, ER-β, and GPER by sequencing with 99%, 95% and 98% identity, respectively, to the basic local alignment search tool (BLAST) database subject sequence. This indicated that the VK2 cells were an appropriate cell model to investigate the effects of estrogen on vaginal AMP expression.

Figure 3.2: VK2 cells express estrogen receptors. End-point PCR was performed on cDNA from VK2 cells for (A) ER-α at 236bp, (B) ER-β at 439bp, and (C) GPER at 680bp. The 100bp ladder (New England BioLabs, USA) is shown in lane 1 of each gel, and the respective PCR product is shown in lane 2. The PCR products were confirmed by sequencing (Genevision, UK) and the nucleotide BLAST alignments are shown. The query sequence is the sequence of the PCR product as determined by sequencing and the subject (sbjct) sequence is the BLAST database sequence.

3.3 Development of qPCR assays

To measure the effects of estrogen on AMP expression in VK2 cells, qPCR assays were developed for AMPs hBD2 and hBD3, in addition to the housekeeping genes GAPDH and ATP5B.

3.3.1 hBD2 qPCR assay

The qPCR assay for hBD2 was designed as a probes-based qPCR assay and the primers for this assay were predesigned by Integrated DNA Technologies (USA). End-point PCR was performed for hBD2 using the probes-based hBD2 primers and the PCR product was electrophoresed, extracted from the gel and cloned into the pGEM-T Easy vector (Promega, USA) as described in the materials and methods. Insertion of the hBD2 qPCR product into the vector was confirmed by sequencing (Figure 3.3A) and the inserted product had 100% identity with the BLAST database subject sequence. The vector containing the hBD2 PCR product was used to produce the standard curve for this assay (Figure 3.3B). The DNA probe of probes-based qPCR assays interferes with the melt peak of the PCR product and thus melt peak analysis was not performed for this assay. However, the qPCR product was electrophoresed on a TBE gel and only one PCR product, with the correct size of 106bp, was detected (Figure 3.3C).

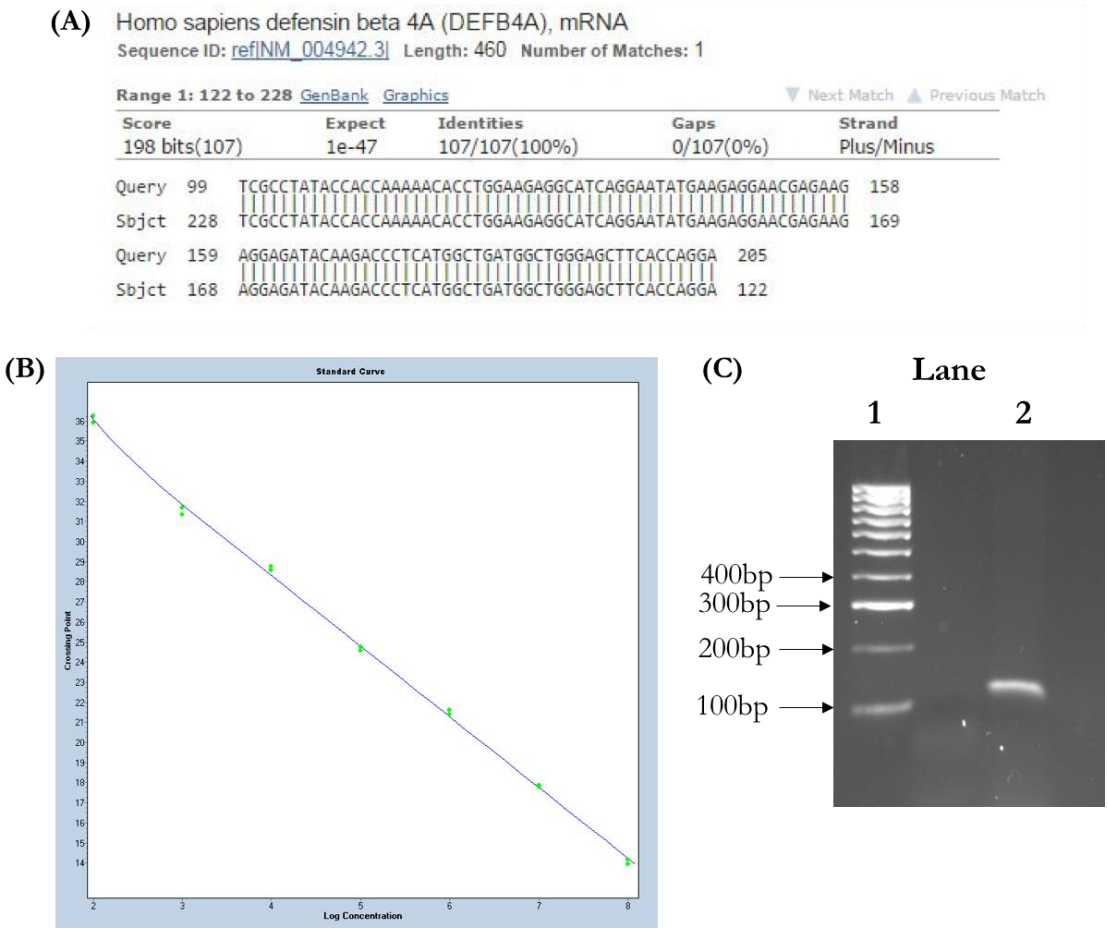

Figure 3.3: Sequencing results and standard curve for hBD2 probes-based qPCR assay plasmid. (A) The hBD2 PCR product was cloned into the pGEM-T Easy vector (Promega, USA) and confirmed by sequencing. The BLAST alignment is shown. The query sequence is the sequence of the PCR product as determined by sequencing and the subject (sbjct) sequence is the BLAST database sequence. (B) qPCR was performed using the vector, containing the hBD2 PCR product, serially diluted 1:10 to produce a standard curve. (C) The qPCR product was electrophoresed with HyperLadder IV (Bioline, USA) in Lane 1 and the 107bp PCR product is shown in Lane 2.

3.3.2 hBD3 qPCR assay

The hBD3 qPCR assay was a SYBR-green based assay and was established by Dr Marcelo Lanz. The hBD3 PCR product was cloned into the pGEM-T Easy vector and confirmed by sequencing. This plasmid was used to produce a standard curve for the hBD3 assay and a melt peak confirmed only one PCR product was amplified (Figure 3.4)[106].

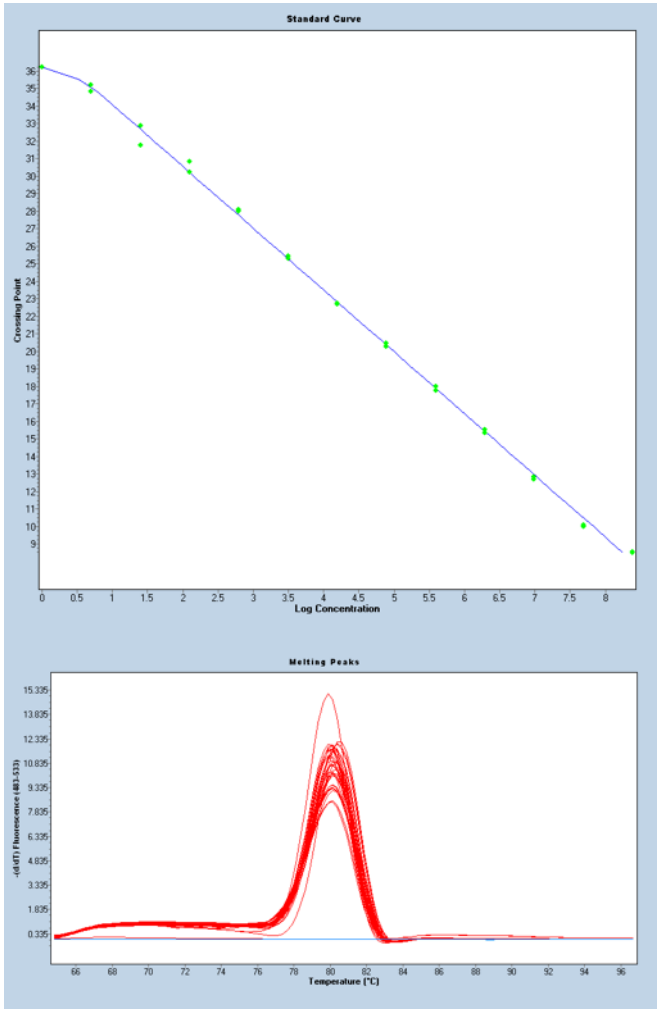

Figure 3.4: Standard curve and melt peak of hBD3 qPCR assay. The figure shows the standard curve and melt peak of the hBD3 qPCR assay designed by Dr Marcelo Lanz[106]. The melt peak confirms amplification of a single PCR product.

The qPCR results were analysed using the standard curve method relative to the housekeeping genes.

3.3.3 Housekeeping gene qPCR assays

qPCR assays for the housekeeping genes, GAPDH and ATP5B, were designed previously by Dr Ased Ali. The primers for these genes were predesigned by Primerdesign (UK). The PCR products were cloned into pGEM-T Easy vectors (Promega, USA) to produce a standard curve for each assay, as shown in Figure 3.5[60]. Melt peak analyses confirmed that each assay detected only one PCR product, as all samples displayed a single melt peak at the same temperature.

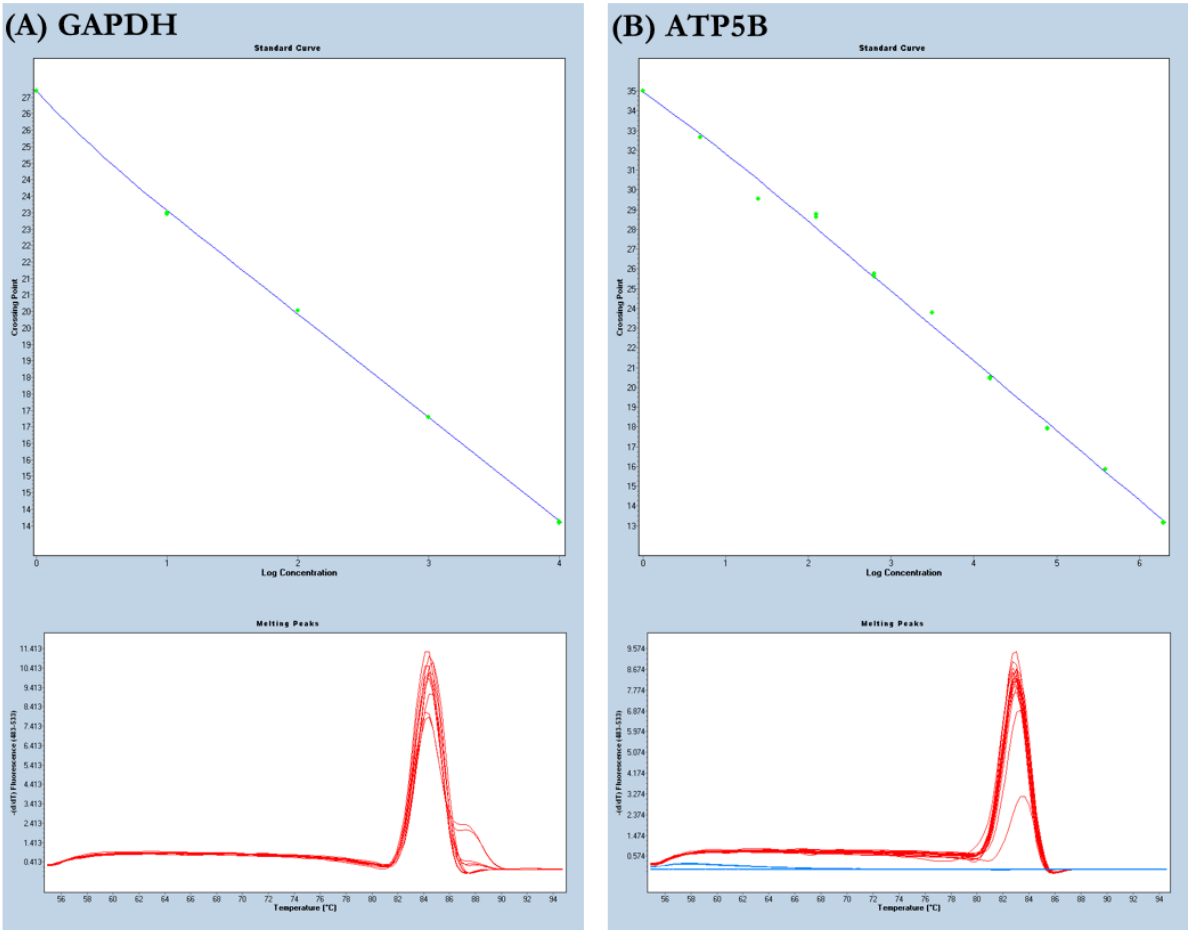

Figure 3.5: Standard curves and melt peaks for GAPDH and ATP5B qPCR assays. The figure shows the standard curves and melt peaks for the (A) GAPDH and (B) ATP5B qPCR assays designed by Dr Ased Ali[60]. Melt peaks confirm that only one PCR product was amplified during each reaction.

The qPCR assays outlined above were used to quantitate the effect of estrogen on hBD2 and hBD3 expression. The qPCR results shown in this thesis were analysed using the standard curve method, relative to the geometric mean of the two housekeeping genes, GAPDH and ATP5B. The results were normalised to the 24 hour flagellin challenge results. This approach was used as the AMPs had very low expression in the control samples with cycle numbers between 30 and 35 recorded. Variability was observed in the cycle numbers reported for the control samples when measuring the AMPs, due to the low cycle numbers for these samples. For example, in-plate replicates of the control samples were observed as having cycle numbers up to two cycles different, indicating a 4-fold difference in the amount of mRNA detected. Thus, as the control samples were less reliable the results were not normalised to control, as this would introduce uncertainty into all of the results. Instead the results were normalised to 24 hour flagellin challenge. As flagellin induced expression of the AMPs, flagellin challenged samples had an earlier cycle number than the control. Minimal variability was observed for these samples (cycle numbers for in-plate sample replicates were within 1% of each other). Thus, normalisation of the results to 24 hour flagellin challenge allowed comparison across different experiments and did

not introduce uncertainty into the data. The qPCR results presented in this thesis, therefore, are shown as arbitrary units (AU) of expression, with 24 hour flagellin challenge normalised to a mean of 100AU for each experiment.

3.4 Effects of acute estrogen on hBD2 and hBD3 expression

3.4.1 qPCR analyses

To investigate the effect of estrogen on hBD2 and hBD3 expression VK2 cells were challenged with 4nM estrogen with and without 50ng/ml flagellin, or PBS. 4nM estrogen is a relevant physiological concentration for premenopausal women[162]. After 0, 8, 12 and 24 hours the RNA was extracted, reverse transcribed into cDNA and analysed for hBD2 and hBD3 expression using the qPCR assays described. The qPCR results were analysed relative to the two housekeeping genes, GAPDH and ATP5B, using the geometric mean and the resultant values were normalised to 24 hour flagellin.

The results, shown in Figure 3.6, indicated that hBD2 expression was significantly induced by flagellin challenge. After 8, 12 and 24 hours flagellin challenge hBD2 expression was determined as 146AU, 167AU and 100AU, respectively, compared to untreated controls, which had mean hBD2 expression of 8AU ($p<0.0001$, Figure 3.6A). This is representative of a 9.9-, 19- and 22-fold change at 8, 12 and 24 hours, respectively, relative to the controls. Estrogen plus flagellin challenge also significantly induced hBD2 expression at 8, 12 and 24 hours ($p<0.0001$), but the addition of estrogen did not significantly increase hBD2 expression compared to flagellin challenge alone at any of the time points. After 24 hours flagellin challenge hBD3 expression increased to 100AU from 46AU in the control, representative of a significant 2.2-fold change in hBD3 expression ($p<0.0001$, Figure 3.6B). This was the only time point where flagellin challenge induced a statistically significant increase in hBD3 expression compared to the control. After 24 hours estrogen plus flagellin challenge hBD3 expression was further increased to 138AU, representative of a 3.0-fold change in hBD3 expression relative to the control ($p<0.0001$) and a significant 1.4-fold increase compared to flagellin ($p=0.0005$). Estrogen plus flagellin did not significantly increase hBD3 expression compared to flagellin challenge at any other time point.

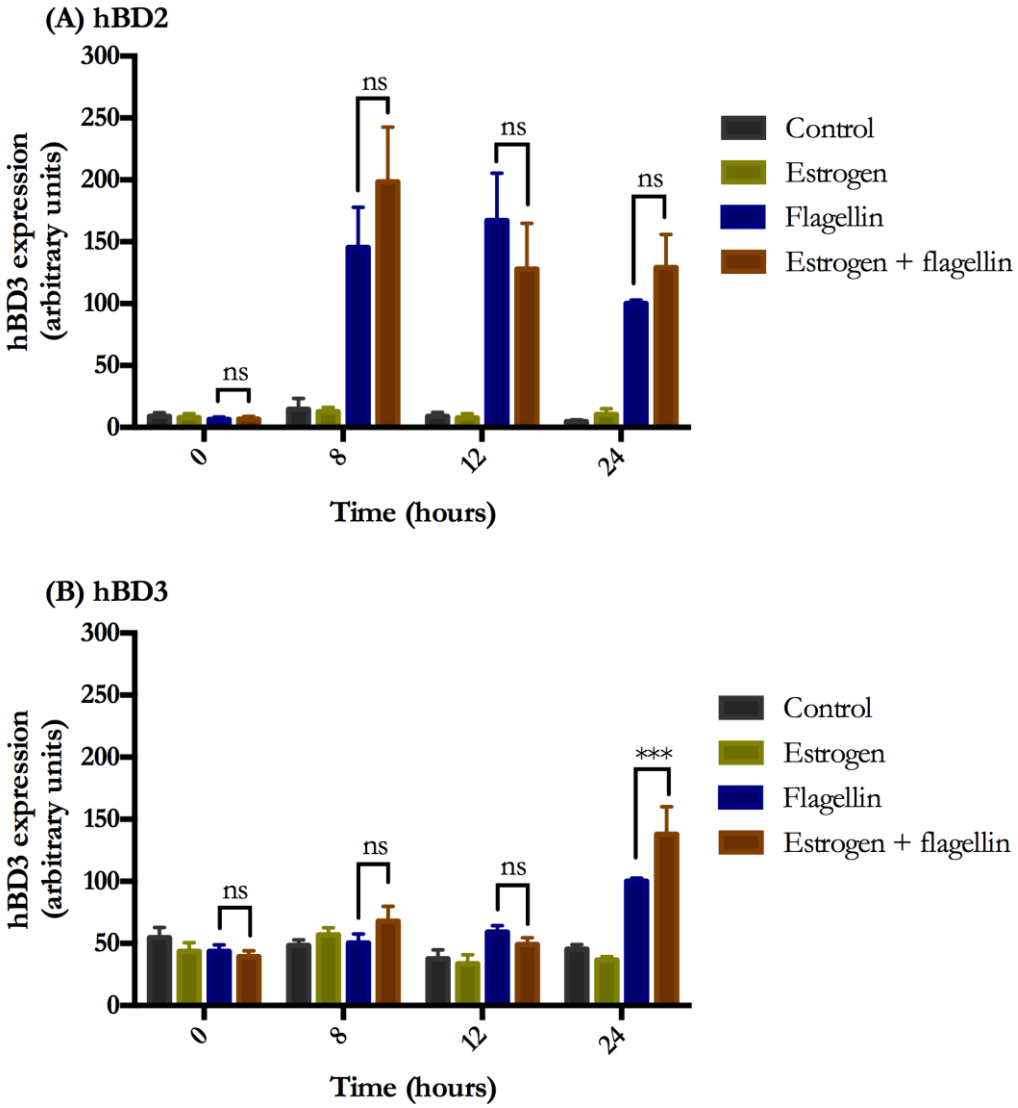

Figure 3.6: Effects of acute estrogen and flagellin on hBD2 and hBD3 expression in VK2 cells. VK2 cells were challenged with 4nM estrogen and/or 50ng/ml flagellin for up to 24 hours. RNA was then extracted and analysed by qPCR for (A) hBD2 and (B) hBD3 expression, and results were normalised to 24 hour flagellin. Error bars represent standard error. Statistical analysis was performed by two-way ANOVA with Tukey's post hoc test. ns=not significant, ***=$p<0.001$. N=3, n=9.

3.4.2 Reporter analyses

To verify these data, hBD2 promoter activity was also measured using a luciferase reporter assay. The phBD-2-Luc reporter plasmid was engineered by Dr Marcelo Lanz and contains a 2032bp hBD2 promoter region insert upstream of the *luc2* luciferase gene[106]. Following transfection of VK2 cells with the reporter plasmid, expression of hBD2 results in luciferase production. When luciferase reacts with the luciferase reporter assay reagent (Promega, USA) light is emitted in the form of luminescence in proportion to the amount of luciferase produced by the cells. This means that greater hBD2 promoter activity results in higher luminescence. Luciferase expression

was quantitated by measurement of luminescence using a plate reader, as detailed in the materials and methods.

3.4.2.1 hBD2 reporter assay optimisation

Transfection of the VK2 cells required optimisation to determine the concentrations of transfection reagent and plasmid DNA that yielded the best results. The pGL4.51 vector (Promega, USA) was used to optimise the transfection protocol. This vector contains the *luc2* gene downstream of the CMV promoter, which results in constitutive luciferase expression in cells that have taken up the plasmid. This is useful for optimisation as the amount of luminescence is directly proportional to the amount of plasmid that has been taken up and therefore, can be used to determine the optimum transfection conditions. Hence, to optimise the transfection reaction, VK2 cells were seeded into a 96-well plate and transfected using 0-0.8µl/well Attractene transfection reagent and 150-250ng pGL4.51 plasmid DNA.

As shown in Figure 3.7, all of the conditions where 0.2µl or greater of Attractene was used resulted in high luminescence levels of approximately 5000AU, compared to the control samples without Attractene, which had a mean luminescence of 22AU. Cytotoxic activity was observed at higher concentrations of Attractene, reflected by 0.7µl and 0.8µl Attractene data, which showed reduced luminescence values of approximately 3500AU. Generally, increasing the concentration of plasmid DNA did not increase the luminescence. Therefore, 0.5µl/well Attractene and 150ng plasmid DNA were the conditions chosen for further transfection experiments, as this resulted in strong luminescence levels of 5033AU, compared to a mean luminescence of 22AU in the controls without Attractene, whilst minimising reagent volumes.

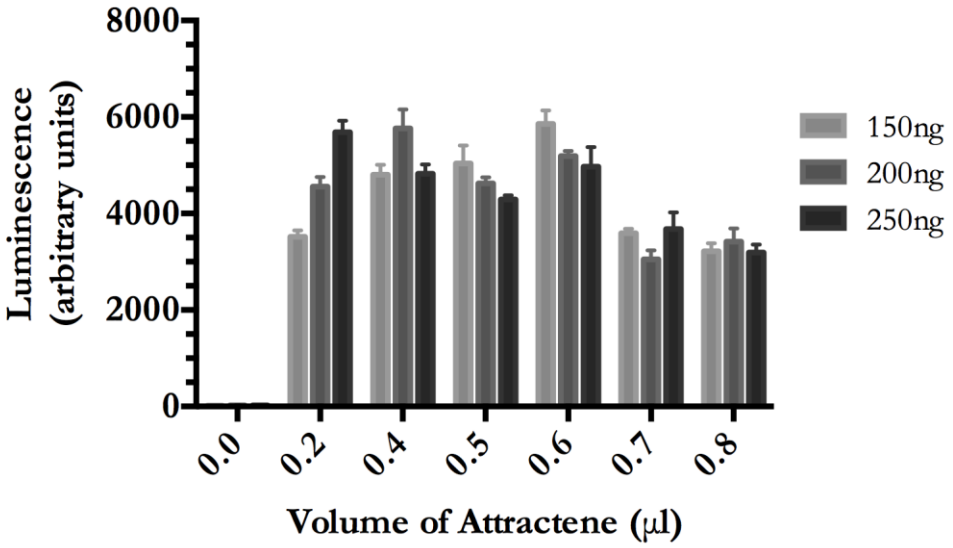

Figure 3.7: Optimisation of VK2 cell transfection. VK2 cells were seeded into a 96-well plate and transfected with 0-0.8µl Attractene (Qiagen, Germany) and 150-250ng pGL4.510 plasmid DNA (Promega, USA) and incubated for 18 hours. The cells were then lysed and the Luciferase Assay System (Promega, USA) and FLOUstar Omega Microplate Reader were used to measure luciferase production. Error bars represent standard error. N=1, n=3.

3.4.2.2 Effects of acute estrogen on hBD2 promoter activity

The VK2 cells were transiently transfected with the phBD-2-luc plasmid using the conditions determined above and then challenged with 4nM estrogen and/or 50ng/ml flagellin, or PBS, for 24 hours. Luminescence levels were determined using the Luciferase Assay Kit (Promega, USA) and FLOUstar Omega Microplate Reader.

The results of the luciferase assay (Figure 3.8) showed that the 24 hour flagellin challenge activated the hBD2 promoter, causing gene transcription. The experimental repeats exhibited variation in the fold change induced, with the first repeat showing a 5.9-fold change in promoter activity following flagellin challenge, compared to control, and the second repeat showing a 42-fold change after flagellin challenge. However, this was not observed for other experiments using the hBD2 reporter assay and thus was likely to be due to technical differences between experimental repeats, such as differences in cell density in the wells at time of challenge. Nevertheless, neither repeat showed a significant increase in luminescence following acute estrogen plus flagellin challenge, compared to flagellin challenge alone. These data supported the qPCR data, showing that acute estrogen treatment did not significantly increase hBD2 expression.

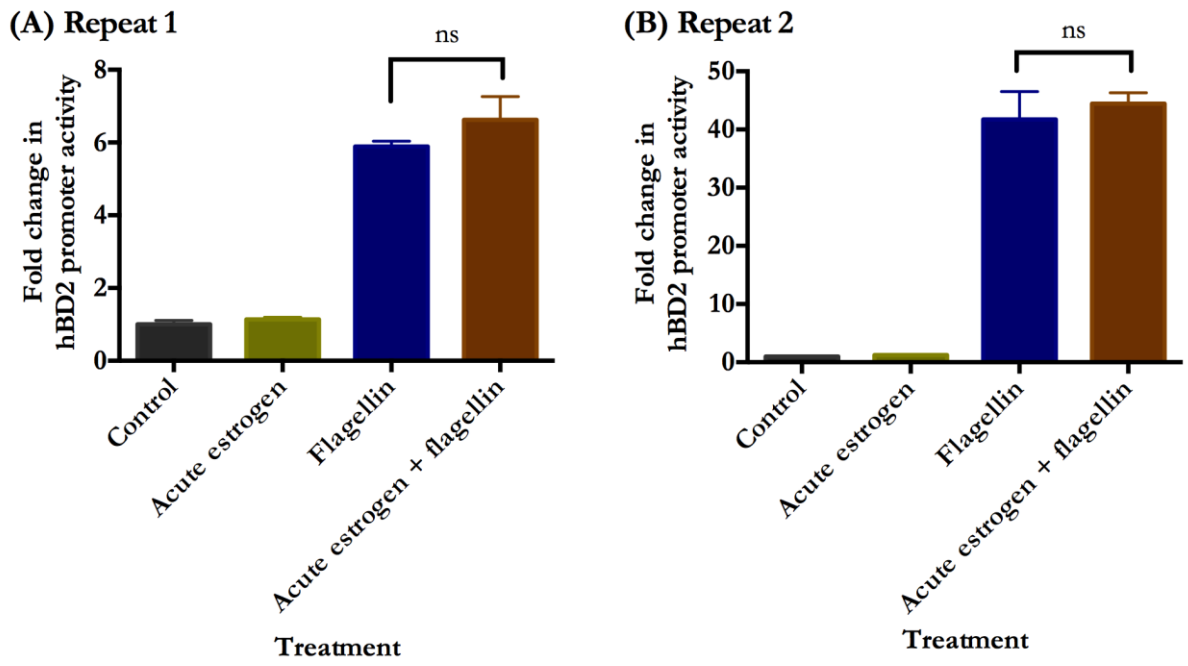

Figure 3.8: Effects of acute estrogen and flagellin on hBD2 promoter activity. VK2 cells were seeded into 96-well plates and transiently transfected with the phBD-2-luc plasmid and then treated with 4nM estrogen and/or 50ng/ml flagellin for 24 hours. The phBD-2-luc plasmid contains a 2032bp hBD2 promoter insert upstream of the *luc2* gene. The cells were lysed, the Luciferase Assay System (Promega, USA) and FLUOstar Omega Microplate Reader were used to determine luminescence, and the results were normalised to the control. (A) and (B) show the results for the first and second biological repeat, respectively. Each graph represents N=1, n=3. Error bars represent standard error. Statistical analysis was performed by one-way ANOVA with Tukey's post hoc test. ns=not significant.

3.4.3 Effects of acute estrogen with reduced flagellin concentrations on hBD2 and hBD3 expression

To ascertain whether a dose of 50ng/ml flagellin was inducing maximum expression of hBD2 and hBD3 such that acute estrogen treatment could not further potentiate gene expression, VK2 cells were challenged with lower concentrations of flagellin, with and without estrogen. It was hypothesised that lower concentrations of flagellin would result in a smaller induction of hBD2 and hBD3 expression, and thus any effects of estrogen would be more marked. VK2 cells were challenged with 2.5pg/ml to 50ng/ml flagellin, with and without 4nM estrogen for 24 hours, and the RNA was extracted, reverse transcribed and analysed by qPCR for hBD2 and hBD3 expression.

The results, in Figure 3.9, showed that acute estrogen plus flagellin treatment did not increase hBD2 or hBD3 expression compared to flagellin alone, at any of the concentrations of flagellin used. The hBD3 expression data suggested a potential increase in gene expression with acute estrogen treatment plus 50ng/ml flagellin (135AU), compared to 50ng/ml flagellin without estrogen (100AU), however, in this experiment the difference was not significant (p=0.1463) as

was seen previously in Figure 3.6. These data indicated that acute estrogen treatment at a concentration of 4nM was not sufficient to increase the expression of hBD2 and hBD3 at any of the flagellin concentrations tested. Thus, the hypothesis that reducing the flagellin concentration may reveal an effect of acute estrogen on hBD2 and hBD3 expression was incorrect. Furthermore, these data demonstrated that 25ng/ml and 50ng/ml flagellin induced hBD2 and hBD3 expression to comparable levels, whilst flagellin concentrations lower than this resulted in lower hBD2 and hBD3 expression. Thus, flagellin at a concentration of 50ng/ml was a strong inducer of AMP expression and this concentration was used for subsequent experiments.

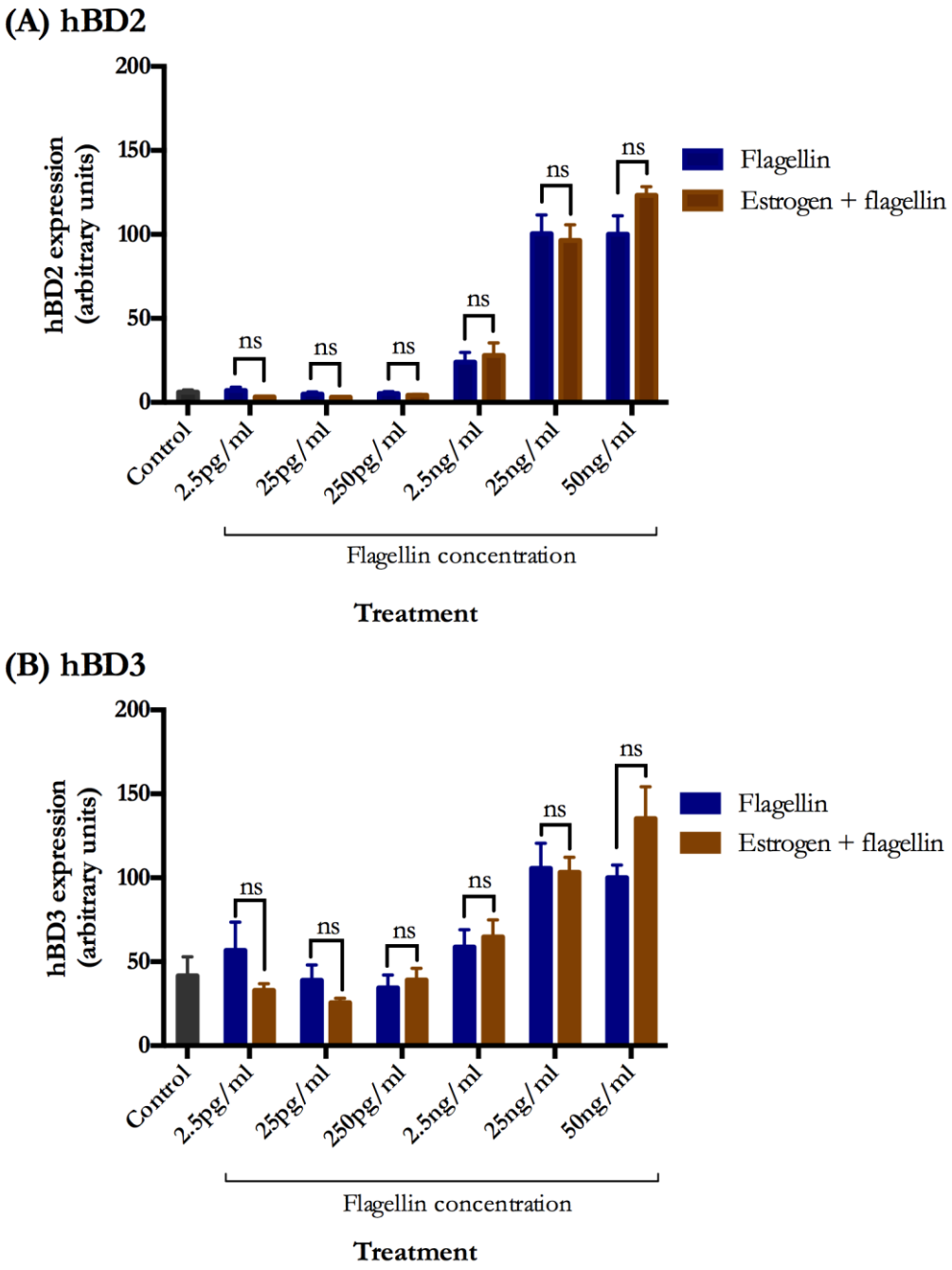

Figure 3.9: Effects of reduced flagellin concentrations, with and without acute estrogen, on hBD2 and hBD3 expression. VK2 cells were challenged with flagellin ranging from 2.5pg/ml-50ng/ml, with and without 4nM estrogen, for 24 hours. The RNA was extracted and analysed by qPCR for (A) hBD2 and (B) hBD3 expression. Error bars represent standard error. Statistical analysis was performed by two-way ANOVA with Sidak's post hoc test. ns=not significant. N=2, n=6.

3.5 Effects of long-term estrogen treatment on hBD2 and hBD3 expression

As acute estrogen treatment plus flagellin challenge did not significantly effect hBD2 and hBD3 expression compared to flagellin alone, the effect of estrogen pretreatment for seven days prior to flagellin challenge on hBD2 and hBD3 expression was investigated. Estrogen pretreatment more accurately represents physiological exposure to estrogen, as well as topical estrogen

treatment, which is applied regularly to the vagina as a prophylactic treatment[7]. The estrogen concentration used in these experiments was representative of physiological estrogen levels, not therapeutic levels.

3.5.1 Effects of estrogen pretreatment on VK2 cell growth

Estrogen has been reported to increase growth of certain cell types[205–208]. Thus, the effect of estrogen pretreatment on VK2 cells was investigated. To do this VK2 cells were seeded at a low density into 6-well plates and treated with 4nM estrogen or 1mM Mitomycin C (Sigma, USA) for seven days. Mitomycin C inhibits cell growth by inhibiting DNA synthesis. On days one, three, five and seven the cells were imaged using an EVOS XL core digital light microscope (AMG, USA), and the CellTiter-Blue Cell Viability Assay (Promega, USA) was used to measure cell growth. At each time point the medium was removed from the wells, the cells were washed with PBS, new medium was added to each well along with CellTiter-Blue Reagent and the cells were incubated at 37°C for 1 hour. CellTiter-Blue Reagent contains highly purified resazurin, which is reduced to resorufin by metabolically active cells causing a colour change. Resazurin and resorufin have distinct absorbance maximums (605nm and 573nm, respectively) and thus reduction of resazurin can be determined by measuring absorbance at both of these wavelengths on a plate reader. The amount of resazurin reduction is directly proportional to the number of cells in the well.

The results showed that untreated control cells and estrogen treated cells grew over the seven day period, reaching confluency at day seven (Figure 3.10). However, Mitomycin C treated cells had significantly reduced growth at days three, five and seven compared to untreated control cells (p-values <0.0001). At each time point, the number of cells in the control wells and the estrogen treated wells were comparable (Figure 3.10A) and both untreated and estrogen treated wells were confluent on day seven (Figure 3.10B). Thus, these data indicated that estrogen pretreatment did not affect the growth of VK2 cells.

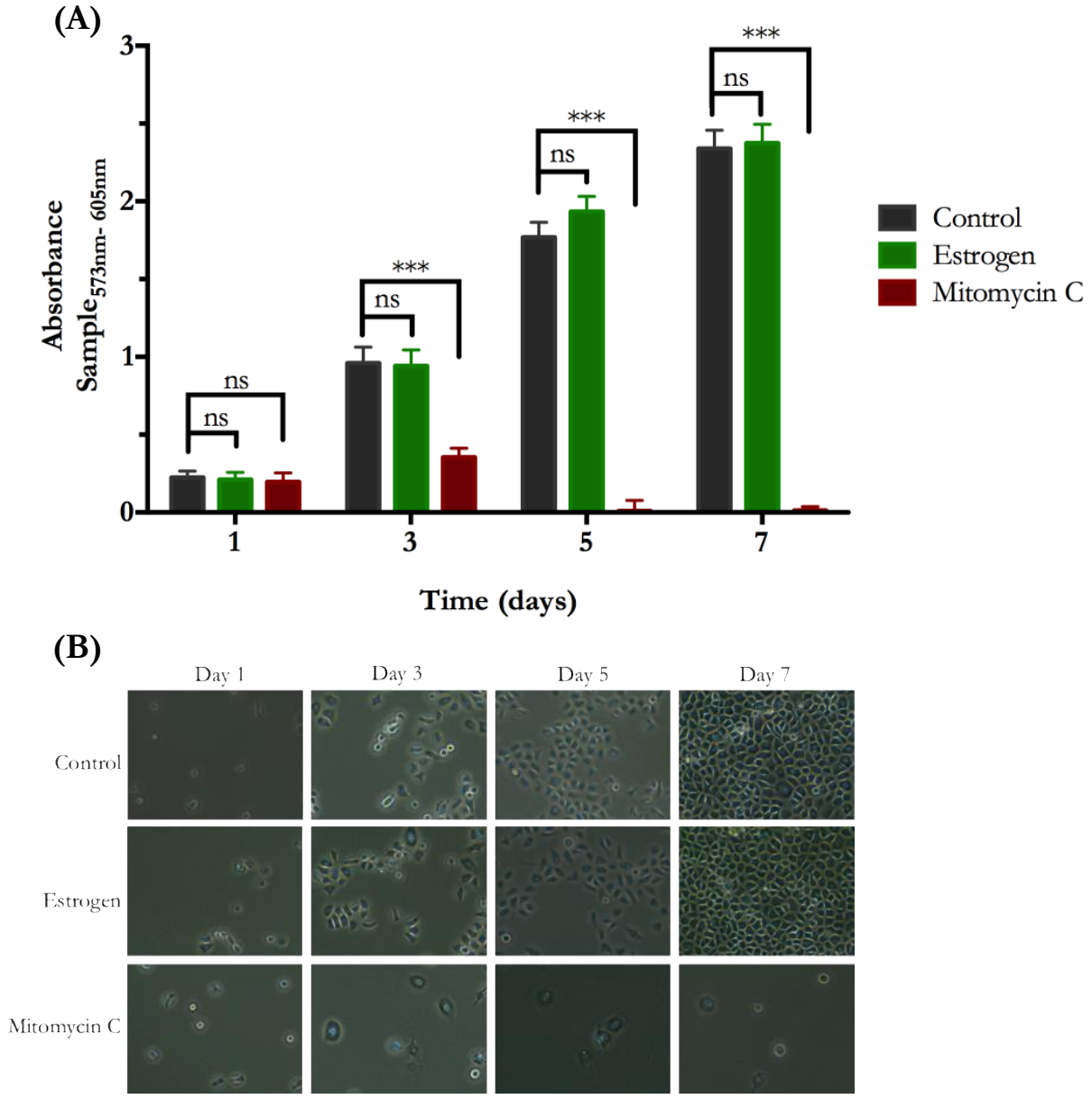

Figure 3.10: Estrogen does not affect the growth of VK2 cells. VK2 cells were seeded into 6-well plates and treated with 4nM estrogen or 1mM Mitomycin C for seven days. (A) CellTiter-Blue Cell Viability Assay (Promega, USA) was used to measure cell viability after 1, 3, 5 and 7 days of treatment. Error bars represent standard error. Statistical analysis was performed by two-way ANOVA with Dunnett's post hoc test. ns=not significant, **=$p<0.01$, ***=$p<0.001$. N=2, n=6. (B) Images taken on an EVOS XL core digital light microscope (AMG, USA) show the cells at each time point for each treatment. Each image was representative of the well.

3.5.2 Effects of estrogen pretreatment on hBD2 and hBD3 expression

To study the effects of long-term estrogen treatment on AMP expression, VK2 cells were pretreated with 4nM estrogen for at least seven days and then challenged with 50ng/ml flagellin (Figure 3.11). The cells were typically washed and given fresh culture medium and estrogen every other day during the seven day period. Once the cells were confluent at day seven, the cell culture medium and estrogen was replaced for the final time, and the cells were incubated in this medium for 24 hours prior to challenge with 50ng/ml flagellin, or PBS, on day 8. RNA was extracted at 0,

8, 12, and 24 hours after flagellin challenge and analysed by qPCR for hBD2 and hBD3 expression.

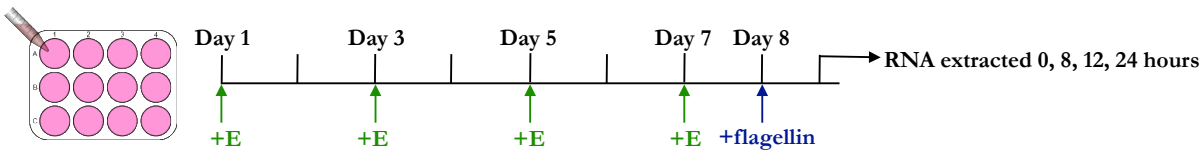

Figure 3.11: Typical timeline of estrogen pretreatment and flagellin challenge of VK2 cells. VK2 cells were seeded into 12-well plates and pretreated with estrogen. Every other day the cell culture medium was removed, the cells were washed with PBS, and fresh medium and estrogen was added to the cells. The medium and estrogen was replaced for the final time 24 hours before flagellin challenge. The RNA was extracted after 0, 8, 12, and 24 hours flagellin challenge.

The results for hBD2 are shown in Figure 3.12. After 8 hours challenge hBD2 expression increased from 15AU in the control samples to 145AU with flagellin challenge. This represented a significant 9.9-fold change in hBD2 expression compared to the control ($p=0.035$). After 8 hours estrogen pretreatment plus flagellin challenge hBD2 expression was determined as 290AU, representative of a 20-fold increase compared to control ($p<0.0001$) and a 2.0-fold increase compared to flagellin challenge alone ($p=0.0374$). After 24 hours challenge hBD2 expression increased from 4.6AU in the control samples to 100AU with flagellin challenge, representative of a 22-fold increase in expression. After 24 hours estrogen pretreatment plus flagellin, hBD2 expression increased to 233AU, which represented a 50-fold change in hBD2 expression relative to the control ($p<0.0001$) and a 2.3-fold increase compared to flagellin challenge ($p<0.0001$).

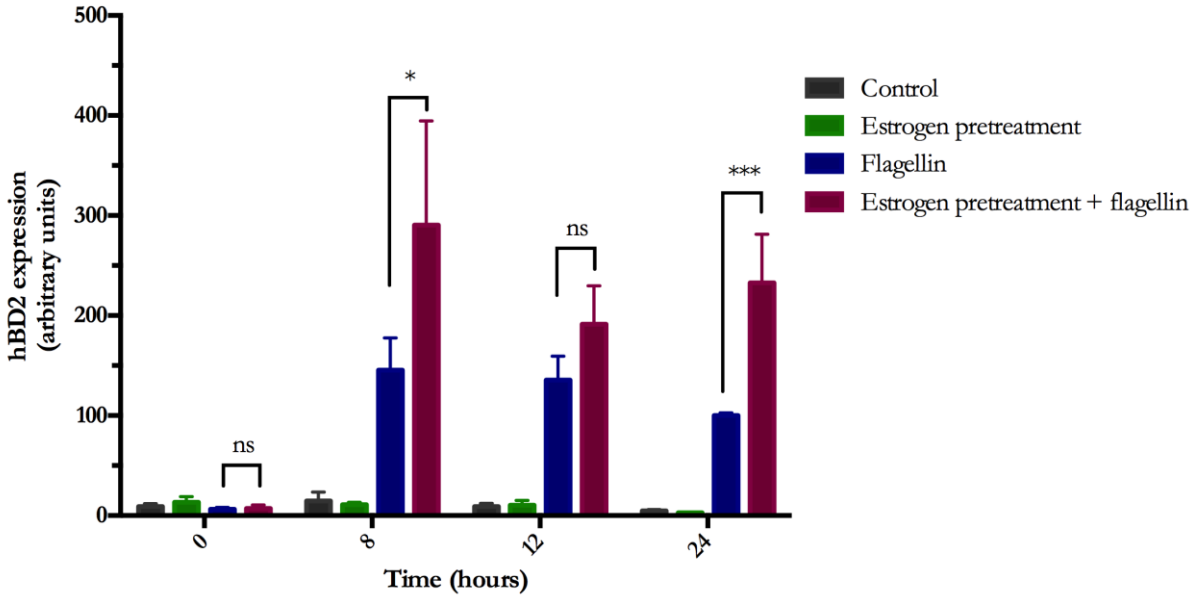

Figure 3.12: Effects of estrogen pretreatment and flagellin on hBD2 expression. VK2 cells were pretreated with 4nM estrogen for 7 days and then challenged with 50ng/ml flagellin, or PBS. RNA was extracted at 0, 8, 12, and 24 hours and analysed for hBD2 expression. The results were normalised to 24 hour flagellin. Error bars represent standard error. Statistical analysis was performed by two-way ANOVA with Tukey's post hoc test. ns=not significant, *=$p<0.05$, ***=$p<0.001$. At 0, 8 and 12 hour N=3, n=9. At 24 hour N=8, n=24.

The promoter activity of hBD2 was measured once again using the luciferase reporter plasmid, this time in response to estrogen pretreatment with flagellin. The results (Figure 3.13) showed that estrogen pretreatment plus flagellin challenge alone resulted in a 27-fold change in promoter activity compared to control ($p<0.0001$), which was a significant 2.1-fold increase on the promoter activity induced by flagellin treatment ($p=0.0367$). Thus, these data mirrored the results obtained by qPCR and supported the hypothesis that estrogen pretreatment increases hBD2 expression during infection.

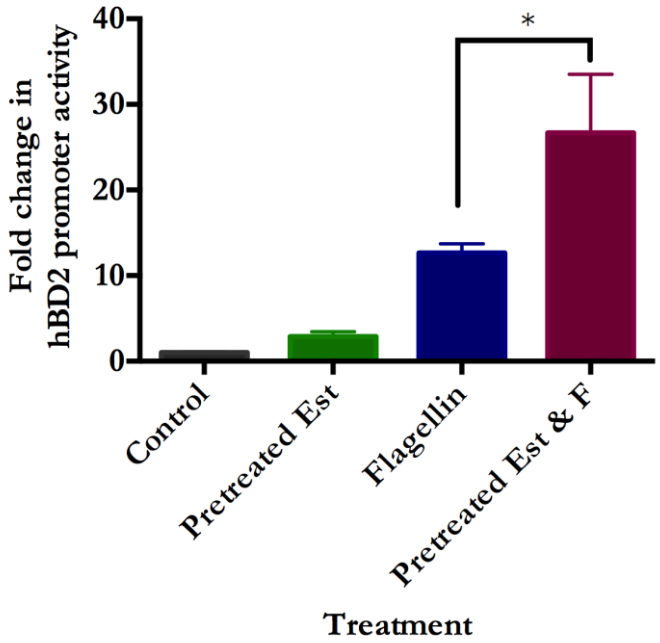

Figure 3.13: Effect of estrogen pretreatment and flagellin on hBD2 promoter activity. VK2 cells were pretreated with 4nM estrogen for 7 days and then seeded into a 96-well plate and transiently transfected with the phBD-2-luc plasmid before being challenged with 50ng/ml flagellin for 24 hours. Promoter activity was determined using the Luciferase Assay System (Promega, USA) and luminescence was measured using a plate reader. The results were normalised to the control. Error bars represent standard error. Statistical analysis was performed by one-way ANOVA with Tukey's post hoc test. *=$p<0.05$. N=4, n=8.

Analysis of hBD3 expression by qPCR showed that after 8 hours estrogen pretreatment plus flagellin challenge hBD3 expression was induced to 139AU, from 48AU in the control. This represented a significant 2.9-fold increase in hBD3 expression relative to control ($p=0.0001$), and a 2.8-fold change compared to flagellin challenge ($p=0.0003$). Whereas, flagellin challenge did not result in a significant increase in hBD3 expression until the 24 hour time point. After 24 hours flagellin challenge, hBD3 expression was determined as 100AU, which represented a significant 2.1-fold increase in expression compared to the controls (47AU, $p=0.0003$). At this time point, estrogen pretreatment plus flagellin resulted in hBD3 expression of 211AU. This represented a 4.5-fold change in hBD3 expression compared to control ($p<0.0001$) and a 2.1-fold change compared to flagellin challenge alone ($p<0.0001$). Thus these data showed that estrogen pretreatment of VK2 cells prior to flagellin challenge not only resulted in higher expression of hBD3, but also induced an earlier hBD3 response than the same challenge without estrogen pretreatment.

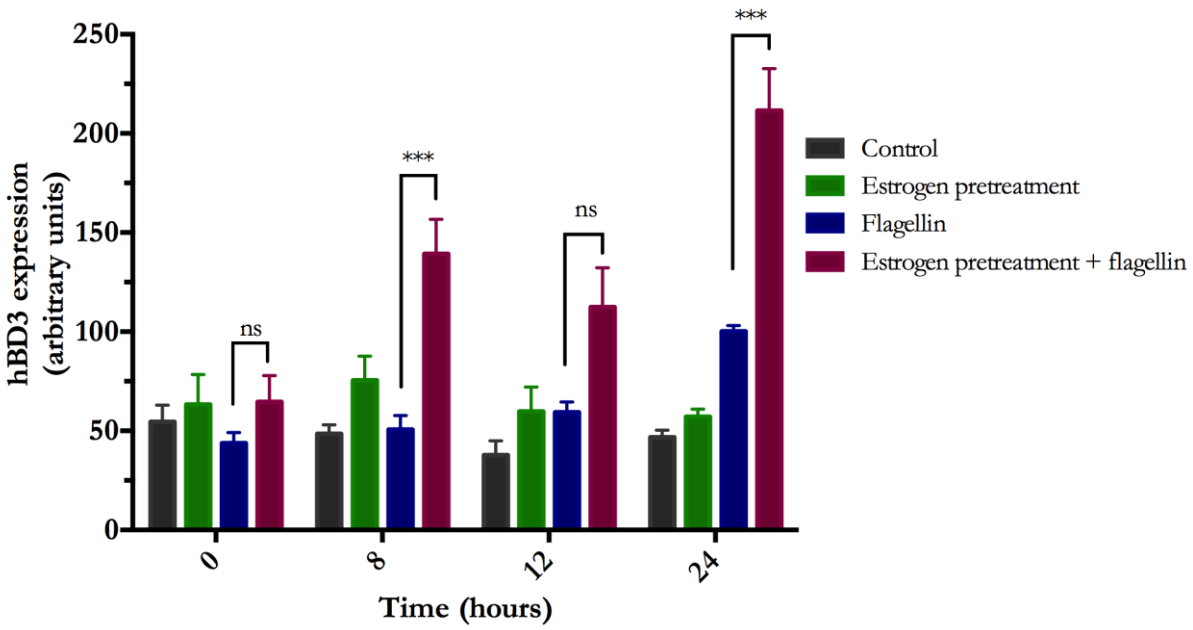

Figure 3.14: Effects of estrogen pretreatment and flagellin on hBD3 expression. VK2 cells were pretreated with 4nM estrogen for 7 days, and then challenged with 50ng/ml flagellin. At 0, 8, 12, and 24 hours RNA was extracted and analysed by qPCR for hBD3 expression. Error bars represent standard error. Statistical analysis was performed by two-way ANOVA with Tukey's post hoc test. ns=not significant, *=$p<0.05$, ***=$p<0.001$. At 0, 8 and 12 hours N=3, n=9. At 24 hours N=8, n=24.

3.6 Effects of cyclodextrin on AMP expression

As indicated in the materials and methods section, the estrogen used to pretreat the VK2 cells was water-soluble 17β-estradiol (Sigma, USA). To facilitate water solubility the 17β-estradiol is encapsulated in 2-hydroxypropyl-β-cyclodextrin (cyclodextrin), which is a compound composed of seven sugar molecules that form a ring structure. The inside of the ring is hydrophobic and the outside of the ring is hydrophilic, which increases the solubility of the compound that is encapsulated. In experiments presented so far within this chapter the cells were pretreated either with estrogen or with water, as the estrogen was reconstituted in water. However, it was also important to consider whether the observed increases in gene expression were attributed to the cyclodextrin that encapsulated the estrogen molecules. The water-soluble estrogen consisted of 48.3mg 17β-estradiol per gram of solid and thus, 4nM estrogen (the concentration used to pretreat the VK2 cells) had a cyclodextrin concentration of 14.8nM. VK2 cells were, therefore, treated with 14.8nM cyclodextrin for seven days and then challenged with 50ng/ml flagellin, or PBS, for 24 hours. The RNA was extracted and analysed by qPCR for hBD2 expression.

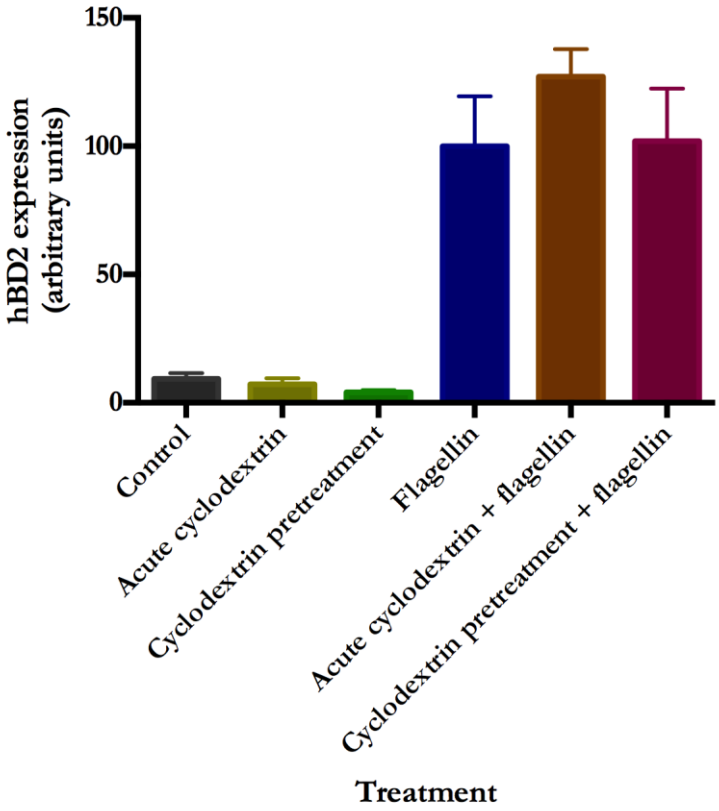

Figure 3.15: Effects of cyclodextrin and flagellin on hBD2 expression. VK2 cells were pretreated with 14.8nM cyclodextrin or vehicle for 7 days and then challenged with 50ng/ml flagellin for 24 hours. Cells were also treated acutely with cyclodextrin (no pretreatment) at the same time as flagellin challenge. RNA was extracted and analysed by qPCR for hBD2 expression. Error bars represent standard error. Statistical analysis was performed by one-way ANOVA with Tukey's post hoc test. N=2, n=6.

The results showed that cyclodextrin (given acutely or as a pretreatment) did not affect hBD2 expression (Figure 3.15). Neither acute cyclodextrin plus flagellin nor cyclodextrin pretreatment plus flagellin significantly affected hBD2 expression compared to flagellin treatment without cyclodextrin. Thus, these data confirmed that the increases in AMP treatment could be attributed to the effects of estrogen, rather than cyclodextrin.

3.7 Effects of estrogen pretreatment and flagellin on hBD2 and hBD3 secretion

Although it was shown that estrogen increased the expression of hBD2 and hBD3 in VK2 cells during a simulated infection, it was also important to examine the effects on hBD2 and hBD3 peptide concentration. Both hBD2 and hBD3 are secreted from epithelial cells and effectuate bacterial killing extracellularly. Thus, the concentration of hBD2 and hBD3 in the cell culture medium bathing the VK2 cells during the challenges was collected and measured by ELISA as described in the materials and methods.

The results for hBD2 showed that control cells displayed a constitutive hBD2 concentration of 235±71pg/ml (standard error of the mean, SEM). Flagellin and estrogen pretreatment plus flagellin significantly increased hBD2 concentration by approximately 3-fold ($p=0.007$, Figure 3.16A), to 716±99pg/ml (SEM) and 693±73pg/ml (SEM), respectively. Thus, an increase in hBD2 concentration was observed following VK2 cell exposure to flagellin.

In contrast to the mRNA data, the ELISA results for hBD2 did not show an increase in peptide concentration with estrogen pretreatment plus flagellin compared to flagellin alone. However, significant variability was observed between in-plate repeats of the same sample. For example, the concentration of hBD2 in in-plate replicates of one control sample was determined as 300pg/ml and 148pg/ml, a more than 2-fold difference. This variability was reflected in the standard curve. The standard curve included on each hBD2 ELISA plate consisted of serial 1:2 dilutions of recombinant hBD2 peptide from 8pg/ml to 2000pg/ml. A typical standard curve for the hBD2 ELISA is shown in Figure 3.17, and this showed that the replicates with peptide levels below approximately 125pg/ml were variable, limiting the fit of the standard curve and the sensitivity of the assay.

The hBD3 ELISA failed to detect any significant increase in hBD3 with any of the treatments, compared to the control. All samples showed a hBD3 concentration of around 140pg/ml (Figure 3.16B). The hBD3 standard curve is shown in Figure 3.18A and demonstrated that the assay was functional despite not detecting any increase in hBD3 with the VK2 cell samples. Similarly to the hBD2 assay, the hBD3 standard curve replicates (Figure 3.18B) showed that the ELISA was not particularly sensitive at hBD3 concentrations below approximately 125pg/ml. Hence the peptide data presented here may reflect poor ELISA assays rather than the true data.

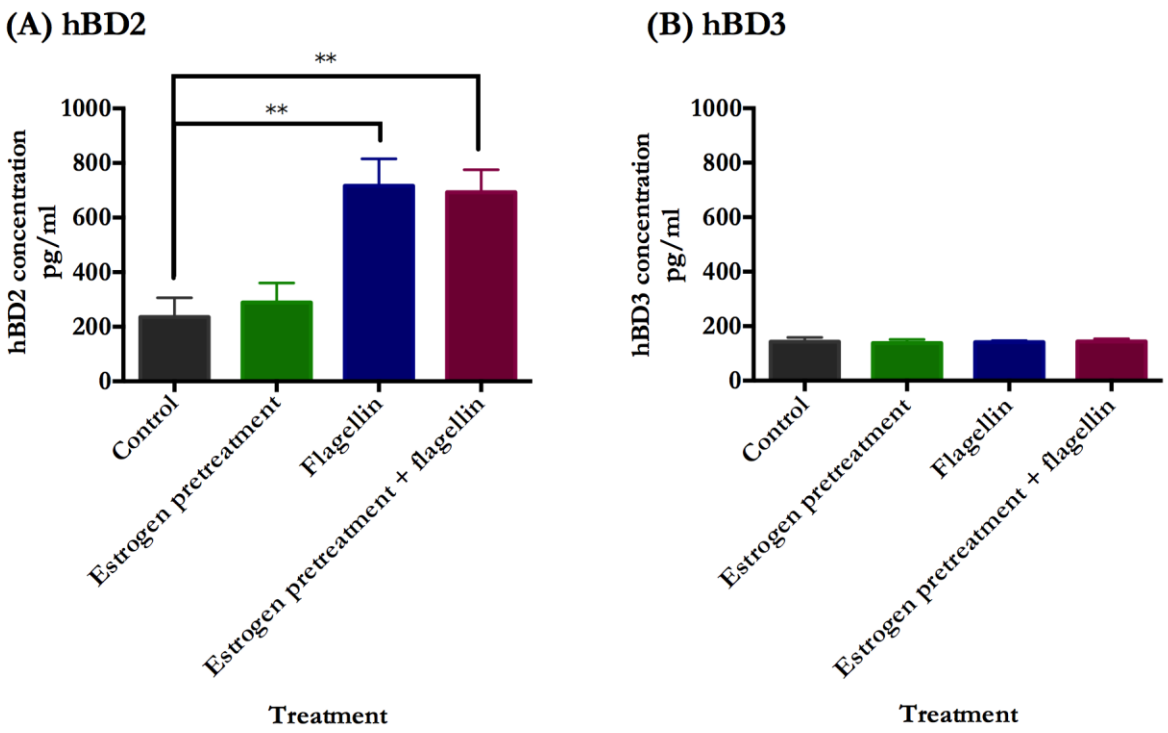

Figure 3.16: Effects of estrogen pretreatment and flagellin on hBD2 and hBD3 secretion. VK2 cells were pretreated with 4nM estrogen for 7 days and then challenged with 50ng/ml flagellin for 24 hours. The medium was removed from the cells and analysed by ELISA for (A) hBD2 (N=2, n=6), and (B) hBD3 (N=1, n=3) secretion. Error bars represent standard error. Statistical analysis was performed by one-way ANOVA with Tukey's post hoc test. **=$p<0.01$.

(A) hBD2 standard curve

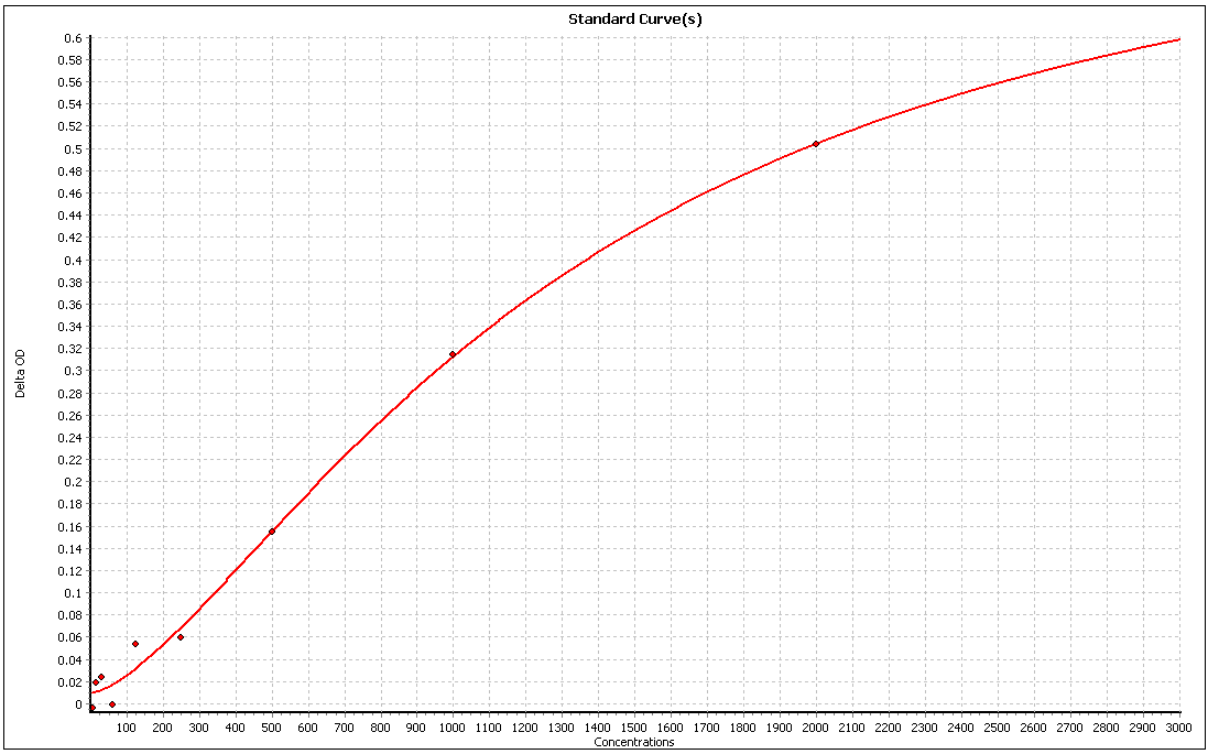

(B) hBD2 standard replicates

Standard curve concentration	Measured concentration (pg/ml)		
pg/ml	Replicate 1	Replicate 2	Average
2000	2294	1752	2023
1000	1068	948	1008
500	494	502	498
250	197	244	220
125	309	71	190
63		125	125
31		148	148
16	76	59	67
8			

Figure 3.17: hBD2 ELISA standard curve. A standard curve was included on each hBD2 ELISA plate and consisted of recombinant hBD2 serially diluted 1:2 from 2000pg/ml to 8pg/ml. (A) shows the standard curve line of best fit. (B) shows the measured concentration of each of the standard replicates. Blanks show where the concentration was too low to be determined.

(A) hBD3 standard curve

(B) hBD3 standard replicates

Standard curve concentration	Measured concentration (pg/ml)		
pg/ml	Replicate 1	Replicate 2	Average
1000	936		936
500	412	346	379
250	239	143	191
125	127	65	96
63	42	37	39
31	45	24	34
16	23	22	23
8	25	31	28

Figure 3.18: hBD3 ELISA standard curve. A standard curve was included on each hBD3 ELISA plate and consisted of recombinant hBD3 serially diluted 1:2 from 1000pg/ml to 8pg/ml. (A) shows the standard curve line of best fit. (B) shows the measured concentration of each of the standard replicates. Blanks show where the concentration was too high to be determined.

3.8 Effects of estrogen pretreatment and flagellin on AMP expression in primary vaginal epithelial cells

It was important to verify the results obtained using VK2 cells in primary vaginal epithelial cells (PVECs) as these are more representative of the *in vivo* vaginal epithelium than the immortalised cell line. Vaginal tissue was obtained from women undergoing gynaecological surgery at the Royal Victoria Infirmary in Newcastle upon Tyne. PVECs were extracted from the vaginal tissue as

described in the materials and methods and were seeded into 12-well plates. The cells were fed every 2-3 days until confluent (Figure 3.19).

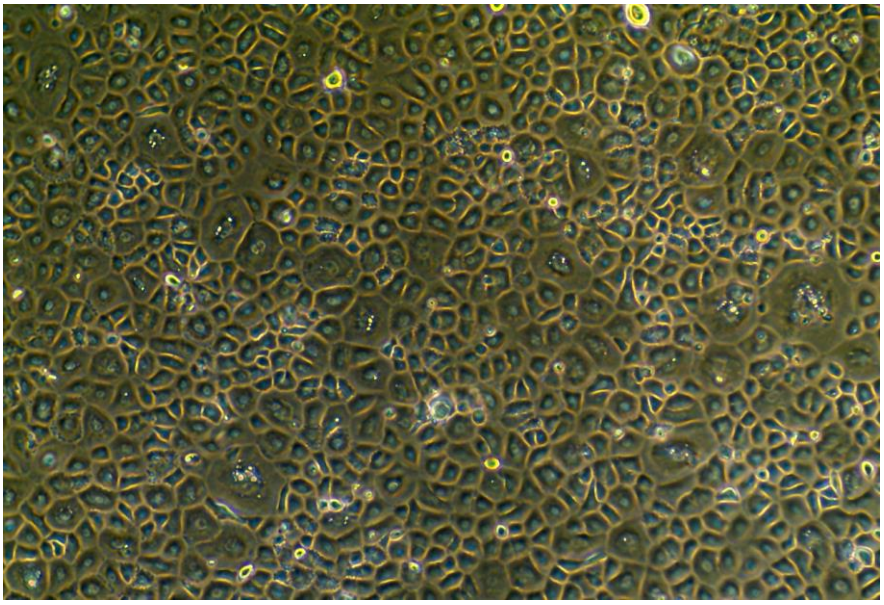

Figure 3.19: Primary vaginal epithelial cells at confluency. The image, taken with an EVOS XL Core digital light microscope (AMG, USA) at x20 magnification, shows PVECs forming a confluent monolayer.

3.8.1 PVECs express estrogen receptors

Prior to conducting experiments with the PVECs, it was important to determine the expression of the estrogen receptors in these cells. End-point PCR was performed for each of the estrogen receptors (ER-α, ER-β, and GPER) to confirm gene expression in PVECs. As shown in Figure 3.20 PCR products representative of ER-α, -β, and GPER were detected at 236bp, 439bp, and 680bp, respectively. Thus, PVECs expressed all estrogen receptors.

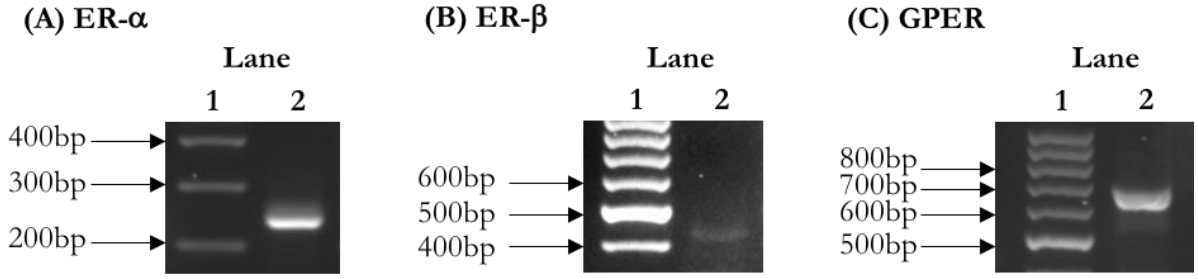

Figure 3.20: Primary vaginal epithelial cells express estrogen receptors. End-point PCR was performed on cDNA from PVECs for (A) ER-α at 236bp, (B) ER-β at 439bp, and (C) GPER at 680bp. The 100bp ladder (New England BioLabs, USA) is shown in lane 1 of each gel, and the respective PCR product is shown in lane 2.

3.8.2 Designing a SYBR-green based hBD2 qPCR assay

The probes-based hBD2 qPCR assay was not very sensitive at high cycle numbers (when gene expression was low). The reported cycle numbers for in-plate replicates of the same sample would vary by 2-3 cycle numbers, in samples with cycle numbers above 28 cycles. This meant a reported difference of 4-8 fold for the same sample. As only a limited number of epithelial cells could be extracted from each patient sample it was important to be able to accurately detect mRNA levels in the primary cell samples without needing to repeat the qPCR experiments to obtain reliable data. Thus, the hBD2 qPCR assay was redesigned as a SYBR-green based assay, as the hBD3 SYBR-green based assay was accurate at high cycle numbers. When designing the SYBR-green based hBD2 assay the primers were designed to anneal to a sequence within the probes-based assay PCR product. This meant the same positive control plasmid could be used with the new assay. A new standard curve was produced using the new primers and SYBR-green reagent and a melt peak confirmed that only one PCR product was amplified. This hBD2 qPCR assay was used for the remainder of the analyses.

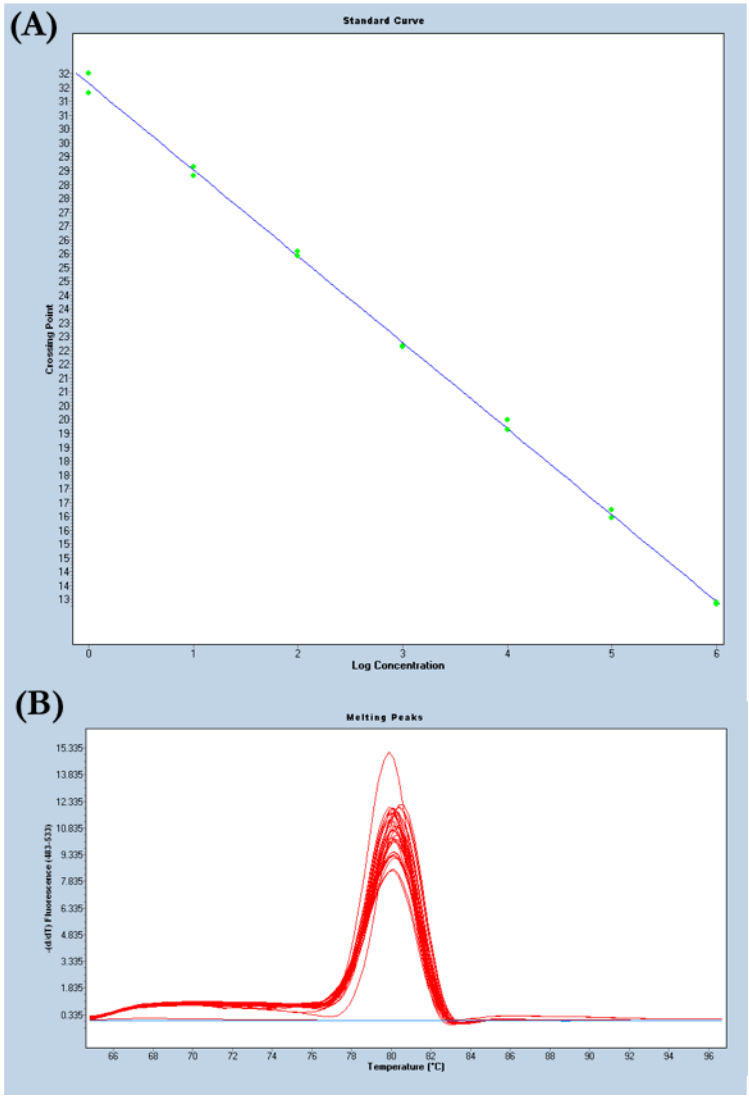

Figure 3.21: Standard curve and melt peak for SYBR-green based qPCR assay. A standard curve (A) was produced for the SYBR-green based hBD2 qPCR assay. The melt peak (B) confirmed that the assay only amplified one PCR product.

3.8.3 Effects of estrogen pretreatment on hBD2 and hBD3 expression in PVECs

To analyse the effects of estrogen pretreatment on hBD2 and hBD3 expression in PVECs, the isolated PVECs were treated with 4nM estrogen, or cyclodextrin vehicle, from seeding to confluency, which took between 5-10 days depending on the tissue sample. Once confluent, the cells were challenged with 50ng/ml flagellin, or PBS, for 24 hours. Initially PVECs were seeded into EpiLife medium (Thermo Fisher Scientific, UK), which is recommended for the growth of human keratinocytes and epithelial cells. Data from one patient sample with two replicates is shown in Figure 3.22 and demonstrated that hBD2 expression increased from 0.4AU in the control to 100AU following 24 hours flagellin challenge. Estrogen pretreatment plus flagellin further increased hBD2 gene expression to 157AU, representative of a 1.6-fold compared to flagellin alone.

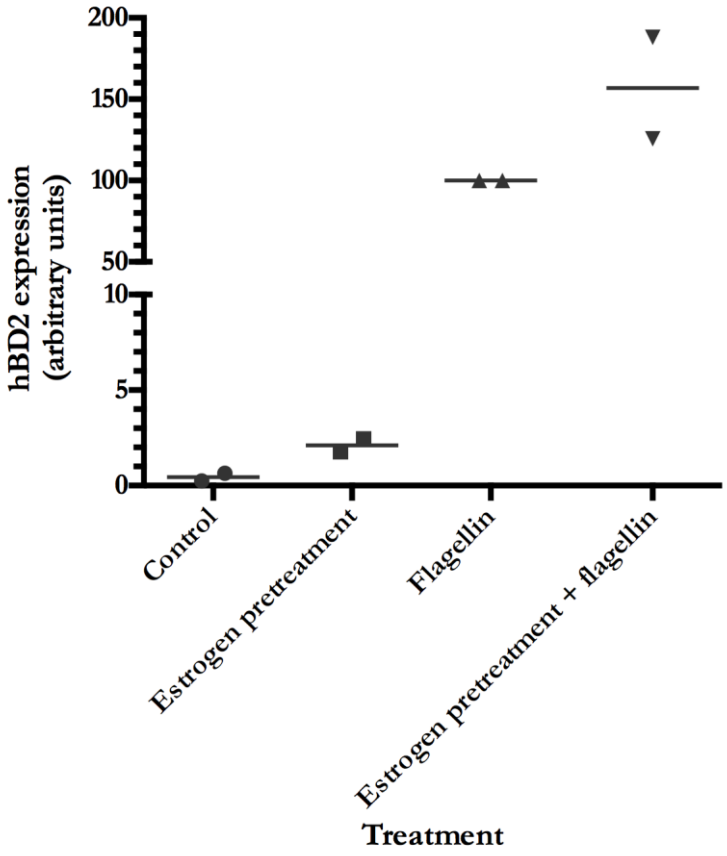

Figure 3.22: Effects of estrogen pretreatment and flagellin on hBD2 expression in primary vaginal epithelial cells growth in EpiLife medium. PVECs were harvested from vaginal tissue samples and seeded into 6-well plates in keratinocyte-SFM. The cells were treated with 4nM estrogen, or cyclodextrin vehicle, for approximately 7 days, and then challenged with 50ng/ml flagellin for 24 hours. RNA was extracted and analysed by qPCR for hBD2 expression. The data represent one patient sample with two replicates.

Results from the same patient sample for hBD3 showed that flagellin challenge increased hBD3 expression from 12AU in the control to 100AU after flagellin challenge. After estrogen pretreatment plus flagellin one replicate exhibited a 20% increase in hBD3 expression, compared to flagellin alone, and the second replicate showed a 40% decrease in hBD3 expression, compared to flagellin alone (Figure 3.23). Thus, on average hBD3 expression with estrogen pretreatment plus flagellin was similar to that with flagellin only (90AU and 100AU, respectively).

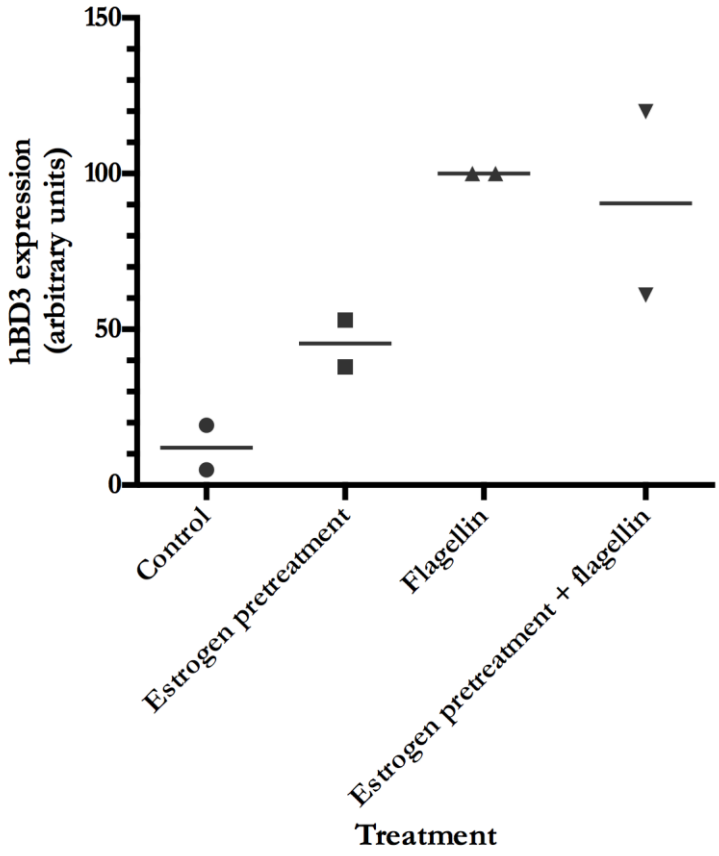

Figure 3.23: Effects of estrogen pretreatment and flagellin on hBD3 expression in primary vaginal epithelial cells growth in EpiLife medium. PVECs were harvested from vaginal tissue samples and seeded into 6-well plates in keratinocyte-SFM. The cells were treated with 4nM estrogen, or cyclodextrin vehicle, for approximately 7 days, and then challenged with 50ng/ml flagellin for 24 hours. RNA was extracted and analysed by qPCR for hBD3 expression. The data represent one patient sample with two replicates.

However, although initial results were encouraging, growth of the PVECs in EpiLife medium proved difficult. Typically, PVECs would adhere to the plate in small numbers, but not divide and grow. Thus, the primary cell culture required optimisation. Growth of the PVECs in keratinocyte-SFM, used to culture VK2 cells, was tried, but the results were similar to those using EpiLife medium in that cell division and growth did not occur. However, culturing PVECs in Dulbecco's Modified Eagle's Medium (DMEM) with 10% fetal calf serum (FCS) resulted in good growth of the PVECs. Thus, PVECs were seeded into 6- or 12-well plates in DMEM containing 10% FCS and were treated with 4nM estrogen, or cyclodextrin vehicle, for approximately seven days. Before the challenge, the DMEM was removed, cells were washed with PBS and keratinocyte-SFM was added to the cells, with estrogen or cyclodextrin. After 24 hours incubation in keratinocyte-SFM, the PVECs were challenged with flagellin for 24 hours. The RNA was extracted and analysed by qPCR for hBD2 and hBD3 expression.

The results for hBD2, in Figure 3.24, showed that both flagellin and estrogen pretreatment plus flagellin significantly increased hBD2 expression compared to control samples ($p<0.0001$). Mean

hBD2 expression in the control samples was 0.7AU, and this increased significantly to 100AU and 93AU following flagellin and estrogen pretreatment plus flagellin, respectively. However, compared to flagellin challenge alone, estrogen pretreatment prior to flagellin challenge did not significantly alter hBD2 expression.

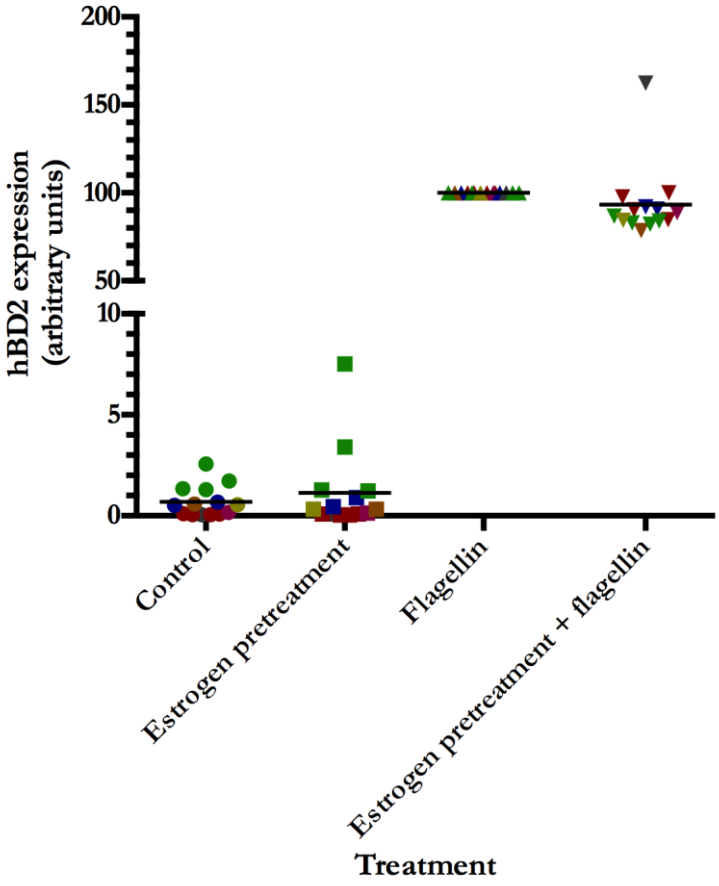

Figure 3.24: Effects of estrogen pretreatment and flagellin on hBD2 expression in primary vaginal epithelial cells grown in DMEM medium. PVECs were harvested from vaginal tissue samples and seeded into 6-well plates in DMEM containing 10% FCS. The cells were treated with 4nM estrogen, or cyclodextrin vehicle, for approximately 7 days, and then challenged with 50ng/ml flagellin for 24 hours. RNA was extracted and analysed by qPCR for hBD2 expression. The data represent 7 patient samples with 14 replicates. Symbols are colour coded according to patient. Statistical analysis was performed by one-way ANOVA with Tukey's post hoc test.

The results for hBD3 showed more variability than those for hBD2. The mean hBD3 expression in the control samples was 35AU. This increased significantly to 100AU and 86AU following flagellin challenge and estrogen pretreatment plus flagellin challenge, respectively ($p<0.001$). Six of the 14 replicates showed increased expression with estrogen pretreatment plus flagellin challenge compared to flagellin alone, however, eight replicates showed reduced expression following estrogen pretreatment plus flagellin. Thus, overall, hBD3 expression showed a 14% decrease in expression following estrogen pretreatment plus flagellin challenge, compared to flagellin challenge alone, but this difference in expression was not statistically significant ($p=0.6789$).

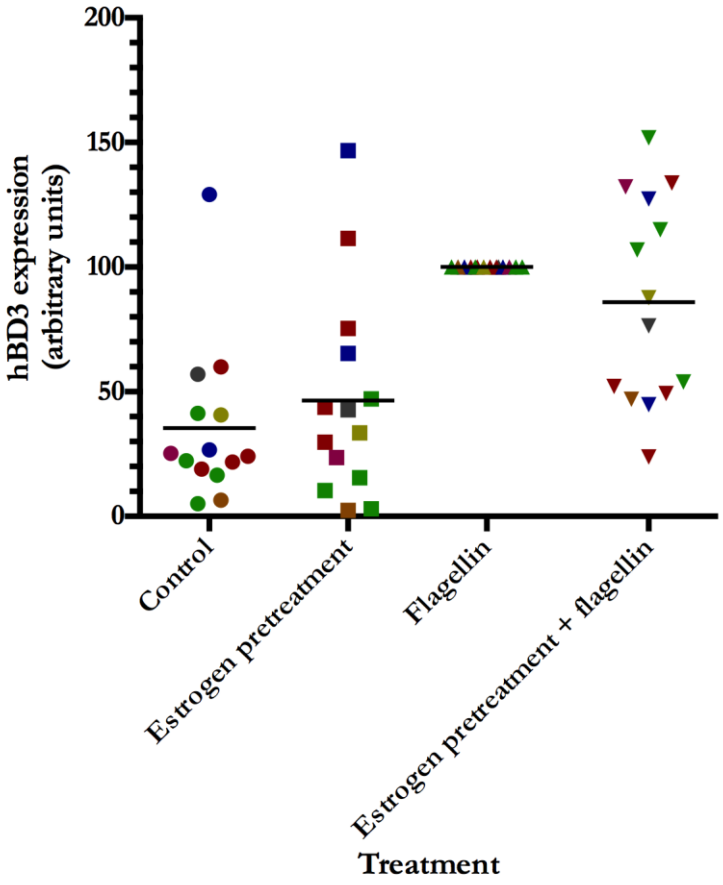

Figure 3.25: Effects of estrogen pretreatment and flagellin on hBD3 expression in primary vaginal epithelial cells grown in DMEM. PVECs were harvested from vaginal tissue samples and seeded into 6-well plates in DMEM containing 10% FCS. The cells were treated with 4nM estrogen, or cyclodextrin vehicle, for approximately 7 days, and then challenged with 50ng/ml flagellin for 24 hours. RNA was extracted and analysed by qPCR for hBD3 expression. The data represent 7 patient samples with 14 replicates. Symbols are colour coded by patient. Statistical analysis was performed by one-way ANOVA with Tukey's post hoc test.

3.8.4 Cultured human primary cells express cytokeratins

The data obtained with PVECs cultured in DMEM with 10% FCS showed a different pattern to the data obtained with PVECs cultured in EpiLife medium. Thus, it was important to analyse the authenticity of the cells and confirm they were indeed epithelial. To investigate this the cytokeratin expression of the PVECs cultured in DMEM was investigated. Cytokeratins constitute the intermediate filaments of all epithelial cells and thus can be used as epithelial cell markers. End-point PCR was performed for cytokeratin 8 and 18 in the PVECs and VK2 cells to confirm that the primary cells were indeed epithelial. Cytokeratin 8 and 18 are typically co-expressed in many epithelial cells, including vaginal cells[209,210]. The end-point PCR detected products at 190bp and 207bp, representative of cytokeratin 8 and cytokeratin 18, respectively, in both VK2 cells and PVECs. This indicated that the PVECs cultured from human vaginal tissue samples were true epithelial cells (Figure 3.26).

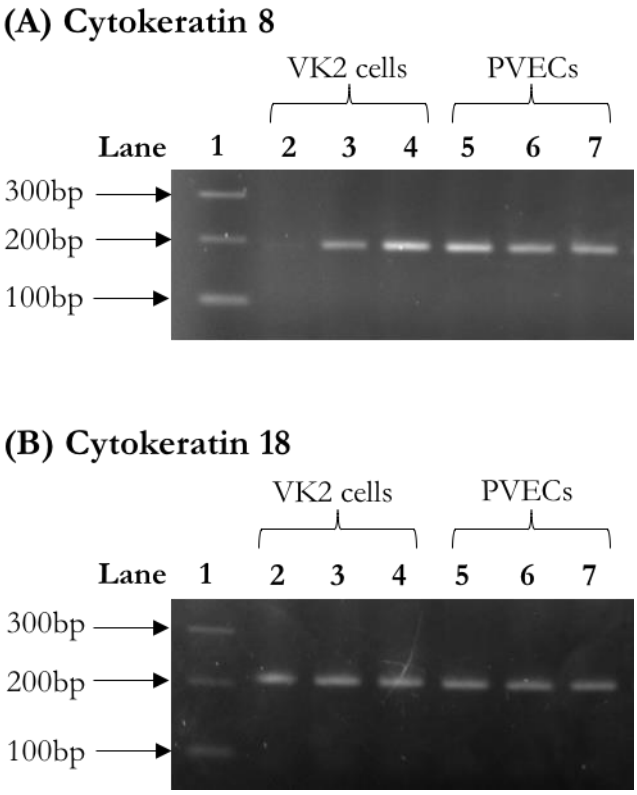

Figure 3.26: End-point PCR for cytokeratins 8 and 18. End-point PCR products for (A) cytokeratin 8 at 190bp and (B) cytokeratin 18 at 207bp in VK2 and primary cells. Lane 1 shows the Generuler 100bp ladder (Thermo Fisher Scientific, USA), lanes 2-4 show PCR products from VK2 cells, and lanes 5-7 show PCR products amplified from primary vaginal epithelial cells (PVECs).

The presence of cytokeratins in the PVECs was also confirmed by immunocytochemistry using a C-11 anti-cytokeratin antibody that detected cytokeratins 4, 5, 6, 8, 10, 13 and 18. For immunocytochemistry, the PVECs were seeded onto sterile glass coverslips in DMEM with 10% FCS, and were grown until confluent. The cells were fixed using methanol and stained using the mouse C-11 anti-pan cytokeratin primary antibody (Abcam, UK) and the Alexa Fluor 488 rabbit anti-mouse secondary antibody (Thermo Fisher Scientific, USA).

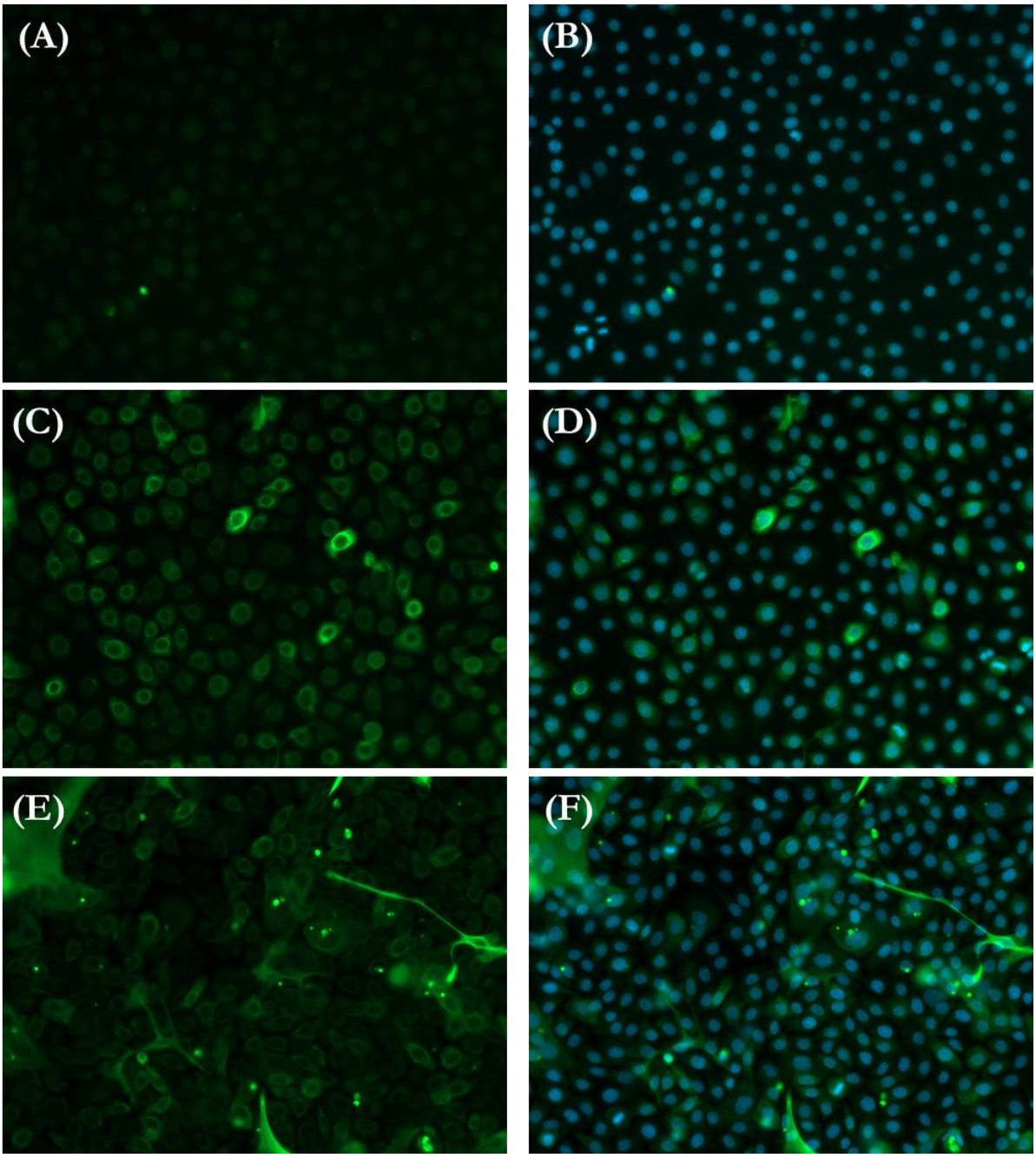

Figure 3.27: Cytokeratin staining in VK2 and primary vaginal epithelial cells. VK2 and PVECs were stained using the mouse C-11 anti-pan cytokeratin primary antibody (1:20, Abcam, UK) and the Alexa Fluor 488 (green) rabbit anti-mouse secondary antibody (1:500, Thermo Fisher Scientific, USA). Nuclei were stained with DAPI (blue). (A) Alexa Fluor 488 and (B) Alexa Fluor 488 +DAPI staining of VK2 cells stained without the primary antibody, as a negative control. (C) Alexa Fluor 488 and (D) Alexa Fluor 488 + DAPI staining of VK2 cells stained with both primary and secondary antibodies. (E) Alexa Fluor 488 and (F) Alexa Fluor 488 + DAPI staining of primary vaginal epithelial cells stained with both primary and secondary antibodies. All images were taken on Zeiss Axio Imager II microscope at x40 magnification with exposure of 274.6ms for Alexa Fluor 488 and 13.8ms exposure for DAPI.

VK2 cells were stained as a positive control, as these cells are known to be epithelial. The VK2 cells stained with both primary and secondary antibodies (Figure 3.27C and D) demonstrated much stronger Alexa Fluor 488 (green) staining, compared to the negative control stained with secondary antibody only (Figure 3.27A and B). This indicated that the VK2 cells synthesised cytokeratins and were epithelial, as expected. The PVECs also stained positively for cytokeratins,

to a similar level as VK2 cells, confirming that the cells isolated from the human vaginal tissue samples were indeed epithelial (Figure 3.27E and F).

3.9 Discussion

It is hypothesised that estrogen has a protective role against UTIs due to the increased risk of women developing rUTI after the menopause[13]. One possible mechanism of protection by estrogen is prevention of uropathogen colonisation of the vagina by increasing vaginal glycogen. This encourages growth of commensal bacteria, such as *Lactobacillus* spp., which metabolise glycogen and produce lactic acid. Although colonisation with *Lactobacillus* spp. has been shown to limit UPEC growth in numerous ways, the primary mechanism of action is thought to be through lowering the pH of the vagina[184,189]. A pH below 4.5 has been shown to prevent the growth of uropathogens[190]. However, few studies have considered the effect of estrogen on innate defences of the urogenital tract.

Data presented in this chapter showed that estrogen has a role in priming the innate immune response to infection, when given as a long-term treatment. Acute estrogen treatment of VK2 cells, an immortalised vaginal epithelial cell line, had no effect on hBD2 expression and a minimal effect on hBD3 expression after 24 hours. However, estrogen pretreatment of VK2 cells prior to challenge with flagellin upregulated both hBD2 and hBD3 expression by greater than 2-fold compared to cells challenged with flagellin without estrogen pretreatment. This potentiation by estrogen was evident after 8 hours challenge for both AMPs. Furthermore, estrogen pretreatment plus flagellin induced hBD3 expression 16 hours earlier than flagellin challenge alone, suggesting that estrogen pretreatment not only promotes a greater antimicrobial response, but also brings about this response quicker than cells not pretreated with estrogen. The qPCR data was supported by hBD2 luciferase reporter assay data, which showed that estrogen pretreatment plus flagellin challenge resulted in greater reporter activity than flagellin challenge alone. Thus, the effects of estrogen on hBD2 expression were confirmed by two separate approaches.

Taken together, these data suggest that vaginal epithelial cells require the presence of estrogen prior to infection for the antimicrobial effects of estrogen to be observed. One possible explanation for the differences observed between acute and long-term estrogen is that estrogen may upregulate components of the flagellin signalling pathway, such as TLR5 and NF-κB. Upregulation of components such as these by estrogen pretreatment prior to challenge would result in greater TLR5 pathway activation upon challenge with flagellin, thus increasing hBD2 and hBD3 expression. Whereas, upregulation of TLR5 pathway components by acute estrogen

would occur too late for any effects to be seen. Broader gene expression analysis of pathway constituents is needed to determine whether this is the mechanism of estrogen action and was conducted using microarray analysis in the next chapter.

Both hBD2 and hBD3 have been shown to have potent killing activity against Gram-negative bacteria. Thus increased expression of these AMPs may promote UPEC clearance from the urogenital tract. *In vivo* activity of AMPs is determined by their salt sensitivity, and the literature reports conflicting findings over the salt sensitivity of hBD2 and hBD3. Some studies suggest that hBD2 is sensitive to physiological concentrations of sodium chloride (0-200mM), limiting its ability to kill *E. coli*[211,212]. However, a study by Zhao *et al.* (2011), showed that transfection of a plasmid containing the hBD2 gene downstream of a CMV promoter into bladder cells of live rats resulted in much faster clearance of UPEC from the bladder than rats transfected with a vector control[213]. This clearly suggests that hBD2 is functional at physiological salt concentrations of the urogenital tract and facilitates bacterial killing. hBD3 is often reported as salt insensitive, however, studies that reported this typically used a maximum of 150mM sodium chloride[214]. More recently, Scudiero *et al.* (2010) used higher concentrations of sodium chloride and found that hBD3 was inactivated by 200mM sodium chloride[215]. Interestingly, a study by Jung *et al.* (2011) reported that at high salt concentrations (>100mM) hBD3 was inactive against *E. coli*, but retained activity against *S. aureus*, whereas, at the same sodium chloride concentrations hBD2 displayed activity against *E. coli*, but not *S. aureus*[216]. This suggests that the salt concentration at the site of antimicrobial peptide action has a role in determining which bacteria AMPs are active against. The vaginal sodium chloride concentration is in the region of 60mM, and thus it is likely that both peptides maintain *E. coli* killing capabilities within the vagina[217–219]. However, further work is required in this area to further understand hBD2 and hBD3 activity during vaginal colonisation with UPEC.

Previous work from our laboratory showed a reduction in hBD2 and hBD3 concentration in vaginal douches of postmenopausal women, compared to premenopausal women[60]. Furthermore, the vaginal concentration of both hBD2 and hBD3 was significantly increased in postmenopausal women receiving estrogen treatment, compared to postmenopausal women not receiving estrogen treatment. This is supportive of the work presented in this chapter as these data suggest regulation of hBD2 and hBD3 by estrogen *in vivo*. Additional evidence of a role for estrogen in *in vivo* AMP regulation comes from a paper by Luthje *et al.* (2013) who measured AMP expression in exfoliated cells from the urine of postmenopausal women before and after a two week course of 25µg/day topical vaginal estrogen treatment[134]. Luthje *et al.* reported an increase in hBD2, hBD3 and psoriasin in exfoliated urothelial cells following estrogen supplementation. The

expression of hBD1, RNase7 and LL-37 were also enhanced by estrogen in immortalised bladder epithelial cells. Thus, this work is intriguing as it not only supports the notion of estrogen regulation of other AMPs, in addition to hBD2 and hBD3, but also suggests that topical estrogen treatment of the vagina may also have protective effects in the bladder. *In vitro* work by Han *et al.* (2010) has also shown that physiological estrogen concentrations increased hBD2 expression from human PVECs during challenge with LPS, supporting a role for estrogen in the vaginal antimicrobial response. However, a conflicting paper from Patel *et al.* (2013) reported that 48 hour treatment of human PVECs with 50nM estrogen reduced hBD2 secretion by approximately 50% compared to PVECs that were not treated with estrogen[199,220]. These differences may perhaps be attributed to the method of vaginal cell collection; Han *et al.* collected vaginal epithelial cells from vaginal tissue removed during surgery, whereas Patel *et al.* collected sloughed vaginal cells in a menstrual cup. The latter is less representative of intact cells in the vaginal epithelium. Furthermore, Patel *et al.* report data from only 2-3 patients and used an estrogen concentration much greater than physiological concentrations, suggesting these data should be interpreted with caution. Analysis of hBD2 and hBD3 expression in PVECs was attempted in this chapter, but proved difficult. Initial results obtained with PVECs cultured in EpiLife medium appeared to mirror VK2 cell data, however, generally this medium was not sufficient to promote primary cell growth and typically resulted in adhesion of primary cells to the culture plate but no cell division. Thus, the cells were cultured in DMEM containing 10% FCS, which did facilitate growth of the PVECs to a confluent monolayer. However, cells cultured in this medium did not show increased hBD2 and hBD3 expression with estrogen pretreatment prior to flagellin challenge. The DMEM contained phenol red and FCS, which are both estrogenic, and therefore, it cannot be excluded that culturing the primary cells in this medium diminished the effects of estrogen supplementation. Further optimisation of the PVEC culture technique is clearly required before conclusions can be drawn from the primary cell data presented here.

The secretion of hBD2 and hBD3 by VK2 cells was measured by ELISA. The hBD2 ELISA showed increased secretion of hBD2 into the cell culture medium following challenge with flagellin. However, estrogen pretreatment prior to flagellin challenge did not increase hBD2 secretion further. In-plate replicates of the cell culture medium samples and recombinant hBD2 standards below 125pg/ml displayed variability in the reported peptide concentration, suggesting the ELISA may not be sufficiently sensitive for this application despite the kit stating the lower limits of detection as 8pg/ml. It is, therefore, possible that the assay is not sensitive enough to detect differences in hBD2 concentration between the flagellin and estrogen pretreatment plus flagellin samples. The hBD3 ELISA showed no increase in hBD3 secretion with any of the treatments. However, the hBD3 standard curve demonstrated a correlation between hBD3

concentration and signal detected, indicating that there was not an issue with the capture or detection antibodies. The mRNA data showed that flagellin only begins to induce hBD3 expression at the 24 hour time point, thus, the 24 hour time point may be too early to detect changes in hBD3 secretion from VK2 cells. Future work should include analysis of both mRNA and peptide levels at later time points, to fully establish the effects of estrogen pretreatment and flagellin on hBD3 secretion. Previous work from our laboratory has utilised these ELISAs to measure the hBD2 and hBD3 concentration of vaginal douches of postmenopausal women. Postmenopausal women who were not receiving topical estrogen treatment had vaginal hBD2 and hBD3 concentrations of 62±6pg/ml (SEM) and 86±9pg/ml (SEM), respectively[60]. Whereas, the vaginal concentration of hBD2 and hBD3 in postmenopausal women who were receiving topical estrogen treatment was 119±13pg/ml (SEM) and 139±17pg/ml (SEM), respectively. These data indicate that estrogen significantly increased hBD2 and hBD3 secretion from vaginal epithelial cells *in vivo*. Furthermore, Han *et al.* (2010) demonstrated that 2nM estrogen increased hBD2 peptide secretion from PVECs *in vitro*[199]. Taken together these data suggest that estrogen increases hBD2 and hBD3 secretion from vaginal epithelial cells and that further investigation and optimisation of the ELISAs used here is needed to confirm this in the VK2 cell model.

The data presented in this chapter is supported by other work showing estrogen has a role in upregulation of AMPs, and especially hBD2 and hBD3, indicating validity of the data[60,134,199]. However, the mechanism behind this upregulation has not been investigated. Understanding the regulation of innate immune defences in response to UTIs is important, as this is the hosts primary defence against uropathogens since an acquired immune response is not protective against rUTIs[136,221,222]. Furthermore, as Luthje *et al.* identified upregulation of multiple other AMPs, it is of interest to investigate the effect of estrogen on other innate immune defences of the urogenital tract and whether the mechanism of estrogen regulation is common among AMPs. This, along with regulation of upstream signalling pathway components, will be investigated in more detail in the next chapters.

Overall, data presented in this chapter identify a role for estrogen in augmenting the innate immune response to vaginal colonisation with UPEC, exemplified here by hBD2 and hBD3. Thus, the benefits of estrogen treatment may go beyond increased vaginal glycogen production, by increasing the vaginal antibacterial response to infection. Hence loss of estrogen following the menopause results in decreased vaginal AMP expression, along with a decrease in vaginal lactobacilli colonisation, facilitating establishment of vaginal colonisation with UPEC, and exacerbating the cycle of rUTI. Identification of other innate immune effectors regulated by

estrogen and the mechanism of regulation may aid development of future therapeutics to prevent rUTI and will be investigated further in the following chapters.

4 Analysis of global gene expression by microarray

4.1 Introduction

Data presented in this thesis has shown that estrogen pretreatment of a vaginal epithelial cell line prior to challenge with flagellin potentiated the expression of the AMPs hBD2 and hBD3, compared to the expression levels measured for flagellin challenge without estrogen pretreatment. Acute estrogen treatment did not potentiate hBD2 expression and only resulted in minimal potentiation of hBD3 expression. This suggested that estrogen pretreatment primes the vaginal epithelial cells prior to exposure to bacterial PAMPs. It is possible that estrogen pretreatment enhanced hBD2 and hBD3 expression by upregulating expression of the signalling pathway components for these genes. Upregulation of signalling pathway components by estrogen pretreatment could facilitate greater activation of the pathway upon flagellin challenge. Thus, it was of interest to utilise microarrays to conduct broad gene expression analysis to investigate the mechanism of hBD2 and hBD3 upregulation by estrogen pretreatment. In addition, whole transcriptome analysis by microarray would identify other genes associated with innate immunity that were upregulated by estrogen pretreatment, such as other AMPs.

For the analysis conducted in this thesis, the Illumina HumanHT-12 v4 Expression Beadchip was used. This microarray chip utilises more than 47,000 50mer probes attached to silica beads to analyse the expression level of 31,000 annotated genes derived from the NCBI RefSeq Release 38. The cDNA samples to be analysed were labelled with biotin and following hybridisation the bound cDNA was visualised by streptavidin-Cy3 staining. Each gene probe is hybridised to a known location on the chip, thus the signal from each probe can be measured. The hybridisation of biotin labelled cDNA to the probe is shown in Figure 4.1.

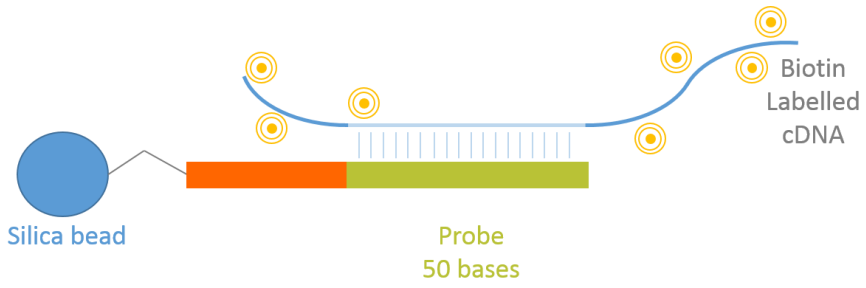

Figure 4.1: Diagram of biotin labelled cDNA binding to probe. 50mer probes are attached to the microarray chip by silica beads. Biotin labelled cDNA hybridises with complementary probes sequences and can be visualised to determine the level of gene expression.

4.2 Sample selection and analysis of RNA quality

To perform microarray analysis RNA samples previously analysed by qPCR were selected. Control cells along with estrogen pretreatment, flagellin, and estrogen pretreatment plus flagellin challenged cells at the 12 and 24 hour time points were selected for microarray analysis, based upon the qPCR results obtained for hBD2 and hBD3. Three technical replicates of each treatment from one biological repeat were analysed. Following RNA extraction, RNA samples were sent to Service XS, The Netherlands for microarray analysis.

Before microarrays were performed the RNA samples were analysed using the Agilent RNA 6000 Nano Kit and the Agilent 2100 Bioanalyser to ensure the RNA was of high enough quality to achieve accurate and reliable results. The kit analyses the quality of the 18S and 28S ribosomal RNA and calculates an RNA integrity number (RIN) out of ten for each sample. An RIN above 7 indicates high quality RNA. The ribosomal RNA quality was very good for all 24 samples (Figure 4.2) and the RIN was calculated to be 10 for each sample. Thus, the RNA was very high quality and was suitable for microarray analysis.

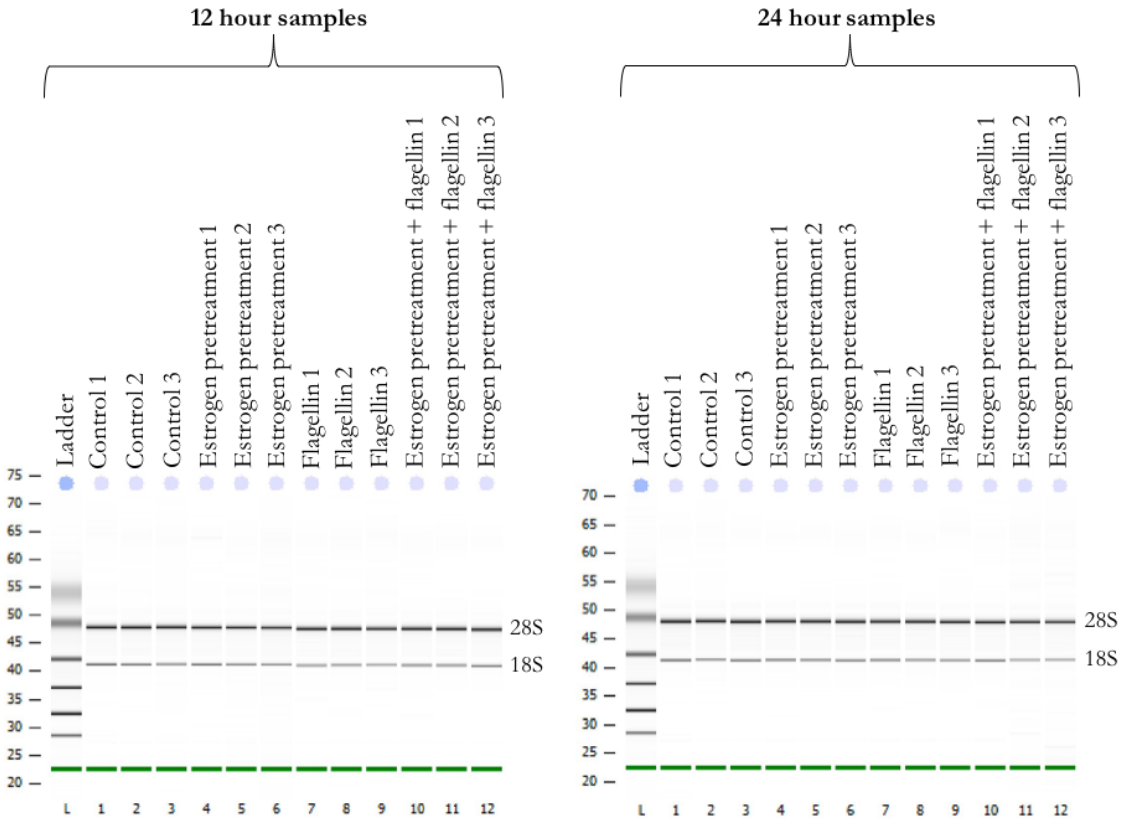

Figure 4.2: RNA quality analysis by ServiceXS. The Agilent RNA 6000 Nano Kit and Agilent 2100 Bioanalyser were used to check the quality of the 18S and 28S ribosomal RNA of the RNA samples.

Microarrays were performed using an Illumina HumanHT-12 v4 Expression Beadchip and the resultant raw expression values were analysed in collaboration with the Bioinformatics Support Unit, Newcastle University, where the raw data was normalised and converted into fold changes relative to the control at each time point using the R software platform with Bioconductor[223,224]. This resulted in six datasets for further analysis and these are shown in Table 4.1. Genes were considered to be significantly differentially expressed if they had a fold change greater than or equal to +2 or less than or equal to -2 and a p-value less than 0.05. The cut off of +/- 2 fold change is a commonly used cut off value which excludes genes with small fold changes and keeps gene lists to a manageable size for initial analysis. The full list of differentially expressed genes after 12 and 24 hours is shown in the Appendix Table 8.1 and Table 8.2, respectively.

Table 4.1: Description of microarray dataset abbreviations.

Dataset abbreviation	Description
EP12	Estrogen pretreatment 12 hours vs control 12 hours
F12	Flagellin 12 hours vs control 12 hours
EP/F12	Estrogen pretreatment + flagellin 12 hours vs control 12 hours
EP24	Estrogen pretreatment 24 hours vs control 24 hours
F24	Flagellin 24 hours vs control 24 hours
EP/F24	Estrogen pretreatment + flagellin 24 hours vs control 24 hours

4.3 Venn diagram analysis

Venn diagrams were constructed to show genes that were commonly differentially regulated by each of the treatments. Each entry in the Venn diagram represents a single probe set. On a microarray chip multiple probe sets may map to the same gene. Figure 4.3 shows the Venn diagram produced for each of the treatments after 12 hours. There were five genes that were differentially expressed by all three treatments (EP12, F12, and EP/F12) and these were lipocalin 2 (LCN2), S100 calcium binding protein A8 (S100A8), S100A9, small proline rich protein 2A (SPRR2A) and SPRR2F. All five of these genes showed significant upregulation with each treatment.

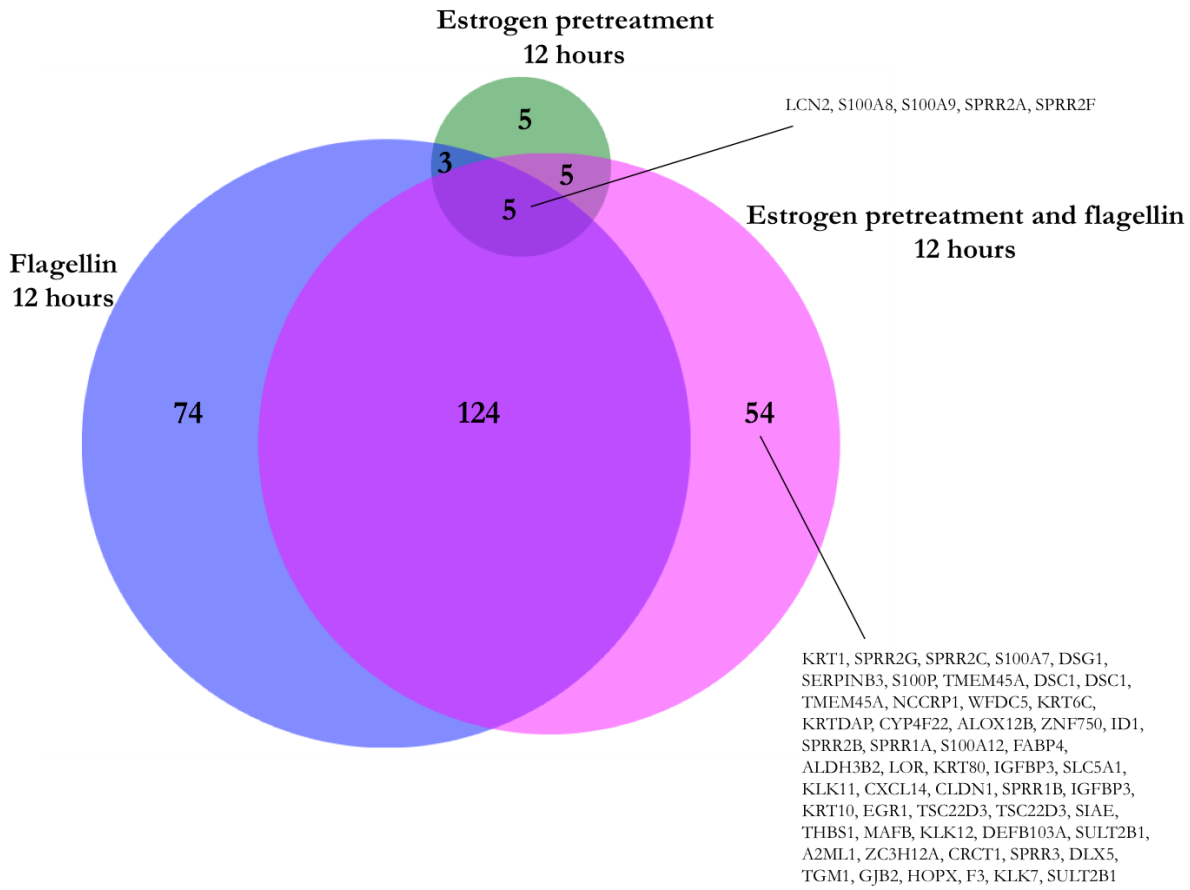

Figure 4.3: Venn diagram of differentially regulated genes after 12 hours. Venn diagrams drawn using BioVenn[201].

LCN2 is an iron sequestering antimicrobial protein, S100 genes encode calcium binding proteins involved in many cellular response including differentiation and immune responses, and the SPRR genes encode proteins involved in keratinisation. Further examination of the microarray data revealed that for each of the five genes EP/F12 resulted in the highest level of expression (Figure 4.4), followed by F12, and then EP12. For each of the genes EP12 alone resulted in an approximate 2.0-fold increase in gene expression, compared to controls, F12 resulted in increased gene expression between 2.2-fold and 6.4-fold, and EP/F12 saw the highest increases in gene expression between 3.4-fold and 15-fold. This pattern was not as marked for S100A8, but was still present as fold changes of 2.0, 2.2, and 3.4 were observed with EP12, F12, and EP/F12 treatments, respectively. In contrast, the increase in gene expression with EP/F12 was particularly notable for SPRR2A and SPRR2F, which exhibited 13- and 15-fold changes in gene expression, respectively, compared to 4.0- and 3.6-fold changes, respectively, with F12 treatment. These data indicate that estrogen pretreatment prior to flagellin challenge potentiated the expression of these genes.

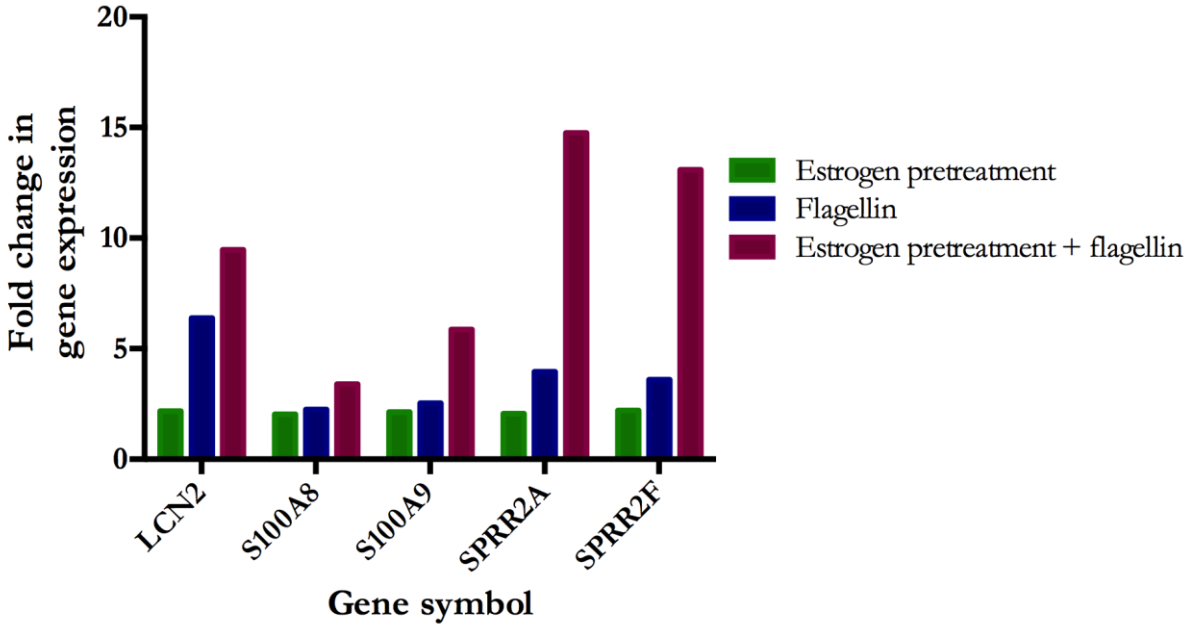

Figure 4.4: Fold change in expression of genes upregulated by estrogen pretreatment, flagellin, and estrogen pretreatment plus flagellin, as determined by microarray.

Previous qPCR data shown in Chapter 3 demonstrated that estrogen pretreatment alone had little effect on the expression of hBD2 and hBD3. Nevertheless, combined estrogen pretreatment plus flagellin challenge potentiated the expression of hBD2 and hBD3 compared to flagellin challenge alone. This may, therefore, be the case for other genes and thus it was important to consider the genes that were upregulated by both F12 and EP/F12, but not EP12.

After 12 hours there were 124 gene probes that fell into this category. All 124 genes showed significant upregulation with the two treatments. Within this set of 124 genes, genes with substantially higher expression with EP/F12 compared to F12 alone were identified. After 12 hours there were only six gene probes out of 124 that exhibited higher expression with EP/F12 than with F12, suggesting potentiation of gene expression by estrogen. These six probes were DEFB4A, IL36G, SERPINB4, SPRR2D, and two probes for SPRR2E. The fold change in gene expression of each of these genes after F12 and EP/F12 treatment is shown in Table 4.2 and ranged from 2.1- to 3.1-fold change with F12 treatment to 4.3- to 13.5-fold change with EP/F12 treatment. As mentioned previously, DEFB4A encodes the antimicrobial peptide hBD2 and the SPRR genes are involved in keratinisation. The SERPINB4 gene encodes the serpin peptidase inhibitor, clade B (ovalbumin), member 4 protein, which is involved in inflammation and immunity, and the IL36G gene encodes the proinflammatory cytokine interleukin 36 gamma.

Table 4.2: Fold change in gene expression of genes upregulated by flagellin and estrogen treatment plus flagellin, after 12 hours.

		Fold change after 12 hours	
Gene ID	**Gene symbol**	**Flagellin**	**Estrogen pretreatment + flagellin**
ILMN_2048043	DEFB4A	2.4	5.1
ILMN_2158713	IL36G	2.7	4.3
ILMN_1782716	SERPINB4	2.9	6.5
ILMN_2191967	SPRR2D	2.1	5.7
ILMN_1701239	SPRR2E	2.5	10.8
ILMN_2211018	SPRR2E	3.1	13.5

Conversely, there were also genes from this group that showed higher expression with F12 treatment than with EP/F12 treatment. Many of these genes have functions related to inflammation and the antiviral response. For example, the 2'-5'-oligoadenylate synthetase 1, 40/46kDa (OAS1) gene, which is involved in inhibition of viral replication, exhibited 17.2-fold change in gene expression with F12 treatment, and 10.4-fold change with EP/F12 treatment. Likewise, the chemokines CXCL10 and CCL5 had fold changes of 42 and 9.6, respectively, after F12 treatment and 16 and 4.6, respectively, after EP/F12 treatment. Additionally, the Venn diagram identified 74 gene probes that were only upregulated by F12 treatment. These were also mostly antiviral and inflammatory genes such as 2'-5'-oligoadenylate synthetase-like (OASL, 4.8-fold change with F12) and interferon-induced protein with tetratricopeptide repeats 3 (IFIT3, 3.5-fold change with F12), which both inhibit viral replication and caspase 1, apoptosis-related cysteine peptidase (CASP1, 2.1-fold change with F12), which induces cell apoptosis. These data suggest a clear role for estrogen in modulating the innate immune response to infection.

There were five genes that were upregulated by EP12 and EP/F12, but not by F12. These genes are shown in Table 4.3 and were cornifelin (CNFN), coagulation factor III (F3), late cornified envelope 3D (LCE3D), suprabasin (SBSN), and secretory leukocyte protease inhibitor (SLPI). These genes mostly have functions related to keratinisation and differentiation, except for F3, which is involved in blood coagulation, and SLPI, which is an AMP important in protecting epithelial cells from proteolytic enzymes. With the exception of F3, these genes show enhanced expression with EP/F12 than with EP12 indicating that the combined treatment amplified gene expression, despite there being no significant increase in the expression of these genes with F12 alone. This expression pattern indicated that these genes are typically expressed in the presence of estrogen and that their expression is augmented by flagellin challenge (i.e. during infection), however, without estrogen these genes were not significantly upregulated following flagellin challenge.

Table 4.3: Fold change in gene expression of genes upregulated by estrogen pretreatment and estrogen pretreatment plus flagellin, after 12 hours.

		Fold change after 12 hours	
Gene ID	**Gene symbol**	**Estrogen pretreatment**	**Estrogen pretreatment plus flagellin**
ILMN_1803838	CNFN	2.0	5.9
ILMN_1797009	F3	2.1	2.2
ILMN_1718395	LCE3D	2.1	5.8
ILMN_1712759	SBSN	2.1	4.4
ILMN_2114720	SLPI	2.2	3.2

There were three gene probes that were differentially regulated by EP12 and F12 but not EP/F12. These genes were lectin, galactose-binding, soluble, 7 (LGALS7) and two different gene probes for LGALS7B, and these genes are involved in cell-cell interactions in keratinocytes. Further examination of the microarray data revealed that these genes were all significantly downregulated by EP12 and F12 with approximately 0.38-fold change for each probe after each treatment. It is interesting that these genes were downregulated by both EP12 and F12, but not by EP/F12.

Finally, the Venn diagram also showed 54 gene probes that were differentially expressed by EP/F12 treatment but not by EP12 or F12 (see Figure 4.3). All 54 of these genes showed significant upregulation. The fact that these genes were not upregulated by EP12 or F12 suggested that neither of these treatments alone was sufficient to stimulate significant upregulation of these genes, however, when the two treatments were combined gene expression was significantly upregulated. Many of these genes, for example keratins (KRTs) and SPRR proteins are involved in keratinisation and differentiation, and may serve to strengthen the epithelial barrier during infection. However, this group of genes also contained the genes S100A7 (also known as psoriasin), S100A12 and DEFB103A, which are antimicrobial peptides. Thus, this suggested that estrogen pretreatment prior to flagellin challenge resulted in upregulation of genes that are not upregulated by estrogen or flagellin alone.

The 24 hour time point samples were also analysed using this method (Venn diagram shown in Appendix Figure 8.1) and this identified the genes RNASE7, SPRR2C, and SPRR2G as additional genes of interest as these genes also showed increased expression with EP/F24 treatment than with EP24 and F24 treatments (see Figure 4.5). Furthermore, analysis of the 24 hour datasets revealed that for many of the genes of interest EP/F24 treatment showed higher gene expression than EP/F12 treatment, whereas, F12 and F24 treatments exhibited similar fold changes in gene expression. These data suggested that estrogen pretreatment prior to flagellin challenge augmented the epithelial response to infection and the response continued to increase

up to at least 24 hours post-challenge, whilst flagellin challenge alone stimulated gene expression that did not increase from 12 to 24 hours.

Overall, these analyses identified a number of genes, detailed in Table 4.4, that are of interest due to their pattern of expression (shown in Figure 4.5) following estrogen and flagellin treatments. Compared to the response seen for genes such as the SPRRs, the increased gene expression with EP/F treatment for some of the genes, such as S100A8 and SLPI, was comparatively small and may not be physiologically relevant with regards to infection. Nevertheless, a number of these genes show a substantial increase in expression with EP/F treatment compared with F treatment alone; the SPRR2G gene exhibited a 22.5-fold increase in expression with EP/F24 treatment compared to a 3.3-fold change with F24. These genes primarily have functions in the immune response to pathogens or the keratinisation/differentiation process.

Table 4.4: Table of genes of interest and their functions after Venn diagram analysis.

Gene symbol	Gene name	Gene function(s)
DEFB103A	Human beta defensin 3	Antimicrobial peptide
DEFB4A	Human beta defensin 2	Antimicrobial peptide
LCN2	Lipocalin 2	Antimicrobial peptide
RNASE7	Ribonuclease, RNase A family, 7	Antimicrobial peptide
SLPI	Secretory leukocyte peptidase inhibitor	Antimicrobial peptide
S100A7	S100 calcium binding protein A7/Psoriasin	Antimicrobial peptide, keratinisation, inflammation
S100A12	S100 calcium binding protein A12	Antimicrobial peptide, keratinisation, inflammation
S100A8	S100 calcium binding protein A8	Keratinisation, inflammation
S100A9	S100 calcium binding protein A9	Keratinisation, inflammation
CNFN	Cornifelin	Keratinisation
LCE3D	Late cornified envelope 3D	Keratinisation
SBSN	Suprabasin	Keratinisation
SPRR2A	Small proline-rich protein 2A	Keratinisation
SPRR2C	Small proline-rich protein 2C	Keratinisation
SPRR2D	Small proline-rich protein 2D	Keratinisation
SPRR2E	Small proline-rich protein 2E	Keratinisation
SPRR2F	Small proline-rich protein 2F	Keratinisation
SPRR2G	Small proline-rich protein 2G	Keratinisation
IL36G	Interleukin 36 gamma	Inflammation
SERPINB4	Serpin peptidase inhibitor, clade B (ovalbumin), member 4	Inflammation

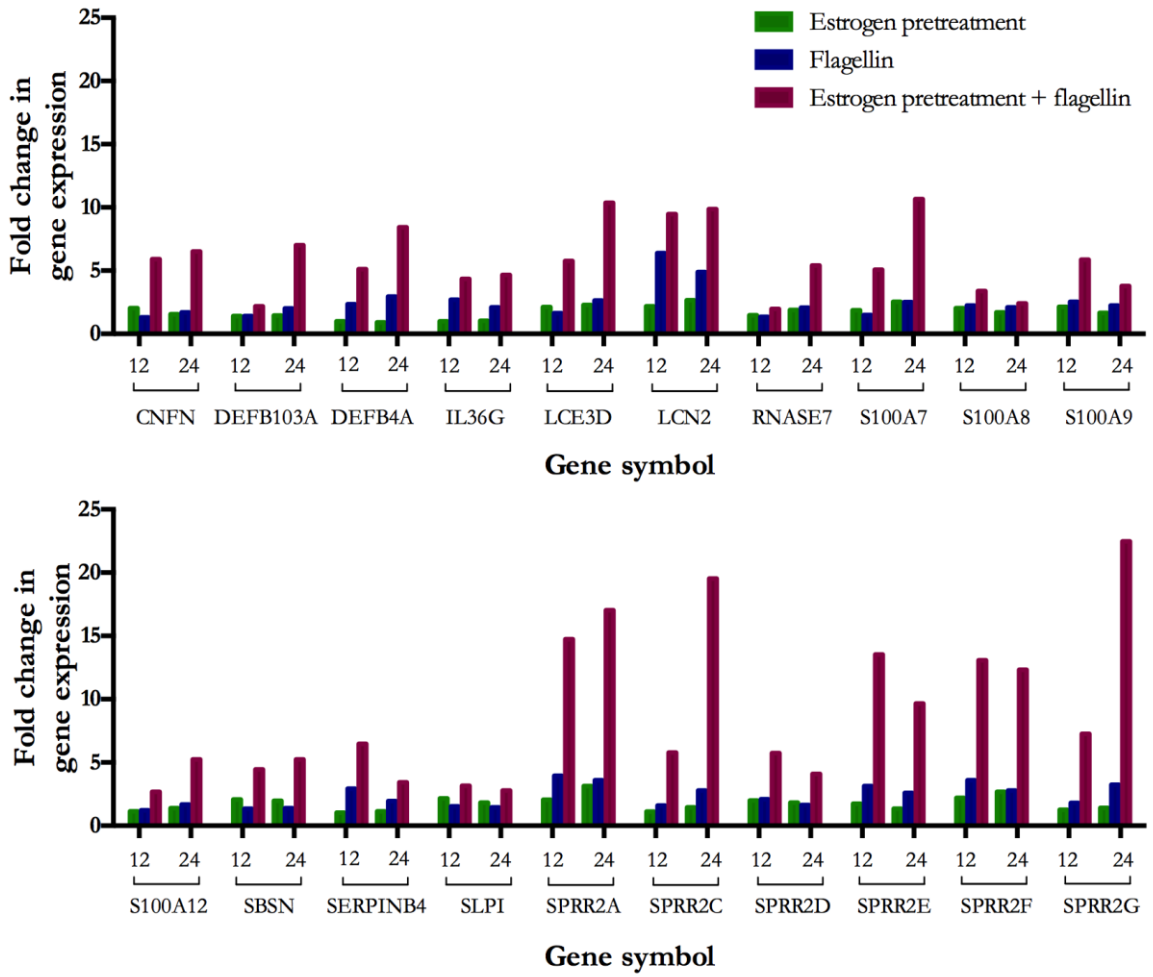

Figure 4.5: Expression pattern of genes of interest identified by Venn diagram analysis.

4.4 Validation of microarray data by qPCR

To validate the microarray data, qPCR was performed for LCN2 and RNASE7 as the encoded proteins have antimicrobial properties. The development of the qPCR assays for these genes is detailed in Chapter 5 section 5.4.1. The qPCR results for LCN2 and RNASE7, and the previous qPCR results for DEFB103A and DEFB4A were compared to the microarray data for these genes (Figure 4.6). The results for DEFB4A are shown on a separate graph, as the fold change in expression of this gene, as measured by qPCR, was substantially greater than the other genes. The data for each of the genes resulted in an R^2 of between 0.9865 and 0.9999 indicating that there was good agreement between the microarray results and the qPCR results for all genes measured. This agreement between the two methods provided confidence that the values measured by microarray for the other genes in the dataset were reliable.

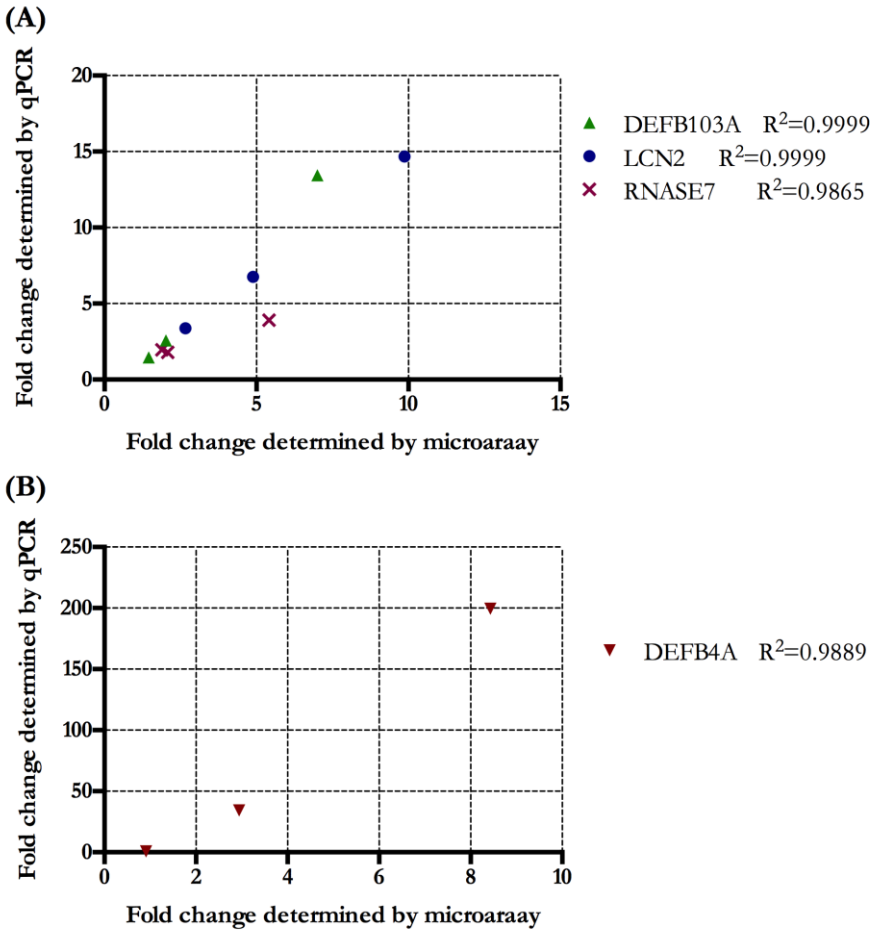

Figure 4.6: Comparison of fold change in gene expression obtained by microarray and qPCR. (A) Fold change in expression of LCN2, DEFB103A, and RNASE7 genes. (B) Fold change in expression of DEFB4A.

4.4.1 Discussion of gene analysis

Analysis of individual genes from the microarray data revealed several genes that may have important roles in innate defence of the urogenital tract during infection and may also be regulated by estrogen. Most of these genes have functions relating to either inflammation, keratinisation, or function as a host defence peptide.

Many genes identified by the microarray contribute to the keratinisation process and are encoded on the epidermal differentiation complex on human chromosome 1q21. This includes the SPRR, S100 and LCE genes.

SPRR genes are a multigene family that are differentially expressed in different types of epithelia. They are a component of the cornified cell envelope and it is thought the differential expression of these genes results in the production of different types of barrier at the epithelial surface[225]. The SPRR genes identified by the microarray all belong to the SPRR2 family. This family of genes has been previously shown to be regulated by estrogen[226].

S100 proteins are calcium binding proteins with a diverse range of functions. One of these functions is thought to be keratinocyte differentiation; the expression of S100A7, A8, and A9 increases during differentiation of primary human keratinocytes[124,227]. Furthermore, treatment of primary human keratinocytes with recombinant S100A7 resulted in upregulation of differentiation markers, such as keratins, and increased expression of tight junction proteins resulting in a stronger tight junction barrier[228]. Similarly overexpression of S100A8 and A9 in a human keratinocyte cell line also increased expression of differentiation markers[229]. Altogether, these results indicate a role for S100 proteins in keratinocyte differentiation and thus, increased expression of these genes following estrogen and flagellin treatment suggested that these treatments caused increased differentiation and strengthening of the tight junction barrier between cells, which may not occur to the same extent with estrogen or flagellin alone.

The late cornified envelope (LCE) genes encode cornified envelope constituents with protein cross-linking abilities and are very similar to SPRR genes[230]. These genes are expressed much later than other keratinisation genes, hence their name. The LCE family are divided into six subgroups, which show tissue specific expression in the skin and contribute to the barrier function of the skin[231]. LCE expression is regulated by stimuli such as ultraviolet light and calcium[232]. Estrogen binding to the GPER receptor results in increased intracellular calcium, indicating a potential mechanism of estrogen regulation of these genes.

Many factors can affect the keratinisation of the vaginal epithelium, one of these being the menopause. After the menopause the vaginal epithelium thins and is less keratinised[203]. It is thought that increased keratinisation protects against infection by preventing penetration of the epithelial layer by pathogens. Increased keratinisation following estrogen treatment has been reported previously and topical estrogen is currently used to treat vaginal atrophy in postmenopausal women. Using topical estrogen treatment to increase keratinisation of the foreskin is also currently being trialled as a preventative to HIV infection[233]. Additionally, research has shown that peptide fragments derived from keratins also have antimicrobial activity and these fragments have been named keratin-derived antimicrobial peptides (KDAMPs)[234]. Keratin 6A-derived peptides from human corneal epithelial cells displayed bactericidal activity against multiple pathogens. The upregulation of numerous genes involved in keratinisation following estrogen pretreatment plus flagellin may therefore serve to protect the vaginal epithelium from infection in a number of ways. Firstly, by strengthening the epithelial barrier to infection and preventing penetration by pathogens. Secondly, by increasing the glycogen content of the vaginal lumen, which supports the growth of *Lactobacillus* spp., which in turn prevents the

growth of pathogenic bacteria. Finally, increased keratinisation may protect the vaginal epithelium from infection by potentially increasing the production of KDAMPs in the vagina to aid in elimination of bacteria from the site of infection. Further examination into the role of keratinisation in protecting against UTIs, and the effect of estrogen on this will be an important area to study further in the future.

Many of the genes upregulated after estrogen and flagellin treatments also have functions related to inflammation. Of the genes highlighted as being of interest due to their expression patterns, IL36G, S100A7, S100A8, S100A9, S100A12 and SERPINB4 have all been reported to play a role in inflammation. IL36G is a proinflammatory cytokine produced by keratinocytes that stimulates MAP kinase and NF-κB signalling upon binding to its receptor and induces the expression of other proinflammatory cytokines[235–238]. S100 proteins are calcium binding proteins with a diverse range of functions, including inflammation. S100A7, also known as psoriasin, has been shown to stimulate proinflammatory cytokine production from neutrophils[239]. Moreover, S100A8 and S100A9 are chemotactic for neutrophils and thus, these proteins together may act to recruit neutrophils to the site of infection and activate the neutrophils to secrete proinflammatory cytokines to promote an immune response[240]. Similarly, S100A12 is chemotactic for mast cells and monocytes and induces the production of proinflammatory cytokines from mast cells[241–244]. However, it has also been reported that S100A8 and S100A9, which work both independently and as a heterodimer, are anti-inflammatory and act to supress acute inflammation by neutralising proinflammatory cytokines produced by neutrophils and macrophages, such as IL-1β, IL-6, and TNF-α, and reducing inflammation[245]. Therefore, as inflammation is a complex area and many proteins involved can function both to stimulate and dampen an immune response, it is difficult to conclude what effect estrogen pretreatment may have on the level of inflammation during a UTI. However, many of the same genes have been reported to be upregulated in inflammatory skin conditions such as atopic dermatitis and contact eczema suggesting that these genes are indeed proinflammatory, and furthermore, that EP/F treatment promotes an inflammatory response[238].

The microarray data also identified several AMPs that showed potentiated expression with estrogen pretreatment plus flagellin than flagellin alone. These were DEFB103A, DEFB4A, LCN2, RNASE7, S100A7, S100A12 and SLPI.

LCN2 is an iron binding protein with antimicrobial properties[246]. A role for LCN2 in defence against UTIs has recently been identified; transurethral inoculation of LCN2 deficient mice with *E. coli* resulted in significantly higher CFUs in the bladder 3 days postinoculation than mice that

were LCN2 competent[247]. LCN2 is also elevated in the urine of women with acute cystitis, suggesting this protein is expressed during episodes of UTI and has an important role in protection against uropathogenic bacteria[247].

RNase 7 was initially identified in skin from healthy individuals in 2002[121]. It was found to have high sequence similarity to the RNase A superfamily of ribonucleases and indeed was found to have high ribonuclease activity. RNase 7 was found to have broad-spectrum antimicrobial activity against Gram-positive bacteria, Gram-negative bacteria and yeast, and thus was deemed to be an AMP. RNase 7 is expressed by epithelial cells throughout the urinary tract and is constitutively present in the urine of healthy patients[248]. Furthermore, in 2013 Kline *et al.* demonstrated that urinary RNase 7 concentrations increase during infection and that RNase 7 facilitates rapid killing of uropathogens by membrane disruption[123]. Altogether, these data suggest that RNase 7 is an important AMP with a role in protecting the urogenital tract from infection. RNase 7 expression has previously been reported in the vulvar, however, the microarray data presented in this thesis is, to the best of our knowledge, the first demonstration of RNase 7 expression in the vaginal epithelium[249]. Furthermore, the microarray data suggested an increase in RNase 7 expression with estrogen pretreatment plus flagellin, compared to flagellin challenge alone indicating a role for estrogen in the regulation of this AMP. Regulation of RNase 7 by estrogen has been reported once previously by Luthje *et al.* (2013); the authors demonstrated that estrogen supplementation increased RNase 7 expression in an immortalised bladder epithelial cell line[134]. Thus, the microarray findings for RNase 7 in the vagina are novel, but supported by observations of RNase 7 expression in the bladder.

The S100 proteins S100A7, S100A8, S100A9 and S100A12 also have antimicrobial properties[127,250,251]. These peptides have been reported to exert their antimicrobial properties through sequestration of metal ions, such as Zn^{2+} and Mn^{2+}[250–252]. S100A8 and S100A9 have previously been identified in both the human and murine vagina however, the microarray data presented in this thesis also demonstrated S100A7 and S100A12 expression in vaginal epithelial cells[253,254]. S100A7 and S100A8/A9 have previously been shown to be upregulated by bacterial flagellin in foreskin-derived keratinocytes[255,256]. Despite having antimicrobial properties these proteins have mainly been studied as chemotactic factors in the context of inflammation, as discussed previously[126]. However, potentiation of the expression of these genes with estrogen pretreatment prior to flagellin challenge indicates that estrogen boosts the antimicrobial properties of the vagina upon exposure to pathogens.

The AMP SLPI was initially identified in lung epithelial cells. The C-terminal domain of SLPI is a protease inhibitor, which protects epithelial cells from serine proteases, and the N-terminal has antimicrobial activity[257]. SLPI has been demonstrated to have broad-spectrum antimicrobial activity against Gram-positive, Gram-negative and fungal pathogens[257–260]. SLPI is expressed in numerous epithelial cells and has been detected in the bladder, kidney, and female reproductive tract[261–264]. However, the role of SLPI in protecting against UTIs has not been studied and thus, the importance of this AMP during UPEC colonisation is not known. Fahey and Wira (2002) previously demonstrated that uterine secretions from premenopausal women contained significantly higher SLPI concentrations than postmenopausal women[265]. This suggested hormonal regulation of SLPI expression and supports the findings of estrogen regulation of SLPI presented here.

In the literature other AMPs have been identified in the urogenital tract and are thought to be important in defence against UTIs. Cathelicidin, with active molecule LL-37, is expressed in the vagina, bladder and kidney, and is upregulated in the urine of during UTIs[263,266–268]. Furthermore, transgenic mice lacking the LL-37 gene had significantly higher levels of bacteria attached to the bladder epithelium following transurethral injection of UPEC, compared to LL-37 competent mice[267]. These data suggest that LL-37 is important in protecting against UTIs. Similarly, the urinary concentrations of lactoferrin and HD5 are increased during UTI episodes[96,269,270]. In addition, treatment of mice with oral lactoferrin significantly reduced the bacterial load in the bladder following transurethral UPEC injection, compared to mice that did not receive oral lactoferrin. However, the effects of deleting the lactoferrin and HD5 genes on the susceptibility of mice to UTIs has not been investigated, so their importance in bacterial clearance from the urinary tract has not been fully substantiated. The microarray data indicated that these AMPs were not upregulated by estrogen pretreatment in vaginal epithelial cells. This demonstrates that topical estrogen treatment may not upregulate all innate factors that may be protective against UTIs.

The Venn diagram identified downregulation of the genes LGALS7 and LGALS7B by EP12 and F12 treatment, but not EP/F12 treatment. Some galectins have been shown to be important in the immune response to bacterial infection, by binding bacteria directly and having a bacteriostatic or bactericidal effect and by recruiting macrophages and neutrophils to the site of infection[271]. Thus, inhibition of these genes by EP12 and F12 treatments may reduce the antimicrobial response of vaginal epithelial cells to infection. Downregulation of these genes was not observed with combined EP/F12 treatment, nor with any treatment at the 24 hour time point making it difficult to speculate on the mechanism behind this regulation pattern and the

importance of this finding. Furthermore, the Venn diagram highlighted that for some genes estrogen pretreatment prior to flagellin challenge resulted in reduced gene transcription, compared to flagellin alone. For example, there were 74 gene probes that were significantly upregulated by F12 treatment, but not by EP/F12 treatment. Many of these genes related to inhibition of viral infection and replication. Flagellin treatment has been shown previously to activate antiviral responses and conferred protection against Cytomegalovirus[272]. Further investigation is required to determine whether downregulation of these antiviral genes is detrimental to clearance of bacterial pathogens from the vagina, or whether downregulation of the host antiviral response is due to the immune response being driven towards antibacterial activity. Chemokines such as CXCL10 and CCL5 also showed increased gene expression with F12 treatment than with EP/F12 treatment. Flagellin induced CXCL10 expression in the cornea has been reported as a crucial factor in innate defence to *Pseudomonas aeruginosa* infection[273]. Thus, reduced expression of CXCL10 after EP/F12 treatment, compared to F12 treatment, may result in reduced bacterial killing and elimination from the vagina. These data, therefore, highlight the importance of understanding the mechanism of action of estrogen, so that key signalling pathways which promote innate immunity may be targeted with novel therapeutics.

The microarray data was verified by qPCR for several AMP genes and the two methods of quantifying mRNA showed good agreement (R^2>0.9865 for each gene). Reporting of validation results varies in the literature, with some groups considering results to be valid if both microarray and qPCR data reported a fold change greater than 2, whilst other groups consider more carefully the magnitude of the difference between the two reported results[274,275]. Furthermore, a 2-fold change has been reported as a cut off below which microarray and qPCR data begin to lose correlation. Thus, consideration of genes with a fold change above 2 should ensure better correlation between microarray and qPCR data. The fold changes measured by qPCR in this thesis are generally consistent with the fold changes measured by microarray however, it is notable that the microarray underestimated the fold change of some samples, particularly those where qPCR reported high fold changes. Svaren *et al.* (2000) also reported greater fold change in gene expression by qPCR than was measured by microarray and found this to be most prevalent for genes where the control sample exhibited low expression of that gene[275]. Examination of the raw gene expression values for the 12 and 24 hour control samples showed that this was indeed the case for hBD2, perhaps indicating why the microarray analysis reported lower fold changes for these genes than qPCR analysis. However, overall there was good agreement between the fold change values reported by microarray and qPCR, providing confidence in the microarray data.

Altogether, initial analysis of the microarray data by Venn diagram highlighted several genes of interest, the expression of which was potentiated in vaginal epithelial cells by estrogen pretreatment prior to exposure to flagellin – a bacterial PAMP important in establishing a UTI. The genes identified have functions relating to three areas: keratinisation, inflammation and microbial killing. However, many of the genes have multiple functions within these. These data suggest, therefore, that estrogen functions to improve innate immunity to infection by increasing the antimicrobial characteristics of the vagina, strengthening the epithelial barrier to pathogens and increasing expression of chemotactic genes involved in migration of immune cells, such as neutrophils and macrophages. All of these functions are involved in facilitating bacterial clearance from the vagina.

4.5 Ingenuity Pathway Analysis

To investigate areas identified by initial microarray analysis in more detail the microarray data was analysed using Ingenuity Pathway Analysis (IPA) software. This allows analysis of the downstream effects of each treatment, the canonical pathways that are involved in producing these effects and the upstream regulators potentially responsible for target gene expression. This type of analysis is useful in beginning to identify potential mechanisms of target gene regulation.

4.5.1 Downstream effects analysis

Using IPA the effects of a treatment on various downstream functions can be predicted. This type of analysis allows a hypothesis to be generated for how a function is regulated by a given treatment. The downstream effect of a treatment is calculated by IPA using interactions published in the literature. For example, the literature may identify a particular set of genes that causes a particular outcome or function, for instance cell cycle activation. The expression values of those genes in any given dataset can then be used to predict the activation state of that function (see Figure 4.7), i.e. to determine whether cell cycle activation is an outcome of a given treatment. This activation state is reported in IPA as a z-score. A z-score is only significant and reported for a function if it is above +2 or below -2[276]. A z-score above +2 shows the function is likely to be activated as a result of the treatment and the higher the z-score the more activated that function is expected to be. Whereas, a z-score below -2 indicates the function may be inhibited in the dataset. Considering the previous example, if genes X, Y and Z are known in the literature to cause cell cycle activation, and these genes are upregulated in a dataset the function "Cell cycle activation" would have a z-score greater than +2 and therefore be predicted to be a downstream effect of the treatment. A p-value is also calculated for each function, however, IPA

typically reports the p-value as –log(p-value). Reporting the p-value in this way means that small p-values are represented by large numbers, whereas large p-values are represented by small numbers. This allows smaller, more significant p-values to be displayed on a graph more clearly. Thus, a significant p-value of less than 0.05 is the equivalent of –log(p-value) of greater than 1.30.

Each of the microarray datasets were analysed with IPA to determine the functions with the highest and lowest z-scores after each treatment (EP, F and EP/F) in VK2 cells.

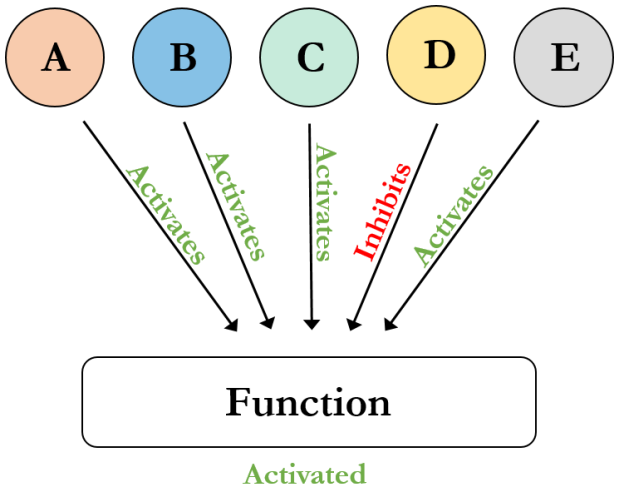

Figure 4.7: Diagram of how the z-score of each function is calculated by IPA. Each function is known to be regulated by a selection of genes (A-E) documented in the literature. The activation state of these genes within a dataset determines the predicted overall activation state of the downstream function. The z-score is calculated for each function based upon the expression values of each of the upstream genes.

4.5.1.1 Most highly activated functions

EP12 treatment did not result in any functions with z-scores above 2. EP24 treatment also resulted in no functions with z-scores greater than 2. This suggested EP treatment alone was not predicted to activate any functions in VK2 cells by IPA. After F12 treatment 85 functions had a z-score above 2 and thus were predicted to be activated. Almost all 85 of the functions were relating to immune cell activation and chemotaxis. However, there were also two relating to transactivation of RNA, two relating to quantity of metal ions, and activation of four diseases (multiple sclerosis, relapsing-remitting multiple sclerosis, inflammatory demyelinating disease and progressive motor neuropathy). The ten functions with the highest z-score after F12 treatment are shown in Figure 4.8A and the differentially expressed genes associated with each of the functions are shown in Table 4.5. In this table groups of genes that are associated with multiple functions are colour coded.

Analysis of the F24 dataset showed predicted activation of similar functions, 64 in total, mostly related to cell movement and migration. The function 'Cell movement of myeloid cells' had the

highest z-score, of 3.664, after F24 treatment, which is comparable with the z-score of 3.710 for the same function after F12 treatment. The ten functions with the highest z-scores after F24 treatment are shown in Figure 4.8B and the differentially expressed genes associated with each function are shown in Table 4.6.

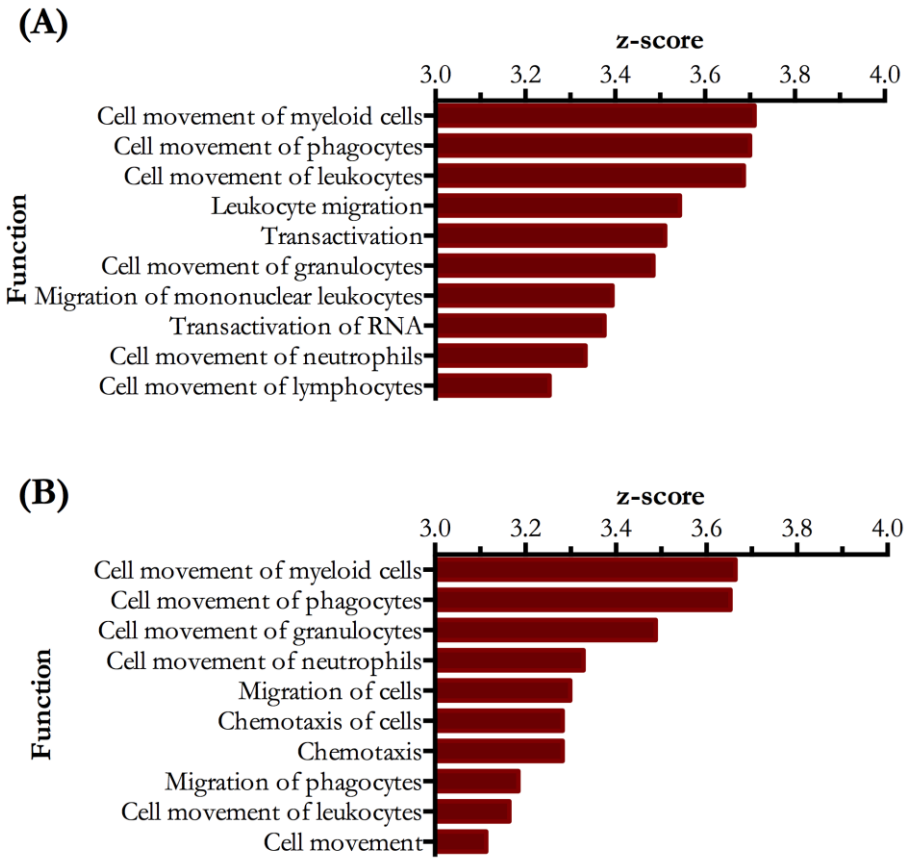

Figure 4.8: Functions with highest z-score after (A) F12 treatment and (B) F24 treatment. Graph shows the ten functions with the highest z-score after (A) 12 hours flagellin (F) treatment and (B) 24 hours F treatment, as calculated by Ingenuity Pathway Analysis. The z-score is calculated based upon the expression values of certain genes within the dataset.

Table 4.5: Table of functions with highest z-score after F12 treatment.

Function	z-score	Number of molecules	Molecules
Cell movement of myeloid cells	3.710	18	CASP1,CCL20,CCL5,CEACAM1,CFB,CXCL10,CXCL8, DEFB4A/DEFB4B,ICAM1,IL1RN,LCN2,LTB,MMP9, S100A8,S100A9,SAA1,SERPINA3,VEGFC = **(a)**
Cell movement of phagocytes	3.700	19	**(a),**CXCL11
Cell movement of leukocytes	3.686	23	**(a)**,CXCL11,DDX58,FYB,STAT1,STAT2
Leukocyte migration	3.544	24	**(a)**,CXCL11,DDX58,FYB,OLR1,STAT1,STAT2
Transactivation	3.511	15	**(c),**MARKCKSL1
Cell movement of granulocytes	3.485	14	**(d),**CEACAM1
Migration of mononuclear leukocytes	3.394	12	CCL20,CCL5,CEACAM1,CXCL10,CXCL11,CXCL8, DDX58,DEFB4A/DEFB4B,FYB,ICAM1,LTB, MMP9 = **(b)**
Transactivation of RNA	3.376	14	CXCL8,DDX58,DDX60L,EIF2AK2,HERC5,IFI16, IRF1,IRF9,LMO2,MMP9,MX1,STAT1,STAT2, TNFSF10 = **(c)**
Cell movement of neutrophils	3.334	13	CASP1,CCL5,CFB,CXCL10,CXCL8, DEFB4A/DEFB4B,ICAM1,IL1RN,LCN2,MMP9, S100A8,S100A9,SAA1 = **(d)**
Cell movement of lymphocytes	3.254	13	**(b)**,SAA1

Table 4.6: Table of functions with highest z-score after F24 treatment.

Function	z-score	Number of molecules	Molecules
Cell movement of myeloid cells	3.664	17	**(b),(c)**,CFB,LTB
Cell movement of phagocytes	3.653	17	**(b),(c)**,CFB,LTB
Cell movement of granulocytes	3.488	13	**(a)**,S100A7
Cell movement of neutrophils	3.328	12	CCL5,CFB,CXCL10,CXCL8,DEFB103A/DEFB103B, DEFB4A/DEFB4B,LCN2,MMP9,PTGS2,S100A8, S100A9,SAA1 = **(a)**
Migration of cells	3.299	24	**(b),(c)**,CFB,CYP2J2,EIF2AK2,LTB,NT5E,PARP9, SOD2,SP100,STAT1
Chemotaxis of cells	3.282	15	**(b),**LCN2,S100A7,SERPINA3,THBS1 = **(c)**
Chemotaxis	3.282	16	**(b),(c)**,TYMP
Migration of phagocytes	3.184	11	CCL20,CCL5,CXCL10,CXCL8, DEFB103A/DEFB103B,DEFB4A/DEFB4B, MMP9,PTGS2,S100A8,S100A9,SAA1 = **(b)**
Cell movement of leukocytes	3.164	19	**(b),(c)**,CFB,LTB,NT5E,STAT1

After EP/F12 treatment 63 functions had a z-score above 2 and, similarly to F12 treatment, almost all 63 functions related to immune cell activation and chemotaxis. However, one function related to 'Transactivation of RNA', one to 'Damage of liver' and five to multiple sclerosis and similar diseases. The ten functions with the highest z-score after EP/F12 treatment are shown in Figure 4.9A with the z-score after F12 treatment represented by blue bars. Observing only the ten functions with the highest z-scores for F12 and EP/F12, EP/F12 resulted in higher z-scores for many of these functions. For example, 'Cell movement by myeloid cells' had a z-score of 3.710 and 4.069 with F12 and EP/F12 treatment, respectively, although it was not possible to determine if this difference was significant. This suggested that EP/F12 treatment resulted in

stronger activation of immune related pathways. However, considering all 63 functions activated by EP/F12, 52 of these functions were common with F12. Of these 26 had a higher z-score with EP/F12 than with F12, 7 had equal z-scores with both treatments and 19 had higher z-scores with F12 than with EP/F12. Furthermore, functions such as 'Cell movement of neutrophils' exhibited a higher z-score with EP/F12 than F12, but the function 'Migration of neutrophils' had a higher z-score with F12 rather than EP/F12. Thus from these data it was difficult to conclude whether estrogen pretreatment prior to flagellin challenge resulted in increased activation of immune functions, as the functions activated by F12 and EP/F12 and their z-scores were mostly comparable. The differentially expressed genes associated with the ten functions with the highest z-scores after EP/F12 treatment are shown in Table 4.7.

Analysis of the EP/F24 dataset once again showed activation of similar functions to the F24 dataset, with 'Cell movement of myeloid cells' having the highest z-score (3.323) followed by 'Cell movement of phagocytes' (3.295). The ten functions with the highest z-scores after EP/F24 treatment are shown in Figure 4.9B, with the data from F24 represented by blue bars. The differentially expressed genes associated with each function are shown in Table 4.8.

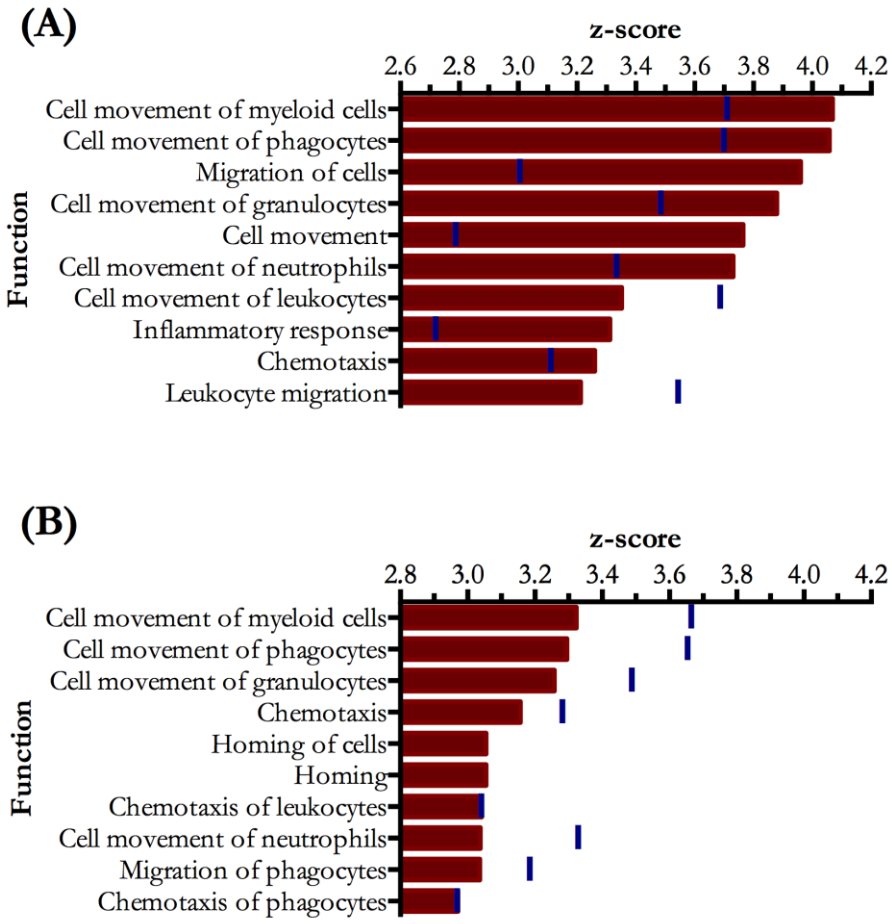

Figure 4.9: Functions with highest z-score after (A) EP/F12 treatment and (B) EP/F24 treatment. Graph shows ten functions with highest z-score after (A) estrogen pretreatment plus flagellin for 12 hours (EP/F12) and (B) estrogen pretreatment plus flagellin for 24 hours (EP/F24). Blue lines indicate values for (A) F12 treatment and (B) F24 treatment.

Table 4.7: Table of functions with the highest z-score after EP/F12 treatment.

Function	z-score	Number of molecules	Molecules
Cell movement of myeloid cells	4.069	22	CASP1,CCL20,CCL5,CFB,CXCL10,CXCL14,CXCL8, DEFB103A/DEFB103B,DEFB4A/DEFB4B,FABP4, GJB2,IL1RN,LCN2,LTB,MMP9,S100A12,S100A7, S100A8,S100A9,SAA1,SERPINA3,THBS1 = **(a)**
Cell movement of phagocytes	4.058	22	**(a)**
Migration of cells	3.960	43	CASP1,CCL20,CCL5,CFB,CXCL10,CXCL14,CXCL8, CYP2J2,DDX58,DEFB103A/DEFB103B, DEFB4A/DEFB4B,EGR1,EIF2AK2,F3,FABP4,GJB2, ID1,IFIT2,IGFBP3,IL1RN,KRT10,LAMA3,LCN2, LTB,MMP9,OLR1,PARP9,S100A12,S100A7,S100A8, S100A9,S100P,SAA1,SERPINA3,SERPINB3,SLPI, SOD2,SP100,STAT1,STAT2,THBS1,TSC22D3, ZC3H12A = **(b)**
Cell movement of granulocytes	3.879	18	**(c)**,S100A7
Cell movement	3.765	46	**(b)**,IL32,MX1,TYMP
Cell movement of neutrophils	3.731	17	CASP1,CCL5,CFB,CXCL10,CXCL14,CXCL8, DEFB103A/DEFB103B,DEFB4A/DEFB4B,FABP4, GJB2,IL1RN,LCN2,MMP9,S100A12,S100A8,S100A9, SAA1 = **(c)**
Cell movement of leukocytes	3.352	29	**(d)**,CASP1,CFB,DDX58,F3,FABP4,GJB2,IL1RN, KRT10,LTB,SERPINB3,STAT1,STAT2, ZC3H12A = **(e)**
Inflammatory response	3.312	21	**(d)**,FABP4,IL1RN,ISG15,OLR1,STAT1
Chemotaxis	3.260	17	TYMP,CCL20,CCL5,CXCL10,CXCL14,CXCL8, DEFB103A/DEFB103B,DEFB4A/DEFB4B,LCN2, MMP9,S100A12,S100A7,S100A8,S100A9, SAA1,SERPINA3,THBS1 = **(d)**
Leukocyte migration	3.212	31	**(d)**,**(e)**,OLR1,SLPI

Table 4.8: Table of functions with highest z-score after EP/F24 treatment.

Function	z-score	Number of molecules	Molecules
Cell movement of myeloid cells	3.323	19	**(a)**,**(b)**,CFB,FABP4,NFKBIZ,PRDM1 = **(c)**
Cell movement of phagocytes	3.295	19	**(a)**,**(b)**,**(c)**
Cell movement of granulocytes	3.258	15	**(a)**,CFB,FABP4,LCN2,MMP9,PRDM1,S100A12, S100A7
Chemotaxis	3.157	16	**(a)**,**(b)**,TYMP
Homing of cells	3.055	16	**(a)**,**(b)**,IGFBP3
Homing	3.055	17	**(a)**,**(b)**,IGFBP3,TYMP
Chemotaxis of leukocytes	3.042	15	**(a)**,CCL20,LCN2,MMP9,S100A12,S100A7, SERPINA3,THBS1 = **(b)**
Cell movement of neutrophils	3.038	14	**(a)**,CFB,FABP4,LCN2,MMP9,PRDM1,S100A12
Migration of phagocytes	3.036	10	CCL20,MMP9,CCL5,CXCL10,CXCL2, DEFB103A/DEFB103B,DEFB4A/DEFB4B,S100A8, S100A9,SAA1 = **(a)**
Chemotaxis of phagocytes	2.971	14	**(a)**,CCL20,LCN2,S100A12,S100A7,SERPINA3,THBS1

4.5.1.2 Most strongly inhibited functions

EP12 and EP24 treatments did not result in any functions with a z-score below -2. This suggested that EP treatment alone was not predicted to inhibit any functions. F12 treatment resulted in 14 functions with a z-score below -2. Other than one function relating to organismal death, all of the inhibited functions after F12 treatment related to replication of pathogens. Thus, F12 treatment resulted in inhibition of pathogen replication within VK2 cells. The ten functions with the lowest z-scores after F12 treatment are shown in Figure 4.10A. F24 treatment resulted in inhibition of seven functions, all relating to viral replication, and these are shown in Figure 4.10B. The genes associated with each function after F12 and F24 treatment are shown in Table 4.9 and Table 4.10, respectively.

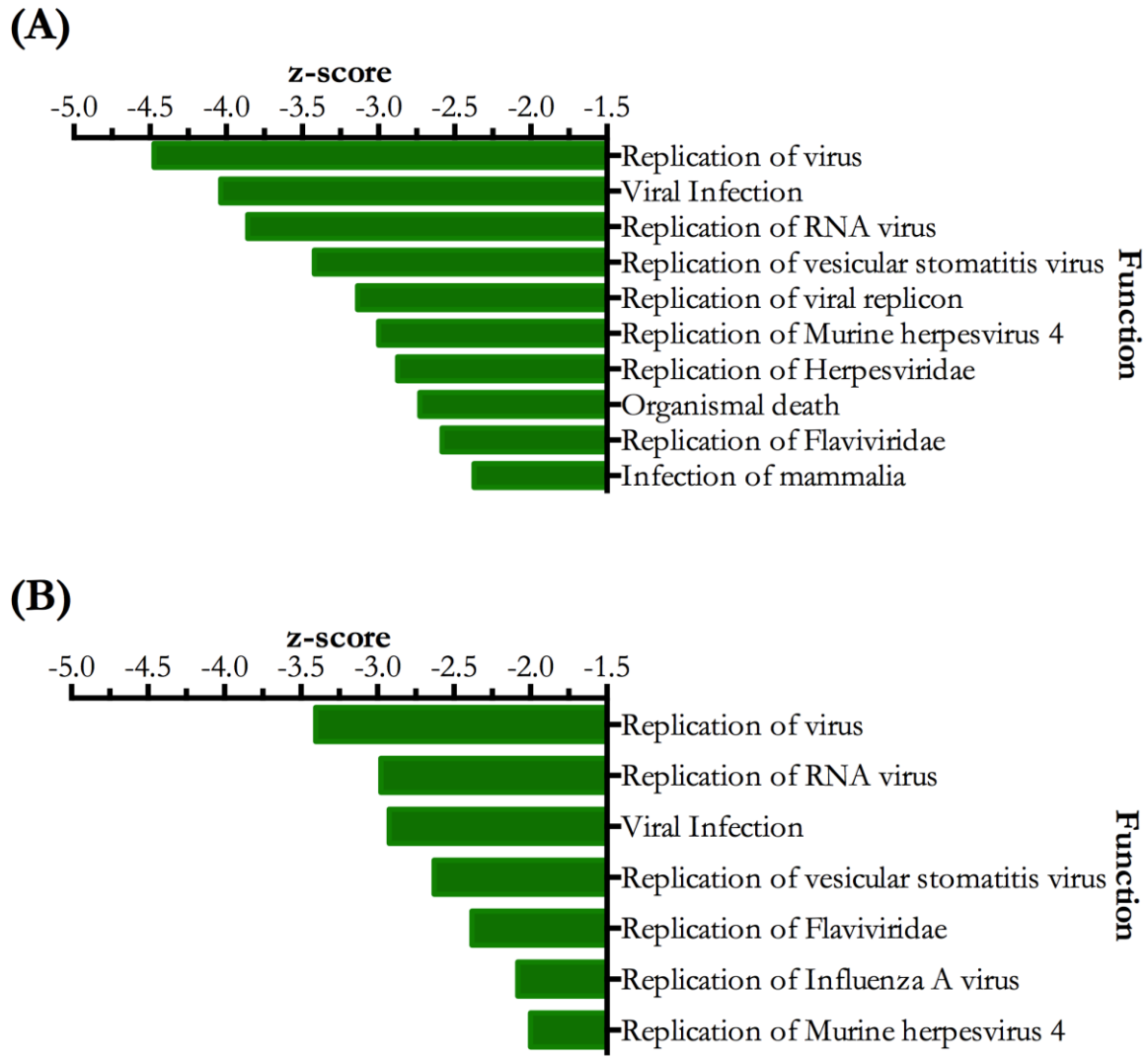

Figure 4.10: Functions with lowest z-score after (A) F12 and (B) F24 treatment. Graph shows the ten functions with the lowest z-score after (A) 12 hour flagellin treatment (F12) and (B) 24 hour flagellin treatment (F24), as calculated by Ingenuity Pathway Analysis.

Table 4.9: Table of functions with lowest z-scores after F12 treatment.

Function	z-score	Number of molecules	Molecules
Replication of virus	-4.474	38	**(a)**,BIRC3,MX2
Viral infection	-4.036	55	**(a)**,BIRC3,DDX60L,DEFB4A/DEFB4B,HLA-B, ICAM1,IFI35,IFIT2,IFIT3,IL1RN,IL32,IL36G,LCN2, MX2,PARP9,PI3,PSME2,SAMD9,SP100,TRIM22
Replication of RNA virus	-3.858	36	ADAR,BST2,CCL5,CEACAM1,CXCL10,CXCL8, DDX58,EIF2AK2,GBP1,IFIH1,IFIT1,IFITM1,IFITM2, IFITM3,IRF1,IRF9,ISG15,ISG20,MMP9,MX1,OAS1, OASL,PARP12,RSAD2,S100A8,S100A9,SP110, STAT1,STAT2,TAP1,TNFSF10,TRIM21,TRIM25, TRIM5,UBE2L6,ZC3HAV1 = **(a)**
Replication of vesicular stomatitis virus	-3.422	14	DDX58,IFIH1,IFITM2,IFITM3,IRF1,IRF9,ISG20, OAS1,OASL,PARP12,SP110,STAT2,TAP1,TRIM25
Replication of viral replicon	-3.138	10	CCL5,EIF2AK2,IFIT1,ISG15,MX1,OAS1,OAS3,OASL, PLSCR1,TNIP1
Replication of Murine herpesvirus 4	-3.000	9	ADAR,CXCL10,DDX58,IFIH1,IRF1,ISG20,MX2, OAS1,PARP12 = **(b)**
Replication of Herpesviridae	-2.874	13	**(b)**,IRF9,RSAD2,STAT1,STAT2
Organismal death	-2.729	25	**(c)**,ADAR,CD68,CFB,CXCL10,CXCL8, DEFB4A/DEFB4B,IL1RN,IRF7,IRF9,MARCKSL1, NINJ1,SDC4,SOD2,STAT2,TNIP1,TRIM21,VEGFC
Replication of Flaviviridae	-2.582	8	CXCL10,EIF2AK2,IFIT1,IFITM1,IFITM3,ISG15, RSAD2,UBE2L6
Infection of mammalia	-2.372	10	LCN2,PI3,CASP1,DDX58,EIF2AK2,IFIH1,ISG15, MMP9,STAT1,USP18 = **(c)**

Table 4.10: Table of functions with lowest z-scores after F24 treatment.

Function	z-score	Number of molecules	Molecules
Replication of virus	-3.404	23	**(a)**,BIRC3,MX2
Replication of RNA virus	-2.978	21	BST2,CCL5,CXCL10,CXCL8,EIF2AK2,IFITM1, IFITM2,IFITM3,IRF9,ISG15,MMP9,MX1,OAS1, PARP12,RSAD2,S100A8,S100A9,SP110,STAT1,TAP1, UBE2L6 = **(a)**
Viral infection	-2.924	36	**(a)**,BIRC3,C1R,DDX58,DEFB103A/DEFB103B, DEFB4A/DEFB4B,HLA-B,IFI35,IL32,IL36G,LCN2, MX2,PARP9,PTGS2,SP100,TRIM22
Replication of vesicular stomatitis virus	-2.630	7	IFITM2,IFITM3,IRF9,OAS1,PARP12,SP110,TAP1
Replication of Flaviviridae	-2.382	7	CXCL10,EIF2AK2,IFITM1,IFITM3,ISG15,RSAD2, UBE2L6
Replication of Influenza A virus	-2.082	9	EIF2AK2,IFITM1,IFITM2,IFITM3,ISG15,MMP9, MX1,RSAD2,STAT1
Replication of Murine herpesvirus 4	-2.000	4	CXCL10,MX2,OAS1,PARP12

After EP/F12 treatment 12 functions had a z-score below -2 (ten functions with lowest z-scores shown in Figure 4.11A with the F12 data overlaid in blue). Eleven of these functions related to infection and replication of pathogens and one function related to organismal death. Of these 12 functions only two had a lower z-score with EP/F12 than with F12, three had an equivalent z-

score after both treatments and seven had a lower z-score after F12 treatment than after EP/F12. For example, "Replication of virus" was the most inhibited function after both treatments, however, the z-score was -4.474 and -3.645 for F12 and EP/F12, respectively. Although it was not possible to test whether this was a significant difference, these data suggested that F12 treatment may result in stronger inhibition of pathogen replication than EP/F12 treatment. EP/F24 treatment resulted in inhibition of nine functions (Figure 4.11B with F24 data overlaid in blue), once again all related to replication of viral pathogens. Of the seven commonly inhibited functions by F24 and EP/F24, four had a lower z-score with EP/F24 than F24, two had equal z-scores with both treatments and one had a lower z-score with F24 than EP/F24. Thus, these data suggested that although at the 12 hour time point F12 treatment potentially resulted in greater inhibition of viral replication, by 24 hours EP/F24 treatment displayed the strongest inhibition of these functions. It is not clear whether regulation of these antiviral responses is important for driving bacterial clearance from the site of infection.

The differentially expressed genes associated with each function after EP/F12 and EP/F24 treatments are shown in Table 4.11 and Table 4.12, respectively.

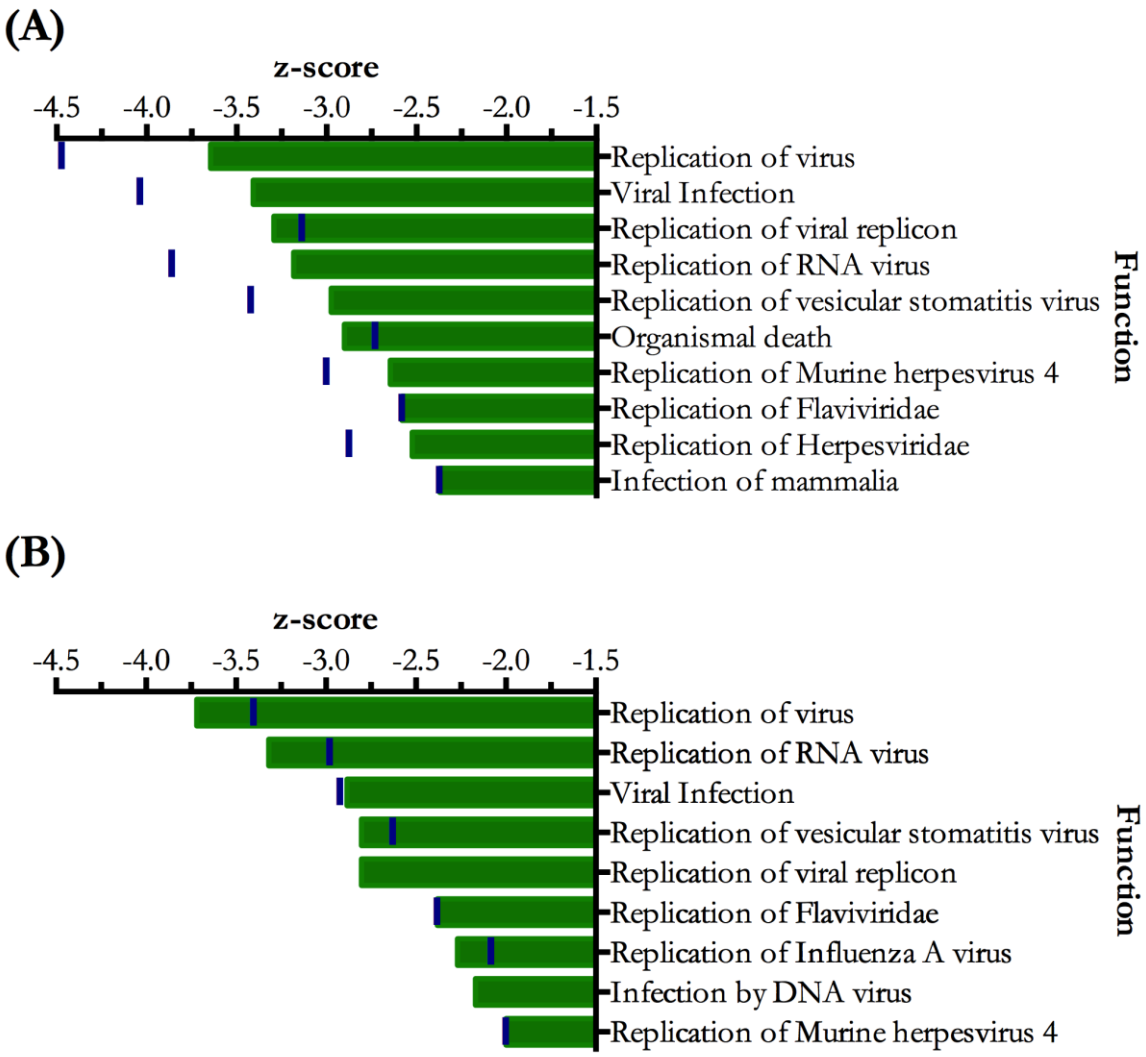

Figure 4.11: Functions with lowest z-score after (A) estrogen pretreatment plus flagellin for 12 hours (EP/F12) and (B) EP/F24 treatment. Blue bars represent the z-score after F12 and F24 treatment.

Table 4.11: Table of functions with lowest z-scores after EP/F12 treatment.

Function	z-score	Number of molecules	Molecules
Replication of virus	-3.645	33	(b),DDX58,IFIH1,IFITM2,IFITM3,IRF9,MX2,OAS1, OASL,PARP12,SP110,STAT2,TAP1 = (a)
Viral infection	-3.409	54	(a),(b),DDX60L,DEFB103A/DEFB103B, DEFB4A/DEFB4B,EGR1,HLA-B,IFI35,IFIT2,IFIT3, IL1RN,IL32,IL36G,KLK12,LCN2,PARP9,PI3,S100P, SAMD9,SERPINB3,SP100,TRIM22
Replication of viral replicon	-3.293	11	CCL5,EIF2AK2,IFIT1,ISG15,MX1,OAS1,OAS3,OASL, PLSCR1,SLPI,TNIP1
Replication of RNA virus	-3.183	32	(c),ADAR,BST2,CCL5,CXCL10,CXCL8,EIF2AK2, GBP1,IFIT1,IFITM1,ISG15,MMP9,MX1,RSAD2, S100A12,S100A8,S100A9,SLPI,STAT1,TRIM21,TRIM5, UBE2L6 = (b)
Replication of vesicular stomatitis virus	-2.975	11	DDX58,IFIH1,IFITM2,IFITM3,IRF9,OAS1,OASL, PARP12,SP110,STAT2,TAP1 = (c)
Organismal death	-2.902	26	(e),ADAR,CFB,CLDN1,CXCL10,CXCL8, DEFB4A/DEFB4B,F3,HOPX,IGFBP3,IL1RN,IRF7, IRF9,SLPI,SOD2,STAT2,TGM1,TNIP1,TRIM21
Replication of Murine herpesvirus 4	-2.646	7	ADAR,CXCL10,DDX58,IFIH1,MX2,OAS1, PARP12 = (d)
Replication of Flaviviridae	-2.582	8	CXCL10,EIF2AK2,IFIT1,IFITM1,IFITM3,ISG15, RSAD2,UBE2L6
Replication of Herpesviridae	-2.525	11	(d),IRF9,RSAD2,STAT1,STAT2
Infection of mammalia	-2.372	10	LCN2,PI3,CASP1,DDX58,EIF2AK2,IFIH1,ISG15, MMP9,STAT1,USP18 = (e)

Table 4.12: Table of functions with lowest z-score after EP/F24 treatment.

Function	z-score	Number of molecules	Molecules
Replication of virus	-3.718	26	(a),BIRC3,MX2
Replication of RNA virus	-3.319	24	BST2,CCL5,CXCL10,EIF2AK2,IFITM1,IFITM2, IFITM3,IRF9,ISG15,MMP9,MX1,OAS1,PARP12, RSAD2,S100A12,S100A8,S100A9,SLPI,SP110,STAT1, STAT2,TAP1,TRIM5,UBE2L6 = (a)
Viral infection	-2.884	45	(a),BIRC3,CYSRT1,DDX60L,DEFB103A/DEFB103B, DEFB4A/DEFB4B,HLA-B,IFI35,IFIT3,IL36G, KLK12,LCE3D,LCN2,MX2,NFKBIZ,PARP9,PI3, S100P,SAMD9,SERPINB3,SP100,TRIM22
Replication of viral replicon	-2.804	8	CCL5,EIF2AK2,ISG15,MX1,OAS1,OAS3,PLSCR1,SLPI
Replication of vesicular stomatitis virus	-2.804	8	IFITM2,IFITM3,IRF9,OAS1,PARP12,SP110,STAT2, TAP1
Replication of Flaviviridae	-2.382	7	CXCL10,EIF2AK2,IFITM1,IFITM3,ISG15,RSAD2, UBE2L6
Replication of Influenza A virus	-2.270	10	EIF2AK2,IFITM1,IFITM2,IFITM3,ISG15,MMP9, MX1,RSAD2,SLPI,STAT1
Infection by DNA virus	-2.170	5	DEFB103A/DEFB103B,NFKBIZ,PI3,SAMD9,STAT1
Replication of Murine herpesvirus 4	-2.000	4	CXCL10,MX2,OAS1,PARP12

4.5.1.3 Most significantly affected functions

In some cases IPA predicts that a function is affected by genes within the dataset, but cannot determine in which direction the function is affected based upon what has been reported in the literature. To consider where this may be the case the functions were sorted by p-value, to establish which were most significantly affected by EP, F and EP/F treatments.

After EP12 treatment the ten most significantly affected functions are shown in Figure 4.12A. Once again, many of the functions related to immune cell activation, however, the most significantly affected function was 'Plaque psoriasis'. Similarly, the function 'Psoriasis' was also the third most significantly affected function for EP12. There were seven differentially expressed genes from the EP12 dataset that were linked to the 'Plaque psoriasis' function and these included LCN2, SLPI, and S100A8/A9 – genes highlighted as potential genes of interest. The full list of differentially expressed genes associated with each function after EP12 and EP24 treatments are shown in Table 4.13 and Table 4.14, respectively. EP24 treatment showed similar most significantly affected functions to EP12 treatment, with 'Plaque psoriasis' being the most significantly affected function with both treatments (Figure 4.12B).

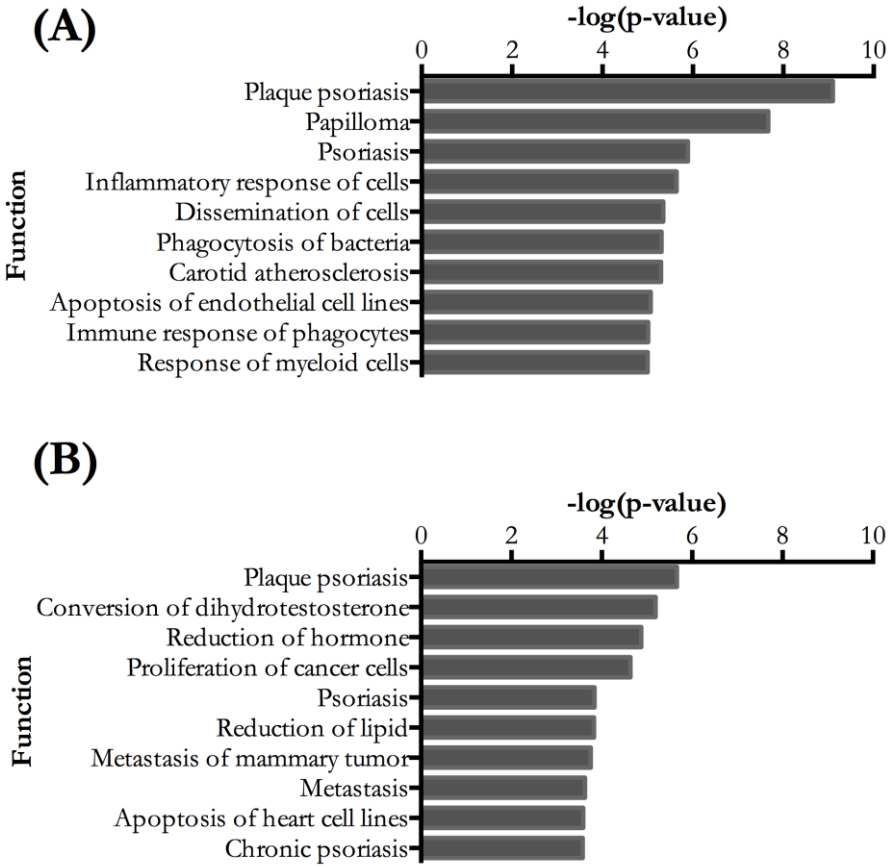

Figure 4.12: Functions with the smallest p-value after (A) estrogen pretreatment at 12 hours and (B) estrogen pretreatment at 24 hours. The p-value is represented as –log(p-value). Grey bars indicate no z-score was calculated for these functions.

Table 4.13: Table of most significantly affected functions after EP12 treatment.

Function	-log(p-value)	Number of molecules	Molecules
Plaque psoriasis	9.10	6	KRT15,LCN2,S100A8,S100A9,SLPI,SPRR2A = **(a)**
Papilloma	7.67	5	CNFN,LCN2,S100A8,S100A9,SLPI
Psoriasis	5.89	7	**(a)**,LCE3D
Inflammatory response of cells	5.64	3	CD14,S100A8,S100A9
Dissemination of cells	5.34	3	CD14,S100A9,SLPI
Phagocytosis of bacteria	5.30	3	CD14,LCN2,S100A9
Carotid atherosclerosis	5.29	2	S100A8,S100A9
Apoptosis of endothelial cell lines	5.07	3	S100A8,S100A9,TFRC
Immune response of phagocytes	5.01	4	CD14,F3,LCN2,S100A9 = **(b)**
Response of myeloid cells	5.00	4	**(b)**

Table 4.14: Table of most significantly affected functions after EP24 treatment.

Function	-log(p-value)	Number of molecules	Molecules
Plaque psoriasis	5.66	4	LCN2,S100A7,SPRR2A,TXNIP = **(a)**
Conversion of dihydrotestosterone	5.19	2	AKR1C1/AKR1C2,AKR1C3 = **(b)**
Reduction of hormone	4.87	2	**(b)**
Proliferation of cancer cells	4.63	4	LGALS7/LGALS7B,RCAN1,S100A7,TXNIP
Psoriasis	3.84	5	**(a)**,LCE3D
Reduction of lipid	3.83	2	**(b)**
Metastasis of mammary tumor	3.75	2	LCN2,S100A4
Metastasis	3.63	5	**(b)**,LCN2,S100A4,TXNIP
Apoptosis of heart cell lines	3.59	2	LCN2,TXNIP
Chronic psoriasis	3.58	3	LCN2,S100A7,SPRR2A

The ten most significantly affected functions after F12 treatment are shown in Figure 4.13A. Six of these ten functions had a z-score associated with them that was above 2 or below -2, but a z-score was not reported for the remaining four functions. 'Psoriasis' was the most significantly affected function and 60 differentially expressed genes from the F12 dataset were linked to this function, once again including previously identified genes of interest DEFB4A, LCN2, S100A8/A9, and SERPINB4 (full list of associated genes in Table 4.15). The three remaining functions without a z-score from the ten most significantly affected functions in the F12 dataset all related to autoimmune diseases, and linked to numerous genes related to inflammation such as interferon-induced proteins.

F24 treatment significantly affected similar functions to F12 treatment, with 'Psoriasis' being the most significantly affected function with both treatments (Figure 4.13B). The genes associated with each function after F24 treatment is shown in Table 4.16.

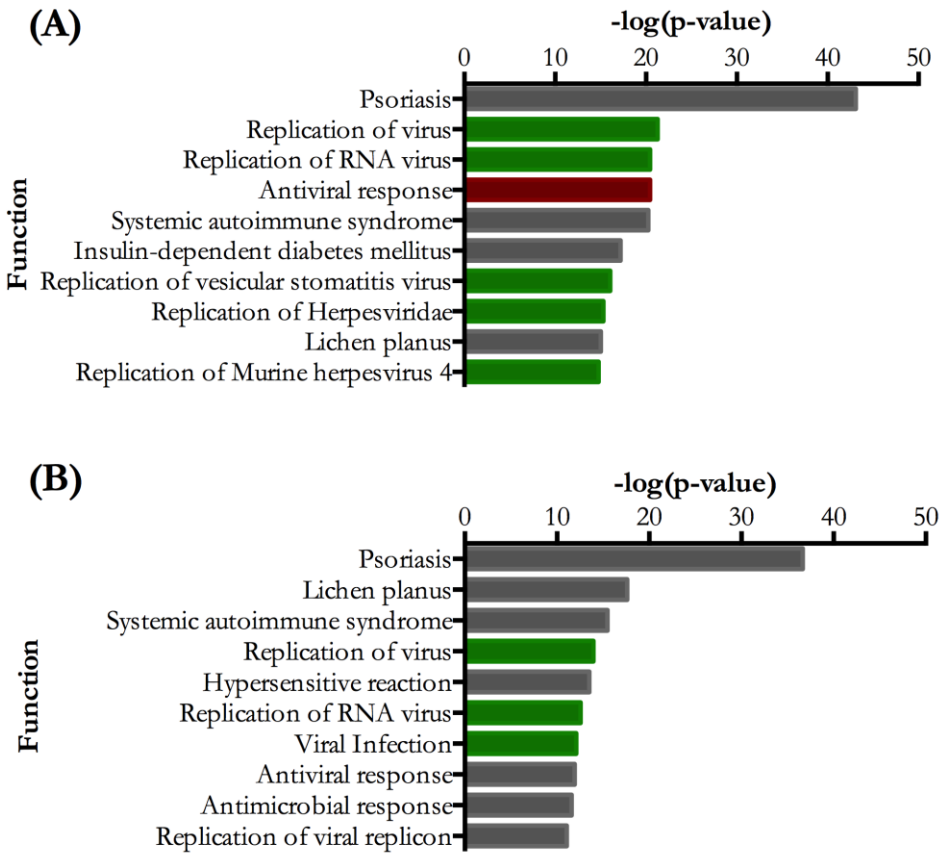

Figure 4.13: Functions with the smallest p-value after (A) 12 hour flagellin treatment (F12) and (B) F24 treatment. The graph shows the ten functions with the most significant p-values after (A) F12 and (B) F24 treatment. Green bars indicate functions with a z-score <-2, red bars indicate functions with a z-score >2, and grey bars indicate functions where no z-score was calculated. The p-value is given as –log(p-value).

Table 4.15: Table of most significantly affected functions after F12 treatment.

Function	-log(p-value)	Number of molecules	Molecules
Psoriasis	43.09	60	(c),ADAR,ALDH1A3,CASP4,CXCL10,CXCL11,CXCL8, DDX58,EPSTI1,GBP1,HERC6,ICAM1,IFI16,IFI35, IFI44,IFI44L,IFIT3,IL36G,IRF7,ISG15,ISG20,LAMP3, LCN2,LGALS3BP,MMP9,NAMPT,OAS1,OAS2,OAS3, OASL,PARP9,PI3,PLSCR1,PSMB10,RSAD2,S100A8, SAMD9,SCO2,SERPINB1,SERPINB2,SERPINB4, SOD2,SPRR2A,SPRR2D,SPRR2E,STAT1,TNC, TNFAIP6,TNIP1,TRIM22,UBE2L6
Replication of virus	21.29	38	**(a)**,BIRC3,MX2
Replication of RNA virus	20.44	36	ADAR,BST2,CCL5,CEACAM1,CXCL10,CXCL8, DDX58,EIF2AK2,GBP1,IFIH1,IFIT1,IFITM1,IFITM2, IFITM3,IRF1,IRF9,ISG15,ISG20,MMP9,MX1,OAS1, OASL,PARP12,RSAD2,S100A8,S100A9,SP110,STAT1, STAT2,TAP1,TNFSF10,TRIM21,TRIM25,TRIM5, UBE2L6,ZC3HAV1 = **(a)**
Antiviral response	20.43	21	ADAR,BIRC3,BST2,CCL5,DDX58,EIF2AK2,IFI44, IFIH1,IFIT1,IFIT2,IRF7,ISG20,LCN2,MX1,OAS1, OAS2,OAS3,OASL,STAT1,TRIM22,ZC3HAV1
Systemic autoimmune syndrome	20.23	46	**(b)**,CCL20,CD68,CEACAM1,HELZ2,IFIT1,IL1RN,LAP3, LCN2,LTB,MMP9,MX1,NAMPT,S100A8,S100A9,SAA1, SDC4,SLFN5,TNFAIP6,TNFSF10,TRIM21,UBE2L6
Insulin-dependent diabetes mellitus	17.19	25	CASP1,CASP4,CCL5,CFB,CXCL10,CXCL8,DDX60, GBP4,HERC6,ICAM1,IFI16,IFI44,IFIH1,IFIT2,IFIT3, IRF7,OAS1,PARP14,PSMB9,SAMD9L,STAT1,STAT2, TAP1,TMEM140,XAF1 = **(b)**
Replication of vesicular stomatitis virus	16.05	14	DDX58,IFIH1,IFITM2,IFITM3,IRF1,IRF9,ISG20, OAS1,OASL,PARP12,SP110,STAT2,TAP1,TRIM25
Replication of Herpesviridae	15.29	13	**(d)**,IRF9,RSAD2,STAT1,STAT2
Lichen planus	15.04	16	HLA-B,IFITM2,IFITM3,IRF1,LAP3,LTB,CCL20, DEFB4A/DEFB4B,IFI27,IFI6,IFIT1,IFITM1,MX1, PSME2,S100A9,TYMP = **(c)**
Replication of Murine herpesvirus 4	14.76	9	ADAR,CXCL10,DDX58,IFIH1,IRF1,ISG20,MX2, OAS1,PARP12 = **(d)**

Table 4.16: Table of most significantly affected functions after F24 treatment.

Function	-log(p-value)	Number of molecules	Molecules
Psoriasis	36.64	43	**(b),**CCL20,DEFB103A/DEFB103B,DEFB4A/DEFB4B, EPSTI1,HERC6,IFI16,IFI27,IFI35,IFI44L,IFI6,IFITM1, IL36G,IRF7,ISG15,LAMP3,LCE3D,LCN2,LGALS3BP, OAS2,OAS3,PARP9,PLSCR1,PTGS2,RSAD2,S100A7, SERPINB2,SOD2,SPRR2A,SPRR2C,SPRR2E,SPRR2G, TNFAIP6,TRIM22,TYMP,
Lichen planus	17.60	15	IFI6,IFITM2,IFITM3,LAP3,TYMP,CCL20, DEFB4A/DEFB4B,HLA-B,IFI27,IFITM1,LCE3D, LTB,MX1,S100A7,S100A9 = **(a)**
Systemic autoimmune syndrome	15.48	30	**(c)**,C1R,CCL20,CCL5,CD68,CFB,DDX60L,HELZ2, HERC6,IFI16,IRF7,LAP3,LCN2,LTB,NT5E,PSMB9, PTGS2,SAA1,TAP1,THBS1,TNFAIP6,XAF1
Replication of virus	13.92	23	BIRC3,BST2,CCL5,CXCL10,CXCL8,EIF2AK2, IFITM1,IFITM2,IFITM3,IRF9,ISG15,MMP9,MX1, MX2,OAS1,PARP12,RSAD2,S100A8,S100A9,SP110, STAT1,TAP1,UBE2L6 = **(b)**
Hypersensitive reaction	13.50	20	**(a)**,CCL5,CXCL8,DEFB103A/DEFB103B,EIF2AK2, LGALS3BP,PLSCR1,PTGS2,S100A8,SOD2,STAT1
Replication of RNA virus	12.56	21	BST2,CCL5,EIF2AK2,IFITM1,IFITM2,IFITM3,IRF9, ISG15,PARP12,RSAD2,SP110,TAP1,CXCL10,CXCL8, MMP9,MX1,OAS1,S100A8,S100A9,STAT1,UBE2L6 = **(c)**
Viral infection	12.08	36	**(b)**,C1R,DDX60L,DEFB103A/DEFB103B, DEFB4A/DEFB4B,HLA-B,IFI35,IL32,IL36G,LCN2, PARP9,PTGS2,SP100,TRIM22
Antiviral response	11.92	12	BIRC3,BST2,CCL5,EIF2AK2,IRF7,LCN2,MX1,OAS1, OAS2,OAS3,STAT1,TRIM22 = **(d)**
Antimicrobial response	11.58	14	**(d)**,DEFB103A/DEFB103B,S100A7
Replication of viral replicon	11.04	8	CCL5,EIF2AK2,ISG15,MX1,OAS1,OAS3,PLSCR1, PTGS2

The ten most significantly affected functions after EP/F12 treatment are shown in Figure 4.14A. Of these 10 functions, only two had an associated z-score. Three out of ten functions related to psoriasis with 'Psoriasis' being the most significantly affected function for this dataset linked to 74 differentially expressed genes within the dataset. 'Plaque psoriasis' and 'Chronic psoriasis' were the second and third most significantly affected functions for EP/F12, and these were linked to 25 and 23 genes in the dataset, respectively. Once again the genes linked to the psoriasis functions included many of the genes highlighted as potential genes of interest due to potentiation of their expression after estrogen treatment. The full list of differentially expressed genes associated with each function after EP/F12 treatment is shown in Table 4.17. The remaining functions mostly related to immune responses, such as 'Antiviral response' and were linked to many interferon-induced genes.

EP/F24 treatment significantly affected similar functions to EP/F12 treatment (Figure 4.14B). Of the ten functions with the smallest p-value after EP/F24 treatment eight functions related to skin diseases such as psoriasis and dermatitis, and these involved genes such as AMPs (hBD2,

hBD3, LCN2), inflammatory genes (interferon-induced genes and chemokines), and epithelial barrier genes (SPRR genes and keratins). The full list of genes associated with each function after EP/F24 treatment is shown in Table 4.18.

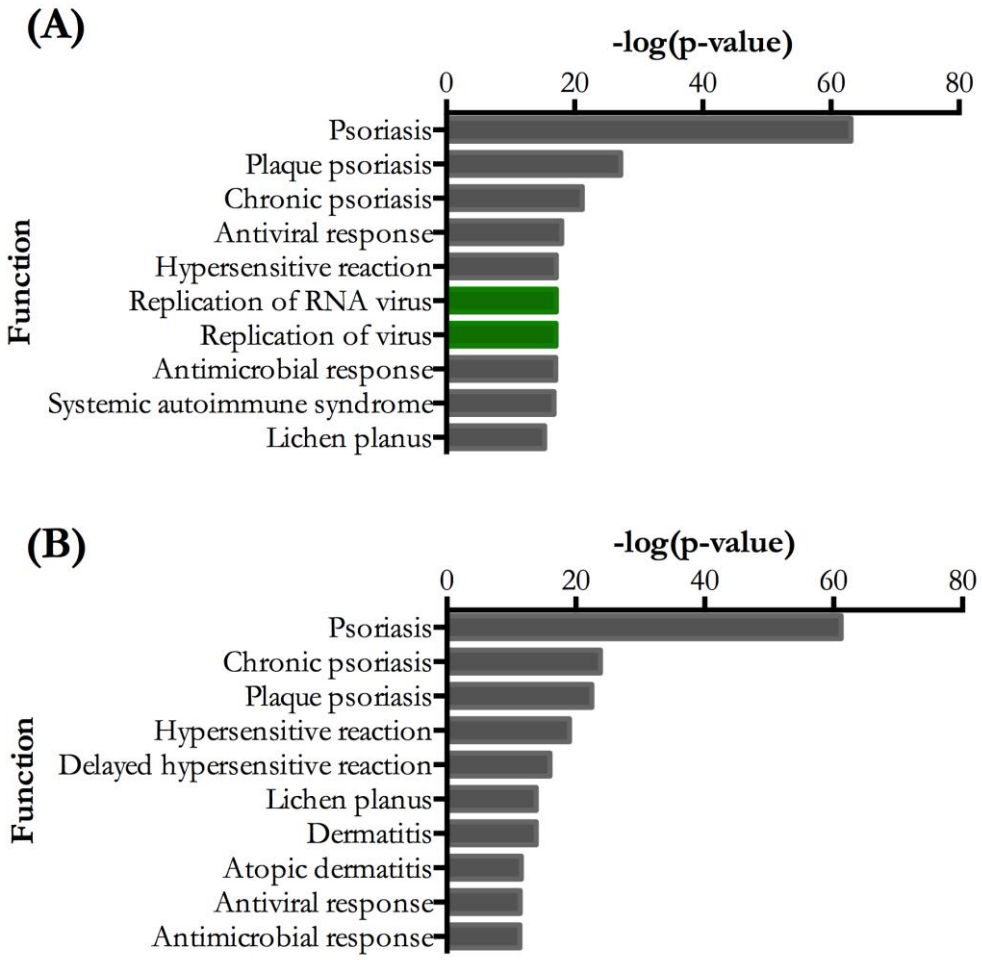

Figure 4.14: Most significantly affected functions after EP/F treatment. Graph shows ten most significantly affected functions after (A) estrogen pretreatment plus flagellin treatment at 12 hours (EP/F12) and (B) EP/F24 treatment. The p-values are represented by –log(p-value). Green bars indicate functions with z-scores <-2, and grey bars indicate functions where no z-score was calculated.

Table 4.17: Table of most significantly affected functions after EP/F12 treatment.

Function	-log(p-value)	Number of molecules	Molecules
Psoriasis	63.12	74	**(a)**,**(b)**,ADAR,ALOX12B,DDX58,DEFB103A/DEFB103B, DSG1,EGR1,EPSTI1,GBP1,HERC6,IFI16,IFI27,IFI35, IFI44,IFI44L,IFI6,IFIT3,IGFBP3,IL36G,ISG15,KLK11, KRTDAP,LAMP3,LCE3D,MMP9,OAS1,OAS2,OAS3, OASL,PARP9,RSAD2,S100P,SAMD9,SERPINB2,SPRR2C, SPRR2G,TNIP1,TRIM22,TYMP,UBE2L6
Plaque psoriasis	27.17	25	CCL20,CXCL10,CXCL8,DEFB4A/DEFB4B,GJB2,KRT1, KRT10,KRT6C,LCN2,LOR,PI3,S100A12,S100A7,S100A8, S100A9,SERPINB3,SERPINB4,SLPI,SPRR1A,SPRR1B, SPRR2A,SPRR2B,SPRR2D,SPRR2E,STAT1 = **(a)**
Chronic psoriasis	21.17	23	DEFB4A/DEFB4B,GJB2,ID1,IFIT1,IFITM1,IRF7,KLK7, KRT6C,LCN2,MX1,PI3,PLSCR1,S100A12,S100A7,S100A9, SERPINB3,SERPINB4,SOD2,SPRR1B,SPRR2A,STAT1, SULT2B1,TGM1 = **(b)**
Antiviral response	17.98	19	ADAR,BST2,CCL5,DDX58,EIF2AK2,IFI44,IFIH1,IFIT1, IFIT2,IRF7,LCN2,MX1,OAS1,OAS2,OAS3,OASL, SERPINB3,STAT1,TRIM22 = **(c)**
Hypersensitive reaction	17.15	29	CCL20,CCL5,CXCL8,DEFB103A/DEFB103B, DEFB4A/DEFB4B,EIF2AK2,FABP4,HLA-B,IFI27, IFITM1,IL1RN,KLK7,KRT1,KRT10,KRT6C,LCE3D,LOR, LTB,MX1,PI3,PLSCR1,S100A7,S100A8,S100A9,SERPINB3, SERPINB4,SOD2,SPRR1B,STAT1
Replication of RNA virus	17.15	32	ADAR,BST2,CCL5,CXCL10,CXCL8,DDX58,EIF2AK2, GBP1,IFIH1,IFIT1,IFITM1,IFITM2,IFITM3,IRF9,ISG15, MMP9,MX1,OAS1,OASL,PARP12,RSAD2,S100A12, S100A8,S100A9,SLPI,SP110,STAT1,STAT2,TAP1, TRIM21, TRIM5,UBE2L6 = **(d)**
Replication of virus	17.10	33	**(d)**,MX2
Antimicrobial response	17.06	22	**(c)**,DEFB103A/DEFB103B,S100A12,S100A7
Systemic autoimmune syndrome	16.78	41	CASP1,CCL20,CCL5,CFB,CXCL10,CXCL14,CXCL8, DDX60,FABP4,GBP4,HELZ2,HERC6,IFI16,IFI44,IFIH1, IFIT1,IFIT2,IFIT3,IL1RN,IRF7,LAP3,LCN2,LTB,MAFB, MMP9,MX1,OAS1,PARP14,PSMB9,S100A12,S100A8, S100A9,SAA1,SAMD9L,STAT1,STAT2,TAP1,THBS1, TRIM21,UBE2L6,XAF1
Lichen planus	15.31	16	CCL20,DEFB4A/DEFB4B,HLA-B,IFI27,IFI6,IFIT1, IFITM1,IFITM2,IFITM3,LAP3,LCE3D,LTB,MX1,S100A7, S100A9,TYMP

Table 4.18: Table of most significantly affected functions after EP/F24 treatment.

Function	-log(p-value)	Number of molecules	Molecules
Psoriasis	61.15	73	**(a)**,**(b)**,ALOX12B,ARG1,CALML5,CDSN,DSC2,DSG1, DEFB103A/DEFB103B,EPSTI1,FLG,HERC6,IFI27,IFI35, IFI44,IFI44L,IFI6,IFIT3,IFITM1,IGFBP3,IL36G,ISG15, KLK11,KLK7,LAMP3,LCE2B,LCE3D,LCE3E,LGALS3BP, MMP9,MX1,OAS1,OAS2,OAS3,PARP9,PLSCR1,RSAD2, S100P,SAMD9,SCO2,SERPINB2,SOD2,SPRR2C,SPRR2G, TRIM22,TYMP,UBE2L6
Chronic psoriasis	23.80	25	**(c)**,CST6,ID1,IRF7,LCN2,S100A12,SPRR2A,STAT1, SULT2B1,TGM1,TGM3 = **(a)**
Plaque psoriasis	22.46	22	CCL20,CST6,CXCL10,DEFB4A/DEFB4B,KRT1, KRT6C,LCN2,LOR,PI3,S100A12,S100A7,S100A8,S100A9, SERPINB3,SERPINB4,SLPI,SPRR1B,SPRR2A,SPRR2B, SPRR2D,SPRR2E,STAT1 = **(b)**
Hypersensitive reaction	19.02	31	**(c)**,**(d)**,EIF2AK2,HLA-B,
Delayed hypersensitive reaction	15.98	15	ARG1,DEFB4A/DEFB4B,IFITM1,KLK7,KRT6C, LGALS3BP,MX1,PI3,PLSCR1,S100A7,S100A9,SERPINB3, SERPINB4,SOD2,SPRR1B = **(c)**
Lichen planus	13.86	15	CALML5,CCL20,DEFB4A/DEFB4B,HLA-B,IFI27,IFI6, IFITM1,IFITM2,IFITM3,LAP3,LCE3D,MX1,S100A7, S100A9,TYMP
Dermatitis	13.85	27	**(d)**,DSC1,EIK2AK2,IRF9,PRDM1,SERPINB4,SLPI,THBS1
Atopic dermatitis	11.53	20	CCL20,CCL5,CST6,DEFB103A/DEFB103B, DEFB4A/DEFB4B,FABP4,FLG,IFI27,KLK7,KRT1, LCE3D,LOR,MX1,NFKBIZ,S100A7,S100A8,S100A9, SERPINB3,STAT1,TGM3 = **(d)**
Antiviral response	11.38	14	BIRC3,BST2,CCL5,EIF2AK2,IFI44,IRF7,LCN2,MX1,OAS1, OAS2,OAS3,SERPINB3,STAT1,TRIM22 = **(e)**
Antimicrobial response	11.30	17	**(e)**,DEFB103A/DEFB103B,S100A12,S100A7

4.5.1.4 Discussion of functions

Analysis of the downstream effects using IPA provides an insight into the functions being activated in cells as a response to a given treatment. Analysis of EP, F and EP/F treatment of VK2 cells at 12 and 24 hour time points revealed that EP treatment alone neither significantly activated nor inhibited any functions within the cells. Furthermore, F and EP/F treatments resulted in activation and inhibition of very similar functions – primarily relating to activation and migration of immune cells. Thus, from these data it was not possible to discern whether estrogen treatment prior to flagellin challenge resulted in stronger activation of the immune system and, therefore, enhanced protection from infections such as UTIs. F and EP/F treatment also significantly affected similar functions; IPA could not determine z-scores for these functions as the software did not have enough information available to make a reliable prediction. It was interesting that functions relating to psoriasis were significantly affected by all three treatments. The pathways and functions linked to psoriasis involved genes such as AMPs, as many AMPs were discovered in psoriatic patients and are often studied within this context, and genes involved in keratinisation. However, AMPs and other related genes are also important for

elimination of bacterial pathogens and, as previously discussed, keratinisation of cells prevents pathogen invasion. Therefore upregulation of psoriasis-related genes after exposure of VK2 cells to flagellin was perhaps not surprising. After 12 hours EP, F and EP/F treatments resulted in differential regulation of 6, 60, and 74 genes linked to the 'Psoriasis', respectively. Other than one gene (KRT15) downregulated by EP12, all of the genes linked to 'Psoriasis' were significantly upregulated. Thus, the increased number of upregulated genes linked to psoriasis after EP/F12 treatment, compared to F12 treatment, was suggestive of EP/F12 treatment increasing the antimicrobial response of VK2 cells to infection. A similar pattern was observed for the 24 hour time point, with EP24, F24 and EP/F24 treatments resulting in upregulation of 4, 43 and 73 genes linked to the function 'Psoriasis', further supporting this theory.

4.5.2 Canonical pathways

In comparison to the downstream effects analysis which predicts functions that are activated and inhibited downstream of the genes within a dataset, canonical pathway analysis determines potential pathways upstream of the differentially expressed genes within a given dataset and reveals interactions between genes. Canonical pathways are different to predicted functions; data relating to predicted functions in IPA is regularly updated whereas canonical pathways are more stable and represent well established pathways in the literature. IPA analyses which canonical pathways are overrepresented in a given dataset by calculating a ratio and –log(p-value). The ratio is the number of genes from a specific canonical pathway that are significantly affected in a dataset and is calculated as follows:

$$Ratio = \frac{Number\ of\ genes\ from\ dataset\ in\ a\ given\ pathway\ that\ meet\ the\ cutoff\ criteria}{Total\ number\ of\ genes\ that\ make\ up\ the\ pathway\ and\ are\ in\ reference\ gene\ set}$$

Thus, a higher ratio indicates that more genes within the pathway are significantly upregulated. The reference gene set for this analysis was the genes included on the Illumina HumanHT-12 v4 Expression Beadchip.

The top 10 canonical pathways after EP12 treatment are shown in Figure 4.15. The grey bars represent the ratio and the orange line shows the –log(p-value) for each canonical pathway. The pathway with the highest ratio after EP12 treatment was 'Role of IL-17A in Psoriasis' with a ratio of 0.154. There were two other pathways relating to IL-17A in the top ten canonical pathways after EP12 treatment, these were 'Differential Regulation of Cytokine Production in Intestinal Epithelial Cells by IL-17A and IL-17F' and 'IL-17A Signalling in Fibroblasts'. EP12 treatment also resulted in several pathways related to innate immunity, such as 'MIF Regulation of Innate

Immunity' and 'MIF-mediated Glucocorticoid Regulation'. Both of these pathways involve activation of NF-κB and result in production of cytokines. The 'iNOS Signalling' pathway is also related to innate immunity and results in production of nitric oxide, which inhibits bacterial DNA replication. The pathways 'Extrinsic Prothrombin Activation Pathway' and 'Coagulation System' are activated by tissue damage and result in secretion of coagulation factors to form a clot and repair the tissue. All ten of the top upregulated pathways by EP12 treatment shown in Figure 4.15 have a significant p-value ($p<0.05$ or $-\log(\text{p-value})>1.30$). The genes associated with each pathway that were upregulated after EP12 treatment are shown in Table 4.19. Similar pathways were upregulated after EP24 treatment and are shown in Table 4.20.

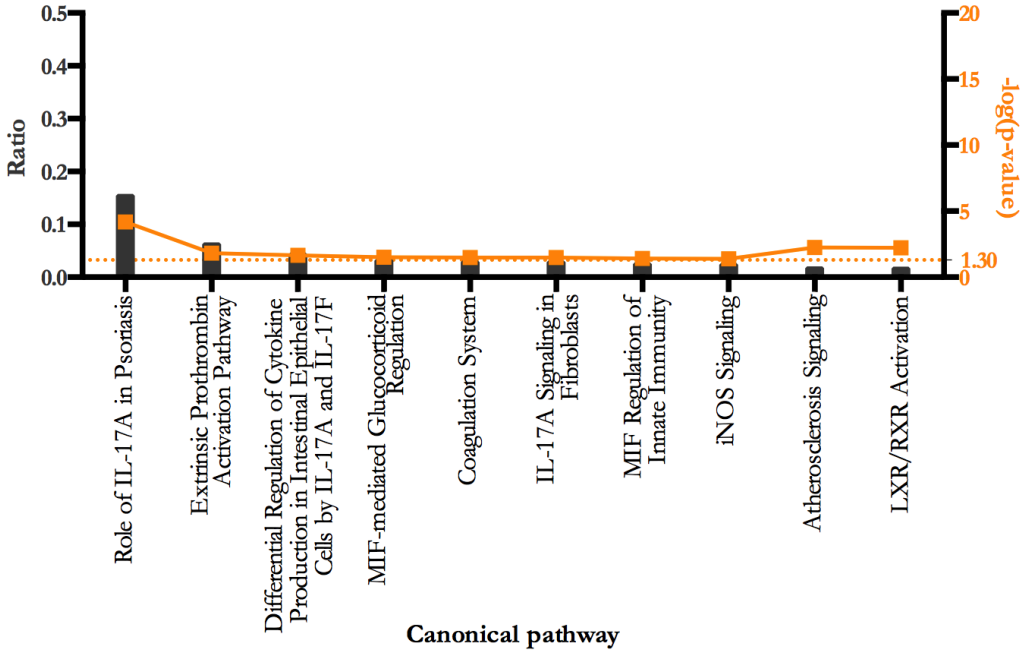

Figure 4.15: Top ten canonical pathways after EP12 treatment. The graph shows the ten canonical pathways with the highest ratio after estrogen pretreatment at 12 hours (EP12), as calculated by Ingenuity Pathway Analysis. Grey bars represent the ratio of each pathway, and orange symbols represent the –log(p-value) which must be >1.30 to be equivalent to a p-value of <0.05. Significance cut off for the –log(p-value) is shown as a dotted orange line.

Table 4.19: Canonical pathways after EP12 treatment.

Function	Ratio	-log(p-value)	Number of molecules	Molecules
Role of IL-17A in Psoriasis	0.1540	4.18	2	S100A9,S100A8
Extrinsic Prothrombin Activation Pathway	0.0625	1.82	1	F3
Differential Regulation of Cytokine Production in Intestinal Epithelial Cells by IL-17A and IL-17F	0.0435	1.66	1	LCN2
MIF-mediated Glucocorticoid Regulation	0.0312	1.52	1	CD14
Coagulation System	0.0286	1.48	1	F3
IL-17A Signaling in Fibroblasts	0.0286	1.48	1	LCN2
MIF Regulation of Innate Immunity	0.0250	1.43	1	CD14
iNOS Signaling	0.0233	1.40	1	CD14
Atherosclerosis Signaling	0.0168	2.25	2	S100A8,F3
LXR/RXR Activation	0.0165	2.24	2	CD14,S100A8

Table 4.20: Canonical pathways after EP24 treatment.

Function	Ratio	-log(p-value)	Number of molecules	Molecules
Methylglyoxal Degradation III	0.2000	4.54	2	AKR1C1/AKR1C2,AKR1C3
Bile Acid Biosynthesis, Neutral Pathway	0.1540	4.30	2	AKR1C1/AKR1C2,AKR1C3
Androgen Biosynthesis	0.0833	2.00	1	AKR1C3
Role of IL-17A in Psoriasis	0.0769	1.97	1	S100A7
Differential Regulation of Cytokine Production in Intestinal Epithelial Cells by IL-17A and IL-17F	0.0435	1.72	1	LCN2
Retinoate Biosynthesis I	0.0333	1.61	1	AKR1C3
MIF-mediated Glucocorticoid Regulation	0.0312	1.58	1	CD14
IL-17A Signaling in Fibroblasts	0.0286	1.54	1	LCN2
Estrogen Biosynthesis	0.0278	1.53	1	AKR1C3
MIF Regulation of Innate Immunity	0.0250	1.48	1	CD14

The top 10 canonical pathways after F12 treatment are shown in Figure 4.16A. The most upregulated pathway after F12 treatment was 'Interferon Signalling'. This pathway is activated by interferons binding to cell surface receptors, initiating transcription of interferon regulated genes, and therefore stimulating an immune response. The 'Activation of IRF by Cytosolic Pattern Recognition Receptors' pathway is similar to the 'Interferon Signalling' pathway, as it results in activation of the interferon regulatory factor (IRF) transcription factor in the cell in response to double-stranded RNA or DNA of viral/bacterial origin. Activation of IRF causes transcription of interferon-stimulated genes (ISGs), which generates an innate immune response. The 'Role of IL-17A in Psoriasis' pathway was once again upregulated with a ratio of 0.385 (compared to 0.154 after EP12 treatment). This pathway involves binding of IL-17 to the IL-17 receptor, which activates transcription of AMPs (including hBD2 and S100A7) and chemokines, which are immune cell attractants. The genes associated with each of the canonical pathways that were upregulated after F12 treatment are shown in Table 4.21. All of the pathways in Figure 4.16A have significant p-values, except for 'Superoxide Radicals Degradation', which had a –log(p-value) of 1.27, equating to a p-value of 0.053 (3dp) (shown in Table 4.21).

The top 10 canonical pathways after EP/F12 treatment are shown in Figure 4.16B. The pathway with the highest ratio after EP/F12 treatment was 'Role of IL-17A in Psoriasis' with a ratio of 0.462. This pathway was also activated by EP12 and F12 treatment, with ratios of 0.154 and 0.385, respectively. Thus, a larger number of genes in this pathway were significantly upregulated after EP/F12 treatment than after EP12 or F12 treatment. Two other pathways relating to IL-17 appeared in the top ten after EP/F12 treatment and these were 'Differential Regulation of Cytokine Production in Intestinal Epithelial Cells by IL-17A and IL-17F' and 'IL-17A Signalling in Gastric Cells'. All three of these pathways involve IL-17A binding to the IL-17 receptor and cause transcription of immune related genes and inflammatory mediators, such as cytokines, chemokines and AMPs. Other immune related pathways were also upregulated, such as

'Interferon Signalling', 'Activation of IRF by Cytosolic Pattern Recognition Receptors' and 'Antigen Presentation Pathway'. The genes associated with the canonical pathways that were upregulated after EP/F12 treatment are shown in Table 4.23. The 'Superoxide Radicals Degradation' and 'Salvage Pathways of Pyrimidine Deoxyribonucleotides' pathways had –log(p-values) of 1.29 and 1.17, respectively (equating to p-values of 0.051 and 0.067) which did not pass the significance threshold. All of the remaining pathways had significant p-values (shown in Table 4.23).

The canonical pathways upregulated after F24 and EP/F24 treatments are shown in Table 4.22 and Table 4.24, respectively, and were similar to that of the 12 hour time point with upregulation of interferon and IL-17 related pathways.

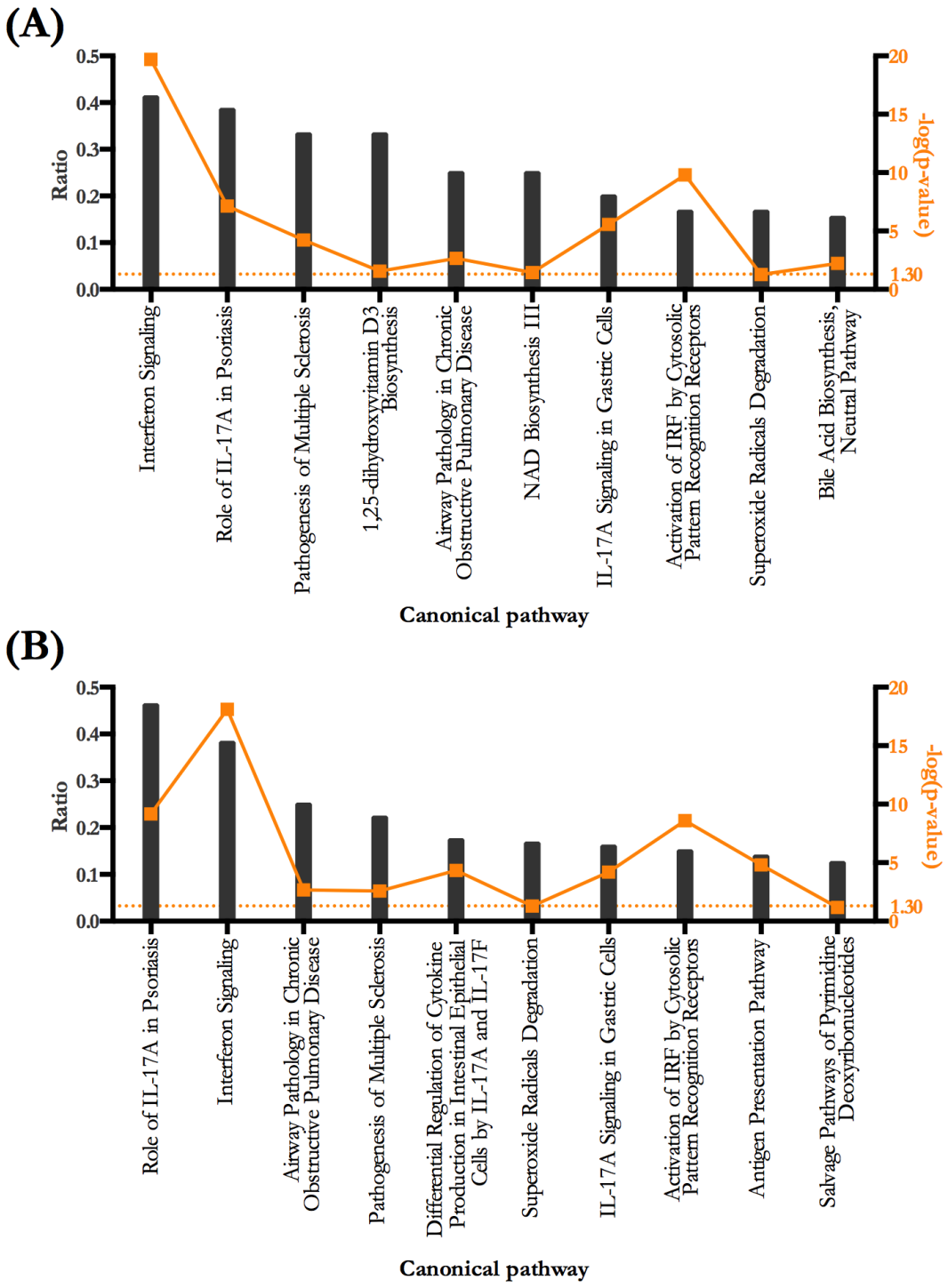

Figure 4.16: Top ten canonical pathways after F12 and EP/F12 treatments. The graphs show the top ten canonical pathways by ratio after (A) 12 hours flagellin treatment (F12) and (B) estrogen pretreatment plus flagellin treatment at 12 hours (EP/F12). The grey bars represent the ratio for each pathway and the orange symbols represent the –log(p-value). The significance cut off of 1.30 for the –log(p-value) is shown with a dotted orange line.

Table 4.21: Table of canonical pathways upregulated after F12 treatment.

Function	Ratio	-log(p-value)	Number of molecules	Molecules
Interferon Signaling	0.4120	19.70	14	IFIT3,OAS1,MX1,IFI35,IRF9,PSMB8, TAP1,IFITM2,IRF1,IFIT1,IFITM3, STAT2,STAT1,IFITM1
Role of IL-17A in Psoriasis	0.3850	7.13	5	CXCL8,S100A9,CCL20,S100A8, DEFB4A/DEFB4B
Pathogenesis of Multiple Sclerosis	0.3330	4.22	3	CXCL10,CXCL11,CCL5
1,25-dihydroxyvitamin D3 Biosynthesis	0.3330	1.56	1	CYP27B1
Airway Pathology in Chronic Obstructive Pulmonary Disease	0.2500	2.65	2	CXCL8,MMP9
NAD Biosynthesis III	0.2500	1.44	1	NAMPT
IL-17A Signaling in Gastric Cells	0.2000	5.56	5	CXCL10,CXCL8,CXCL11,CCL20,CCL5
Activation of IRF by Cytosolic Pattern Recognition Receptors	0.1670	9.80	10	DHX58,IFIH1,IRF7,DDX58,STAT2, IRF9,STAT1,ADAR,IFIT2,ISG15
Superoxide Radicals Degradation	0.1670	1.27	1	SOD2
Bile Acid Biosynthesis, Neutral Pathway	0.1540	2.22	2	AKR1C1/AKR1C2,AKR1C4

Table 4.22: Table of canonical pathways upregulated after F24 treatment.

Function	Ratio	-log(p-value)	Number of molecules	Molecules
Role of IL-17A in Psoriasis	0.4620	10.60	6	S100A7,CXCL8,S100A9,CCL20,S100A8, DEFB4A/DEFB4B
Glutathione Redox Reactions II	0.3330	1.82	1	TXNDC12
Interferon Signaling	0.2650	13.10	9	IFITM3,OAS1,MX1,IFI35,IRF9,STAT1, TAP1,IFITM2,IFITM1
Airway Pathology in Chronic Obstructive Pulmonary Disease	0.2500	3.15	2	CXCL8,MMP9
Pathogenesis of Multiple Sclerosis	0.2220	3.04	2	CXCL10,CCL5
Differential Regulation of Cytokine Production in Intestinal Epithelial Cells by IL-17A and IL-17F	0.1740	5.28	4	DEFB103A/DEFB103B,LCN2,CCL5, DEFB4A/DEFB4B
Superoxide Radicals Degradation	0.1670	1.52	1	SOD2
IL-17A Signaling in Gastric Cells	0.1600	5.13	4	CXCL10,CXCL8,CCL20,CCL5
Salvage Pathways of Pyrimidine Deoxyribonucleotides	0.1250	1.40	1	TYMP
Prostanoid Biosynthesis	0.1110	1.35	1	PTGS2

Table 4.23: Table of canonical pathways upregulated after EP/F12 treatments.

Function	Ratio	-log(p-value)	Number of molecules	Molecules
Role of IL-17A in Psoriasis	0.4620	9.16	6	S100A7,CXCL8,S100A9,CCL20,S100A8, DEFB4A/DEFB4B
Interferon Signaling	0.3820	18.10	13	IFITM3,IFIT1,IFIT3,OAS1,MX1,STAT2, IRF9,IFI35,PSMB8,STAT1,IFITM2,TAP1, IFITM1
Airway Pathology in Chronic Obstructive Pulmonary Disease	0.2500	2.68	2	CXCL8,MMP9
Pathogenesis of Multiple Sclerosis	0.2220	2.57	2	CXCL10,CCL5
Differential Regulation of Cytokine Production in Intestinal Epithelial Cells by IL-17A and IL-17F	0.1740	4.35	4	DEFB103A/DEFB103B,LCN2,CCL5, DEFB4A/DEFB4B
Superoxide Radicals Degradation	0.1670	1.29	1	SOD2
IL-17A Signaling in Gastric Cells	0.1600	4.20	4	CXCL10,CXCL8,CCL20,CCL5
Activation of IRF by Cytosolic Pattern Recognition Receptors	0.1500	8.60	9	IFIH1,IRF7,DDX58,STAT2,IRF9,STAT1, ADAR,IFIT2,ISG15
Antigen Presentation Pathway	0.1390	4.82	5	PSMB9,HLA-B,PSMB8,HLA-F,TAP1
Salvage Pathways of Pyrimidine Deoxyribonucleotides	0.1250	1.17	1	TYMP

Table 4.24: Table of canonical pathways upregulated after EP/F24 treatments.

Function	Ratio	-log(p-value)	Number of molecules	Molecules
Role of IL-17A in Psoriasis	0.3850	7.19	5	S100A7,S100A9,CCL20,S100A8, DEFB4B/DEFB4B
Ascorbate Recycling (Cytosolic)	0.3330	1.58	1	GLRX
Glutathione Redox Reactions II	0.3330	1.58	1	GLRX
Interferon Signaling	0.3240	14.30	11	IFIT3,IFITM3,OAS1,MX1,IFI35,STAT2, IRF9,STAT1,TAP1,IFITM2,IFITM1
Arginine Degradation I (Arginase Pathway)	0.2500	1.45	1	ARG1
Pathogenesis of Multiple Sclerosis	0.2220	2.56	2	CXCL10,CCL5
Differential Regulation of Cytokine Production in Intestinal Epithelial Cells by IL-17A and IL-17F	0.1740	4.32	4	DEFB103A/DEFB103B,LCN2,CCL5, DEFB4A/DEFB4B
Urea Cycle	0.1670	1.28	1	ARG1
Arginine Degradation VI (Arginase 2 Pathway)	0.1670	1.28	1	ARG1
Superoxide Radicals Degradation	0.1670	1.28	1	SOD2

The 'Role of IL-17A in Psoriasis' pathway diagram in Figure 4.17 shows the molecules involved with this pathway. Red shading of a molecule indicates upregulation in the dataset and the intensity of the colour indicates the degree of fold change in gene expression. The pathway shows IL-17A acting upon the IL-17 receptor, which is made up of IL-17RA and IL-17RC subunits, and causing transcription of genes involved in either an antimicrobial response, such as hBD2, or genes involved in psoriasis, such as CCL20. After EP12 treatment S100A8 and S100A9 are the only molecules in this pathway that were upregulated, by 2.03 and 2.13-fold respectively (Figure 4.17A). However, after F12 treatment S100A8/9 were upregulated but hBD2, CCL20 and IL-8 were also upregulated (Figure 4.17B). After EP/F12 treatment these molecules and S100A7 were all upregulated (Figure 4.17C). Furthermore, as shown in Figure 4.5 in section 4.3 the expression of genes S100A7, S100A8, S100A9, and hBD2 was higher with EP/F treatment than just F treatment and this is reflected in Figure 4.17 by more intense colouring on the pathway. Thus, the

'Role of IL-17A in Psoriasis' canonical pathway was on the whole more upregulated with EP/F treatment than with EP or F treatment separately.

(A) EP12

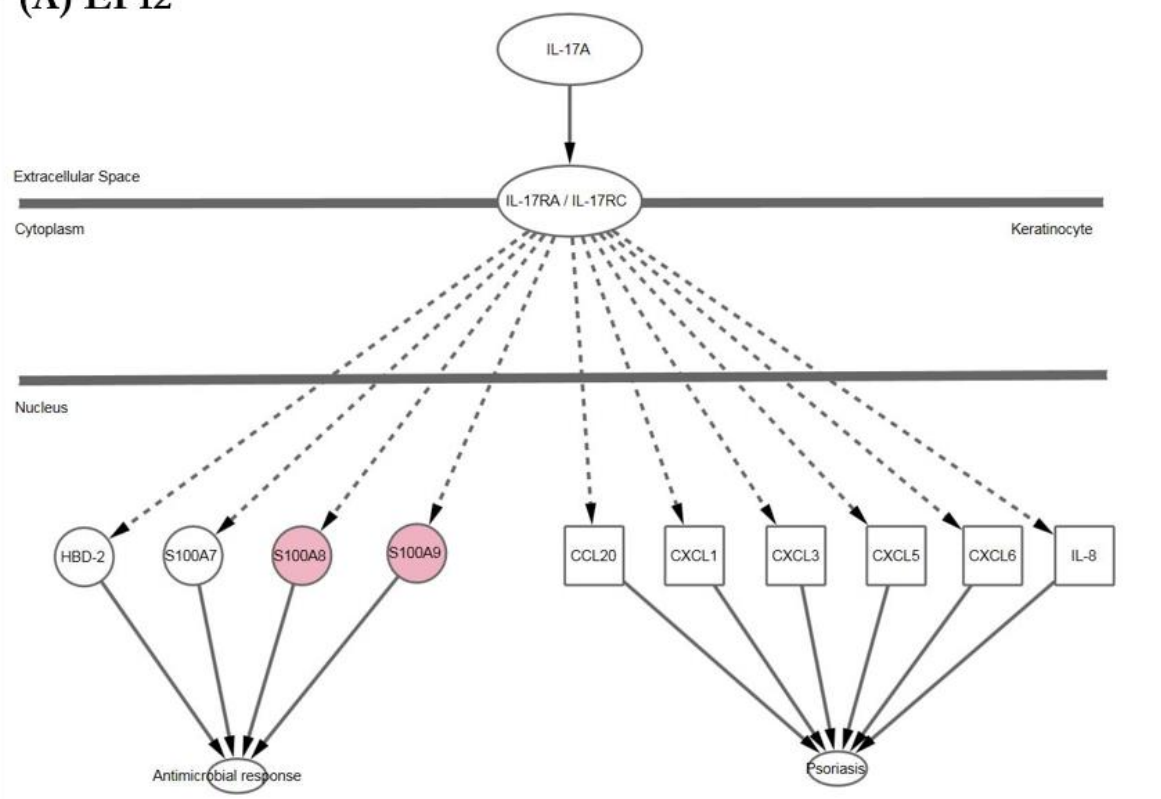
IL-17A
Extracellular Space
IL-17RA / IL-17RC
Cytoplasm
Keratinocyte
Nucleus
HBD-2
S100A7
S100A8
S100A9
CCL20
CXCL1
CXCL3
CXCL5
CXCL6
IL-8
Antimicrobial response
Psoriasis

(B) F12

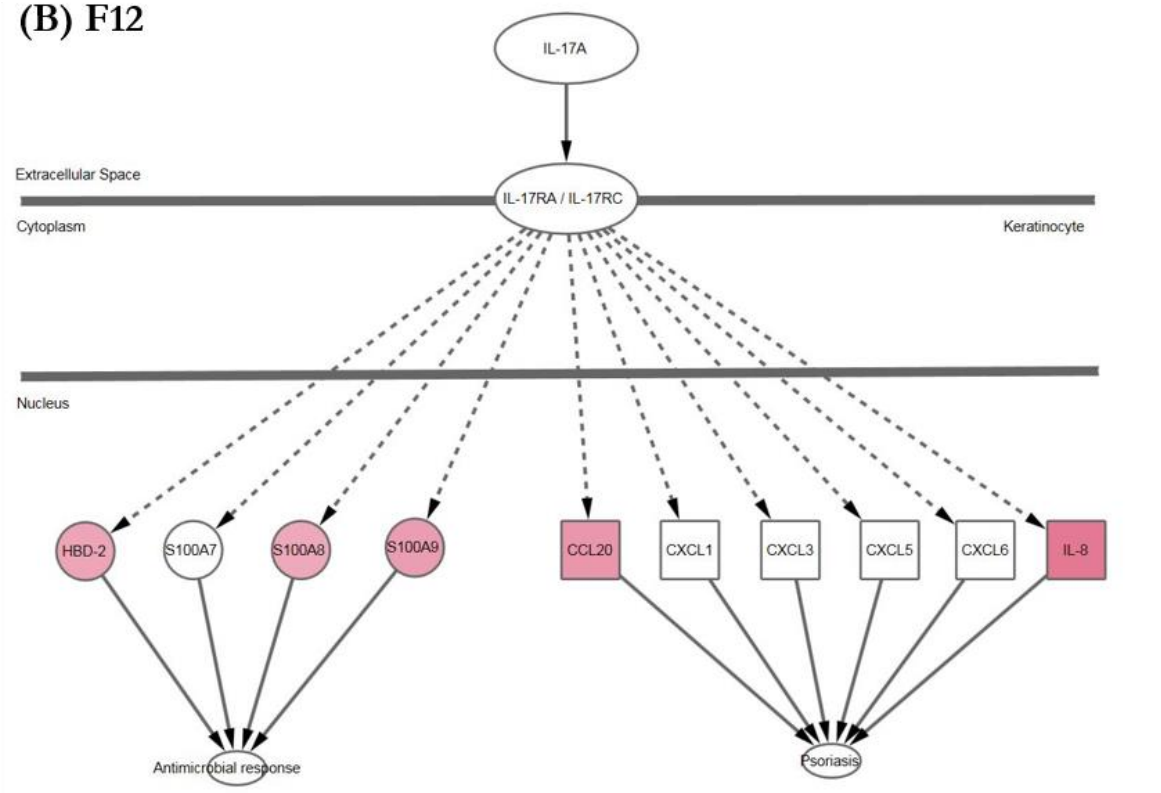
IL-17A
Extracellular Space
IL-17RA / IL-17RC
Cytoplasm
Keratinocyte
Nucleus
HBD-2
S100A7
S100A8
S100A9
CCL20
CXCL1
CXCL3
CXCL5
CXCL6
IL-8
Antimicrobial response
Psoriasis

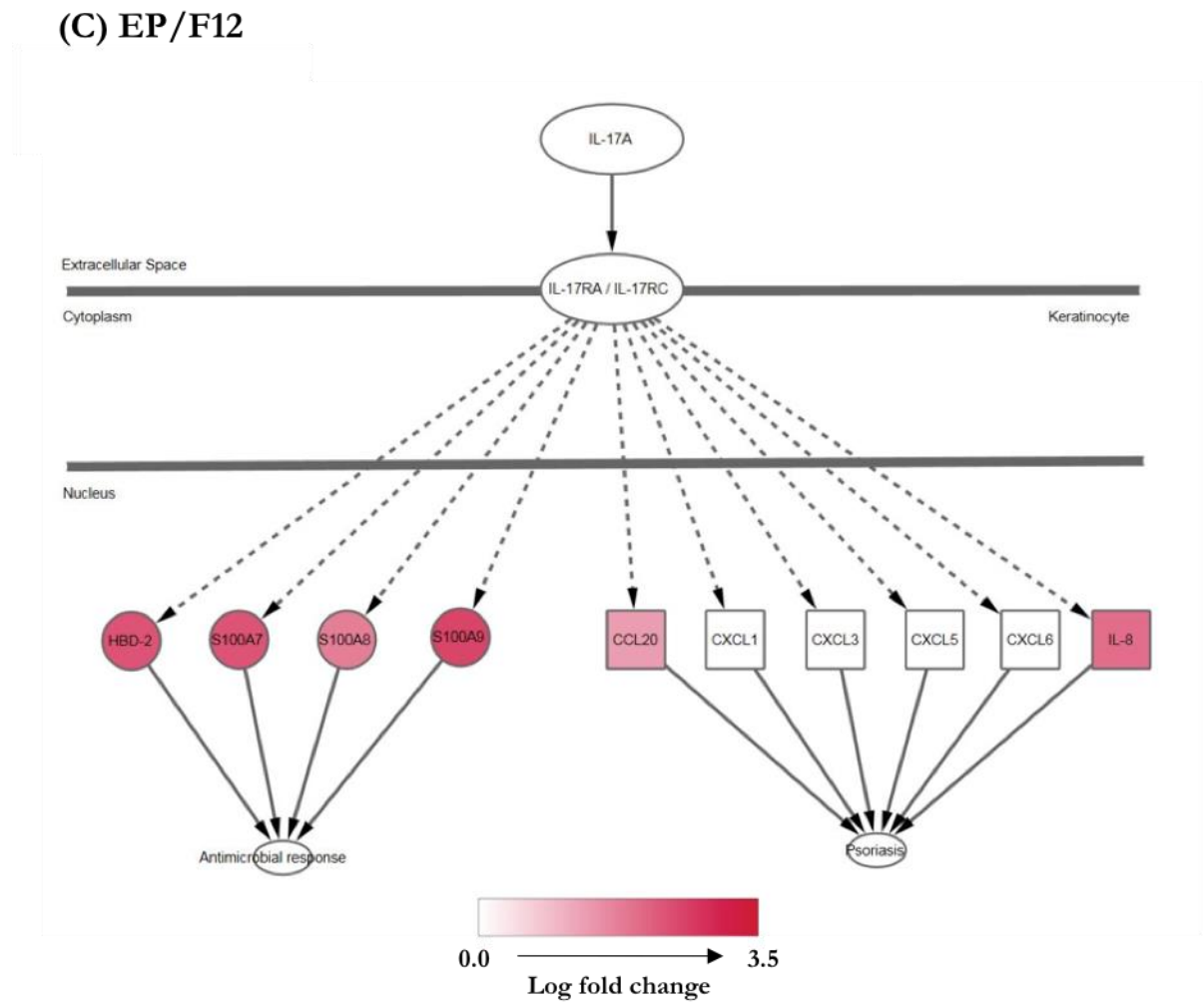

Figure 4.17: 'Role of IL-17A in Psoriasis' pathway diagram. The data from (A) Estrogen pretreatment at 12 hours, EP12, (B) Flagellin treatment after 12 hours, F12, and (C) Estrogen pretreatment plus flagellin after 12 hours, EP/F12, is overlaid on the pathway diagram for the 'Role of IL-17A in Psoriasis' pathway, using Ingenuity Pathway Analysis. The intensity of the red colouring indicates the degree of upregulation.

4.5.2.1 Discussion of canonical pathways

IPA was used to analyse the six microarray datasets for canonical pathways that were overrepresented after each treatment. Canonical pathways associated with interferon production and signalling were upregulated after F and EP/F treatments. However, perhaps more notable, all three treatments resulted in upregulation of multiple pathways associated with IL-17. The 'Role of IL-17A in Psoriasis' pathway was overrepresented in every dataset indicating that after EP, F and EP/F treatments at both the 12 and 24 hour time points genes from this pathway were significantly upregulated. In the case of psoriasis, activation of this pathway resulting in expression of chemokines that attract immune cells aggravates the condition by promoting influx of proinflammatory cytokine-producing immune cells to the psoriatic lesion, driving inflammation. However, in the case of an infection, such as a UTI, activation of this pathway may stimulate both an innate (AMP) immune response and an adaptive immune response. Thus, it is possible that increased activation of this pathway may improve bacterial clearance from the

site of infection. However, IL-17 is not produced by epithelial cells, and hence, expression of this gene in VK2 cells was not detected by the microarray. IL-17 is mainly produced by Th17 cells. Th17 cells are recruited to sites of infection by secretion of the chemokine CCL20, which was significantly upregulated by F12 and EP/F12 treatment[277,278]. The expression of IL-36G, a proinflammatory cytokine identified as a potential gene of interest, was also potentiated by EP/F treatment and has been shown to stimulate IL-17 production from CD4+ T cells[237]. Thus, increased IL-36G expression following estrogen pretreatment may result in increased IL-17 secretion from CD4+ T cells at the site of infection. Furthermore, the downstream functions analyses indicated that immune cell migration was activated in all datasets. Even though IL-17 was not present in the VK2 cell model, the genes downstream of this cytokine show upregulation. Consequently, it is possible to hypothesise that addition of IL-17 to VK2 cells would further increase the expression of the AMPs, cytokines, and chemokines in this pathway. Furthermore, addition of IL-17 to the VK2 cells would more accurately model the cytokine environment that vaginal epithelial cells are exposed to during infection, as IL-17 secreting Th17 cells would likely be recruited to the site of infection by CCL20.

4.5.3 Upstream regulator analysis

Upstream regulator analysis identifies molecules, such as transcription factors, that are upstream of the genes in a given dataset and may be responsible for the observed gene expression changes. IPA uses the gene expression data to predict which upstream regulators are activated or inhibited in a dataset. For example, if it is reported in the literature that a set of genes are transcribed by a particular transcription factor, and these genes are upregulated in a given dataset, IPA predicts that the upstream regulator is active. However, if the gene expression mostly contradicts the literature IPA predicts that the upstream regulator is inhibited. If the gene expression data do not follow a clear pattern with the literature a prediction of the upstream regulator activity cannot be made. Following identification of important upstream regulators, IPA also identifies mechanistic networks; these are used to determine which, if any, transcription factors are working together to regulate the genes within a dataset.

The upstream regulators and mechanistic networks were analysed for each dataset. After EP12 treatment only one transcription factor was predicted to be activated by IPA and this was E26 transformation-specific (ETS) homologous factor (EHF) with an activation z-score of 2.00. This transcription factor belongs to the family of ETS transcription factors that possess a conserved DNA binding domain, the ETS domain[279]. No mechanistic network was predicted for this transcription factor. Four genes from the EP12 dataset were predicted to be downstream of this

transcription factor and these were cornifelin (CNFN), S100A8, S100A9 and SPRR2A. EHF is a member of the epithelial specific expression (ESE) family of transcription factors and is reported to have roles epithelial cell differentiation and barrier function[280,281]. Therefore, this transcription factor may be involved in the keratinisation process of vaginal epithelial cells in response to estrogen treatment identified by downstream functional analysis.

After F12 treatment 17 transcription factors were predicted to be upregulated (see Table 4.25) by IPA. Interferon regulatory factor 3 (IRF3) had the highest activation z-score (5.715) suggesting this was the most activated transcription factor for this dataset. IRF1, 5 and 7 were also predicted to be activated, with z-scores of 3.071, 4.383 and 5.381, respectively. These transcription factors are involved in transcription of interferon-induced genes and were upstream of several genes, such as IFIT3 and OAS1, involved in the 'Interferon Signalling' canonical pathway discussed previously. Three of the 17 transcription factors that were predicted to be activated after F12 treatment also had increased gene expression in the dataset compared to controls (see Table 4.25). These three transcription factors are IRF1, IRF7 and signal transducer and activator of transcription 1 (STAT1). Transcriptional upregulation of these transcription factors further indicated a role for these transcription factors after flagellin treatment.

Table 4.25: Table of activated upstream regulators after flagellin treatment at 12 hours. The mechanistic network is shown as: number of target genes in network (number of transcription factors in network).

Upstream Regulator	Fold Change	Predicted Activation State	Activation z-score	Mechanistic Network
IRF3		Activated	5.715	73 (8)
IRF7	7.41	Activated	5.381	61 (8)
STAT1	11.48	Activated	4.985	87 (16)
IRF5		Activated	4.383	47 (5)
NFATC2		Activated	3.606	65 (7)
RELA		Activated	3.522	86 (16)
TP53		Activated	3.273	89 (19)
STAT3		Activated	3.075	75 (15)
IRF1	2.17	Activated	3.071	19 (2)
EZH2		Activated	2.926	
EHF		Activated	2.714	
PPRC1		Activated	2.598	
JUN		Activated	2.491	45 (11)
SMARCB1		Activated	2.449	
FOXO1		Activated	2.408	55 (9)
FOXO3		Activated	2.333	61 (11)
CTNNB1		Activated	2.000	11 (2)

Observation of the mechanistic networks associated with the transcription factors revealed that many of the mechanistic networks are in fact highly similar, and only differ by perhaps one or two transcription factors. For example, the IRF3, STAT1, tumour protein P53 (TP53) and V-rel avian reticuloendotheliosis viral oncogene homolog A (RELA) mechanistic networks, shown in

Figure 4.18, share many common transcription factors, such as STAT1, STAT3, NF-κB (complex) and forkhead box O1 (FOXO1), and result in transcription of similar groups of genes.

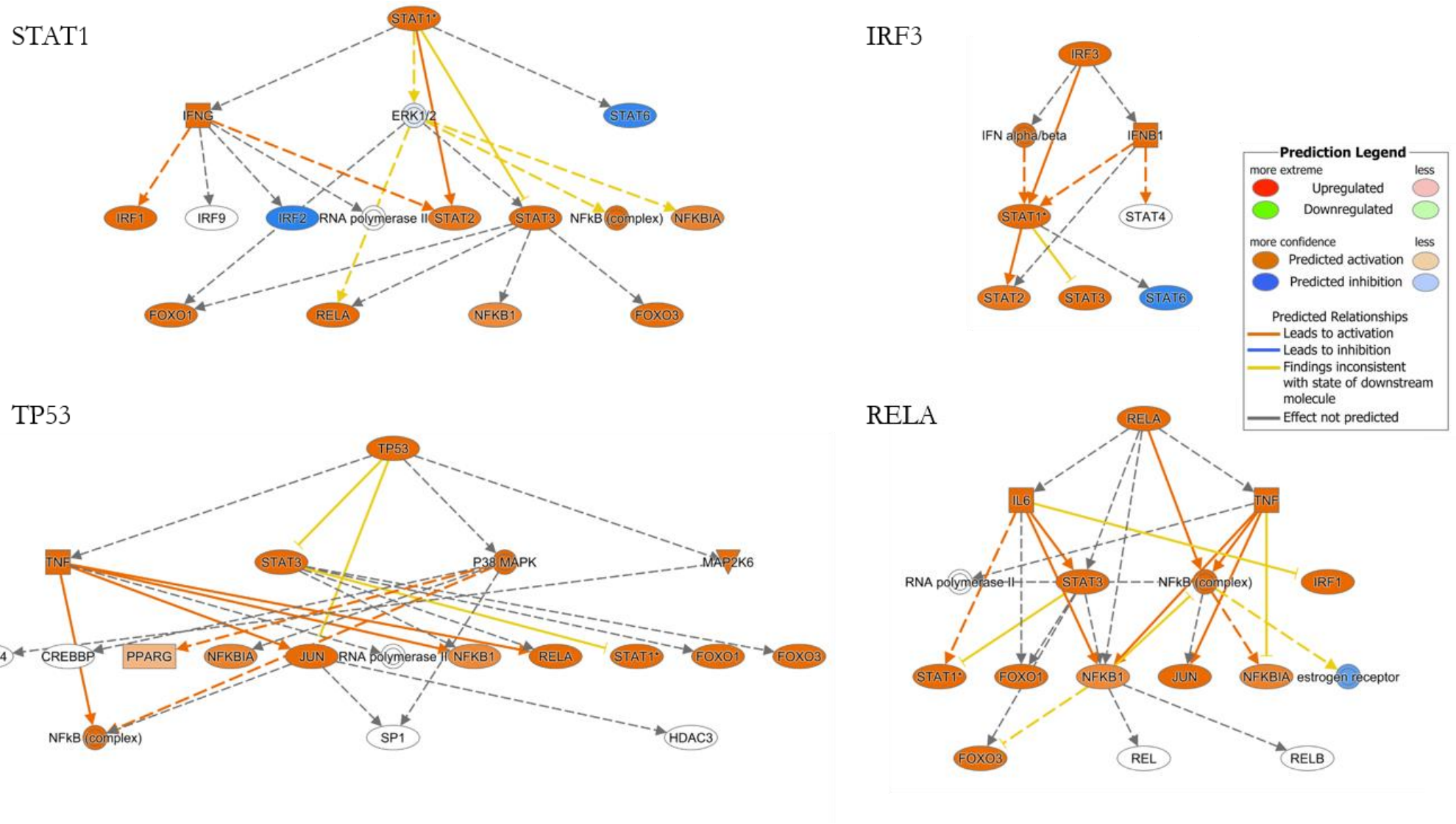

Figure 4.18: Examples of mechanistic networks after flagellin treatment for 12 hours.

The transcription factor STAT1 was present in many of the mechanistic networks and was upregulated 11.48-fold after F12 treatment indicating that this was potentially a crucial transcription factor in VK2 cell response to flagellin challenge. The STAT1 mechanistic network after F12 treatment consisted of 16 transcription factors working together to upregulate 87 genes. These genes included interferon-induced genes, cytokines, chemokines and AMPs. The full list of genes downstream of the STAT1 mechanistic network after F12 treatment is shown in Table 4.26.

Table 4.26: Genes downstream of the STAT1 mechanistic network after flagellin treatment at 12 hours.

Gene	Fold Change	Gene	Fold Change	Gene	Fold Change	Gene	Fold Change
ALDH1A3	2.08	IFI27	16.47	LGALS3BP	2.13	SDC4	2.34
BIRC3	2.77	IFI35	6.84	LTB	10.91	SERPINA3	8.67
CASP1	2.30	IFI44	4.03	MARCKSL1	3.47	SERPINB2	2.80
CASP4	2.04	IFI44L	15.81	MMP9	3.72	SERPINB4	2.92
CCL20	2.68	IFI6	14.36	MX1	16.02	SERPINE2	2.28
CCL5	9.61	IFIH1	5.09	MX2	24.78	SLC15A3	5.56
CEACAM1	2.07	IFIT1	7.00	NAMPT	2.07	SLFN5	2.56
CFB	7.63	IFIT2	5.34	OAS1	17.20	SOD2	8.06
CMPK2	2.35	IFIT3	13.45	OAS2	14.99	SP100	2.70
CXCL10	41.73	IFIT5	2.34	OAS3	5.85	SP110	8.78
CXCL11	2.32	IFITM1	14.02	OASL	4.79	STAT1	11.48
CXCL8	3.59	IFITM2	3.19	PI3	2.05	STAT2	4.81
DDX58	4.66	IFITM3	3.50	PLSCR1	5.27	TAP1	5.37
DEFB4A/DEFB4B	2.35	IL1RN	2.66	PSMB10	2.23	TNFSF10	3.98
EIF2AK2	3.11	IL32	2.39	PSMB8	3.43	TNIP1	3.56
GBP1	8.84	IRF1	2.17	PSMB9	2.72	TRIM22	8.78
GBP4	4.03	IRF7	7.41	PSME2	2.10	TYMP	5.26
HERC6	3.13	IRF9	3.21	RSAD2	8.71	USP18	5.43
HLA-B	4.16	ISG15	4.89	S100A8	2.24	VEGFC	2.14
HLA-F	3.22	ISG20	3.40	S100A9	2.53	WARS	2.49
ICAM1	2.41	LAMP3	7.48	SAA1	3.65	XAF1	6.19
IFI16	2.71	LCN2	6.38	SAMD9	4.16		

The EHF transcription factor was also predicted to be activated for the F12 dataset with a z-score of 2.714, compared to a z-score of 2.000 after EP12 treatment. Furthermore, after F12 treatment 11 upregulated genes from the dataset were predicted to be downstream of the EHF transcription factor, when only four genes downstream of this transcription factor were upregulated after EP12 treatment.

Upstream analysis of the EP/F12 revealed that IPA predicted activation of 20 transcription factors (see Table 4.27). IRF3 was once again the transcription factor with the highest z-score (5.355), and similar transcription factors were predicted to be activated for both F12 and EP/F12 treatments (see Figure 4.19A). Furthermore, most of the transcription factors exhibited similar z-scores after both F12 and EP/F12 treatments. EP/F12 treatment resulted in the predicted activation of four transcription factors that were not predicted to be activated after F12 treatment; these were V-myc avian myelocytomatosis viral oncogene homolog (MYC), nuclear receptor coactivator 2 (NCOA2), STAT2 and CEBPB.

Table 4.27: Table of transcription factors predicted to be activated after estrogen pretreatment plus flagellin treatment at 12 hours. The mechanistic network is shown as: number of target genes in network (number of transcription factors in network).

Upstream Regulator	Fold Change	Predicted Activation State	Activation z-score	Mechanistic Network
IRF3		Activated	5.355	69 (10)
IRF7	5.47	Activated	4.902	54 (8)
EHF		Activated	4.000	
IRF5		Activated	3.918	
STAT1	7.90	Activated	3.861	78 (15)
STAT3		Activated	3.339	65 (15)
NFATC2		Activated	3.162	42 (4)
RELA		Activated	2.936	76 (16)
TP53		Activated	2.866	82 (21)
IRF1		Activated	2.742	30 (3)
SMARCB1		Activated	2.611	
PPRC1		Activated	2.598	
MYC		Activated	2.577	
JUN		Activated	2.397	50 (9)
FOXO1		Activated	2.395	42 (7)
NCOA2		Activated	2.383	63 (11)
EZH2		Activated	2.359	19 (3)
FOXO3		Activated	2.317	33 (8)
STAT2	3.31	Activated	2.234	52 (5)
CEBPB		Activated	2.159	45 (7)

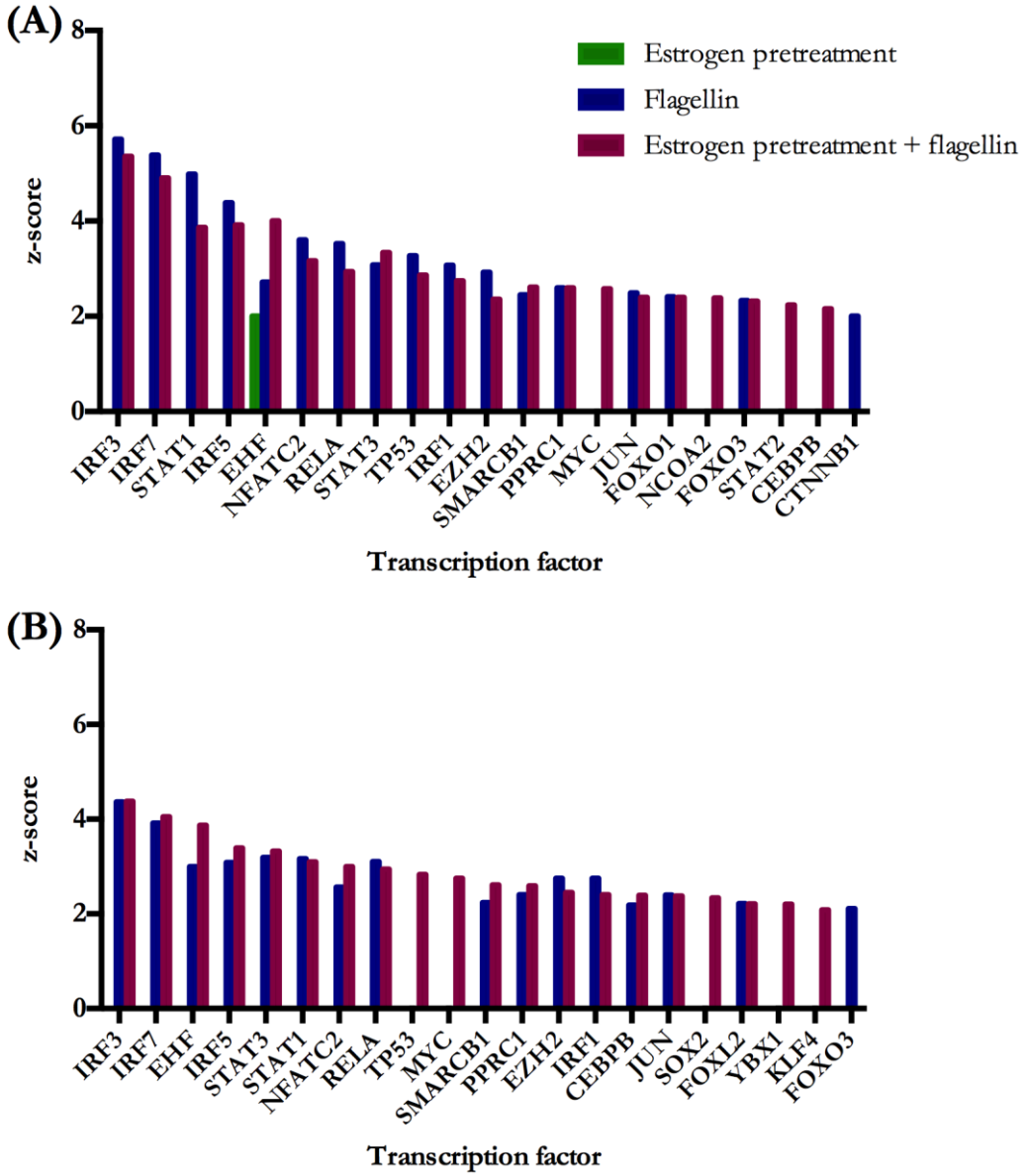

Figure 4.19: Comparison of transcription factors predicted to be activated after estrogen pretreatment, flagellin, and estrogen pretreatment plus flagellin treatments. (A) transcription factors predicted to be activated after 12 hours and (B) transcription factors predicted to be activated after 24 hours.

The transcription factor EHF was predicted to be most active after EP/F12 treatment with a z-score of 4.000, compared to 2.714 after F12 treatment and 2.000 after EP12 treatment. Furthermore, after EP/F12 16 upregulated genes in this dataset were downstream of this transcription factor. These genes are mostly related to keratinisation and cell differentiation, such CNFN, S100 proteins and SPRR genes. The fold change in gene expression for these 16 genes and the genes downstream of EHF that were upregulated after EP12 and F12 treatments are shown in Table 4.28.

Table 4.28: Table of genes downstream of the EHF transcription factor that are upregulated after estrogen pretreatment (EP12), flagellin (F12), and estrogen pretreatment plus flagellin (EP/F12) at 12 hours.

	Fold Change		
Gene Symbol	**EP12**	**F12**	**EP/12**
CCL20		2.68	2.54
CNFN	2.04		5.90
IL1RN		2.66	2.32
KLK7			2.02
S100A7			5.07
S100A8	2.03	2.24	3.39
S100A9	2.13	2.53	5.86
S100A12			2.69
SAA1		3.65	2.25
SERPINA3		8.67	8.92
SPRR1B			2.38
SPRR2A	2.06	3.95	14.74
SPRR2D		2.09	5.73
SPRR2E		3.14	13.54
SPRR2G			7.27
SPRR3			2.11
TNC		2.41	
VEGFC		2.14	

Analysis of the 24 hour datasets showed similar transcription factors were predicted to be activated to those of the 12 hour datasets (Figure 4.19B). After EP/F24 treatment there were five transcription factors that were predicted to be activated that were not predicted to be activated for F24 treatment. These were TP53, MYC, SYR box 2 (SOX2), Y-box binding protein 1 (YBX1), and Kruppel-like factor 4 (KLF4). Altogether, there were eight transcription factors that were predicted to be activated by EP/F treatment at either the 12 or 24 hour time point that were not predicted to be activated by F treatment at the same time point. These were CEBPB, KLF4, MYC, NCOA2, SOX2, STAT2, TP53 and YBX1. The upregulated genes downstream of these transcription factors at each time point are shown in Table 4.29. Of note, from the genes of interest identified by Venn diagram analysis, DEFB4A, LCN2 and SLPI were identified downstream of YBX1, CEBPB and KLF4, respectively. Thus, increased activation of these transcription factors following EP/F treatment may result in increased transcription of these AMPs.

Table 4.29: Genes downstream of transcription factors upregulated after EP/F treatment but not F treatment.

Transcription factor	12 hour downstream genes	24 hour downstream genes
CEBPB	ARG1,CCL5,FABP4,IGFBP3,IRF9,LCN2,SBSN, SERPINB2	
KLF4		ASPRV1,CNFN,CST6,LOR,PRDM1,SERPINB2,SLPI,SPRR3,TGM1,USP18
MYC	(a),CASP1,EGR1,GBP4,IFI16,SPRR1A	ARG1,ASPRV1,CST6,PRDM1,CNFN,FABP4,LOR,MMP9,PLSCR1,SPRR3, TGM1,THBS1,USP18 = (a)
NCOA2	CCL5,CXCL10,EGR1,FABP4,IFIT2,ISG15,OASL	
SOX2		ASPRV1,CNFN,CST6,HOPX,LOR,PRDM1,SPRR3,TGM1,USP18
STAT2	CCL5,GBP1,IFI27,IFI6,IFIT2,IFIT3,IFITM1,IRF7, IRF9,ISG15,MX1,OAS1,OAS2,RSAD2	
TP53	(b),CASP1,CXCL8,GBP1,IFI16,TSC22D3,ZC3H12A	BIRC3,GLRX,PRDM1,SCO2,FABP4,ID1,IFI35,IGFBP3,IRF7,IRF9,ISG15, MAFB,MMP9,OAS1,SERPINA3,SOD2,STAT1,TAP1,THBS1,TRIM22 = (b)
YBX1		CCL5,CXCL2,DEFB4A/DEFB4B,ID1,IGFBP3

4.5.3.1 Discussion of upstream regulator analysis

Analysis of upstream regulators using IPA is utilised to predict which transcription factors may be activated depending on which genes are differentially expressed in a dataset. The activation state and associated z-score of a transcription factor is determined based upon known relationships in the literature. A transcription factor is predicted as being activated if it has a z-score above +2. This type of analysis is useful as transcription factors may be highly activated in a sample but not show increased expression, as many transcription factors are activated by phosphorylation events, or by dissociation from an inhibitor. Therefore, the expression values of transcription factors are not sufficient to determine the activation state.

The six microarray datasets were analysed in this way to examine whether particular transcription factors may be responsible for the observed potentiation of the expression of certain genes with estrogen pretreatment before flagellin challenge in VK2 cells.

The analysis revealed that the EHF transcription factor is predicted to be activated after all three treatments. Furthermore, EHF is predicted to be most active following EP/F treatment. This transcription factor is upstream of several of the potential genes of interest. Increased activation of this transcription factor after EP/F12 treatment, compared to F12 treatment, may explain the substantial gene expression potentiation of genes such as the SPRR genes after EP/F12 treatment (shown in section 4.3 in the Venn diagram analysis), as these genes are downstream of EHF. Thus, estrogen pretreatment prior to flagellin challenge may result in increased keratinisation and a strengthened epithelial barrier to infection through activation of this transcription factor, resulting in transcription of genes crucial to this process. Other transcription

factors in the ETS family have been shown to be activated by hormones such as gonadotropin-releasing hormone via a MAP kinase pathway. Binding of estrogen to GPER results in MAP kinase activation. This reveals a potential pathway of estrogen regulation of EHF and therefore, keratinisation and differentiation in VK2 cells.

Similar transcription factors were predicted to be upregulated after both F12 and EP/F12 treatments, and many of these transcription factors had similar z-scores, for example IRF3, STAT1 and RELA. Thus, it was difficult to determine from this analysis alone which transcription factors were involved in the potentiation of the expression of the AMPs identified by Venn diagram analysis following estrogen treatment. There were eight transcription factors that were predicted to be activated by EP/F treatment at either 12 or 24 hours that were not predicted to be activated by F treatment at the same time point. These were CEBPB, KLF4, MYC, NCOA2, SOX2, STAT2, TP53 and YBX1. KLF4, SOX2 and TP53 were identified as being upstream of genes mostly involved in keratinisation, such as CNFN and SPRR genes, and therefore may activate the keratinisation response alongside the EHF transcription factor. The AMP SLPI was also identified as being downstream of the transcription factor KLF4. CEBPB was identified as being upstream of genes involved in both keratinisation and inflammation, and the AMP LCN2. STAT2 and YBX1 were predicted to be upstream of genes that were mostly chemokines or interferon-induced genes. However, YBX1 was predicted to be upstream of hBD2, suggesting that activation of this transcription factor may be responsible for the observed increase in gene expression of hBD2 after EP/F treatment. NCOA2 is a transcription factor that interacts with nuclear hormone receptors to aid in DNA transcription. NCOA2 has been shown to co-localise with ER-α in nuclei after estrogen treatment[282]. Thus, EP/F treatment may increase gene expression through activation of NCOA2. Therefore, these analyses highlight transcription factors that were predicted to be more activated following EP/F treatment, compared to F treatment, and thus, may be involved in upregulation of the AMPs hBD2, LCN2 and SLPI. However, the upstream regulator analysis did not reveal potential transcription factors for all AMPs identified by Venn diagram analysis, such hBD3 and RNase 7. Hence for these AMPs other transcription factors not identified by IPA (such as the genomic ERs) may require further investigation.

4.6 Summary

This chapter focussed on the use of microarrays to perform whole transcriptome analysis, enabling the identification of both downstream effector genes and pathways involved in

regulating expression of target genes. Microarrays were performed upon eight conditions: control, estrogen pretreatment, flagellin, and estrogen pretreatment plus flagellin at the 12 and 24 hour time points. This generated six datasets for analysis via examining the expression patterns of individual genes by employing Venn diagrams and utilising IPA for downstream effect, canonical pathway, and upstream regulator analyses.

Initial analysis of the datasets by Venn diagram resulted in identification of 20 genes of interest. The expression of these genes was potentiated by estrogen pretreatment prior to challenge with flagellin, compared to flagellin challenge without prior estrogen treatment. The genes of interest are all either AMPs, or are involved in keratinisation, inflammation, or have multiple roles within these three areas. This suggested that pretreatment of vaginal epithelial cells with estrogen prior to exposure to the bacterial PAMP flagellin served to increase the keratinisation of the vaginal epithelial barrier, as well as the inflammatory and antimicrobial response of the vagina. Thus, these factors promote rapid clearance of bacteria from the site of infection.

Analysis of the microarray data via IPA identified a potential role for IL-17 in the production of AMPs. This pathway has been predominantly studied in psoriasis and shows that binding of IL-17 to the IL-17 receptor results in expression of AMPs and chemokines in keratinocytes. IL-17 is expressed by Th17 cells, not epithelial cells, and thus this element was absent from the VK2 cell model. However, the microarray data showed that F and EP/F treatments both caused expression of CCL20 – the chemokine responsible for Th17 cell migration. Therefore, it was possible to hypothesise that the presence of pathogenic bacteria in the vagina stimulates expression of CCL20, causing migration of Th17 to the vagina, which stimulates AMP production facilitating bacterial killing. This notion is supported by downstream function analysis of the microarray data showing that F and EF treatments activated immune cell migration. However, the literature suggests that estrogen and IL-17 levels may be conversely expressed *in vivo*, as serum IL-17 increases after the menopause when estrogen levels decline[283]. Initial investigations into the effect of IL-17 on vaginal AMP expression are presented in Chapter 6.

It is difficult to conclude from the upstream regulator analysis which transcription factors may be involved in increasing gene expression with EP/F treatment as IPA predicted similar levels of activation for most of the transcription factors with both F and EP/F treatments. However, there were transcription factors that were only predicted to be activated after EP/F treatment that will need further investigation, along with the genomic ERs which can directly cause

transcription of target genes upon binding to estrogen. The role of the ERs in vaginal AMP expression is explored in the next chapter.

Altogether, these microarray data indicated a role for estrogen in potentiation of AMP gene expression, in addition to genes involved in keratinisation and the inflammatory response. Thus, the data presented in this chapter have revealed that estrogen promotes a multipronged defence against vaginal UPEC colonisation.

5 Investigating the mechanisms of AMP regulation by estrogen

5.1 Introduction

Analyses of the microarray data in Chapter 4 revealed upregulation of several AMP genes, along with genes involved in keratinisation and inflammation, in response to estrogen pretreatment plus flagellin. The finding that estrogen upregulated many AMPs is supported by unpublished work from our laboratory that showed estrogen treatment of postmenopausal women significantly increased vaginal douche concentrations of hBD2, hBD3 and LCN2, compared to postmenopausal women not receiving estrogen treatment (unpublished data). Furthermore, Luthje *et al.* (2013) have also reported that estrogen treatment increased AMP expression in exfoliated bladder cells in the urine of postmenopausal women[134]. However, the mechanism behind this upregulation has not been investigated. Upstream regulator analysis of the microarray data predicted activation of many transcription factors as a result of flagellin and estrogen pretreatment plus flagellin. Specifically, YBX1, CEBPB and KLF4 were identified as being upstream regulators of hBD2, LCN2 and SLPI, respectively, and were predicted to be activated by estrogen pretreatment plus flagellin but not flagellin challenge alone. However, none of the transcription factors that were predicted by Ingenuity Pathway Analysis to be more activated by estrogen pretreatment plus flagellin than flagellin alone were upstream of other important AMPs, such as hBD3 and RNase 7. In addition, ER-α and –β can regulate gene transcription directly, by interacting with estrogen response elements in the promoter region of estrogen responsive genes. Thus, it was feasible that AMP gene regulation by ER-α and –β did not involve the transcription factors IPA predicted to be activated. It was, therefore, of interest to determine the contribution of ER-α/β and GPER to AMP expression, to establish their roles in the signalling pathways that upregulate AMP expression in response to estrogen.

Understanding the mechanisms by which estrogen regulates AMP expression may aid in development of novel therapeutics for UTI, for example by highlighting common signalling molecules involved in AMP expression. Increased serum estrogen levels are associated with higher breast cancer risk and topical estrogen application has been shown to increase the serum estrogen concentration in postmenopausal women[284,285]. As a result, topical estrogen treatment is contraindicated for breast cancer patients, due to increased risk of cancer recurrence. This highlights concerns over the safety of estrogen therapy and indicates that there are patients for whom estrogen treatment is not suitable. Thus, there is a need for alternative treatments to estrogen; hence, greater understanding of the mechanisms by which estrogen is protective against UTIs may facilitate development of non-hormonal alternatives that function in the same manner.

To explore the effects of the different estrogen receptors an agonist and antagonist were used and the effects of estrogen receptor agonism/antagonism on AMP expression were measured. The microarray data identified upregulation of the AMPs hBD2, hBD3, LCN2, RNase 7, S100A7, S100A12 and SLPI by estrogen pretreatment plus flagellin. LCN2, RNase 7 and S100A7 were chosen, in addition to hBD2 and hBD3, for initial investigations in this chapter into the mechanism of AMP regulation. LCN2 and RNase 7 have been identified as important antimicrobial effectors against UTIs and S100A7 has been shown to be an effective killer of *E. coli* in the vagina[123,129,247,248].

5.2 Mechanism of hBD2 expression regulation by estrogen

5.2.1 Inhibition of ER-α and –β and VK2 cell growth

To determine which estrogen receptors were involved in AMP upregulation following estrogen pretreatment, the ER-α and –β receptors were inhibited using ICI 182,780 (fulvestrant). Fulvestrant is a high affinity antagonist of ER-α and –β, with agonistic activity on the GPER receptor[286]. As the VK2 cells were to be pretreated with fulvestrant, the effect of 1μM fulvestrant on the growth of VK2 cells was determined using the CellTiter-Blue Cell Viability Assay (Promega, USA) as detailed in the materials and methods. The results showed (Figure 5.1) that estrogen, fulvestrant, or estrogen plus fulvestrant pretreatments did not significantly affect the growth of VK2 cells, compared to a vehicle treated control. Thus, after seven days there was approximately the same number of cells in the well, regardless of the pretreatment received. Thus, inhibition of ER-α and –β did not affect cell growth.

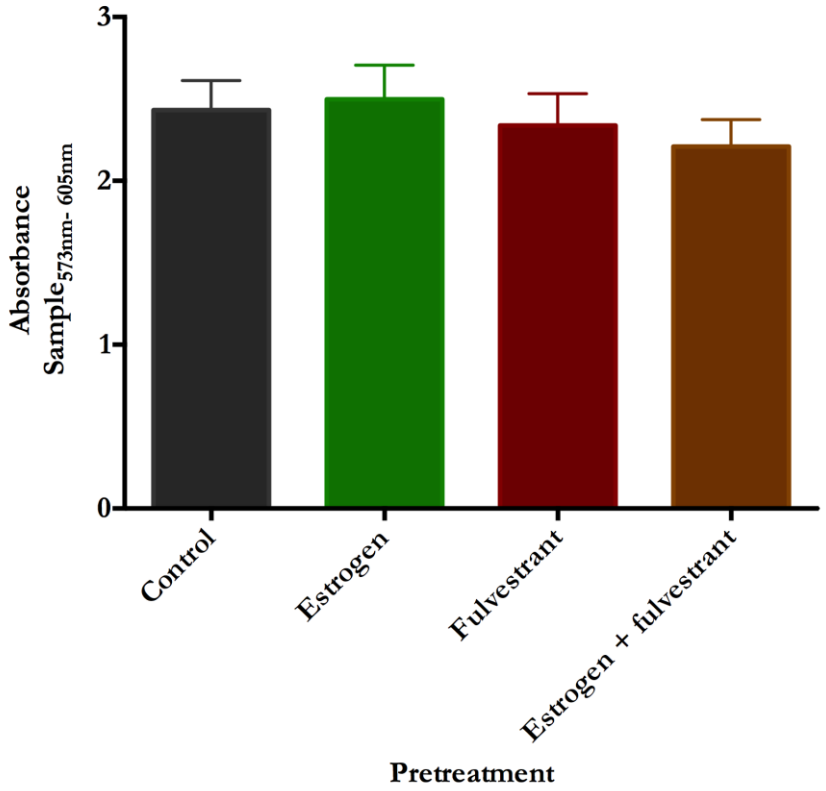

Figure 5.1: Effects of fulvestrant on VK2 cell growth. VK2 cells were seeded in 12-well plates and treated with 4nM estrogen with and without 1μM fulvestrant, or vehicle, for seven days. CellTiter-Blue Cell Viability Assay (Promega, USA) was used to measure cell viability. Error bars represent standard error. Statistical analysis was performed by one-way ANOVA with Dunnett's post hoc test. N=3, n=9.

5.2.2 Effects of inhibition of ER-α and –β on hBD2 expression

To investigate the effects of inhibiting ER-α and –β on hBD2 expression VK2 cells were treated with 4nM estrogen with and without 1μM fulvestrant (Tocris Bioscience, UK) for seven days and then challenged with 50ng/ml flagellin, or PBS, for 24 hours. This concentration of fulvestrant has been shown previously to inhibit estrogen challenge concentrations up to 10μM[287,288]. Hence, this concentration is argued to be sufficient to inhibit an estrogen challenge concentration of 4nM. If the potentiation in hBD2 expression following estrogen pretreatment was regulated through ER-α and/or –β, then following inhibition of these receptors it was predicted that the potentiation would no longer be observed. Alternatively, if the potentiation of hBD2 expression by estrogen was regulated by GPER the potentiation would still occur and may even be slightly enhanced, as fulvestrant is a GPER agonist. After 24 hour flagellin challenge the RNA was extracted, reverse transcribed into cDNA and then analysed by qPCR for the expression of hBD2. The qPCR results were analysed relative to two housekeeping genes, GAPDH and ATP5B, using the geometric mean and the resultant values were normalised to 24 hour flagellin.

The results showed (Figure 5.2) that estrogen pretreatment prior to flagellin challenge resulted in a significant increase in hBD2 expression compared to flagellin challenge alone ($p<0.0001$). However, inhibition of ER-α and –β by fulvestrant abolished this effect, so that the difference in hBD2 expression between flagellin challenge with and without estrogen pretreatment was no longer significant. Following fulvestrant treatment, flagellin and estrogen pretreatment plus flagellin induced hBD2 expression from 0.8AU in the control to 25AU and 23AU, respectively. Thus, inhibition of ER-α and –β prevented potentiation of hBD2 expression by estrogen. Fulvestrant also appeared to reduce overall hBD2 expression, even in the absence of estrogen pretreatment; flagellin challenge without fulvestrant induced a 63-fold change in hBD2 expression (from 1.6AU in the control to 100AU after flagellin challenge), whereas flagellin challenge with fulvestrant only induced a 31-fold change in hBD2 expression (from 0.8AU in the control to 25AU after flagellin). The CellTiter-Blue assay data showed fulvestrant did not affect the growth of VK2 cells, so this was not due to a reduced number of cells following fulvestrant treatment. It is not fully understood why this occurred but it may have been due to inhibition of background estrogen in the media, for example small amounts of estrogen in the bovine pituitary extract, which activated hBD2 expression.

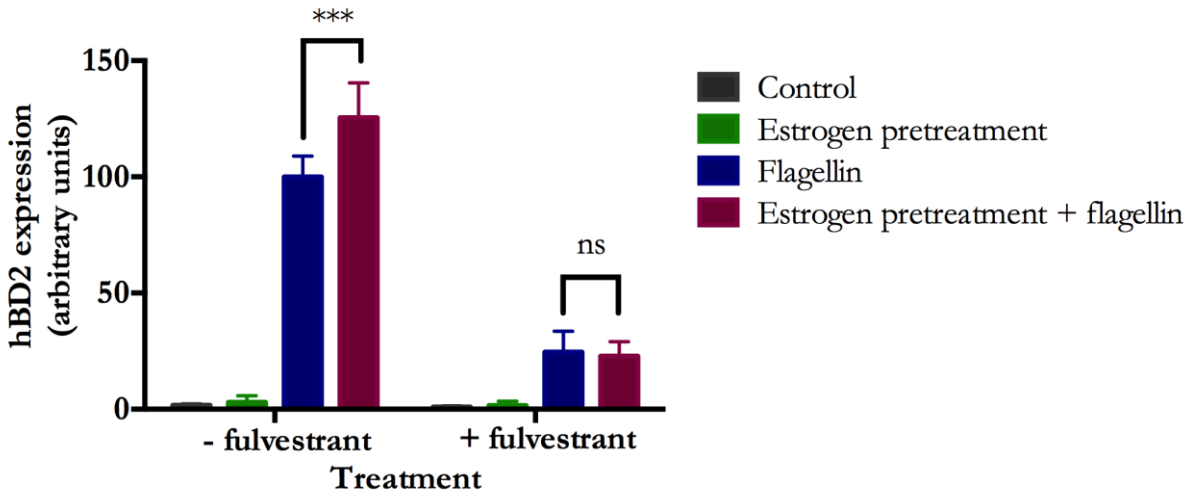

Figure 5.2: Effects of inhibition of ER-α and –β on hBD2 expression. VK2 cells were seeded into 12-well plates and then treated with 4nM estrogen and/or 1μM fulvestrant, or vehicle, for seven days before challenge with 50ng/ml flagellin or PBS for 24 hours. The RNA was extracted, reverse transcribed into cDNA and analysed by qPCR for hBD2 expression. Results were normalised to 24 hour flagellin challenge. Error bars represent standard error. Statistical analysis was performed by two-way ANOVA with Tukey's post hoc test. ns=not significant, ***=$p<0.001$. N=3, n=9.

5.2.3 Effects of estrogen pretreatment on expression of TLR5 pathway components

Regulation of hBD2 expression by ER-α and –β may occur directly, through ERs binding to the hBD2 promoter region and causing gene transcription, or indirectly, through upregulation of

TLR5 pathway components. The TLR5 signalling pathway is shown in Figure 5.3A and consists of activation of the adaptor protein MYD88 by TLR5. MYD88 then initiates the signal transduction by activating the IRAK1/IRAK2/IRAK4/TRAF6 complex, which in turn activates the TAB2/TAB3/TAK1 complex. This TAK1 kinase complex phosphorylates the IKKα/β complex, which results in NF-κB activation. Examination of the microarray data showed that estrogen pretreatment did not upregulate components of the TLR5 pathway (Figure 5.3B). Interestingly, flagellin and estrogen pretreatment plus flagellin did result in increased expression of the molecule IRAK2, however, overall estrogen pretreatment did not upregulate the TLR5 signalling pathway. Thus, upregulation of hBD2 by estrogen is likely to occur through direct interaction of ER-α and/or –β with the hBD2 promoter, independently of the TLR5 pathway.

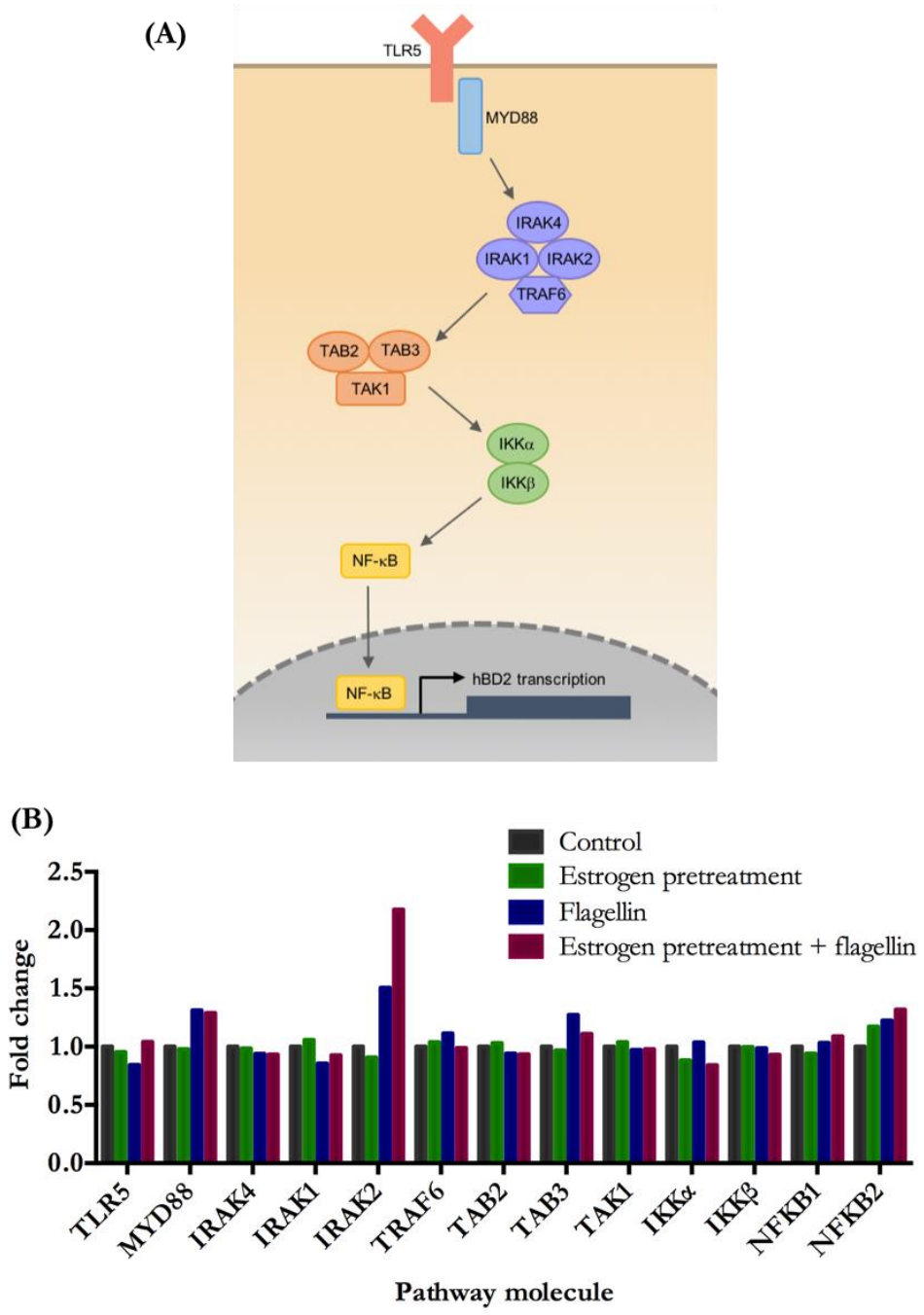

Figure 5.3: Effects of estrogen pretreatment and flagellin on expression of TLR5 pathway molecules. The figure shows (A) the molecules involved in the TLR5 signalling pathway and (B) the expression levels of these molecules after seven days estrogen pretreatment and flagellin challenge, relative to control samples. The expression was measured by microarray on an Illumina HumanHT-12 V4 Expression BeadChip.

5.2.4 Effects of mutagenesis of estrogen response elements in hBD2 promoter on hBD2 expression

To establish whether ER-α and –β regulation of hBD2 occurred through direct interaction of the receptors with the promoter, the role of estrogen response elements (EREs) in the hBD2 promoter was investigated. Following estrogen binding to ER-α/β the receptors dimerise,

migrate to the nucleus, bind EREs in the promoter of estrogen responsive genes and initiate transcription of the gene. An ERE typically consists of two palindromic ERE half-sites, with sequence GGTCA or TGACC, separated by three base pairs of any nucleotide sequence. Thus, EREs have the consensus sequence GGTCAnnnTGCAA. However, most estrogen responsive genes do not contain the consensus ERE sequence in their promoter[289]. One arm of the palindromic sequence is often imperfect. Furthermore, ERE half-sites have been reported to regulate gene transcription without a full ERE[290,291]. Therefore, PROMO software was used to search for ERE half-sites in the hBD2 promoter[292,293]. Six ERE half-sites were identified in the 2032bp hBD2 promoter region in the phBD-2-luc plasmid engineered by Dr Marcelo Lanz[106]. These are shown in Figure 5.4 highlighted in red. The sequence highlighted in green is the start of the first exon.

```
          CTGGACACTGGTCTCATCTGGTGAAAGACTGTGGGTAATGGAAGCATTTCTGTGGGGTGGTGGCAGGACATGTGCATGGTGAGG
ERE1      CAGGTCATCAGCAGCAAGTGAGAGCTGCCTCTTACTTTCTAAAGGTGACATAGCAAGTATACAAAAAAAAAATAAAATATTAAT
          TTAGGCAGAGCACATAAAGGCTTTATTTCATATTCCATTTCTCTGTATGCTTTCTTCACCAGGAAGAAATAGTTTTAGTGTCAG
          GAATGAATGAGTCTGCCCCTCAATTCCAGCCTGCTCAGCACACAAGGAAACAAAGCCCTGACAATCAGAGTGACTCCCTGGTGA
ERE2      CTAAGCTCCAGTCCTGGATGCATATTTGTTTAGCAGTTCTGACAGCATCTGACCCAGCCCTCTCTTTGCATACCCCACCAGAAC
          CTTCTTTTTTTTTTTTTTTCTTTGAGACTGAGTCTTGCTCTGTCGGAAGCGATTCCCGTGCCTCAGCCTCCCAAATACCTGGAA
ERE3      TTATAGGCGTAAGCCATCATGCCTGGCTAATTTTTGTATTTTTCATGGAGATGGGGTTTTGCCATGTTGGTCAATTGGTCTCA
ERE4      CACTCCTGACCTCATGTGATCCACCTGCCTCAGCCTCCCAAAGTGCTGGGATGACAGGTGTAAGCCACCATGCTAGGCTCAGAA
          ATTTCCTTTTATAAAAATGTCATTAAGGATCTTGGCTGCACAATATCGTTACCAGCTTCCTTTAAATCCACCTCTGGCCTGCCA
ERE5,ERE6 GGAATCAGGGTTCTTCAGAACCTGACATTTTAAATGAAGAGGTCAGGCAGGTCATGAGGAAAGCCTCATTGTCCCCATGTCTCT
          GTCACTGCTGCACCCCTGAGACATCACAGACATGGACACTGGGGCCTGCTTGTTTCTCAAACTGCCCTTAGATCGAAAGAGGGA
          GGAACCAGGATGAATGCCACTCATTTTCCCAAGAAAGGCCCTCTCCTGAGTGCCCGGGATGGGGCTCTGTCCATTGCCTGGGGC
          CGCCAATTGCTACTCTGGGTTACGGAAGAAGGACAGGGTCCTGAGAGACACCAGAGACCTCACACAGCCCTGAAAACATGGGGC
          TCCTTCATAAGTGTTTCCCATCACCAACAGGGAGACCACGTGGAGGCCTTGCAGCCCTACTCGGTGCTTCTCCACCAAATCCCA
          AGGGCAGTGACGCTGACGTCTGTGGAAAGCAGAGAAAGCCCTGGCTCCCAAAGCCCTGAAGTCCTGTGGAGCTGACATTCCCTG
          AGTGACGGTGTGAATGGAAGGAACTCAAGTGCGGGTGGTAGGCCACCTCCTGGCCCAGGCCTGGGTGAACTCTGAGGGGACACA
          TGTAGTCACAATCCCATCCTCCCATTCTCCTTCTCAGAGGAAGGAAGTGGGCATCCATCTGCCTCATCTCTCTCCCGTGGGGAA
          GATGGGGAGTTTCAGGGGAACTTTCACATAAATTTCACCAGCTCAGATCTCCTGTGAGGATGGGGCCCACCATGCTCCCGGTGC
          TGCCAGAGGCCCTGAGCCCCTCCAGGGTCCCTGGGTTTGAGCCAGCCCTGTATCATCCCCAGGAGCTGAATGTCCGAGCAATGG
          ATAGAATTAGATGGAAAGAGCTCTCAATTTGGCCTGAGACTGTCCCCAGATACTCAGGAAAAACAGGACGTCGCACAGAGTGGG
          CAGCAGGTGAGTGGCAGGTTATAGGTCCTGAGTTTGAGTTTGTTCTCACGTGAGACAGACCCAGCCCCTCACTCCATTCACACA
          CTGGGTTTTAAATGGTGCAAGATAGGAGGAATTTTCTGGTCCCAAGAGCAGGAGGAAGGGATTTTCTGGGGTTTCCTGAGTCCA
          GATTTGCATAAGATCTCCTGAGTGTGCATTGTTCTTTGAGGACCATTCTCTGACTCACCAGGTAAGTGGCTGAATTCTAACCTC
          TGTAATGAGCATTGCACCCAATACCAGTTCTGAACTCTACCTGGTGACCAGGGACCAGGACCTTTATAAGGTGGAAGGCTTGAT
          GTCCTCCCCAG
```

Figure 5.4: Estrogen response element half-sites in the 2032bp hBD2 promoter region. The sequence shown is the 2000bp hBD2 promoter region in the phBD-2-luc plasmid engineered by Dr Marcelo Lanz. ERE half-sites identified by PROMO are highlighted in red. The start of the first exon is shown in green.

To assess the role of each ERE half-site in the regulation of hBD2 expression, each ERE half-site of the parental, or wild type (WT), plasmid was mutated in turn by site-directed mutagenesis in collaboration with Tom Powell (MRes student, 2014), to produce six mutant plasmids. The results of the mutagenesis were confirmed by sequencing and are shown in Figure 5.5.

Figure 5.5: Sequencing of hBD2 promoter ERE mutants. Site-directed mutagenesis was used to mutate each of the six ERE half-sites in the 2032bp hBD2 promoter region in the phBD-2-luc plasmid. The figure shows the BLAST alignments of the sequencing results for (A) the WT plasmid, (B) ERE1 mutant, (C) ERE2 mutant, (D) ERE3 mutant, (E) ERE4 mutant, (F) ERE5 mutant, (G) ERE6 mutant. The ERE sites of the plasmids are highlighted in green, and the ERE sequence from the human genomic and transcript DNA database is highlighted in blue. The query sequence is the sequence of the PCR product as determined by sequencing and the subject (sbjct) sequence is the BLAST database sequence.

To analyse the effects of the ERE mutations, VK2 cells were pretreated with 4nM estrogen for seven days and then transiently transfected with each of the seven plasmids, using the conditions determined in Chapter 3 section 3.4.2.2. Following transfection, the VK2 cells were challenged with 50ng/ml flagellin, or PBS, for 24 hours. After challenge, the medium was removed, the cells were washed, lysed and the Luciferase Assay System (Promega, UK) used to determine the level of hBD2 luciferase reporter activity.

After transfection with the WT phBD-2-luc plasmid, challenging the VK2 cells with flagellin resulted in a 12-fold change in hBD2 expression, compared to control (Figure 5.6). Estrogen pretreatment prior to flagellin challenge of VK2 cells transfected with WT phBD-2-luc plasmid induced a 27-fold change in hBD2 expression, compared to control. This represents a statistically significant 2.1-fold change in hBD2 expression ($p=0.0012$) with estrogen pretreatment plus flagellin, compared to flagellin challenge without estrogen pretreatment. Flagellin challenge of VK2 cells transfected with phBD-2-luc plasmids with mutations in ERE1-6 resulted in induction of hBD2 expression to a comparable level to that of the WT transfected cells. However, estrogen pretreatment of the VK2 cells transfected with ERE mutant phBD-2-luc plasmids did not result in statistically significant potentiation of hBD2 expression above that observed with flagellin challenge without estrogen pretreatment. Thus, estrogen regulation of hBD2 expression occurs through direct interaction of ER-α/β with the hBD2 promoter to stimulate gene transcription. Furthermore, these data suggested all EREs in the hBD2 promoter were necessary for potentiation of hBD2 expression by estrogen.

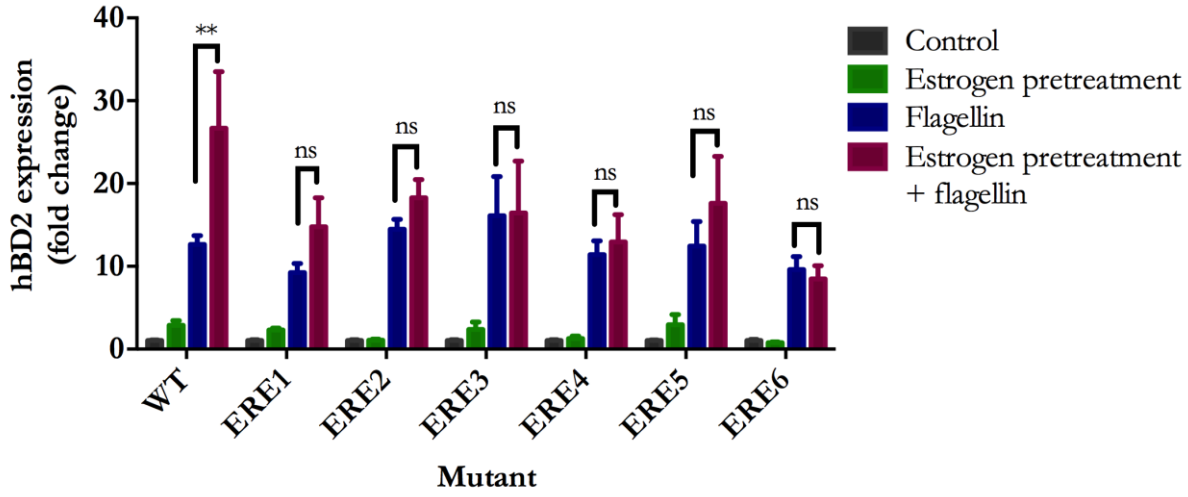

Figure 5.6: Effects of mutating estrogen response elements (EREs) in the hBD2 promoter on hBD2 expression. VK2 cells were pretreated with 4nM estrogen, or cyclodextrin vehicle, for seven days and then transiently transfected with WT and mutant phBD-2-luc plasmids, before challenged with 50ng/ml flagellin or PBS for 24 hours. After challenge, the medium was removed, the cells were washed and lysed, and luciferase production was determined using the Luciferase Assay System (Promega, USA) and FLUOstar Omega Microplate Reader. The results were normalised to the cyclodextrin-treated control for each plasmid. Error bars represent standard error. Statistical analysis was performed by two-way ANOVA with Tukey's post hoc test. ns=not significant, **=$p<0.01$. N=4, n=8.

5.2.5 Effects of GPER stimulation on hBD2 expression

Data presented in this chapter indicated that regulation of hBD2 expression by estrogen was dependent on ER-α/β; inhibition of these receptors abolished the potentiation of hBD2 expression observed with estrogen pretreatment plus flagellin challenge. To verify these data, VK2 cells were treated with G-1, a selective GPER receptor agonist with no activity against ER-α and –β. It was hypothesised that stimulation of GPER with G-1 would not affect hBD2 expression with estrogen pretreatment plus flagellin, compared to flagellin alone.

As the VK2 cells were to be pretreated with G-1, it was important to investigate any effects of G-1 on VK2 cell growth. The cells were pretreated for one, five and seven days with 100nM G-1 or vehicle control. This concentration of G-1 has been shown previously to stimulate estrogenic effects[294]. At each time point the cells were imaged using an EVOS XL core digital light microscope and the cell viability was determined using the CellTiter-Blue Cell Viability Assay (Promega, USA). The results, shown in Figure 5.7, indicated that 100nM G-1 pretreatment did not affect the growth of VK2 cells. No statistically significant difference in the number of viable cells was observed between G-1 and vehicle treated VK2 cells at any time point up to seven days. In contrast, Mitomycin C significantly reduced the growth of VK2 cells, compared to the control cells, after five and seven days of pretreatment.

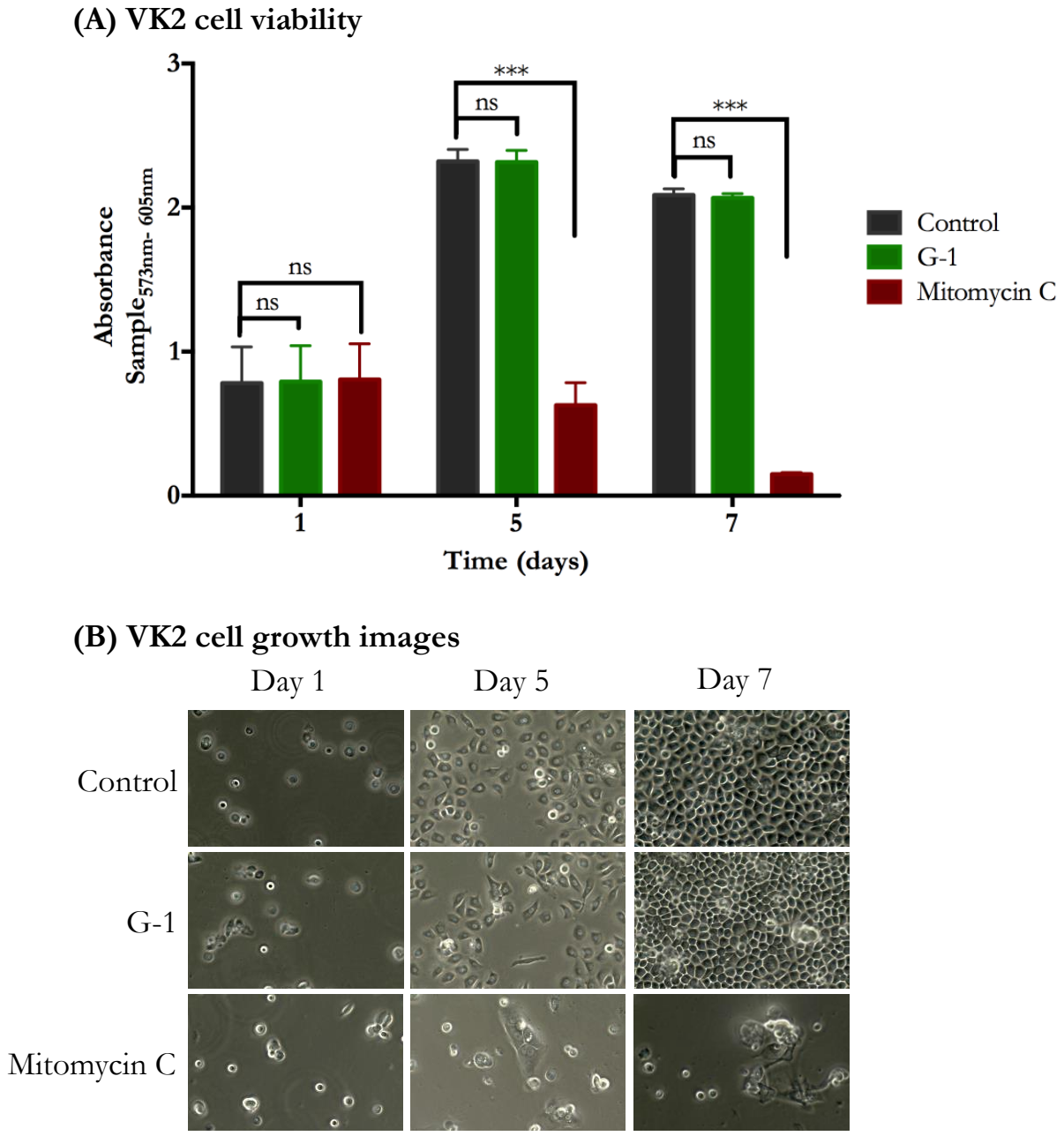

Figure 5.7: Effects of G-1 pretreatment on the growth of VK2 cells. VK2 cells were treated with 100nM G-1, DMSO vehicle, or 1mM Mitomycin C for 1, 5, and 7 days. (A) CellTiter-Blue Cell Viability Assay (Promega, USA) was used to measure cell viability after 1, 5, and 7 days of treatment. Error bars represent standard error. Statistical analysis was performed by two-way ANOVA with Dunnett's post hoc test. ns=not significant, ***=$p<0.001$. At days 1 and 5 N=2, n=6, and at day 7 N=1, n=3. (B) Images taken on an EVOS XL Core digital light microscope (AMG, USA) at x20 magnification show the confluency of the cells at each time point with each treatment. Each image was representative of the well.

Having established that G-1 did not affect VK2 cells growth, the VK2 cells were pretreated with 100nM G-1, or DMSO vehicle, for one, five and seven days, and then challenged with 50ng/ml flagellin or PBS for 24 hours. RNA was extracted from these cells, reverse transcribed into cDNA and analysed by qPCR for hBD2 expression.

The results from this experiment revealed that hBD2 expression was not significantly increased by G-1 pretreatment plus flagellin, compared to flagellin challenge alone, for any of the time points studied (Figure 5.8). Following one day pretreatment, flagellin challenge increased hBD2 expression to 89AU, from 0.2AU in the control. G-1 pretreatment plus flagellin induced hBD2 expression to 105AU, which was not statistically significant different from flagellin challenge alone ($p=0.261$). Similarly, after five days pretreatment flagellin challenge induced hBD2 to 113AU, from 0.4AU in the control, and G-1 pretreatment plus flagellin resulted in hBD2 expression of 105AU. Once again this did not represent a statistically significant difference ($p=0.7851$). After seven days pretreatment, flagellin induced hBD2 expression to 100AU from 0.5AU in the control. Interestingly, G-1 pretreatment plus flagellin challenge resulted in hBD2 expression of 74AU, a significant 26% reduction ($p=0.0156$) in hBD2 expression compared to flagellin challenge alone.

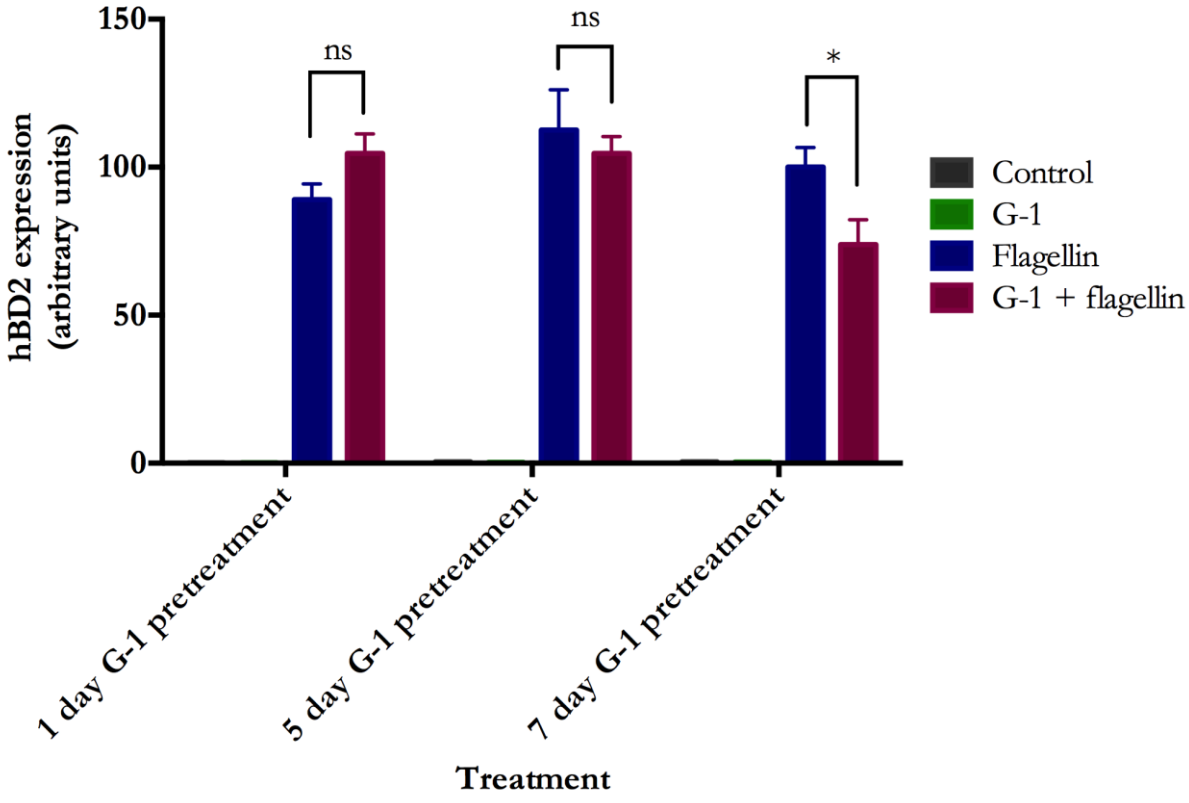

Figure 5.8: Effects of G-1 pretreatment and flagellin on hBD2 expression. VK2 cells were pretreated with 100nM G-1, or DMSO vehicle, for 1, 5, and 7 days, before challenged with 50ng/ml flagellin or PBS for 24 hours. The RNA was extracted, reverse transcribed, and analysed by qPCR for hBD2 expression. The results were normalised to 24 hour flagellin challenge after seven day vehicle pretreatment. Error bars represent standard error. Statistical analysis was performed by two-way ANOVA with Tukey's post hoc test. ns=not significant, *=$p<0.05$. N=2, n=6.

To summarise, inhibition of ER-α and/or -β abolished the potentiation of hBD2 expression by estrogen pretreatment plus flagellin, suggesting that hBD2 is regulated through ER-α and/or –β. Mutation of the six ERE half-sites in the hBD2 promoter also inhibited hBD2 potentiation by estrogen pretreatment plus flagellin. Moreover, these data indicated that all six ERE half-sites were needed for estrogen regulation of hBD2 expression. In support of this, stimulation of GPER with G-1 agonist did not result in potentiation of hBD2 expression. Thus, these data indicated that upregulation of hBD2 by estrogen pretreatment occurred via ER-α and/or –β and required all six ERE half-sites in the hBD2 promoter region.

5.3 Mechanism of hBD3 expression regulation by estrogen

5.3.1 Effect of inhibition of ER-α and ER-β on hBD3 expression

Receptor agonists/antagonists were again used to determine the roles of ER-α, ER-β, and GPER in hBD3 induction by estrogen. VK2 cells were pretreated with 4nM estrogen and/or 1μM fulvestrant, or vehicle, for seven days and then challenged with 50ng/ml flagellin or PBS for 24 hours. The RNA was extracted, reverse transcribed and analysed by qPCR for hBD3 expression.

The results, presented in Figure 5.9, showed that flagellin challenge without fulvestrant induced hBD3 expression to 100AU from 56AU in the control, representative of a 1.8-fold increase in hBD3 expression ($p=0.0171$). Estrogen pretreatment prior to flagellin challenge resulted in hBD3 expression of 169AU, representing a significant 3.0-fold change in hBD3 expression relative to the control ($p<0.0001$) and a significant 1.7-fold change compared to flagellin challenge ($p<0.0001$). Following fulvestrant pretreatment, flagellin challenge induced hBD3 expression to a comparable level as flagellin challenge without fulvestrant (1.6-fold change vs. 1.8-fold change). However, inhibition of ER-α and –β by fulvestrant attenuated the potentiation of hBD3 expression by estrogen pretreatment plus flagellin. In fact, fulvestrant plus estrogen pretreatment prior to flagellin challenge induced hBD3 expression to 92AU, which was comparable to expression of 104AU observed with fulvestrant pretreatment plus flagellin challenge ($p=0.8238$). Hence, inhibition of ER-α and –β prevented potentiation of hBD3 expression by estrogen pretreatment.

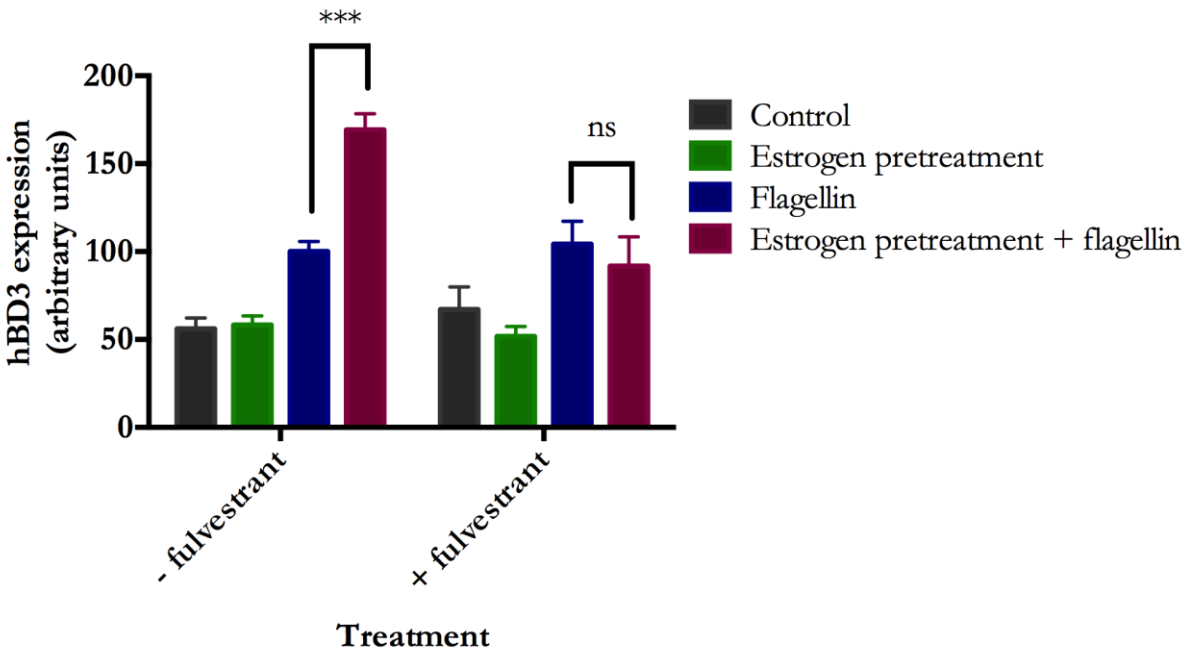

Figure 5.9: Effects of inhibiting ER-α and –β on hBD3 expression. VK2 cells were treated with 4nM estrogen and/or 1μM fulvestrant, or vehicle, for seven days, and then challenged with 50ng/ml flagellin or PBS for 24 hours. The RNA was extracted, reverse transcribed, and analysed by qPCR for hBD3 expression. The results were normalised to 24 hour flagellin challenge. Error bars represent standard error. Statistical analysis was performed by two-way ANOVA with Tukey's post hoc test. ns=not significant, ***=p<0.001. N=3, n=9.

5.3.2 Development of a hBD3 promoter luciferase reporter plasmid

To further explore the mechanisms of ER-α and –β upregulation of hBD3 expression, the role of EREs in the hBD3 promoter was investigated. Promoter analysis using the PROMO software identified one ERE half-site in the 2000bp hBD3 promoter region directly upstream of the first exon and this is highlighted in red in Figure 5.10. The sequence highlighted in green is the start of the first exon.

AAGTCCCCCTCAAAACGGATTTTGTGTGTCTGGAGTATGTCCAAACTTGAAAAGGCTGATTGTCACAGCCCAATCTCCAATTCCCAGCTCCCAAACTAGTTGACA
AGAAAAAGTGGCATTTTTCCTCACCAAGGAACTTTTATGAAATAGTGGTGTTGCCATAAAAATGCCTCCCAGTCTATGAAGGAACAGGTTAGACCAGGGGTTCAC
CTGTGGAAGTCTATTCTCCATGTGGAAAAGCAAGTCATCTCCAGCGTCTGACTGTCCTCACCCCAGGCTGAGAGCTGGTGCTAACCCTCTACAACGCCCAATGCC
ATCGTTATGTCTGACATAGTAAGACTGTGAAGTCAGCACCCATCCCACCCACACTCACCTCCTTCCCCCATTTATAAATATCTCCAATTGCTTTGTCTCAAATCA
TGAACTAAAGAGGAAAGTTAGATTTTAAAAAGTAGCATCTACCTATCTAAAGTCTTAAATCTGCTGATTGAGCTCCACTCTTGGCTCAAAGAGTTATCTTTGAGT
TATGATGAGTTATCTTTCTTCTACGTTTCTGCAGCCCTGTGCTTGAAATCTTCCTATGACTCCCATTAGAATTCATCCTAAATTTATCATTTGACTGTCTGCCCA
TCTACCTGGCCCTACATGGAGCTTCTGGAGAGAAAGAACCAAGACTGGTCCCTCTTGGTATCTCATCCACTTCACCCTCACCTATGCTGAAGACATGATACTTGT
CCCTTCCTATAGTATGTGTTCAGAGTTTTCTTACTGAATCTGACAGGTGTGGTGCACCCAAATTCTGAACACACACTCCCAGAACTAACACACCCTTGATCCTTA
GTGGATCCGTTATAATTGCATTCACACGAAGCAGCAGCTAGGAGACATCACGGTGACTTCAGCTCCCAATTGAATTGTCATTGACTTACTTAGTTCCCAATTGAT
AGTCAACCAAATACAACCCATCCATTGGATTCCTGAACATTTAAGTTTAATAGCTGTTTTTTTTTTCTTTTTTAGCATTTTTCCCTCTAAACGTTGAATCTATAT
GCAGGGGAAATCATCTGGCCCCTGGACTGCCTTGAATGCTCCTGAGCCAAGAGTAACTTGAGGTCTTAAATGTCTATTCTGAAGCCCCTCTTTTGCACAGGGACA
GTCATTGACTAGGAGGAGATGCCAGTCTATTAAATCTATCATCCCAGCATCCTCTTTCTCTGATGAAGTAAAATTAAACACCTTCTTTACTCATAAATTTGGTAG
GTTTTAGACAATGATGAAGAATCGGACATGGGCCGCACACAGTGGCTCATACCAGTAATCCCAGCAATTTAGGAGGCTGAAGCAGGAGGATTGCTTGAGCCCAGG
AGTTCACATCTGGGCTCGAAACCAGTCTGGGCAGCATAGTGAGACCCCATTTTATTTTCTACAGAAAATTTAAAATTTAGCCATGTGTGGAGGCATGCGTTTGTG
GTCCCAGCTACTCAGGGGGCTGAAGTGGGAGGACCTCTTGAGCCTGACAGCTCAAGCTGTTGTGAGCTGTAATCATGCCACTGCACTCCAGCCTGCACAAAAAAG
TGAGACTCTGTCTCTCAAAAAAAAAAAAAAAAAAATGAAAGAATGAGACATGTTTCACTCAAATTATAGCACCCCATCATAGGCCAAGGGCCAGGTGCAAATCCAT
AGG**GGTCA**GCTAACCTTGAATGTAGCCCATTTTCCTCCCTTACCTCACTACCAAAAAGCCAGTCCTATTGCCAGATATTGAATATGTCCAGGGCTGGATTTATTT
GGTCCCCAGGAGGGTCTTAGACTCTCCCAGCATTTTAGGAAGAGAAAAAAAGCTCCAAAGCAGCAAAGTACGGACAAGTCAGCCCCCAGCCACATGCCCTGAGAC
TATTCCCCAAAGGGGGCATACTTGCTCATGCCAGCCCTATCTGTACCCACAACCCAATCTGACCCACACCCAGACAAGCCCCTGGAGTCCAGAGAGCACCCGGAC
AGCCACAAATCCATAGGGAGCTCTGCCTTACCATTGGGTTCCTAATTAACTGAGTGAGTGGGTGTGTTC

Figure 5.10: Identification of EREs in the hBD3 promoter. PROMO software was used to identify ERE half-sites in the 2000bp hBD3 promoter region directly upstream of the first exon[292,293]. ERE half-sites are highlighted in red. The start of the first exon is shown in green.

To analyse the effects of this ERE half-site on hBD3 expression attempts were made to engineer a luciferase reporter plasmid containing the hBD3 promoter region containing the ERE. Initially 1000bp and 2000bp 5' upstream regions of the hBD3 promoter were amplified from genomic DNA. The forward and reverse primers used to amplify the PCR products contained KpnI and HindIII restriction enzyme sites, respectively, to introduce these restriction enzyme sites at either end of the PCR products. The amplified 1kp and 2kb hBD3 promoter products are shown in Figure 5.11. Electrophoresis of the products after gel extraction is shown in Figure 5.11C. These products were digested, along with the pGL4.10 reporter plasmid, using KpnI and HindIII restriction enzymes, ligated and transformed into competent DH5α cells, as detailed in the materials and methods. Following transformation, plasmid DNA was isolated from the DH5α cells by miniprep. However, despite repeated attempts sequencing data showed that the 1kb and 2kb hBD3 promoter products were not successfully cloned into the pGL4.10 luciferase reporter plasmid.

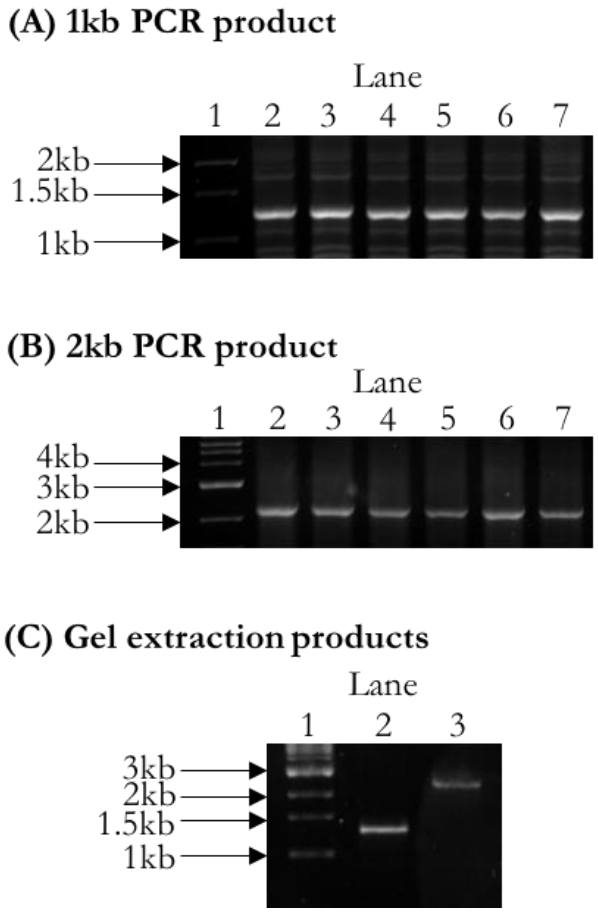

Figure 5.11: Amplification of 1kb and 2kb hBD3 promoter region from genomic DNA. Amplification of (A) 1kb and (B) 2kb region of the hBD3 promoter. The 1kb DNA ladder (New England BioLabs, USA) is shown in lane 1 and the PCR products are shown in lanes 2-7. (C) The DNA bands were extracted from the gel and the gel extraction product was electrophoresed. The 1kb DNA ladder is shown in lane 1, the gel extraction products of the 1kb and 2kb PCR are shown in lanes 2 and 3, respectively.

As attempts to clone 1kb and 2kb fragments of the hBD3 promoter into pGL4.10 were not successful, the forward primer for the hBD3 promoter region was redesigned to amplify a smaller 500bp region of the hBD3 promoter containing the ERE half-site. End-point PCR was performed for the 500bp hBD3 promoter region (Figure 5.12A), and the product purified (Figure 5.12B). Single and double digests of the pGL4.10 reporter vector were performed using the HindIII and SacI restriction enzymes. Gel electrophoresis of the digested products (Figure 5.12C) showed that both double and single digests resulted in complete digestion of the plasmid, with no plasmid left uncut. This confirmed that the restriction digest reaction was efficient.

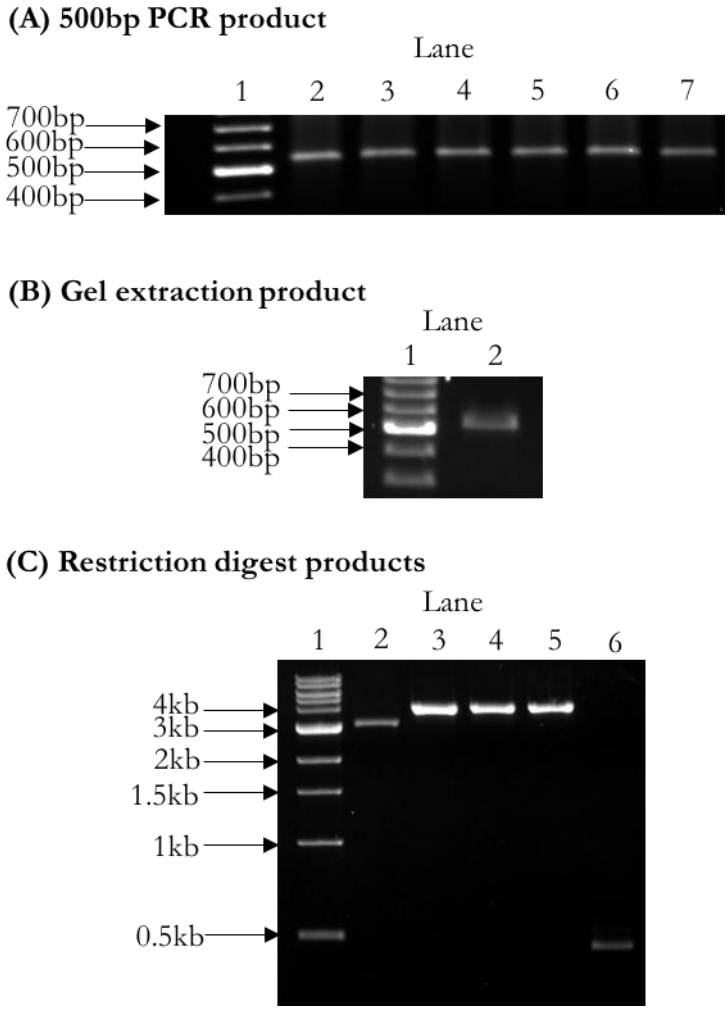

Figure 5.12: Amplification, gel extraction and restriction digest of 500bp hBD3 promoter product. (A) The 500bp hBD3 promoter region was amplified and gel electrophoresed. The 100bp DNA ladder (Thermo Scientific, USA) is shown in lane 1, and 500bp hBD3 promoter PCR products are shown in lanes 2-7. (B) The PCR products were extracted from the gel and electrophoresed to confirm extraction of the product. The 100bp DNA ladder is shown in lane 1, and the gel extraction product is shown in lane 2. (C) The pGL4.10 luciferase reporter plasmid and the 500bp hBD3 promoter product were digested with restriction enzymes HindIII and SacI. The 1kb DNA ladder (New England BioLabs, USA) is shown in lane 1. The uncut pGL4.10 plasmid is shown in lane 2. A double digest of pGL4.10 with HindIII and SacI is shown in lane 3. Single digests of pGL4.10 with HindIII and SacI are shown in lanes 4 and 5, respectively. A double digest of the 500bp hBD3 promoter product with HindIII and SacI is shown in lane 6.

The digested pGL4.10 vector and 500bp hBD3 promoter insert were ligated together, transformed into DH5α cells and plated onto LB/ampicillin plates as detailed in the materials and methods. Typically, less than five colonies grew on the LB/ampicillin plates after transformation and sequencing results revealed that the 500bp hBD3 insert was not successfully integrated into the pGL4.10 luciferase reporter vector. Control reactions were performed in parallel with the 500bp hBD3 promoter insert reaction. As the pGL4.10 vector contains the gene for ampicillin resistance, only bacteria that have successfully taken up the pGL4.10 vector, with or without the 500bp insert, are able to grow on LB/ampicillin plates. The first of the control reactions (V + L) included the doubly digested vector with DNA ligase, but with no 500bp insert. As expected, no colonies grew as a result of this transformation reaction indicating that minimal amounts of the vector were undigested, or religated without incorporating the insert (Figure 5.13C). The second control reaction consisted of doubly digested vector only (V), without DNA ligase and again the results showed (Figure 5.13D) that no colonies grew after this transformation reaction, supporting the notion that the vector was entirely digested during the restriction digest. The third reaction consisted of the pGL4.10 vector singly digested, by HindIII only, plus DNA ligase (V_{single} + L). The results (Figure 5.13E) showed that >100 colonies grew on the LB/ampicillin plates after this transformation reaction, indicating that the ligation reaction was functional. The final control reaction consisted of undigested pGL4.10 vector only (V_{uncut}) and the results (Figure 5.13F) showed that >300 colonies grew on the LB with ampicillin plate following this reaction and thus, the transformation step was working efficiently. Thus, altogether the control reactions suggested that the vector was being fully digested by HindIII and SacI, and that both the ligation and transformation steps were working efficiently. Thus, it was not clear why cloning the hBD3 promoter region (500bp, 1kb, or 2kb) into the pGL4.10 luciferase reporter vector was not successful, but the data were reproducible and hence, this experiment was not pursued any further.

(A) Reaction details

Reaction name	V + I + L	V + L	V	V_{single} + L	V_{uncut}
Reason for reaction	Reaction of interest	Quantifies undigested and religated vector	Quantifies undigested vector	Verifies ligase	Verifies transformation
10x ligase buffer (µl)	1	1	1	1	1
MQ water (µl)	6	7	8	7	8
DNA ligase (µl)	1	1	-	1	-
Vector (µl)	double digest 1	double digest 1	double digest 1	single digest 1	undigested 1
Insert (µl)	1	-	-	-	-
Total volume (µl)	10	10	10	10	10

(B) V + I + L
Reaction of interest

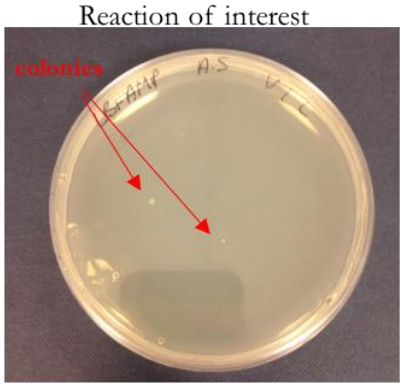

(C) V + L
Quantifies undigested and religated vector

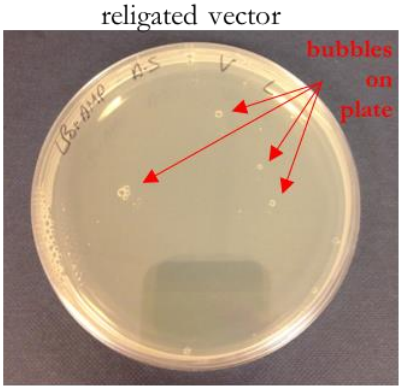

(D) V
Quantifies undigested vector

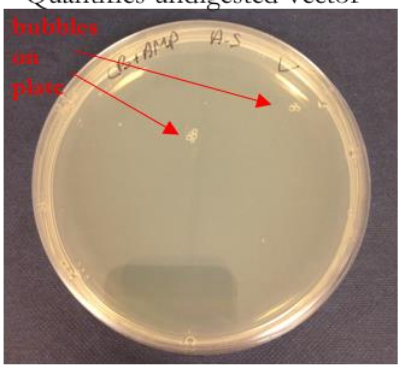

(E) V_{single} + L
Verifies ligation

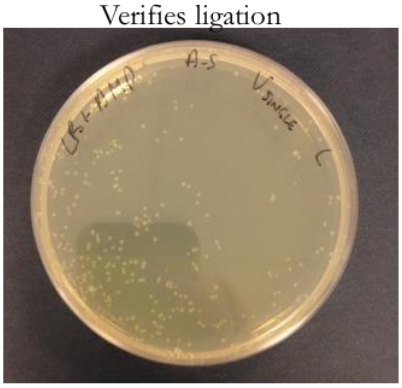

(F) V_{uncut}
Verifies transformation

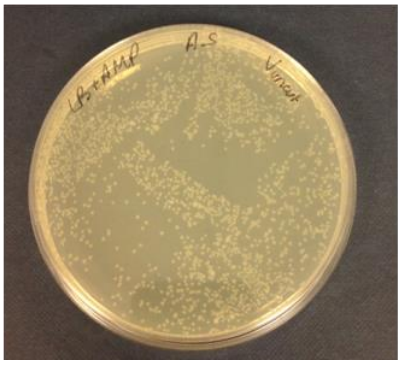

Figure 5.13: Results of hBD3 promoter cloning. (A) shows the components of the ligation reactions for the 500bp hBD3 insert and control reactions. (B)-(F) show the results of the transformation plated out on LB/ampicillin agar plates for each of the reactions.

5.3.3 Effects of GPER stimulation on hBD3 expression

As previous data suggested that hBD3 expression in response to estrogen pretreatment was regulated through ER-α and/or –β, it was hypothesised that stimulation of GPER with the G-1 agonist would not result in significant induction of hBD3 expression in the VK2 cells. VK2 cells were pretreated with 100nM G-1, or DMSO vehicle, for one, five and seven days, and then challenged with 50ng/ml flagellin or PBS for 24 hours. The RNA was extracted, reverse transcribed and analysed by qPCR for hBD3 expression. The results were normalised to 24 hour flagellin challenge.

The results, shown in Figure 5.14, showed that none of the pretreatments with G-1 resulted in significant upregulation of hBD3 expression. After one day pretreatment, flagellin challenge induced hBD3 expression to 104AU, from 37AU in the control samples. This represented a significant 2.8-fold change in hBD3 expression ($p<0.0001$). One day G-1 pretreatment plus flagellin challenge resulted in hBD3 expression of 114AU, which was comparable to hBD3 expression observed with flagellin challenge without G-1 ($p=0.7275$). Similarly, after five days pretreatment, flagellin challenge alone induced hBD3 expression to 110AU from 58AU in the control and G-1 pretreatment for five days prior to flagellin challenge resulted in hBD3 expression of 87AU. This also did not represent a statistically significant change in hBD3 expression compared to flagellin challenge without G-1 ($p=0.1030$). Following seven days pretreatment, flagellin challenge alone induced hBD3 expression to 100AU from 43AU in the control ($p<0.0001$), comparable to the level of induction with flagellin challenge after one and five day vehicle pretreatment. Interestingly, seven day G-1 pretreatment plus flagellin challenge resulted in hBD3 expression of 45AU, a level comparable with that of the control ($p=0.99$), and which represented a significant 55% reduction in hBD3 expression compared to flagellin challenge ($p<0.0001$). Consistently, seven day G-1 pretreatment alone also significantly reduced hBD3 expression 64% compared to the control ($p=0.0231$). Thus, this result suggested that long-term stimulation of GPER resulted in downregulation of hBD3 expression, which was not seen with shorter G-1 treatments.

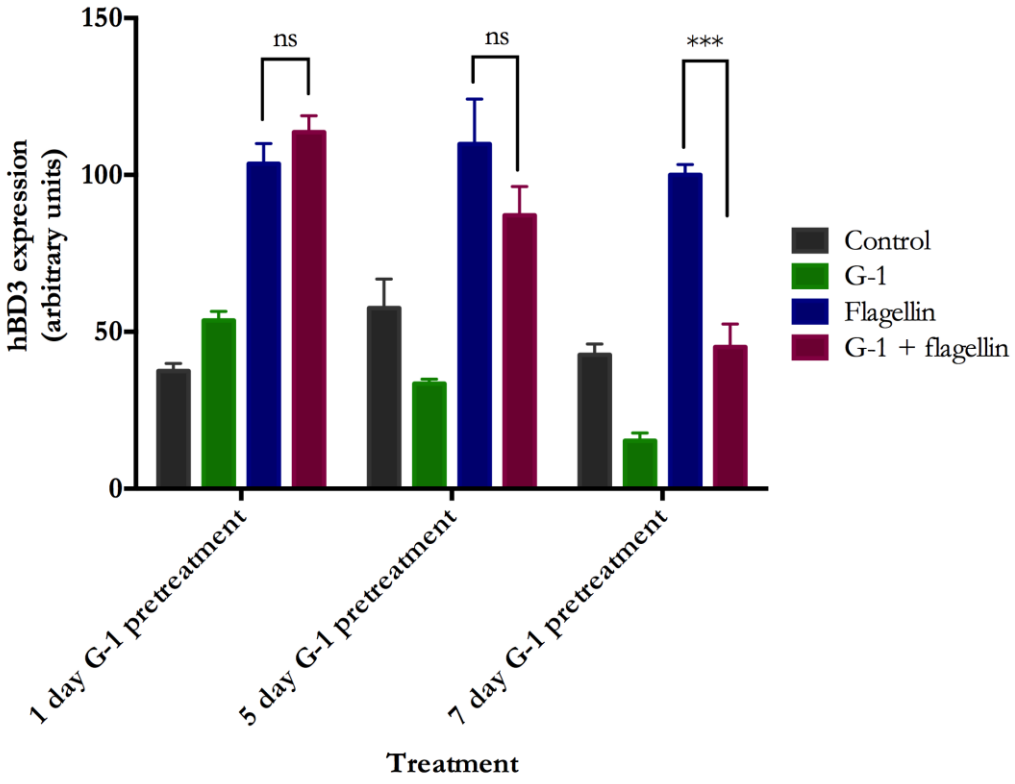

Figure 5.14: Effects of G-1 pretreatment on hBD3 expression. VK2 cells were pretreated with 100nM G-1, or DMSO vehicle, for one, five, and seven days and then challenged with 50ng/ml flagellin, or PBS, for 24 hours. The RNA was extracted, reverse transcribed, and then analysed by qPCR for hBD3 expression. The results were normalised to 24 hour flagellin challenge after 7 days vehicle pretreatment. Error bars represent standard error. Statistical analysis was performed by two-way ANOVA with Tukey's post hoc test. ns=not significant, ***=$p<0.001$. N=2, n=6.

5.4 Mechanisms of LCN2, RNase 7, and S100A7 gene expression regulation by estrogen

5.4.1 Development of LCN2, RNase 7 and S100A7 qPCR assays

As microarray analysis in Chapter 4 identified upregulation of several antimicrobial peptide genes by estrogen pretreatment plus flagellin, compared to flagellin challenge alone, qPCR assays were developed for LCN2, RNase 7, and S100A7 so that expression of these AMP genes could be further investigated. These AMPs have been shown to be important in clearance of *E. coli* from the urogenital tract[123,129,247,248].

The qPCR assay for LCN2 and positive control plasmid was previously established by Dr Ased Ali[60]. The plasmid, containing the LCN2 PCR product, was used to produce a standard curve for the LCN2 assay and the melt curve confirmed that only one product was amplified (Figure 5.15).

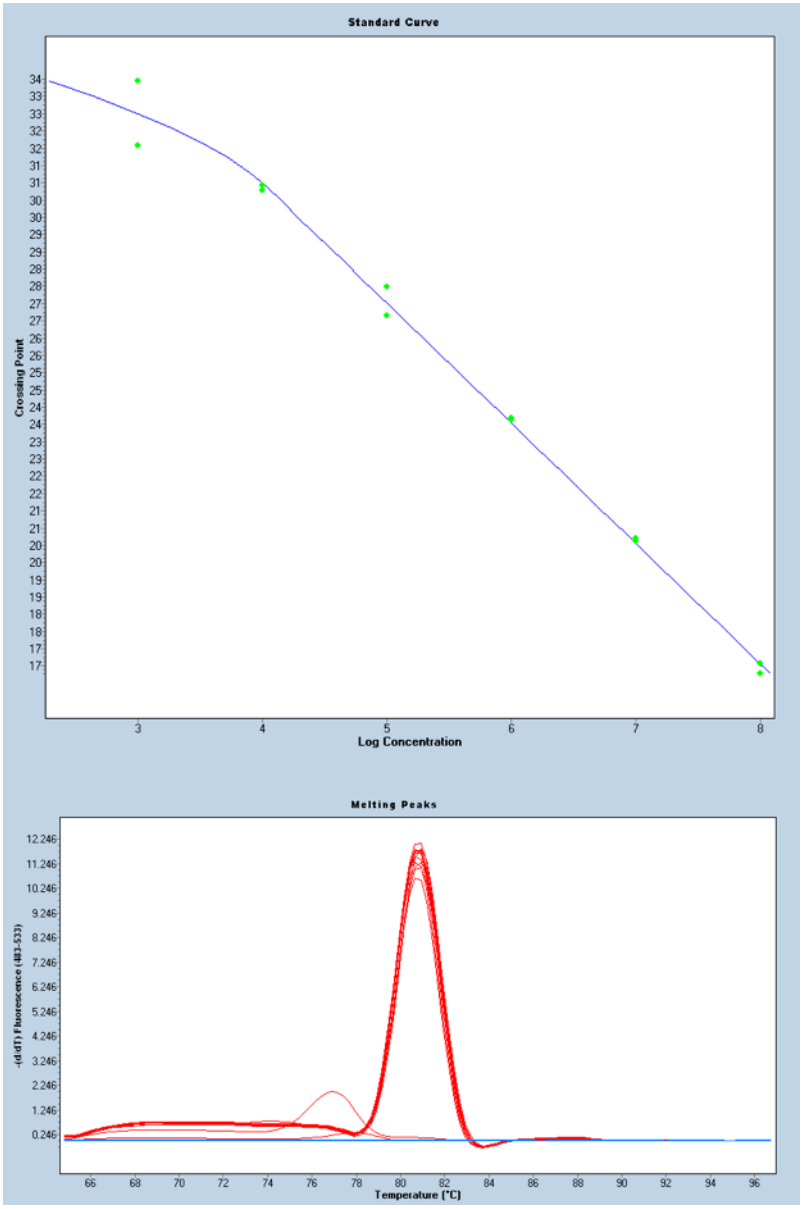

Figure 5.15: Standard curve and melt peak of the LCN2 qPCR assay. The figure shows the standard curve and melt peak of the LCN2 qPCR assay designed by Dr Ased Ali[60]. The melt peak confirmed amplification of a single qPCR product.

A qPCR assay was also developed for RNase 7. End-point PCR was performed for RNase 7 and the resultant PCR product was cloned into the pGEM-T easy vector as detailed in the materials and methods. Sequencing confirmed the presence of the PCR product in the plasmid (Figure 5.16A). The plasmid insert had 98% identity to the BLAST subject sequence. This plasmid was serially diluted and used to produce a standard curve for the RNase 7 qPCR assay (Figure 5.16B). Melt peak analysis confirmed that only one product was amplified by the qPCR reaction (Figure 5.16B). A slight shoulder was observed on the melt peak, however, this only occurred in very highly concentrated plasmid samples and was not observed for VK2 cDNA samples.

(A) RNase 7 sequencing results

Homo sapiens ribonuclease A family member 7 (RNASE7), mRNA

Sequence ID: ref|NM_032572.3| Length: 1511 Number of Matches: 1

Range 1: 141 to 226 GenBank Graphics ▼ Next Match ▲ Previous Match

Score	Expect	Identities	Gaps	Strand
148 bits(80)	1e-32	84/86(98%)	0/86(0%)	Plus/Plus

```
Query  73   ATTTGACAGCCTATGAGTGCGTGGACACCACCTCAGCCCACTGAGCAGGAGTCACAGCAC  132
            ||||||||||| ||||||||||||||||||||||||||||||||||||||||||||||
Sbjct  141  ATCTGACAGCCTAGGAGTGCGTGGACACCACCTCAGCCCACTGAGCAGGAGTCACAGCAC  200

Query  133  GAAGACCAAGCGCAAAGCGACCCCTG  158
             |||||||||||||||||||||||||
Sbjct  201  GAAGACCAAGCGCAAAGCGACCCCTG  226
```

(B) RNase 7 standard curve and melt peak

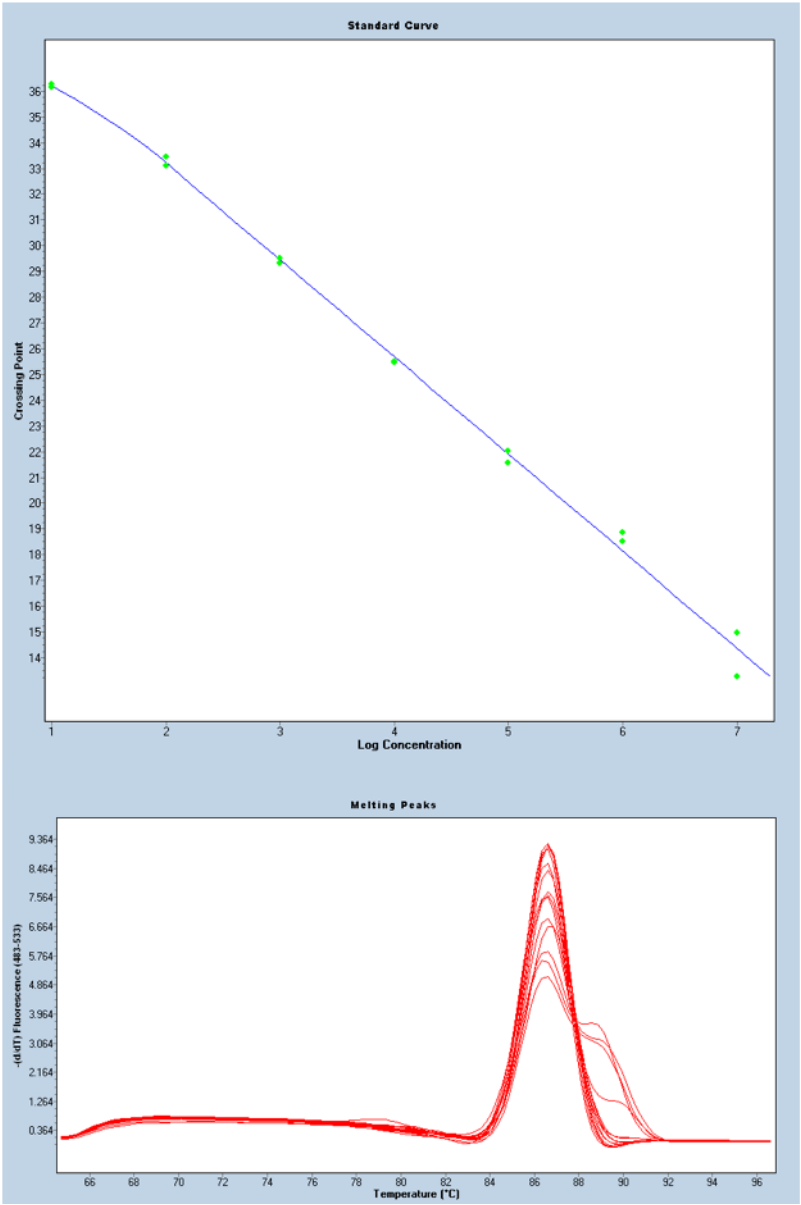

Figure 5.16: Sequencing data, standard curve, and melt peak of the RNase 7 qPCR assay. (A) Sequencing results confirmed the insertion of the RNase 7 PCR product into the pGEM-T easy vector. Sequencing was performed by Genevision (UK). The query sequence is the sequence of the PCR product as determined by sequencing and the subject (sbjct) sequence is the BLAST database sequence. (B) This vector was used to produce a standard curve and melt peak for the RNase 7 qPCR assay. The melt peak showed only one PCR product was amplified.

A similar approach was used to develop a qPCR assay for S100A7. End-point PCR was performed for S100A7 and the PCR product was cloned into the pGEM-T easy vector as outlined in the materials and methods. Sequencing, performed by Genevision (UK), confirmed the presence of the S100A7 PCR product in the pGEM-T easy vector (Figure 5.17A) with 97% identity to the BLAST subject sequence. The vector was serially diluted and used to produce a standard curve and melt peak for the S100A7 qPCR assay (Figure 5.17B). The qPCR reaction for the standard with the highest S100A7 concentration amplified multiple products, represented by multiple peaks on the melt curve, however, only one PCR product was amplified for the other standards and multiple products were not observed for the VK2 cDNA samples.

(A) S100A7 sequencing results

Homo sapiens S100 calcium binding protein A7 (S100A7), mRNA

Sequence ID: ref|NM_002963.3| Length: 450 Number of Matches: 1

Range 1: 176 to 243 GenBank Graphics ▼ Next Match ▲ Previous Match

Score	Expect	Identities	Gaps	Strand
115 bits(62)	1e-22	66/68(97%)	1/68(1%)	Plus/Plus

```
Query  25   GATG-ANGAGAACTTCCCCAACTTCCTTAGTGCCTGTGACAAAAAGGGCACAAATTACCT  83
            |||| | ||||||||||||||||||||||||||||||||||||||||||||||||||||
Sbjct  176  GATGAAGGAGAACTTCCCCAACTTCCTTAGTGCCTGTGACAAAAAGGGCACAAATTACCT  235

Query  84   CGCCGATG  91
            ||||||||
Sbjct  236  CGCCGATG  243
```

(B) S100A7 standard curve and melt peak

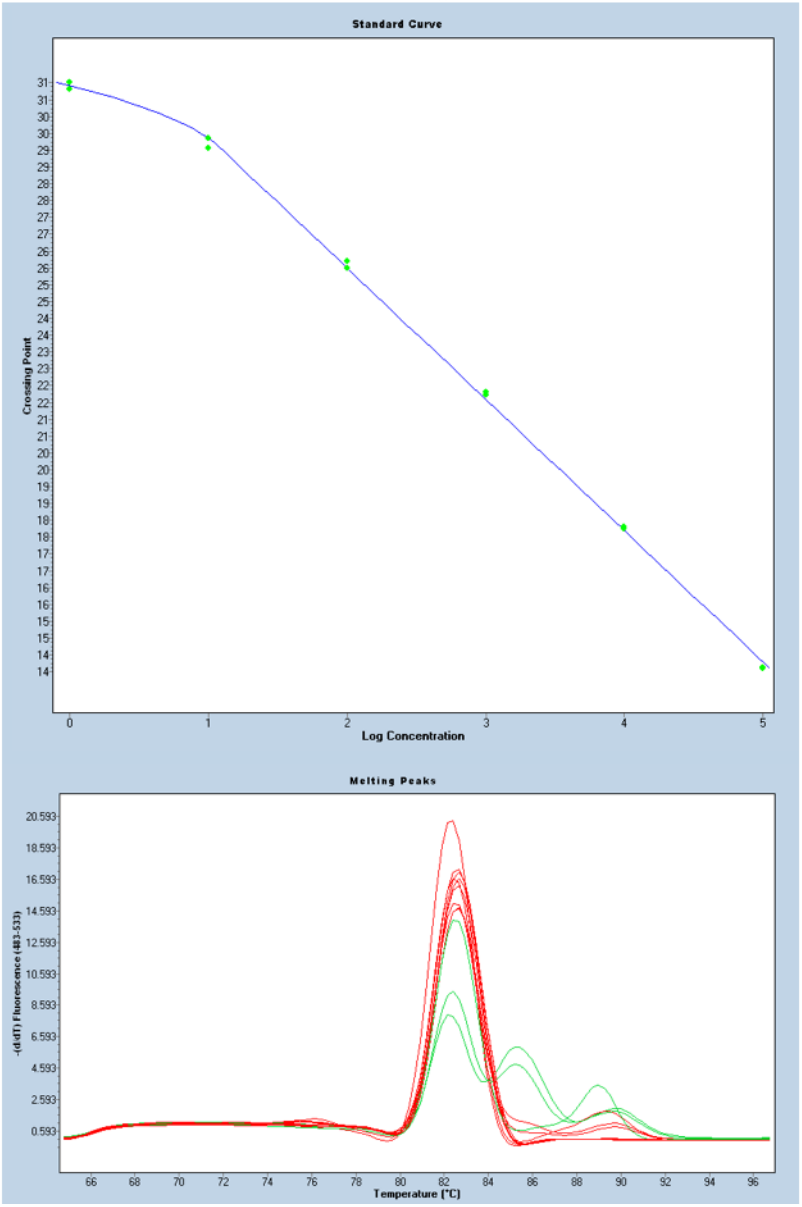

Figure 5.17: Sequencing data, standard curve, and melt peak of the S100A7 qPCR assay. (A) Sequencing results confirmed the insertion of the S100A7 PCR product into the pGEM-T easy vector. Sequencing was performed by Genevision (UK). The query sequence is the sequence of the PCR product as determined by sequencing and the subject (sbjct) sequence is the BLAST database sequence. (B) This vector was used to produce a standard curve and melt peak for the S100A7 qPCR assay.

These qPCR assays were used to analyse expression of LCN2, RNase 7, and S100A7 in the next sections.

5.4.2 Effects of estrogen pretreatment and flagellin on LCN2, RNase7 and S100A7 expression

To verify the microarray data, qPCR was performed for LCN2, RNase 7 and S100A7 following estrogen pretreatment for seven days followed by 50ng/ml flagellin challenge for 24 hours.

The results for LCN2, presented in Figure 5.18A, showed that flagellin treatment significantly induced LCN2 expression to 100AU from 12AU in the control, representing an 8.5-fold change ($p<0.0001$). Estrogen pretreatment prior to flagellin challenge further increased LCN2 expression to 125AU, a significant 25% increase in LCN2 expression, compared to flagellin challenge without estrogen ($p=0.0059$). Similarly, flagellin challenge induced a significant 1.6-fold change in RNase 7 expression (Figure 5.18B), to 100AU from 62AU in the control. Estrogen pretreatment prior to flagellin challenge resulted in RNase 7 expression of 125AU, suggesting a trend towards increased expression with estrogen pretreatment. However, this difference was not statistically significant. Finally, flagellin challenge significantly increased S100A7 expression from 39AU in the control to 100AU ($p<0.0001$). Estrogen pretreatment prior to flagellin challenge increased S100A7 to 141AU, a significant 41% increase in expression, compared to flagellin challenge alone ($p<0.0001$). Thus, altogether, these data were supportive of the microarray findings, and suggested a role for estrogen potentiation of LCN2, S100A7 and potentially RNase 7.

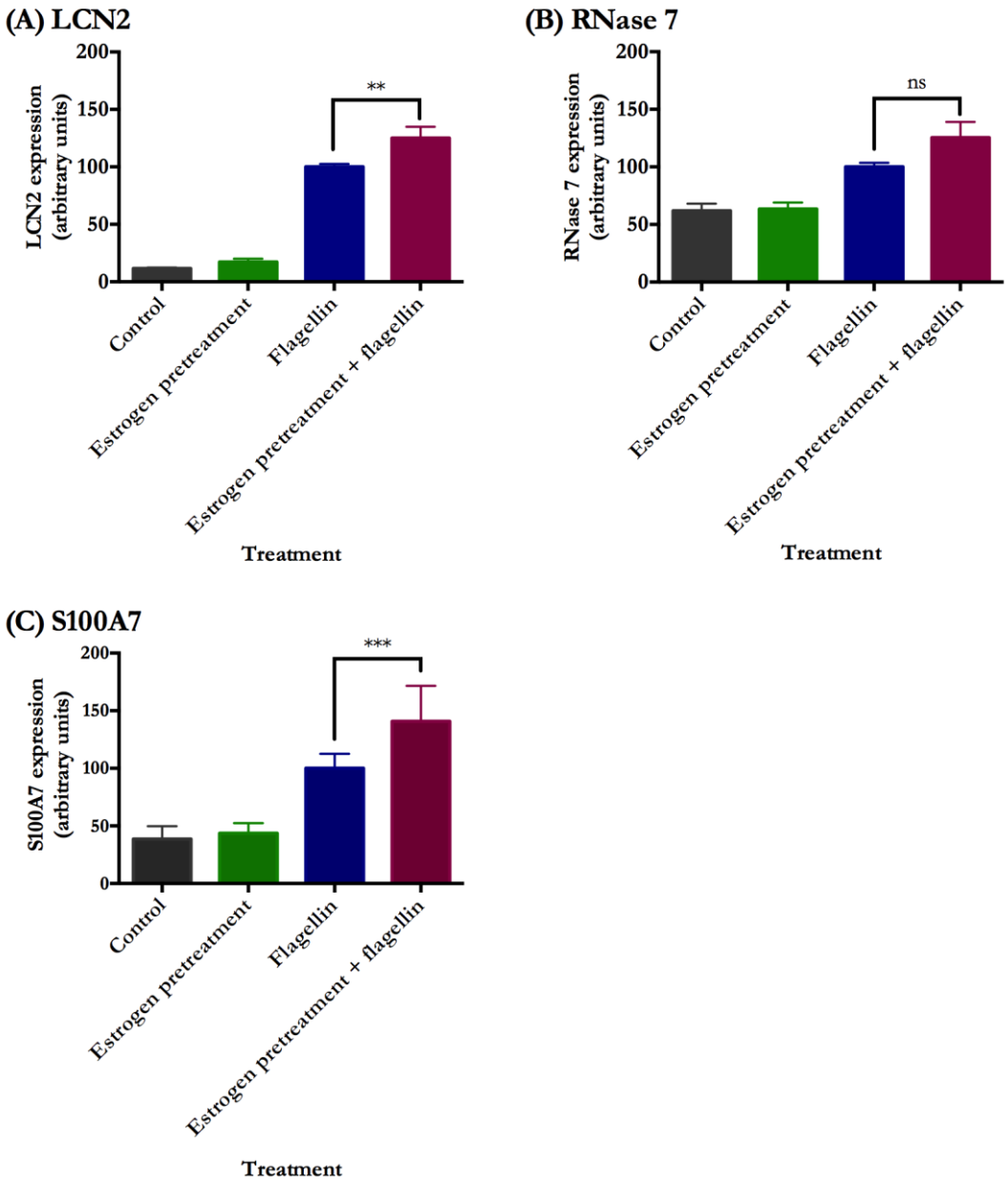

Figure 5.18: Effects of estrogen pretreatment and flagellin on LCN2, RNase 7 and S100A7 expression. VK2 cells were pretreated with 4nM estrogen, or cyclodextrin vehicle, for seven days and then challenged with 50ng/ml flagellin, or PBS, for 24 hours. After challenge the RNA was extracted, reverse transcribed, and analysed by qPCR for (A) LCN2, (B) RNase 7, and (C) S100A7 expression. The results were normalised to 24 hour flagellin challenge. Error bars represent standard error. Statistical analysis was performed using one-way ANOVA with Tukey's post hoc test. ns=not significant, **=$p<0.01$, ***=$p<0.001$. For LCN2 and RNase 7 N=8, n=24 and for S100A7 N=5, n=15.

5.4.3 Effects of ER-α and –β inhibition on LCN2, RNase 7, and S100A7 expression

To investigate the potential role of ER-α and –β in the regulation of LCN2, RNase 7 and S100A7, the 2000bp promoter regions of these genes were analysed for the presence of ERE half-sites using PROMO. Several ERE half-sites were identified in the promoter region of each gene (highlighted in red in Figure 5.19); nine ERE half-sites were identified in the LCN2

promoter, eight in the RNase 7 promoter and eight in the S100A7. These data demonstrated the potential for interaction of ER-α and –β with binding sites in the promoter region of these genes.

Figure 5.19: Identification of EREs in the promoter regions of LCN2, RNase 7, and S100A7. The figure shows the 2000bp promoter region of (A) LCN2, (B) RNase 7 and (C) S100A7. Estrogen response element half-sites identified by PROMO software are shown in red[292,293]. The start of the first exon is shown in green.

To investigate the roles of ER-α and –β in LCN2, RNase 7 and S100A7 expression, the expression of these genes was analysed following inhibition of ER-α and –β. VK2 cells were pretreated with 4nM estrogen with and without 1μM fulvestrant, or vehicle, for seven days, and

then challenged with 50ng/ml flagellin or PBS for 24 hours. After the challenge the RNA was extracted, reverse transcribed and analysed by qPCR for LCN2, RNase 7 and S100A7 expression. The results were normalised to 24 hour flagellin.

The results for LCN2, shown in Figure 5.20A, revealed that flagellin challenge induced LCN2 expression to 100AU, from 11AU in the controls ($p<0.0001$). Estrogen pretreatment prior to flagellin challenge significantly increased LCN2 expression, to 110AU, compared to flagellin challenge ($p=0.0006$). However, following inhibition of ER-α and –β by fulvestrant, potentiation of LCN2 expression by estrogen was not observed. Following fulvestrant pretreatment, flagellin challenge induced LCN2 expression to 20AU, from 3.6AU in the control, and estrogen pretreatment plus flagellin resulted in LCN2 expression of 17AU. This did not represent a significant change in LCN2 expression (0.5218). These results also reflected the results for hBD2 (Figure 5.2), which showed an approximate 50% decrease in the level of induction of gene expression with flagellin following fulvestrant pretreatment. For LCN2, without fulvestrant pretreatment flagellin challenge resulted in a 9.4-fold increase in expression, whereas, after fulvestrant pretreatment flagellin challenge induced a 5.6-fold increase in LCN2 expression. Again this may have been due to potential estrogenic compounds in components of the cell culture medium, such as bovine pituitary extract, which induced a baseline level of LCN2 expression. Inhibition of ER-α and –β with fulvestrant may have, therefore, reduced this exogenous effect.

The results for RNase 7 (Figure 5.20B) showed that estrogen pretreatment prior to flagellin challenge did not significantly increase RNase 7 expression, compared to flagellin challenge alone, with or without fulvestrant treatment. Furthermore, inhibition of ER-α and –β by fulvestrant increased baseline expression of RNase 7, from 59AU in the control samples without fulvestrant pretreatment, to 173AU in the control samples with fulvestrant pretreatment. These data suggested that inhibition of ER-α and –β increased RNase 7 expression.

Without fulvestrant pretreatment expression of S100A7 was significantly induced 2.4-fold to 100AU by flagellin challenge, compared to 42AU in the control ($p<0.0001$, Figure 5.20C). Estrogen pretreatment prior to flagellin challenge further increased S100A7 expression to 134AU, a significant 1.3-fold change compared to flagellin alone ($p<0.0001$). Following fulvestrant pretreatment the potentiation of S100A7 expression by estrogen pretreatment plus flagellin challenge was attenuated, and no statistically significant difference was observed between S100A7 expression with flagellin challenge (32AU) and estrogen pretreatment plus flagellin

(30AU). Once again fulvestrant pretreatment resulted in a reduced baseline gene expression in the control samples, with S100A7 expression determined as 42AU in controls without fulvestrant and 13AU in controls plus fulvestrant pretreatment. Nevertheless, the level of induction of S100A7 gene expression by flagellin was comparable with and without fulvestrant treatment; flagellin challenge without fulvestrant treatment resulted in a 2.4-fold change in S100A7 expression, whilst flagellin challenge with fulvestrant pretreatment resulted in a 2.5-fold change, compared to the controls.

Thus, taken together these data did not suggest that estrogen pretreatment upregulated RNase 7 expression and thus, these results did not reflect the microarray findings for RNase 7. Nevertheless, these data did indicate a role for ER-α and –β in upregulation of LCN2 and S100A7 by estrogen, as inhibition of these receptors blocked potentiation of LCN2 and S100A7 expression by estrogen.

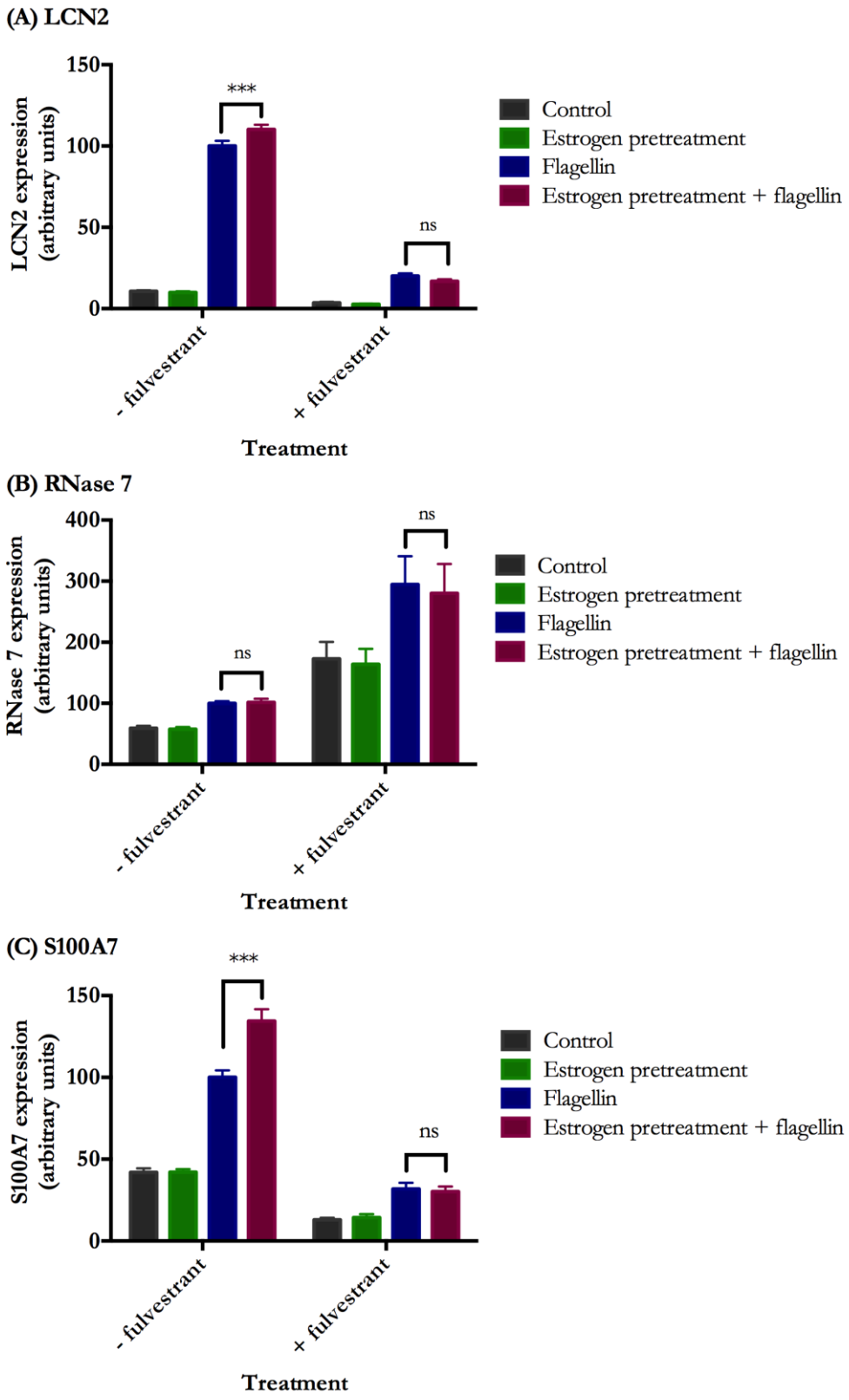

Figure 5.20: Effects of ER-α and –β inhibition on LCN2, RNase 7 and S100A7 expression. VK2 cells were pretreated with 4nM estrogen with and without 1μM fulvestrant (Tocris, UK), or vehicle, for seven days and then challenged with 50ng/ml flagellin or PBS for 24 hours. The RNA was extracted, reverse transcribed, and analysed by qPCR for (A) LCN2, (B) RNase 7, and (C) S100A7 expression. The results were normalised to 24 hour flagellin challenge. The error bars represent standard error. Statistical analysis was performed by two-way ANOVA with Tukey's post hoc test. ns=not significant, ***=$p<0.001$. N=3, n=9.

5.4.4 Effects of GPER stimulation on LCN2, RNase 7 and S100A7 expression

Inhibition of ER-α and –β by fulvestrant attenuated the potentiation of LCN2 and S100A7 gene expression by estrogen, which indicated that expression of these AMP genes was regulated in part through the genomic estrogen receptors. To verify these results VK2 cells were treated with G-1, a GPER agonist, and it was hypothesised that activation of GPER would not affect LCN2 and S100A7 expression. Although the previous experiments with fulvestrant did not suggest that RNase 7 was upregulated by estrogen through ER-α and –β, the effects of G-1 on RNase 7 expression were also investigated, to determine whether RNase 7 is upregulated by activation of GPER. VK2 cells were pretreated with 100nM G-1, or DMSO vehicle, for one, five and seven days and then challenged with 50ng/ml flagellin or PBS for 24 hours. The RNA was extracted, reverse transcribed and analysed by qPCR for LCN2, RNase 7 and S100A7 expression.

The results for LCN2, presented in Figure 5.21A, showed that for one, five and seven day pretreatments flagellin challenge alone induced LCN2 expression to approximately 100AU, from approximately 15AU in the control samples. However, G-1 pretreatment plus flagellin challenge resulted in significant downregulation of LCN2 expression at one, five and seven days pretreatment (p-values<0.05). The level of downregulation increased with the length of pretreatment; one day G-1 pretreatment plus flagellin resulted in a significant 25% decrease in LCN2 expression compared to flagellin ($p=0.0104$), five day G-1 pretreatment plus flagellin resulted in a significant 41% decrease in LCN2 expression compared to flagellin ($p=0.0001$), and seven day G-1 pretreatment plus flagellin resulted in a significant 66% reduction in LCN2 expression compared to flagellin ($p<0.0001$).

Following one day pretreatment, flagellin induced RNase 7 expression to 103AU, compared to 41AU in the control ($p=0.0023$). G-1 pretreatment plus flagellin further increased this to 127AU, suggesting potentiation of RNase 7 expression by G-1 after one day pretreatment, however, this increase was not statistically significant ($p=0.4377$). Five and seven day G-1 pretreatment plus flagellin resulted in reduced RNase 7 expression by approximately 30%, compared to flagellin alone, however, again these results were not statistically significant (p-values of 0.2252 and 0.1207, respectively).

The results for S100A7 expression following G-1 pretreatment echoed the results for LCN2 and RNase 7, whereby, G-1 pretreatment resulted in downregulation of S100A7 expression. After one day pretreatment, flagellin induced S100A7 expression to 121AU, compared to 36AU in the control. One day G-1 pretreatment plus flagellin induced S100A7 expression to 111AU, which

did not represent a statistically significant difference in S100A7 expression compared to flagellin challenge. Five and seven day G-1 pretreatment plus flagellin resulted in significant 34% and 29% decreases in S100A7 expression, respectively, compared to flagellin challenge alone ($p=0.0025$ and $p=0.0297$, respectively).

Therefore, a similar pattern was seen for LCN2, RNase 7 and S100A7 expression whereby G-1 pretreatment plus flagellin resulted in lower AMP expression than flagellin challenge.

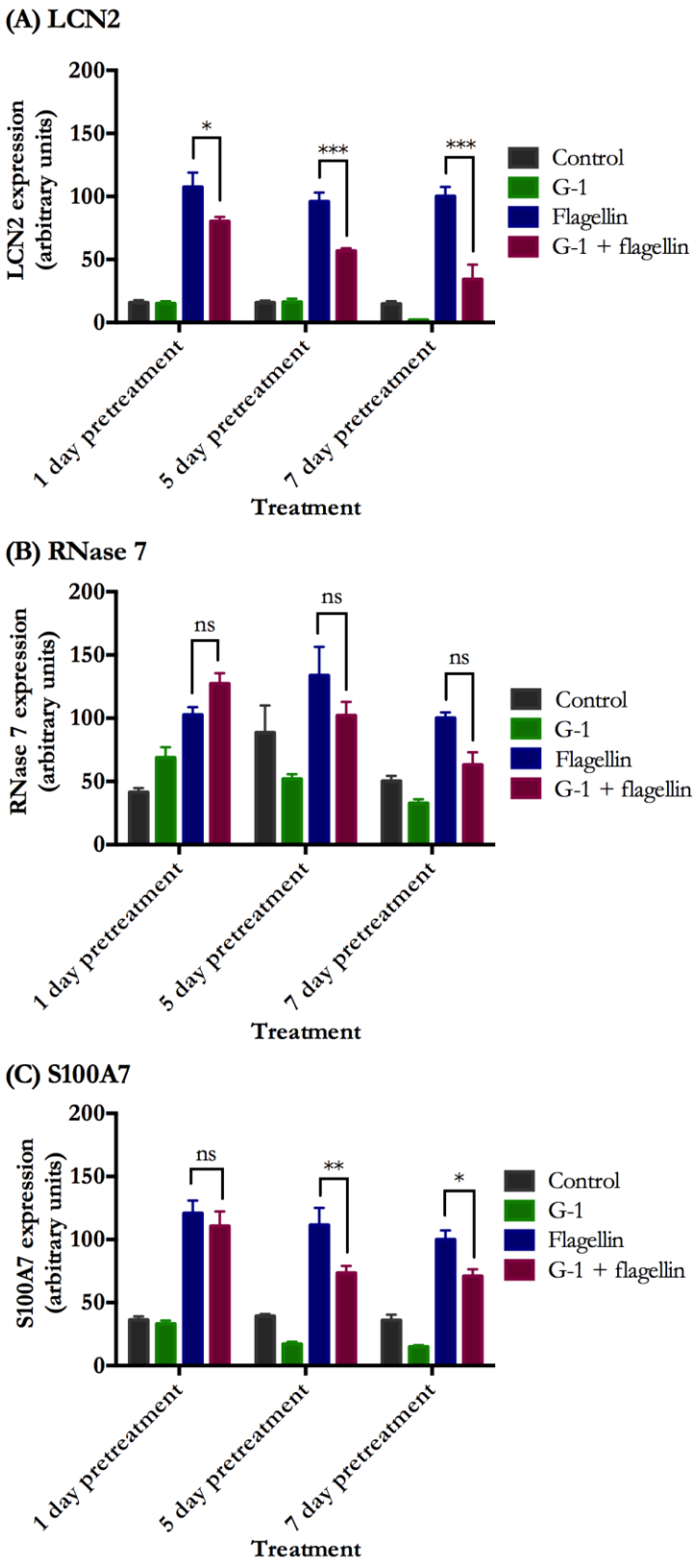

Figure 5.21: Effects of G-1 pretreatment and flagellin on LCN2, RNase 7, and S100A7 expression. VK2 cells were pretreated with 100nM G-1 (Tocris, UK), or DMSO control, for one, five, or seven days and then challenged with 50ng/ml flagellin or PBS for 24 hours. The RNA was extracted, reverse transcribed, and analysed by qPCR for (A) LCN2, (B) RNase 7, and (C) S100A7 expression. The results were normalised to 24 hour flagellin challenge with 7 day vehicle pretreatment. Error bars represent standard error. Statistical analysis was performed by two-way ANOVA with Tukey's post hoc test. ns=not significant, *=$p<0.05$, **=$p<0.01$, ***=$p<0.001$. N=2, n=6.

5.5 Discussion

This chapter investigated potential mechanisms of estrogen regulation of AMP expression in VK2 cells. Data presented in this thesis indicated upregulated expression of a number of AMP genes in response to estrogen pretreatment prior to flagellin challenge, and this finding is supported by other published literature[134,199]. However, prior to this no investigation into the mechanism by which estrogen upregulates AMP gene expression had been conducted. To determine the contribution of estrogen receptors to AMP expression, estrogen receptor agonists/antagonists were used.

The ER-α and –β agonist, fulvestrant, was used to inhibit ER-α and –β during seven day pretreatment of VK2 cells with estrogen. Fulvestrant is a pure antagonist of ER-α and –β, with agonistic activity on GPER[286,295]. Thus, expression of AMPs regulated through ER-α/β would not be potentiated with estrogen and fulvestrant pretreatment plus flagellin challenge. Whereas, following fulvestrant pretreatment AMPs regulated through GPER would still show increased gene expression with estrogen pretreatment plus flagellin compared to flagellin challenge alone. It is of interest to note that patients receiving fulvestrant treatment for breast cancer experience a greater incidence of UTIs, hinting at an important role for ER-α and -β in protection against UTIs[296]. Analysis of hBD2 expression revealed that the potentiation observed with estrogen pretreatment plus flagellin was indeed inhibited by fulvestrant treatment, suggesting regulation of hBD2 by ER-α/β. The classical mechanism of hBD2 induction is through activation of NF-κB, which binds to NF-κB binding sites in the hBD2 promoter[60,106,297–300]. Data obtained by microarray revealed that estrogen pretreatment did not upregulate components of the TLR5 pathway, indicating that ER-α/β regulation of hBD2 expression was likely to be through direct interaction of the ERs with EREs in the hBD2 promoter region. ERE half-sites were identified in the 2032bp hBD2 promoter region inserted into the phBD-2-luc vector, engineered by Dr Marcelo Lanz, using PROMO software[106,292,293]. Although EREs are reported as having the consensus sequence GGTCAnnnTGACC, most estrogen responsive genes contain imperfect, non-palindromic EREs in their promoter. For example, functional EREs were identified in the c-fos and lactoferrin gene promoters with sequences of CGGCAgcgTGACC and GGTCAaggCGATC, respectively[301,302]. EREs with mutations in both sides of the palindrome have much lower transcriptional activity than EREs with mutations in only one side[289,303]. Thus, searching for ERE half-sites, rather than full ERE sequences, was a valid approach for identifying potential EREs in a gene promoter region. PROMO identified six ERE half-sites in the hBD2 promoter region and mutation of these six ERE half-sites by site-directed mutagenesis resulted in attenuation of hBD2 gene expression by estrogen pretreatment. Thus, these data indicated that

hBD2 is regulated through ER-α/β, and that all six ERE half-sites are required for potentiation by estrogen. Interestingly, a similar result has been found previously for the chicken ovalbumin gene, whereby four ERE half-sites, separated by more than 100bp were identified in the promoter region and all contributed to induction of gene expression by estrogen[290]. Furthermore, evidence suggested that ER dimers could cause a conformational change in the ovalbumin promoter region and bind to two widely spaced ERE half-sites. This therefore, suggests a mechanism by which the ERE half-sites may regulate hBD2 expression in response to estrogen. Examination of the hBD2 promoter region showed that two of the six ERE half-sites, ERE3 and ERE4, were separated from imperfect palindromes by 3bp, suggesting that two full EREs may exist within the hBD2 promoter. The six ERE half-sites are highlighted in red in Figure 5.22, with the imperfect palindromes of ERE3 and ERE4 highlighted in blue. Thus, hBD2 may be regulated through ER dimers binding to two separate ERE half-sites, and/or by interaction of ER dimers with imperfect EREs in the hBD2 promoter, but further work is needed to determine the precise mechanism of ER-α/β regulation of hBD2 through the ERE half-sites identified here.

```
          CTGGACACTGGTCTCATCTGGTGAAAGACTGTGGGTAATGGAAGCATTTCTGTGGGGTGGTGGCAGGACATGTGCATGGTGAGG
    ERE1  CAGGTCATCAGCAGCAAGTGAGAGCTGCCTCTTACTTTCTAAAGGTGACATAGCAAGTATACAAAAAAAAAATAAAATATTAAT
          TTAGGCAGAGCACATAAAGGCTTTATTTCATATTCCATTTCTCTGTATGCTTTCTTCACCAGGAAGAAATAGTTTTAGTGTCAG
          GAATGAATGAGTCTGCCCCTCAATTCCAGCCTGCTCAGCACACAAGGAAACAAAGCCCTGACAATCAGAGTGACTCCCTGGTGA
    ERE2  CTAAGCTCCAGTCCTGGATGCATATTTGTTTAGCAGTTCTGACAGCATCTGACCCAGCCCTCTCTTTGCATACCCCACCAGAAC
          CTTCTTTTTTTTTTTTTTTCTTTGAGACTGAGTCTTGCTCTGTCGGAAGCGATTCCCGTGCCTCAGCCTCCCAAATACCTGGAA
    ERE3  TTATAGGCGTAAGCCATCATGCCTGGCTAATTTTTGTATTTTTCATGGAGATGGGGTTTTGCCATGTTGGTCAAATTGGTCTCA
    ERE4  CACTCCTGACCTCATGTGATCCACCTGCCTCAGCCTCCCAAAGTGCTGGGATGACAGGTGTAAGCCACCATGCTAGGCTCAGAA
          ATTTCCTTTTATAAAAATGTCATTAAGGATCTTGGCTGCACAATATCGTTACCAGCTTCCTTTAAATCCACCTCTGGCCTGCCA
ERE5,ERE6 GGAATCAGGGTTCTTCAGAACCTGACATTTTAAATGAAGAGGTCAGGCAGGTCATGAGGAAAGCCTCATTGTCCCCATGTCTCT
          GTCACTGCTGCACCCCTGAGACATCACAGACATGGACACTGGGGCCTGCTTGTTTCTCAAACTGCCCTTAGATCGAAAGAGGGA
          GGAACCAGGATGAATGCCACTCATTTTCCCAAGAAAGGCCCTCTCCTGAGTGCCCGGGATGGGGCTCTGTCCATTGCCTGGGGC
          CGCCAATTGCTACTCTGGGTTACGGAAGAAGGACAGGGTCCTGAGAGACACCAGAGACCTCACACAGCCCTGAAAACATGGGGC
          TCCTTCATAAGTGTTTCCCATCACCAACAGGGAGACCACGTGGAGGCCTTGCAGCCCTACTCGGTGCTTCTCCACCAAATCCCA
          AGGGCAGTGACGCTGACGTCTGTGGAAAGCAGAGAAAGCCCTGGCTCCCAAAGCCCTGAAGTCCTGTGGAGCTGACATTCCCTG
          AGTGACGGTGTGAATGGAAGGAACTCAAGTGCGGGTGGTAGGCCACCTCCTGGCCCAGGCCTGGGTGAACTCTGAGGGGACACA
          TGTAGTCACAATCCCATCCTCCCATTCTCCTTCTCAGAGGAAGGAAGTGGGCATCCATCTGCCTCATCTCTCTCCCGTGGGGAA
          GATGGGGAGTTTCAGGGGAACTTTCACATAAATTTCACCAGCTCAGATCTCCTGTGAGGATGGGGCCCACCATGCTCCCGGTGC
          TGCCAGAGGCCCTGAGCCCCTCCAGGGTCCCTGGGTTTGAGCCAGCCCTGTATCATCCCCAGGAGCTGAATGTCCGAGCAATGG
          ATAGAATTAGATGGAAAGAGCTCTCAATTTGGCCTGAGACTGTCCCCAGATACTCAGGAAAAACAGGACGTCGCACAGAGTGGG
          CAGCAGGTGAGTGGCAGGTTATAGGTCCTGAGTTTGAGTTTGTTCTCACGTGAGACAGACCCAGCCCCTCACTCCATTCACACA
          CTGGGTTTTAAATGGTGCAAGATAGGAGGAATTTTCTGGTCCCAAGAGCAGGAGGAAGGGATTTTCTGGGGTTTCCTGAGTCCA
          GATTTGCATAAGATCTCCTGAGTGTGCATTGTTCTTTGAGGACCATTCTCTGACTCACCAGGTAAGTGGCTGAATTCTAACCTC
          TGTAATGAGCATTGCACCCAATACCAGTTCTGAACTCTACCTGGTGACCAGGGACCAGGACCTTTATAAGGTGGAAGGCTTGAT
          GTCCTCCCCAG
```

Figure 5.22: Position of potential imperfect full EREs in the 2032bp hBD2 promoter region. ERE half-sites identified by PROMO software are shown in red. Imperfect ERE half-sites separated from these by 3bp are shown with consensus base pairs highlighted in blue and imperfect base pairs underlined in black. The start of the first exon of hBD2 is shown in green.

Analysis of hBD3 expression also revealed inhibition of gene expression following fulvestrant treatment. This suggested that hBD3, in addition to hBD2, may be regulated by ER-α/β. PROMO software identified one ERE half-site in the hBD3 promoter and to investigate the contribution of this ERE half-site to hBD3 expression attempts were made to engineer a luciferase reporter plasmid containing the hBD3 promoter region. However, these attempts were not successful for reasons that were not clear, as the control reactions did not highlight any

technical issues with the experiment protocols. Thus, this avenue was not explored further. Future attempts to engineer a hBD3 luciferase reporter plasmid could involve the use of a different bacterial strain for transformation, such as JM109, or a strain suitable for transformation by electroporation rather than chemical transformation. The genotype of the bacterial transformation strain and the transformation method may affect the efficiency of the cloning reaction. Examination of the DNA sequence flanking the ERE half-site in the hBD3 promoter did not reveal any further imperfect ERE sequences. Furthermore, as only one ERE half-site was identified, cooperative binding of an ER dimer to separate ERE half-sites is implausible. Thus, the bioinformatics analysis does not support regulation of hBD3 by ER-α/β. To investigate the role of GPER in hBD3 expression, VK2 cells were pretreated with the GPER agonist G-1 for one, five and seven days prior to flagellin challenge. Interestingly, seven day pretreatment of VK2 cells with G-1 followed by flagellin challenge resulted in significant downregulation of hBD3 expression of 55% compared to flagellin challenge without G-1 pretreatment. This suggested that stimulation of GPER resulted in a reduction in hBD3 expression and was unexpected. This result may be explained by desensitisation of GPER. Desensitisation of G protein-coupled receptors (GPCRs) is the loss of response due to prolonged administration of an agonist. During desensitisation the GPCR is endocytosed and then either recycles back to the membrane or is targeted for degradation. Desensitisation has been reported previously with GPER, whereby the receptor was endocytosed and degraded by the ubiquitin-proteasomal pathway[304]. Thus, it is possible that seven day stimulation of GPER with G-1, at a concentration much higher than that used for the estrogen pretreatment, resulted in desensitisation and degradation of the GPER in the VK2 cells. This notion was also supported by the fulvestrant data. Pretreatment of the VK2 cells with fulvestrant inhibited the potentiation of hBD3 expression by estrogen. This initially indicated that hBD3 was regulated through ER-α/β. However, as fulvestrant also has agonistic effects on GPER, fulvestrant treatment of the VK2 cells for seven days may also have resulted in GPER desensitisation. Therefore, paradoxically, downregulation of hBD3 expression following G-1 and fulvestrant treatments may indicate regulation of hBD3 through GPER. This premise is supported by the findings from the hBD3 promoter analysis, which did not support regulation of hBD3 by ER-α and ER-β. As G-1 treatment did not cause an increase in hBD3 expression even after only one day pretreatment, it is possible that desensitisation began within the first 24 hours following G-1 treatment. Hence, further experiments may indicate whether G-1 treatment at this concentration (100nM) significantly induces hBD3 expression at earlier time points than one day G-1 pretreatment.

Induction of hBD3 expression has previously been reported to occur through activation of the epidermal growth factor receptor (EGFR) and MAP kinases[305]. Interestingly, GPER has been shown to activate MAP kinase signalling through transactivation of EGFR[306]. Thus, a mechanism is proposed whereby estrogen binding to GPER results in activation of EGFR, MAP kinases and consequently, increases hBD3 expression. Further work using EGFR inhibitors is needed to fully investigate this hypothesis.

The results for LCN2 and S100A7 were similar to that of hBD3. Pretreatment of VK2 cells with fulvestrant prevented potentiation of LCN2 and S100A7 expression by estrogen pretreatment plus flagellin. In addition, G-1 pretreatment prior to flagellin challenge also resulted in significant downregulation of LCN2 and S100A7 expression compared to flagellin challenge without G-1 pretreatment. However, unlike hBD3, several ERE half-sites and at least two imperfect full ERE sequences are present in the promoter regions of LCN2 and S100A7 (Figure 5.23). Thus, for these AMP genes it is difficult to determine which estrogen receptor(s) were responsible for increasing AMP expression in response to estrogen. The downregulation in response to G-1 may be attributed to GPER desensitisation, however, further work examining GPER protein levels following G-1 treatment is required to confirm this. Furthermore, the loss of gene expression potentiation with fulvestrant may either be due to inhibition of ER-α and –β, or may be due to agonism of GPER causing desensitisation of this receptor. Thus, these data alone are not sufficient to ascertain the role of each estrogen receptor in LCN2 and S100A7 expression.

qPCR analysis to verify the microarray data showed a trend towards potentiation of RNase 7 expression with estrogen pretreatment plus flagellin, compared to flagellin alone. However, repetition of this challenge with and without fulvestrant pretreatment, showed that estrogen pretreatment plus did not enhance RNase 7 expression, compared to flagellin challenge without estrogen pretreatment, even when fulvestrant was not present. Thus, these data do not fully support previous findings suggesting a role for estrogen in RNase 7 regulation. Furthermore, following fulvestrant pretreatment, baseline expression of RNase 7 appeared to be increased from 59AU in control samples without fulvestrant to 172AU in control samples with fulvestrant. These data suggested that inhibition of ER-α and –β and potential desensitisation of GPER resulted in increased RNase 7 expression. Contradictory to this, a decrease in RNase 7 expression was observed following seven day G-1 pretreatment plus flagellin challenge, compared to flagellin challenge without G-1 pretreatment, which did suggest a role for estrogen receptors in regulation of RNase 7 gene expression. However, this downregulation was not statistically significant. Eight ERE half-sites and one imperfect full ERE was also identified in the RNase 7 promoter (Figure

5.23). Therefore, the results of these experiments are complex and it is not possible to determine, from these experiments alone, the role of the estrogen receptors in RNase 7 expression.

(A)

LCN2 promoter region:

TATCATCCAGGCTGGAGTGCAGTGGCACAATCATAGCTCACTGCAGCCTCGGCTTCCTGGGCCCAAGTGATCCTCCCACCTCAGCCTCCCCGAGGATACGTGGTTTT
TTTTTTCTTTTTTCAGACAGGGTCTCACTCTGTCTCCCAGGCTGGAGTGCAGTGGTGCGATCTTGGCTCACTGCAGCCTCCGCCTCCCGGGTTCAAGCCATTCTCCT
GCCTCAGCCTCCTGAGTAGTTGGGATCATAGGCATGCATCACCCCACCTGGCTAATTTTTGTATTTTTAGTAGAGACGGGGTTTTGCCATATTGGCCAGGCTAGTCC
CTGAGGATACATTTTTTTTTTCCCCGAGATGGAGTCTCCCTCTGTCGCCCAGGCTGGAGTGCAATGGCGCAACCTTGGCTCACTGCAACCTCCGCCTCCCAGGTTCA
AGCAATTCTTCTGCCTCAGCTTCCCGAGTAGTTGGGATTACAGGCATGCGCCACCATGCCCAACTAATCTTTGTATTTTTACTAGAGACAGGGTTTCACCATGTTGG
TCAGGCTGGTCTTGAACACCTGACCTCAGGTTATCCACCCGCCTCAGTCTCCCAAAGTGCTGGAGTTACAGGCGAGAGCCACTGCGCCCAGCCGAGGATACCTTTTT
TTTTTTTTTTTTAAGACAGAATATCGCTCTGTTCCAGGCTAAAGTGCAAAGGCGTGATCTCGGCTCACTGCAACCTCCGCCTCCCAGGTTCAAGCTGTTCTTCTGCC
TCAGCCTCCCGAGTAGCTGGGATTACAGGCGCCTGCCACCATGCCCTGCTAATTTTTGTATTTTTAGTAGAGATGGGGTTTCACCGTGTTGGCCAGACTGGTCTCGA
ACTCCTGACCTCGTGATCCACCCGCCTCAGCCTCCCAAATGCTGGGATTACAGATGTGAGCCACCGCACCCGGCCTGGCAGAGGATACTTTTTAAGGTCAAAGACAG
TAGCAGAGGTGGAGTTCCTGGGAACAGGGTCATGAGGGAAGAGGGGGTTCGGAGGGAGCGAGTAGCCACTGGCTACCTCTAGAAAGGGAAGGCTTTGGTGCAACAT
CGTTCCCCTGCAGTTTTACTCATCTTTGCTTCCTGCCCTTTCATCATCCAATCGGGCAGGCAGGACAGGGCCTGAGGGGGCAGGGATCCAGTGGGTGCCTCTCTAGA
CTAACCCCAGCTCAGGACTCCCAGAGCCCCTTCCCTGAGGCCCTGCTGCCCCCAAGCCCAGATTGGGGATCCCAAGCAGCACGTAGGCAGAGCCAGTGAGGTCCCCG
TTAGTCCCATTGAAAGCTCTAAAACCAGCGAACCCTCAGTCCAGCCTCAGGTCAGGCATCCAGGACGGCCTCAGCCCTCATGGGTGAGCCATCTCTGCGGACACTGC
ACAGGGCCTACGATCCATCGCTGCCTCCCGAGGATGCCAGCCAGGCCCCCGTTGAGATAACTGCTTCCCTGCTGGACAAGGCTGGGACCAGCCATCTCGGTGACAGT
TCCAGAACCCCTGGCCTGGGCTGCTGGGTTCAATGGAAAAAGGCTGTGACTAGAGTCAGGGGGATGGTCTCAGTGACCTCAAGGATAAGGCCAGATCCTTGCACTGT
CAGTGACCCAAAGCAACAGGTGTCCAGAGCAGCAGTGTGGCGCCTTCACGCCCCCACACATCAGCCCAACTCACCCAGGACAGGGACTGTAGCCTCAGCACTCAACC
CATGTGCCCTGTGTGGGGTCTCTTCCCACTGCACTCACAGGAGAGGAAGGGTCCCTCAGGGGTCCACTGGGGTCCCCTCCTGCAAATGGGGCAAGGAGAGGGGCAAG
GGGCTGTCTCAAGGCCCCTGGAGCACATGCAGGTCCTGGACTGGGGCTCCTGGGAGGGCCATGATTCTGGGCTCCATGAGTTCAGAGCAGACGCCTTGTTTTTCCTT
GTCCACTGTCAGCCACCCCACCCTTCCCTGACCCTTAAAAGAACCAGGAAACAGCACATGATCTGTTGGAAGGAGGCATTCATTCTTTCCTTTCTGTGGGTGTGGGG

(B)

RNase 7 promoter region:

CAGAAGAGCCAGAGGCCTGTGTGAACTTGTTCTTGATTCTCTTTTGCCATCTAGTGGCATTTCTCATCTCCAGCACCACTTTTGCTTCTAAAGATCCTTCATCCTGA
CCCCCAACCCACAGCTGTGCTGTCCAGCTACTAAAATAATGTCCTCCTGGCCTCAAAACAAACTCCCCATCCTCCTGACTTAGAATCATAAATTCTGGACCAGAACA
CAAACTTTATGATCAGGATGGGTTGTGCGACTTCTCCACAGTTATAATCCACACAACAGCCAGGTAATCCTTTAAGCTGACACGTTCTTTATTCATCTACTTAGAAC
CCTTCCAGGGTTCCCTACTGTGCTTGGAGTAAAAGCCACAGGCCTTCAAATGGTCCGTAAGTCTTCCCAATGACCTGGTCTCTGGTCCCTCTCTGAACTCTCAGTTA
CCTGCTCCAGCCACACTGGACACACTGCTGTTCCTCCAACACCTCAGGCATCTGTCTGCTCTGGGGCTTTTGCAGTGCTAGTCTCTTCACTTGGAACATTCTTCCTC
CGGATAATCACAAGTTCACTCTTATCTTCAAGTCTCTGCCCCAGAGTCAGCGATTTCAACGATGTTACGTAAAATTACTGACCACCAACCCCTATACTGTTCTACTT
TTTTCCCTAGCCATTATCACTTTGAGCAAAGTATACGTATTTTTTTTTACTGTCTTTCTCCAATGGAATGTAAGCTCTACAAAGGCAGGGACTTTTGTCTTTGTTTT
TTGTTGTTGTTTGTTTGTTTGTTTGTTTGTTTTTTGAGACAGGGTCTCACTCTGTGACCCAGGCTGGAGTGCAGTGGTGCAATCATGATTTTCACTGCAGATTTTAT
CTCTCAAGCTCAAGCAATCCTCCCTCCTCAGCCTCTGGAGTAGCTGGGACCACAGGCATGCACCACCATGCCTGGCTAATTTTTCAAATTTTTTATAGAGACAGGGT
TTCGCCACATTGCCCAGGCTGGTCTTGAATTCGTGGCCTTAGGCAATCCTCCTGCCATGGCCTCCCAAAGTGCTAGGATTACAGGTGTGGGCCACCGTACCTGGCCA
TTTTTGCCTTTTTTTGTTCAGTGATATATCCCAAGTATCTTGACACTTAGTAGATGCTCGATAAATGTTTGTTGACCACATGAATGAAGCATGCCCAAGATTCTGAGA
TTGCCTACTACTTACAGGTAAATTCTGAAAACAAAAATATTCCTCATCTCAGTTTTACAGGCCTTCTCACCCACAGAGGGTGATGCTTCTCTGCCTTGGTGTCTCGG
TTCTCCTGAGTGTCATATTCCAAGCTCACAAGAGCTTGGAGTAGCACTGACCCAGATGCTCCACACAGCTGTAACCACCACAAGGAACAGGACATACAAGGTGAAGG
AAGCACTAAGGCAGGATGTCGAGAGCAGCAACAGCATTTTAAACACAAACATTTGGGCAGTATTAAATTTTTGCAATTTTCAATAAAAAAGGGAGGGAACAAGTGAA
ATTGAGAGGTGTTGGCTGCCTTCTCCAGCTAAAGCCATGTGGCCTTGGTTGGTACCTGGAACTGGAGAGGCCTGTGAATCATTGTGGAATGGCTTCGCTATTGGGGA
TGGTGCCAGGCCTCGTGACAGTGATGATTCATTCACCCACTTCCCTCGTGTCTGTTCCATCTCCTCCGAAAGATAACCAGTATCTCCAGATGACAAGGAACCAGACA
AAGCATCTTTCTAGGCTGTCCTATCTGTGCCTCAGGTCAGAGAAGAAGCAACCCTTAACACCACAGTGATTGACTCTTCCCAGGATCAAGGGCCAGAAGTGTATATG
AGAGGATATGAATGACAACTCTTCCTGAAATTGATTTCAGTTGACACCTGGGTCAGGTGCTCTATTAAAGAGTCATTAAAATCATGTGGCCAGGGAACAAATACAGT
CTTCGAATGTGACGATTCAAGCTTCCTCATTGCTGAACATGTTTAGGCAGGTACAGGCATCCTTAGGTGTCCACGTATTTGGGACATGTAAGTGGAGAGGCATGAAC

(C)

S100A7 promoter region:

AACTCTTAAAACTCAACGATAAGAACACAAACCAAACAATTAGAAAATGGGCCAAAGACCTTAACAGATATCTCATCAAAGAAGATACAGAAGGTGACAAATAAGCA
TATCAGAAGATGCTCCACATCATATGTCCTCAAGGAAATGCAAATTAAAACAACAATGAGATACCAGTACACACTTATGAGAATGCCCAAAATCTGGAACACTGGAC
AACAGCAAATGCTGAAGAAGGATGTGGAGCAACAGGAACTCTCATTCATTGATGGCAGGAACACAAAATAGTACAGCCACTTTGGAAGACAGTTTAGTGCTTTCTTA
AAAAACTAAACATACTCTTACCATAGGATCCAGAAATCACACTCCTTGGGATTTACCCAAAAGAAGTGAAAACTTATGTCCACACAAAAACCTGCATACACATATAT
ATGAATATATGGCACAATGGTGAAGTCTGGGCTTTTAATGAAGCCATCCTAAATAGCATGCATTGTACCCACTAAGAAATGTCTCATCCTTCACCCACCGCCTCACC
TGCTGCCCTTCACAGTCTCCAGTGTCTATGATTCTACTCTCTACCTCCATCTGTATGCATGATGTAGCTCCCACTTACACATGAGGTTGCACAGTATTTGACTTTCT
GAGTAATTTCACTTAAGATAATAGCCTCCAGTTCCATCCATGTTGCCGCAAAAAGCGTGATTTCATTCTTTTTTTATAGCTGAGTAGCATTCCACTGTGTGTGTGTG
TATGTATCTTTTGCTGTTAAAAGTAATATTGCCATCACATGGGGAACTGGGAGAGGGAGAAACAGGTCCCCCTGGTTACATAGGTACTGACGAGAAGGAAGTTGAAG
AAAGATGATGGGTGGAGAAAATAGGTCCCACCTAGGGAGACATCACATCAGCTCTGTGGAGCCCCAGAGTGCTTAAAGGGCTGGCACTAAATGAACCTGGAACTCTC
TTGCACCCTAAAAGGAACATTGCAAGGGGGTAGCAGAAAAAGTCCATTTCAGTGATTCATCATCTCCCTTTCCTCACCATGCCCCAGGGATTCCCATGCCTTCCCAA
CCCTCTTGCCCCTACCTGGGTCAGCCTTTCCACAGCAGGTTAGGGCACATTATAGCCAAGGGCACAACTCCCAACTCCTACACAGGCTGTTTTGCATAGGAGGAGGA
AAAACACTGAAGACTTTCTGGGAAGTTAGTGCCATGGGGCAGGAAAGAACTTTTCCCACTCCCTGCCTCCAGGCTCATTCCATGGGGGGGTCACTCCACCACTCAAC
CTAGATAGTGAGGCCCCTGACCCCAGTCCCCCCACCTAATTCCAGGGCTTCTGTGAGGGGCTGACCAATGGTTAGCAATGAAGTAACCCTGCTTCCCTCCCTGGACT
TTGAGTTCCCATAGGGCAGACCCTGATGTGACCCAAGACCTATAGCACAGGGGATAAGAGTAAGGATTTGATTCAGGCTTTTCTGAGTCCATATAATGATTTGTTGT
GTTTACTAGCTGAGTAAACTTGGGAACATCTCAACTTCTCCTTTCCTAAAATAGAGATTGAAGCACCTCTTAGGACTATGAGGGTTGAGGAGGATGCAGGAGCAGCA
GGTATCTTGATATCTAGACATTAAAATGCTCAGTCAGCGGTGGGGGTCATAGAACAGGCTGTCATAACAAATGTGTGGAAGGATAAGGGGAGGGAACAAACAAGACC
ATGCTGCCTTCAGGAGTCTGAAACTCCATCCTCTTTGGGTCCAGAGGCCCAGTGCTCTTTTCTCCCATTTTCTGACCTGCTACTACACATGTACCGCTGCCTTACCC
TCAAATCAAGGTTGAGCCAGAGAAGACTCCAGGTGAGGTCTCTGGGGTGGGGTGGGACCTGGTGACCTGGGACACTGGCCAGAAATCCTGAGCACAGCCTCCTGGGT
GTGTCCCACCCACCTGATGTGGGGCAAGCCTCCAAGAAACAGATGACAGAGGTGGCCCCAGGCCTCCCAGCCCCTGGGAAGAGCCAGGCTGAGCCTTATAAAGGACT

Figure 5.23: Identification of imperfect ERE sequences in the 2000bp LCN2, RNase 7, and S100A7 promoter regions. ERE half-sites in identified by PROMO in the (A) LCN2, (B) RNase 7, and (C) S100A7 promoters are highlighted in red. Imperfect ERE half-sites within 3bp of another ERE half-site are shown with consensus base pairs in blue and mismatched base pairs underlined in black. The start of the first exon is shown in green.

It is possible to speculate, from findings published in the literature, how estrogen treatment may increase expression of LCN2, RNase 7 and S100A7. LCN2 has been reported to be regulated through induction of NF-κB in epithelial cells[307]. A recent paper has also shown collaboration of

NF-κB with the ETS transcription factor E74-like factor 3 (ELF3) to induce LCN2 expression, although this work was performed in chondrocytes from cartilage tissue and not epithelial cells[308]. Analysis of the microarray data in Chapter 4 identified upregulation of another ETS transcription factor, ETS homologous factor (EHF) by estrogen pretreatment plus flagellin. Thus, LCN2 regulation by EHF is a potential avenue for further work. NF-κB can be activated by EGFR, which can be transactivated by GPER[306,309]. Thus, this suggests a mechanism by which estrogen may increase NF-κB activation, and consequently induce expression of downstream genes, such as LCN2. The microarray data did not show increased expression of NF-κB following estrogen treatment, however, this does not rule out that estrogen increases NF-κB activation at the protein level, rather than mRNA level, and is an area that warrants further research. The literature reports conflicting findings with some papers reporting that estrogen activates NF-κB and others reporting that estrogen inhibits NF-κB[310–314]. Cerillo *et al.* (1998) reported cell-type specific differences in the cross-talk between estrogen receptors and NF-κB signalling. Thus, the effects of estrogen on NF-κB activation in vaginal epithelial cells provide an interesting area for future investigations. In addition, the microarray data identified LCN2 downstream of the transcription factor CEBPB. CEBPB was predicted to be more activated following estrogen pretreatment plus flagellin than following flagellin challenge without estrogen. Furthermore, CEBPB has been shown to be activated by EGFR, through MAP kinase signalling, suggesting a mechanism whereby estrogen binding to GPER may cause upregulation of CEBPB, and hence, LCN2 expression[315]. Overall, there are several pathways by which estrogen may upregulate LCN2, including potential NF-κB and CEBPB activation and direct interaction of ER-α/β with the LCN2 promoter. Further work is required to determine the contribution of these pathways to LCN2 expression in response to estrogen.

RNase 7 is reported to be regulated through activation of MAP kinases, ERK1 and ERK2, but not NF-κB[316]. RNase 7 activation through STAT3 has also been reported[317]. STAT3 was highlighted in the microarray pathway analysis as being a strongly activated transcription factor following flagellin and estrogen pretreatment plus flagellin. ERK1/2 and STAT3 are all downstream of the EGFR, indicating that estrogen binding to GPER may result in increased RNase 7 gene expression via activation of EGFR and, in turn, MAP kinases and STAT3[306,318]. However, promoter analysis identified several ERE half-sites, as well as one imperfect ERE, in the promoter region of RNase 7. Thus, potential pathways exist for induction of RNase 7 expression by GPER and ER-α/β.

Finally, the regulation of S100A7 is less clear, however, S100A7 has been shown to be induced by IL-1β, which is upstream of both NF-κB and MAP kinase signalling pathways[319]. As discussed for LCN2 and RNase 7, both NF-κB and MAP kinase signalling pathways may be activated by binding of estrogen to GPER. The promoter region of S100A7 showed multiple ERE half-sites, and two imperfect full EREs. Thus, potentiation of S100A7 expression by estrogen may occur through GPER or ER-α/β. ER-β regulation of S100A7 has been reported in breast cancer cells, and thus further work using site-directed mutagenesis may confirm this and reveal which of the ERE half-sites are important for S100A7 expression[320].

A diagram summarising potential pathways of estrogen regulation of LCN2, RNase 7, and S100A7 is shown in Figure 5.24.

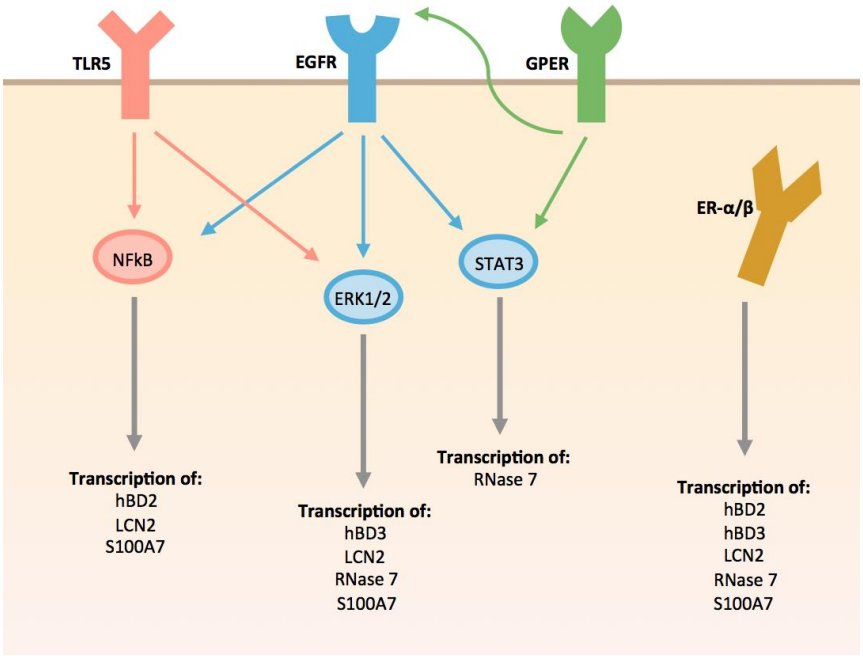

Figure 5.24: Regulatory pathways of hBD2, hBD3, LCN2, RNase 7, and S100A7. The figure shows potential pathways of hBD2, hBD3, LCN2, RNase 7, and S100A7 regulation by estrogen and flagellin.

Interestingly, the microarray data in Chapter 4 also identified potentiation of the proinflammatory cytokine IL-36G by estrogen pretreatment plus flagellin, compared to flagellin challenge alone. IL-36G has been reported to activate NF-κB and MAP kinase signalling in T cells and breast cancer cells[235,236]. This indicates that upregulation of IL-36G by estrogen may activate pathways involved in AMP gene transcription. In support of this, stimulating primary human keratinocytes with exogenous IL-36G has been shown to upregulate the expression of S100A7[321].

Further work to decipher the roles of the estrogen receptors in AMP expression should employ ER-α and –β inhibitors without agonist activity on GPER. Fulvestrant is the only combined ER-α and –β inhibitor, which is why it was used here, however, MPP dihydrochloride and PHTPP are selective antagonists for ER-α and –β, respectively, and could be used separately, or in combination, to inhibit ER-α and –β without agonism on GPER. Inhibition of GPER with the selective antagonist G-15, which has no affinity for ER-α or –β, may also elucidate the role of GPER in AMP expression.

To summarise, this chapter investigated the potential mechanisms by which estrogen regulates AMP expression. Although the results for some of the AMP genes were not clear-cut, data corresponding to mutagenesis of the ERE half-sites in the hBD2 promoter were strongly suggestive of a role for ER-α/β in hBD2 gene transcription, and this was a novel finding. Conversely, the presence of only a single ERE half-site in the hBD3 promoter and no imperfect full ERE sequence makes it unlikely that hBD3 is regulated by estrogen in the same manner as hBD2. Results relating to LCN2, RNase 7 and S100A7 were more ambiguous and require further experiments to clarify the regulation of these genes by estrogen. Nevertheless, the results for hBD2 and hBD3 indicate that multiple mechanisms for AMP expression by estrogen may exist, and that a broad range of cellular responses activated by estrogen, through GPER and ER-α/β, may be needed to mount an effective antimicrobial response to infection. This will be important to consider in the development of novel therapeutics for UTIs. In addition to this, the suggestion of GPER desensitisation in response to prolonged stimulation may have important repercussions on the use of long-term estrogen as a prophylactic treatment for UTIs, and should be explored further.

6 Role of IL-17 in antimicrobial peptide expression

6.1 Introduction

Analyses of the microarray data in Chapter 4 identified 'The Role of IL-17A in Psoriasis' as the canonical pathway most activated by estrogen pretreatment plus flagellin challenge (shown in Figure 6.1). This pathway consists of IL-17A binding to the IL-17 receptor complex (IL-17RA/RC) and activating transcription of the AMPs hBD2 and S100A7, as well as genes such as S100A8/A9, CCL20 and IL-8, which are associated with an inflammatory response. This was suggestive of a role for IL-17 in AMP transcription in the vaginal epithelium and warranted further investigation.

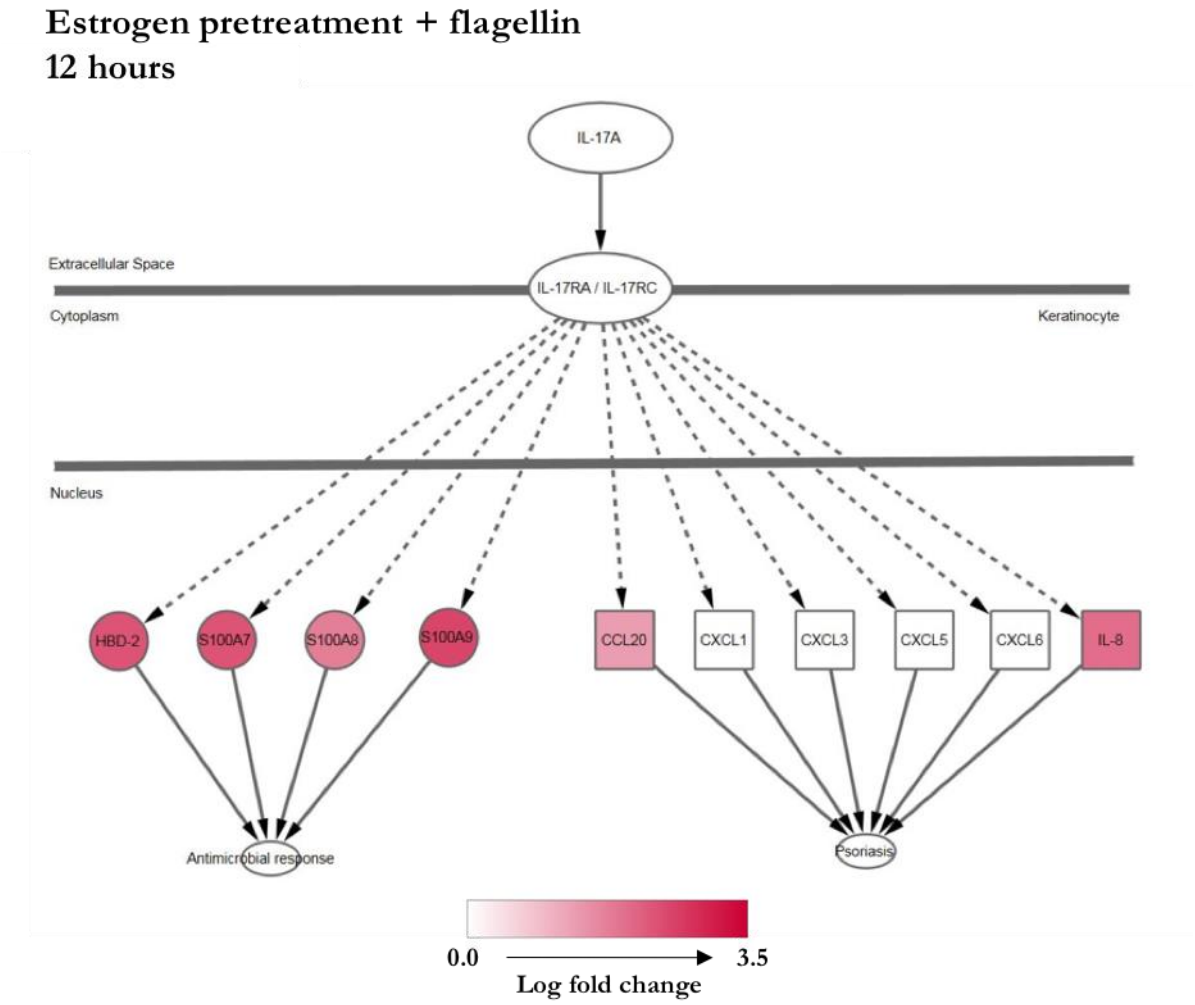

Figure 6.1: 'Role of IL-17A in Psoriasis' pathway. Shading of the molecules shows their upregulation following estrogen pretreatment plus flagellin after 12 hours, the darker red the more upregulation.

IL-17 was initially identified in 1993 and was found to function as a proinflammatory cytokine[322,323]. Its discovery also lead to the identification of a new subset of T helper cells, named

T helper 17 (Th17) cells, which are the main source of IL-17 secretion. IL-17 is also secreted from other cell types, such as γδT cells and mast cells[324,325]. T helper cells secrete a specific cytokine profile that ensures the host mounts an appropriate immune response for the invading pathogen. For example, Th1 cells produce IFN-γ and TNF-α, which aid in the clearance of intracellular pathogens[326]. Th2 cells produce cytokines such as IL-4 and -5, which drive the immune system towards an anti-parasitic response. Th17 cells are a distinct subset from Th1 and Th2 cells, and produce cytokines such as IL-17 and IL-22[327]. Th17 cells protect mucosal surfaces from invading pathogens and promote extracellular bacterial killing[328].

There are six members of the IL-17 family, IL-17A to IL-17F, with IL-17A and IL-17F being the most well characterised members. IL-17A and IL-17F are encoded on the same gene locus on chromosome 6; the other four IL-17 family members are encoded elsewhere in the genome, but share structural similarity[329]. IL-17A and IL-17F can form homodimers or heterodimers of the two subunits. IL-17A is a more potent inducer of cytokine secretion than IL-17F, and IL-17A/F heterodimers have intermediate activity[330]. IL-17B, IL-17C, and IL-17D are also considered to be proinflammatory cytokines, but they are not well understood. Emerging evidence suggests IL-17C can be expressed by epithelial cells, however microarray analysis in Chapter 4 did not identify IL-17C expression in VK2 cells[331,332]. IL-17E, also known as IL-25, shares the lowest homology with the rest of the family and is involved in Th2 cell responses to parasites and allergies[333].

To initiate cell signalling IL-17 binds to the IL-17 receptor, a cell membrane receptor ubiquitously expressed on many cells throughout the body[334–338]. The IL-17 receptor family consists of five members, IL-17RA to IL-17RE, the genes of which are mostly clustered on chromosome 3. IL-17RA and IL-17RC subunits form a receptor complex that binds IL-17A and IL-17F homodimers and heterodimers[339]. Binding of IL-17A/F to the IL-17RA/RC complex activates signalling through several pathways including NF-κB, MAPK and C/EPB, resulting in production of proinflammatory cytokines, chemokines, and other important immune response effectors such as antimicrobial peptides[327,340–342]. In addition to inducing expression of inflammatory genes, activation of MAPK by IL-17 also results in stabilisation of the mRNA of cytokines and chemokines, such as IL-6 and IL-8[343,344]. This increased stability prevents degradation of the mRNA before translation and thus results in greater production of these cytokines. Consequently, IL-17 has been identified as having an important role in host defence against pathogens.

Clinically, the importance of IL-17 signalling during an infection is demonstrated by patients with mutations in the IL-17F and IL-17RA genes[345]. These patients have recurrent infections of the skin, nails and oral and genital mucosa by *C. albicans* and *S. aureus*. This is supported by mouse models, which show that IL-17 signalling is crucial to protect against *C. albicans* and *S. aureus*, but also several other pathogens including *Helicobacter pylori* and *Neisseria gonorrhoeae*[346–349]. IL-17A has also been shown to be important for murine defence against uropathogenic *E. coli* during a UTI by stimulating a neutrophil migration response; mice lacking a neutrophil response were unable to clear *E. coli* from the bladder and kidney and suffered from a persistent infection[79]. Furthermore, neutrophil recruitment and bacterial clearance were attenuated in IL-17A null mice, indicating this as an important cytokine in bacterial clearance during a UTI[350].

The microarray data reported in Chapter 4 revealed upregulation of genes downstream of the 'Role of IL-17A in Psoriasis' pathway following estrogen pretreatment plus flagellin challenge, despite the cells not being exposed to IL-17A during this experiment. This suggested that, in addition to estrogen, IL-17A may also have a role in AMP expression. Thus, production of IL-17A by Th17 cells during an infection may affect the regulation of AMPs. It was, therefore, of interest to investigate the potential roles of IL-17A in vaginal AMP expression and consider the combined effects of estrogen and IL-17A on AMP expression during simulated infection. Such analyses were attempted to determine whether estrogen retains the ability to potentiate AMP expression in the presence of the proinflammatory cytokine IL-17A, or whether introduction of IL-17A to the VK2 cells negates the potentiation of AMP gene expression by estrogen.

6.2 IL-17 receptor expression in VK2 cells

To determine whether the VK2 cells were able to bind to IL-17A, end-point PCR was performed for the IL-17 receptor complex subunits IL-17RA and IL-17RC. These two members form a heterodimer on the cell surface, bind IL-17A and IL-17F homo/heterodimers, and initiate a signalling cascade[339,351]. PCR products of 132bp and 338bp, representing IL-17RA and IL-17 RC, respectively (Figure 6.2), were detected. The IL-17RA and IL-17RC PCR products were confirmed by sequencing and had 98% and 99% identity, respectively, to the BLAST database subject sequence. The VK2 cells were therefore expected to be responsive to IL-17A.

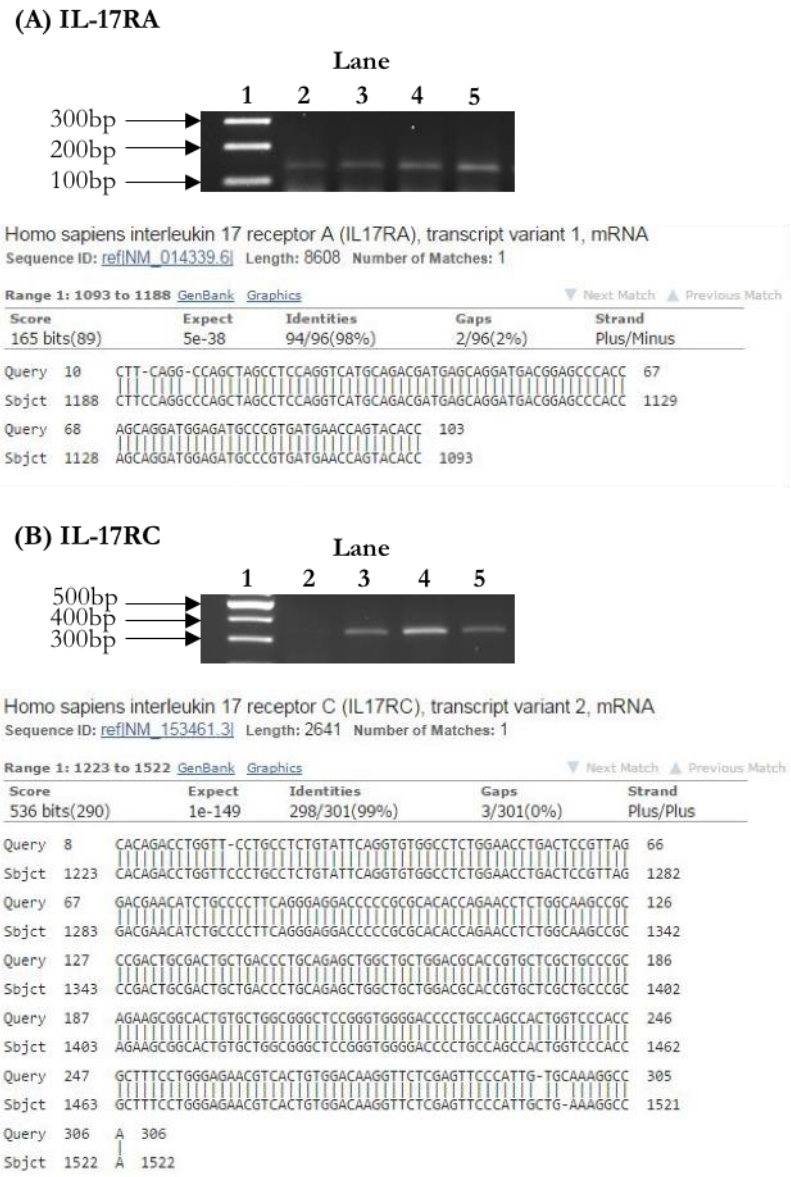

Figure 6.2: Expression of IL-17RA and IL-17RC in VK2 cells. End-point PCR performed on cDNA from VK2 cells shows (A) IL-17RA PCR products at 132bp and (B) IL-17RC PCR products at 338bp. In each gel a 100bp DNA Ladder (New England BioLabs, USA) is in lane 1, and PCR products are shown in lanes 2-5. The PCR products were confirmed by sequencing (Genevision, UK) and the nucleotide BLAST alignment is shown. The query sequence is the sequence of the PCR product as determined by sequencing and the subject (sbjct) sequence is the BLAST database sequence.

6.3 Effects of IL-17A concentrations on AMP expression

To determine the effects of IL-17A on AMP expression, VK2 cells were treated with recombinant IL-17A (Sigma, USA) at concentrations ranging from 0.1ng/ml to 100ng/ml for 24 hours. This broad range of concentrations was investigated, initially, to establish at what IL-17A concentration (if any) significant AMP induction was observed. Control cells were treated with vehicle only. After challenge the RNA was extracted, reverse transcribed into cDNA, and analysed by qPCR for the expression of hBD2, hBD3, LCN2, RNase7 and S100A7 (Figure 6.3).

The qPCR results were normalised to the two housekeeping genes GAPDH and ATP5B, and then to 100ng/ml IL-17A. These AMPs were identified by the microarray as being upregulated by estrogen pretreatment, and have been studied in previous chapters of this thesis. The 'Role of IL-17A in Psoriasis' pathway showed only hBD2 and S100A7 downstream of IL-17A, thus it was of interest to determine whether other AMPs were also regulated by IL-17A signalling.

AMP expression typically exhibited an IL-17A dose dependent response, with higher concentrations of IL-17A resulting in higher expression of AMPs (Figure 6.3). For hBD2, IL-17A at concentrations of 0.1ng/ml and 1ng/ml did not significantly increase expression compared to control (Figure 6.3A). However, 10ng/ml IL-17A significantly increased hBD2 expression to 49AU from 4.7AU in the control samples ($p<0.0001$). This was representative of a 10-fold increase in hBD2 expression compared to control. 100ng IL-17A further increased hBD2 expression to 100AU, a 21-fold increase relative to control ($p<0.001$). In contrast, hBD3 expression did not appear to be affected by exogenous IL-17A (Figure 6.3B), as none of the concentrations used resulted in a statistically significant increase in hBD3 expression.

IL-17A induced a dose dependent response in LCN2 expression; 1ng/ml, 10ng/ml and 100ng/ml IL-17A resulted in expression levels of 31AU, 78AU and 100AU, respectively. This was reflective of a significant 5.3-, 13- and 17-fold change in LCN2 expression, respectively, compared to the control ($p=0.0252$, $p<0.0001$ and $p<0.001$, respectively, Figure 6.3C). Interestingly, all of the concentrations of IL-17A administered to the VK2 cells resulted in a significant increase in RNase 7 expression, ranging from a 1.5-fold change with 0.1ng/ml IL-17A ($p=0.0108$) to a 1.9-fold change with 100ng/ml IL-17A ($p<0.0001$), compared to the control samples (Figure 6.3D). Conversely, S100A7 expression was only increased by 100ng/ml IL-17A, which resulted in a significant 2.0-fold upregulation of S100A7, compared to the control samples ($p<0.0001$).

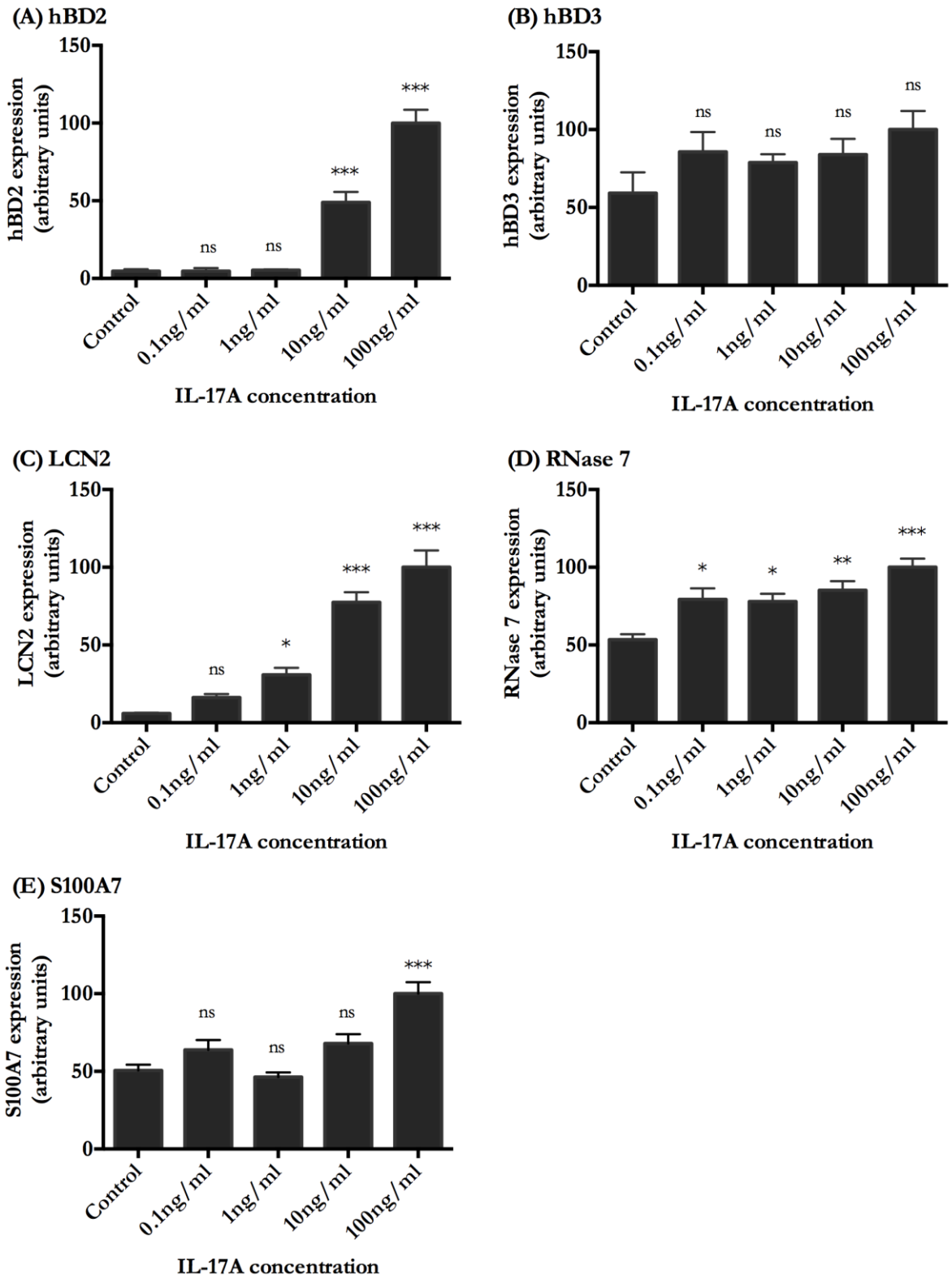

Figure 6.3: Effects of IL-17A concentrations on antimicrobial peptide gene expression. VK2 cells were challenged with 0.1-100ng/ml IL-17A or vehicle only for 24 hours. RNA was then extracted and analysed by qPCR for the expression of (A) hBD2, (B) hBD3, (C) LCN2, (D) RNase 7, and (E) S100A7. Results were normalised to 100ng/ml IL-17A challenge. Error bars represent standard error. Statistical analysis was performed by one-way ANOVA with Dunnett's post hoc test. ns=not significant, *=$p<0.05$, **=$p<0.01$, ***=$p<0.001$. N=2, n=6.

Thus, all of the AMPs, with the exception of hBD3, were responsive to IL-17A, typically showing a dose dependent upregulation of gene expression. The AMPs hBD2 and LCN2 showed the strongest gene expression induction in response to IL-17A. These data indicated that, in addition to estrogen, IL-17A is also an inducer of AMP expression and may be an important regulator during infection. Therefore, it was of interest to establish whether estrogen and IL-17A work synergistically to further increase AMP expression, or whether either treatment results in maximal expression that is not increased by further treatments. As 100ng/ml IL-17A induced significant upregulation of all the AMPs measured, except hBD3, this concentration of recombinant IL-17A was used for further experiments. Additionally, use of this concentration examined whether high concentrations of proinflammatory cytokines, such as IL-17A, negated the beneficial effects of estrogen on AMP expression, or whether estrogen potentiated AMP expression over and above that observed with 100ng/ml IL-17A.

6.4 Effects of estrogen pretreatment, IL-17A, and flagellin on AMP expression

To examine potential synergistic effects of IL-17A and estrogen on AMP expression during infection VK2 cells were pretreated with 4nM estrogen, or cyclodextrin vehicle, for seven days and then challenged with 100ng/ml IL-17A and/or 50ng/ml flagellin for 24 hours. The RNA was extracted and qPCR analysis was performed for the AMPs hBD2, hBD3, LCN2, RNase 7 and S100A7 to determine gene expression.

Following the challenge, hBD2 expression increased from 0.3AU in the control samples to 23AU with IL-17A alone, and 41AU with estrogen pretreatment plus IL-17A. This represented a 77-fold change with IL-17A without estrogen pretreatment and a 137-fold change with estrogen pretreatment plus IL-17A, compared to control, supporting increased gene expression following estrogen pretreatment (Figure 6.4A). A similar trend was seen with flagellin challenge, which increased hBD2 expression to 100AU (333-fold change compared to control) without estrogen pretreatment, and 159AU (531-fold change compared to control) with estrogen pretreatment prior to flagellin challenge. Statistical analyses of these data did not indicate this to be a significant difference, although this response was found to be significant in previous experiments in Chapters 3 and 5. Combined IL-17A and flagellin treatment without estrogen pretreatment resulted in a substantial 2307-fold change in gene expression, compared to the control samples. Nevertheless, estrogen pretreatment prior to combined IL-17A and flagellin challenge potentiated hBD2 expression and resulted in a 3712-fold increase in gene expression compared

to the control. This represented a significant 1.6-fold increase in hBD2 expression compared to IL-17A plus flagellin challenge without estrogen ($p=0.014$).

A similar trend was also seen for hBD3 (Figure 6.4B), whereby there was a clear trend towards increased expression with estrogen pretreatment compared to the same challenges without estrogen pretreatment. IL-17A challenge without estrogen pretreatment increased hBD3 expression to 51AU, from 30AU in the control. Estrogen pretreatment prior to IL-17A challenge further increased hBD3 expression to 85AU, representative of a 1.7-fold change compared to IL-17A challenge without estrogen. Flagellin challenge alone resulted in a 3.3-fold change in expression to 100AU, from 30AU in the control. This again increased to 154AU when estrogen pretreatment was given prior to flagellin challenge, representative of 5.1-fold change in hBD3 expression relative to control. This result supported the data shown in previous chapters. Combined IL-17A and flagellin challenge upregulated hBD3 expression to 238AU without estrogen pretreatment, representative of a 7.8-fold change compared to control samples. This increased to 331AU after estrogen pretreatment, IL-17A and flagellin, representative of an 11-fold change compared to control, and a significant 1.4-fold change compared to IL-17A plus flagellin without estrogen pretreatment ($p=0.014$).

The results also suggested an increase in LCN2 expression in response to estrogen pretreatment prior to IL-17A and/or flagellin challenge, although the difference was not statistically significant for any of the challenges (Figure 6.4C). Combined IL-17A and flagellin challenge without estrogen pretreatment induced LCN2 expression from 8.8AU in the control to 189AU, a 22-fold change in LCN2 expression. This further increased to 227AU with estrogen pretreatment, IL-17A and flagellin, representing a 26-fold change in LCN2 expression, compared to the control. Thus, the results for LCN2 were suggestive of potentiation of gene expression by estrogen pretreatment, although these results were not statistically significant.

Likewise, the results for RNase 7 suggested increased expression with estrogen pretreatment prior to each challenge compared to the same challenge without estrogen, but again these differences were not statistically significant (Figure 6.4D). IL-17A challenge without estrogen pretreatment resulted in RNase 7 expression of 67AU, compared to 35AU in the control samples, representative of a 1.9-fold change. Estrogen pretreatment plus IL-17A increased RNase 7 expression to 99AU, which represented a 2.9-fold change compared to control samples, and a 1.5-fold change compared to IL-17A without estrogen pretreatment. Flagellin challenge without estrogen pretreatment resulted in RNase 7 expression of 100AU, which rose to 136AU following

estrogen pretreatment plus flagellin, representative of 2.9 and 3.9-fold changes, respectively, when compared to the control. RNase 7 showed further induction to 183AU with combined IL-17A and flagellin challenge, which represented a 5.3-fold change in RNase 7 expression compared to the control. Estrogen pretreatment prior to IL-17A plus flagellin challenge resulted in the greatest induction of RNase 7 expression to 246AU, which represented a 7.1-fold change in gene expression compared to control samples and a 1.3-fold change compared to IL-17A plus flagellin without estrogen pretreatment.

Finally, induction of S100A7 expression by IL-17A was also augmented by estrogen pretreatment (Figure 6.4E). S100A7 expression was determined as 34AU for control samples. This increased to 62AU with IL-17A challenge without estrogen pretreatment and 80AU with estrogen pretreatment plus IL-17A challenge, representative of 1.8- and 2.4-fold changes in S100A7 expression compared to controls, respectively. Similarly, flagellin challenge induced S100A7 expression to 100AU, which increased to 150AU following estrogen pretreatment plus flagellin challenge, representative of a significant 1.5-fold change ($p=0.0126$). In addition, IL-17A plus flagellin challenge resulted in S100A7 expression of 166AU, representative of a 4.9-fold change compared to control samples. However, this increased by a significant 1.5-fold to 255AU following estrogen pretreatment, IL-17A and flagellin ($p<0.0001$).

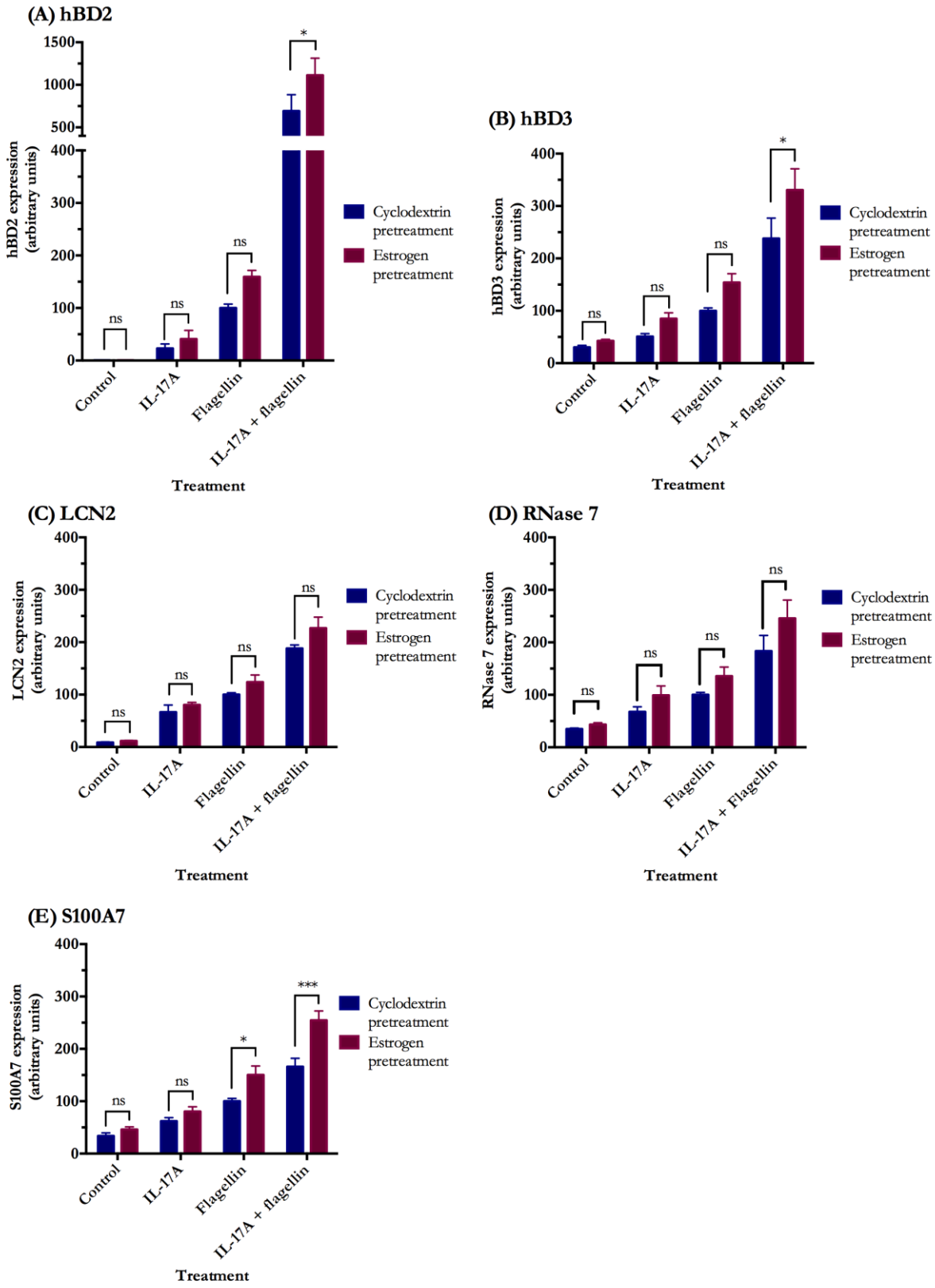

Figure 6.4: Effects of estrogen pretreatment, IL-17A, and flagellin on antimicrobial peptide expression. VK2 cells were pretreated with 4nM estrogen or 14.8nM cyclodextrin for 7 days and challenged with 100ng/ml IL-17A and/or 50ng/ml flagellin for 24 hours. The RNA was extracted and analysed by qPCR for the expression of (A) hBD2, (B) hBD3, (C) LCN2, (D) RNase 7, and (E) S100A7. Error bars represent standard error. Statistical analysis was performed by two-way ANOVA using Sidak's post hoc test. ns=not significant, *=$p<0.05$, ***=$p<0.001$. N=2, n=6.

Altogether, these results clearly indicated that there was a trend for increased AMP expression with estrogen pretreatment prior to challenging the cells with IL-17A and/or flagellin. Estrogen pretreatment, IL-17A and flagellin resulted in the greatest induction of gene expression for all of the AMPs measured. Thus, these data are indicative of a beneficial role for estrogen, by enhancement of AMP gene expression, even in the presence of proinflammatory cytokines such as IL-17A.

6.5 Effects of estrogen pretreatment, IL-17A and flagellin on AMP secretion

ELISAs were performed to examine the effect of estrogen pretreatment, IL-17A and flagellin on AMP peptide levels. As AMPs effectuate bacterial killing extracellularly, the AMP concentrations in the cell culture media were measured. Following pretreatment with estrogen for seven days, the VK2 cells were challenged with IL-17A and/or flagellin for 24 hours, the cell culture media was removed and stored at -80^{o}C prior to quantification of peptide concentration by ELISA. ELISAs were performed for hBD2, hBD3 and LCN2.

The ELISA results for hBD2 are shown in Figure 6.5. Combined data from two biological repeats of the experiment (with three technical replicates of each treatment within each repeat) showed the concentration of hBD2 in control samples was 235±71pg/ml. This increased to a mean peptide concentration of 713±101pg/ml for IL-17A and flagellin without estrogen pretreatment. Estrogen pretreatment prior to combined IL-17A and flagellin challenge resulted in a mean hBD2 concentration of 1433±310pg/ml, which represented a significant 2.0-fold increase in hBD2 peptide concentration compared to IL-17A and flagellin without estrogen pretreatment ($p=0.0048$, Figure 6.5A). However, variability was detected between the two repeats of the experiment (shown in Figure 6.5B and Figure 6.5C). The first repeat showed that IL-17A plus flagellin resulted in a mean hBD2 concentration of 885±47pg/ml, which increased significantly to 1950±174pg/ml with estrogen pretreatment, IL-17A and flagellin challenge ($p=0.0004$). Whereas, the second repeat resulted in mean hBD2 concentrations of 541±11pg/ml with IL-17A plus flagellin challenge and 915±104pg/ml after estrogen pretreatment, IL-17A and flagellin challenge. The increase in peptide concentration following the addition of estrogen in the second repeat was not statistically significant. Thus, the concentration of hBD2 after a given challenge varied between experimental repeats. Variability was also observed between in-plate replicates of the same sample; for example, the hBD2 concentration following IL-17A plus flagellin challenge was

determined as 721pg/ml and 955pg/ml for in-plate replicates of the same sample. As discussed in Chapter 3 this variability was also reflected in the standard curve and probably reflected reduced sensitivity of the ELISA.

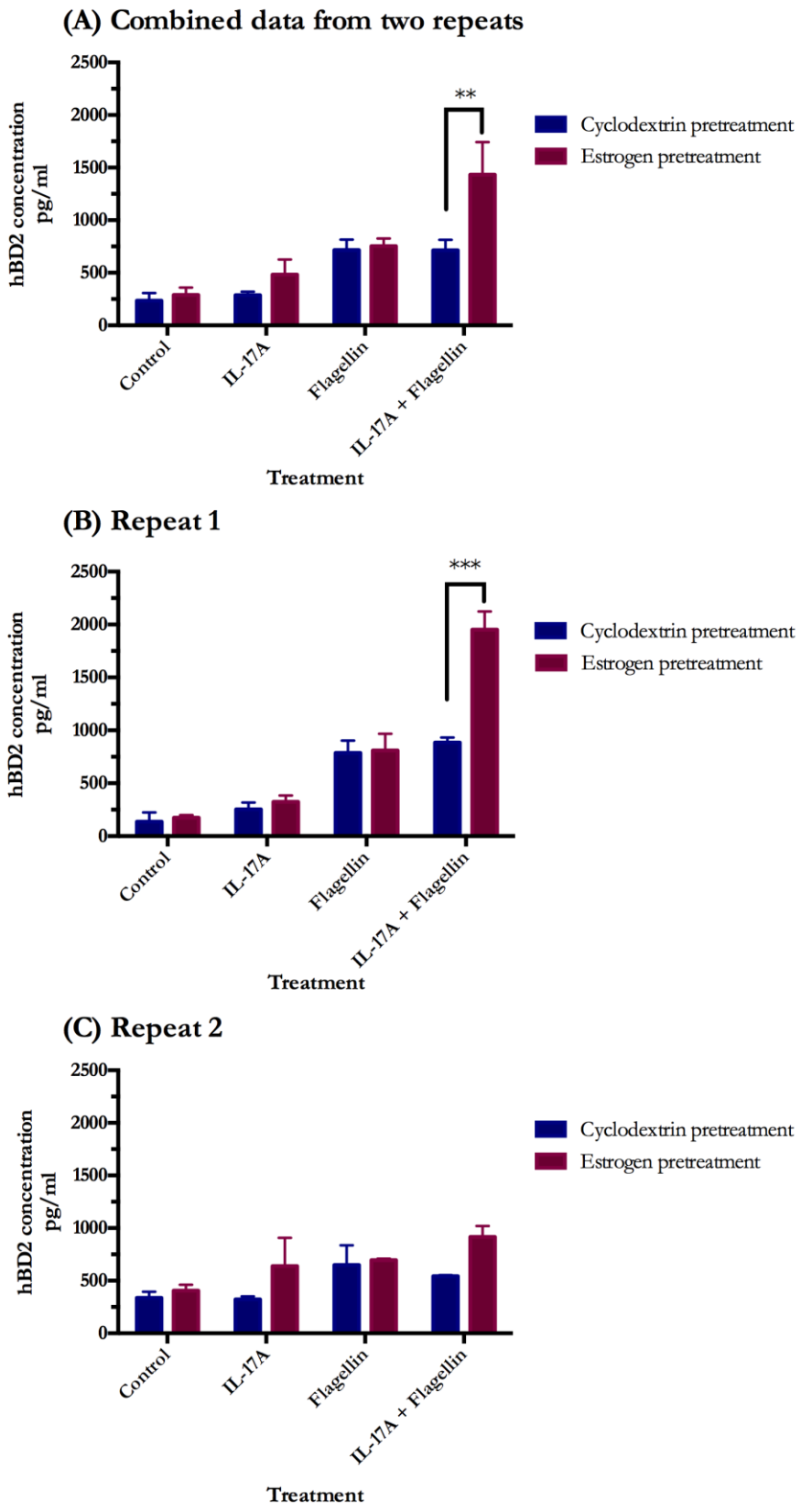

Figure 6.5: Effects of estrogen pretreatment, IL-17A, and flagellin on hBD2 secretion. VK2 cells were pretreated with 4nM estrogen or 14.8nM cyclodextrin for 7 days and then challenged with 100ng/ml IL-17A and/or 50ng/ml flagellin for 24 hours. The medium was removed from the cells and analysed by ELISA for hBD2 secretion**.** (A) shows combined results from two experiments, N=2, n=4. (B) and (C) show the results from each biological repeat of the experiment separately, N=1, n=2. Error bars represent standard error. Statistical analysis was performed by two-way ANOVA with Sidak's post hoc test. **=$p<0.01$, ***=$p<0.001$.

The data for hBD3 is shown in Figure 6.6. Similar to data reported in Chapter 3, the ELISA results did not show a significant change in hBD3 protein concentrations for any of the treatments. These data did not fit with mRNA data, which showed an 11-fold increase in hBD3 expression with estrogen pretreatment, IL-17A, plus flagellin after 24 hours, compared to control samples.

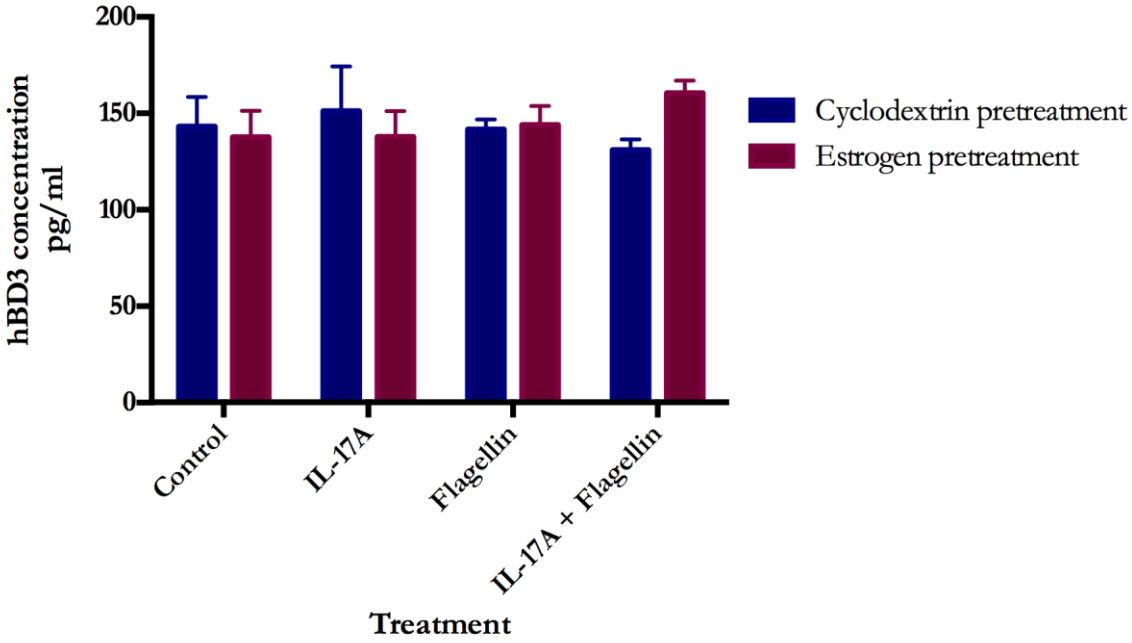

Figure 6.6: Effects of estrogen pretreatment, IL-17A, and flagellin on hBD3 secretion. VK2 cells were treated with 4nM estrogen or 14.8nM cyclodextrin for 7 days and then challenged with 100ng/ml IL-17A and/or 50ng/ml flagellin for 24 hours. The medium was removed from the cells and analysed by ELISA for hBD3 secretion. Error bars represent standard error. Statistical analysis was performed by two-way ANOVA with Sidak's post hoc test. N=1, n=3.

The ELISA results for LCN2 are shown in Figure 6.7. Combined data from two repeats of the experiment showed that IL-17A plus flagellin both with and without estrogen pretreatment significantly increased LCN2 protein secretion compared to control samples ($p=0.0048$ and $p=0.0166$, respectively). However, the addition of estrogen did not significantly increase the protein concentration compared to IL-17A plus flagellin challenge without estrogen (Figure 6.7A). Flagellin challenge did not significantly increase LCN2 protein concentration compared to control, and once again no significant differences in LCN2 protein concentrations were observed between flagellin challenge with and without estrogen pretreatment. IL-17A challenge with and without estrogen also did not significantly increase LCN2 concentrations compared to the control. Variability was detected in the LCN2 peptide concentration measured in the two repeats of the experiment. The first repeat showed a mean peptide concentration of 1217±184pg/ml in the control samples which increased to 8574±23pg/ml following estrogen pretreatment, IL-17A

and flagellin (Figure 6.7B). The second repeat exhibited a mean LCN2 concentration of 1538±163pg/ml in the control samples, which was comparable with the level measured in the first repeat (Figure 6.7C). However, following estrogen pretreatment, IL-17A and flagellin the peptide concentration in the second repeat was determined as 3692±432pg/ml, which was substantially lower than the 8574pg/ml measured for the first repeat following the same treatment. The trend of lower AMP secretion in the second repeat was also seen for hBD2, suggesting this difference may have reflected technical issues in the repetition of the experiment.

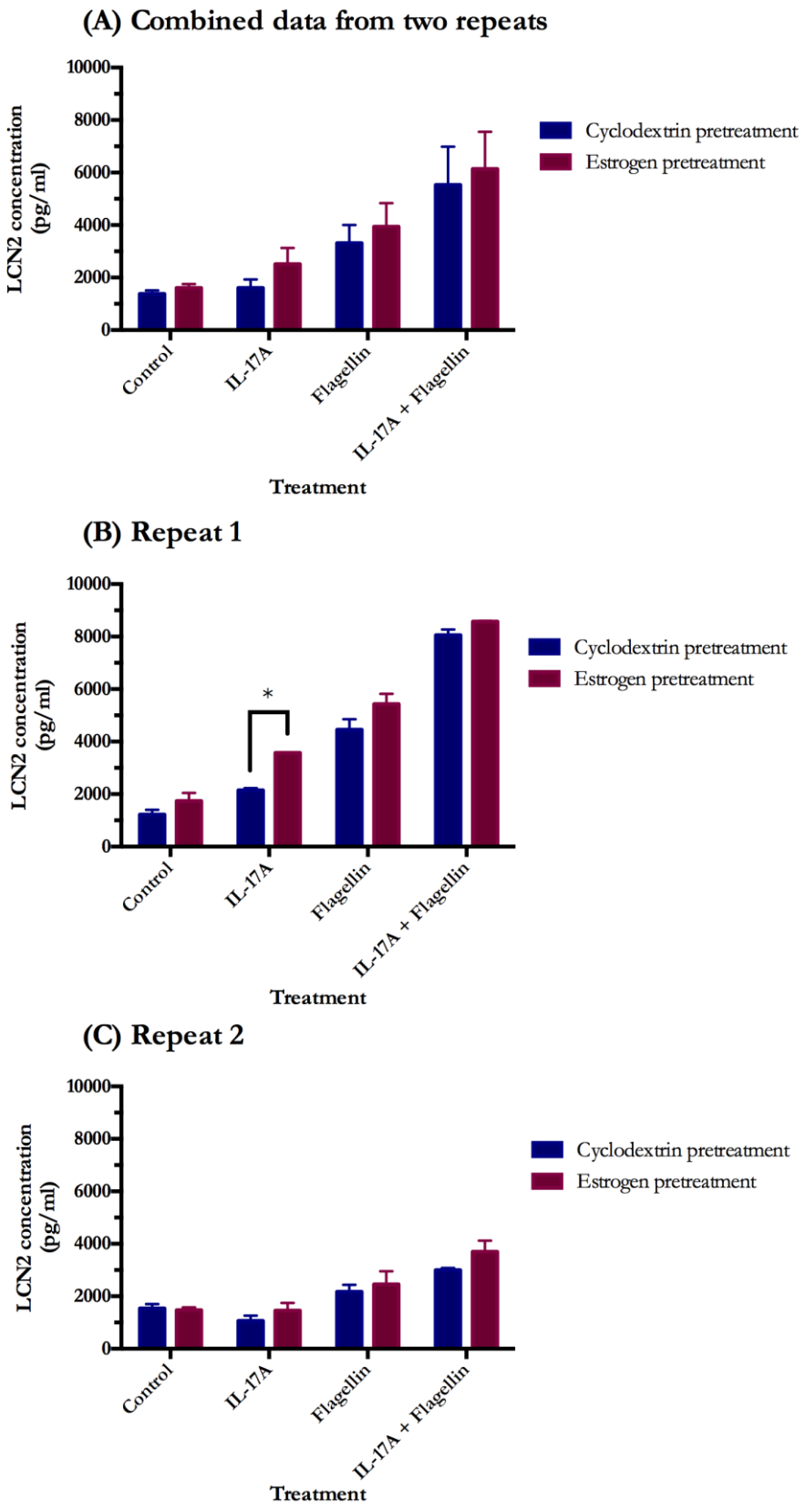

Figure 6.7: Effect of estrogen pretreatment, IL-17A, and flagellin on LCN2 secretion. VK2 cells were treated with 4nM estrogen or 14.8nM cyclodextrin for 7 days and then challenged with 100ng/ml IL-17A and/or 50ng/ml flagellin for 24 hours. The medium was removed from the cells and was analysed by ELISA for LCN2 secretion. (A) shows the combined results from two biological repeats, N=2, n=4. (B) and (C) show the results from each biological repeat separately, N=1, n=2. Error bars represent standard error. Statistical analysis was performed by two-way ANOVA with Sidak's post hoc test. *=$p<0.05$.

Unlike the hBD2 and hBD3 ELISAs, the LCN2 ELISA showed good agreement between in-plate replicates of the samples. This was reflected in the standard curve (Figure 6.8), which demonstrated that the LCN2 ELISA assay accurately detected the LCN2 concentration of the standards. This suggested that the assay was very sensitive and reliable.

The peptide data for hBD2, hBD3 and LCN2 is summarised in Table 6.1.

(A) LCN2 standard curve

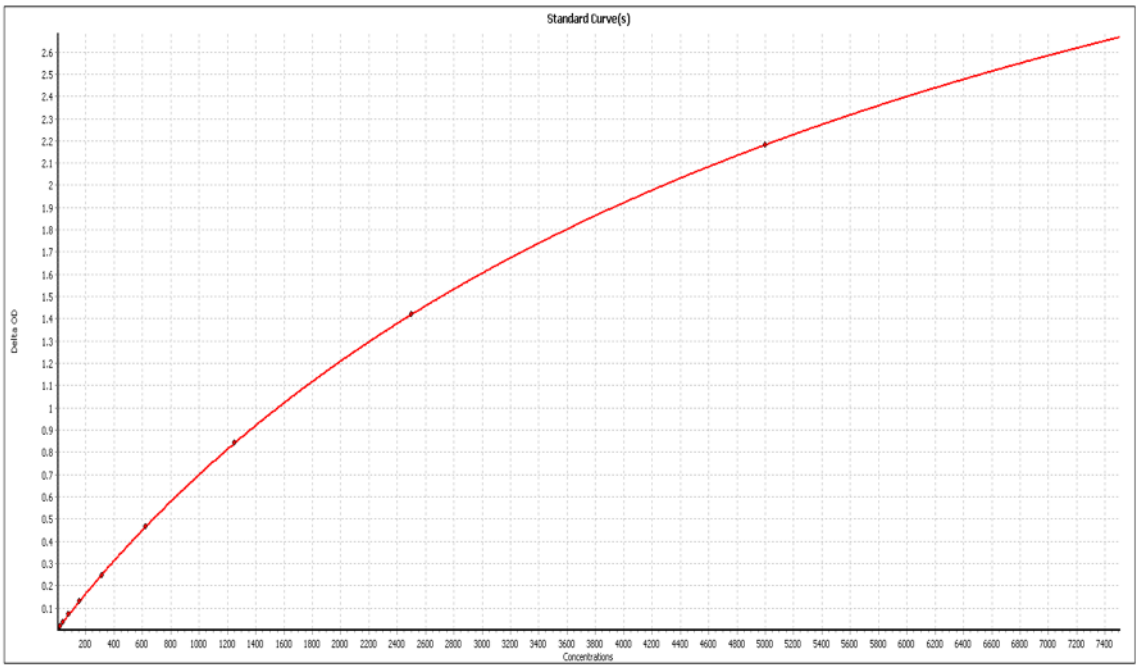

(B) LCN2 standard replicates

Standard curve concentration	Measured concentration (pg/ml)		
pg/ml	Replicate 1	Replicate 2	Average
5000	5132	4873	5003
2500	2424	2571	2498
1250	1259	1250	1255
625	617	629	623
313	314	305	310
156	161	154	158
78	81	82	82
39	39	39	39
20	17	18	18

Figure 6.8: LCN2 ELISA standard curve. A standard curve was included on each LCN2 ELISA plate and consisted of recombinant LCN2 serially diluted 1:2 from 5000pg/ml to 20pg/ml. (A) shows the standard curve line of best fit. (B) shows the measured concentration of each of the standard replicates.

Table 6.1: Summary of hBD2, hBD3 and LCN2 peptide data. The table shows the peptide concentration measured for each repeat of the experiment and the overall average and standard error of the mean (SEM).

		hBD2 (pg/ml)			hBD3 (pg/ml)		LCN2 (pg/ml)		
		Repeat 1 n=2	Repeat 2 n=2	**Average (SEM) n=4**	**Repeat 1 n=3**	**SEM**	Repeat 1 n=2	Repeat 2 n=2	**Average (SEM) n=4**
Control	- Estrogen	137	334	**235 (71)**	**143**	**15**	1217	1538	**1377 (137)**
	+ Estrogen	174	404	**289 (71)**	**138**	**14**	1734	1467	**1601 (155)**
IL-17A	- Estrogen	254	319	**286 (34)**	**151**	**23**	2150	1064	**1607 (326)**
	+ Estrogen	325	638	**481 (145)**	**138**	**14**	3568	1451	**2510 (623)**
Flagellin	- Estrogen	786	646	**716 (99)**	**142**	**5**	4455	2173	**3314 (687)**
	+ Estrogen	810	696	**753 (73)**	**144**	**10**	5428	2451	**3940 (898)**
IL-17A + Flagellin	- Estrogen	885	541	**713 (101)**	**131**	**6**	8058	2996	**5527 (1464)**
	+ Estrogen	1950	915	**1433 (310)**	**160**	**7**	8574	3692	**6133 (1420)**

6.6 Discussion

Analyses of microarray data in Chapter 4 revealed that IL-17A may be an important regulator of AMP expression in epithelial cells through interaction with the IL-17 receptor IL-17RA/RC. Examination of the activated canonical pathways showed that after estrogen pretreatment plus flagellin challenge the most activated pathway was the 'Role of IL-17A in Psoriasis' (Figure 6.1). This pathway involves IL-17A binding to the IL-17A receptor (IL-17RA/RC) and initiating transcription of antimicrobial genes (DEFB4A, S100A7, S100A8, S100A9) and inflammatory genes (CCL20, CXCL1, CXCL3, CXCL5, CXCL6, IL-8). IL-17A was not present in the VK2 cell challenge with estrogen pretreatment plus flagellin, as IL-17A is not produced by epithelial cells. Nevertheless, qPCR data showed that estrogen pretreatment plus flagellin challenge potentiated the expression of a number of these genes compared to flagellin challenge alone. Taken together, these qPCR and microarray data suggest that both estrogen and IL-17A have a role in AMP regulation. Thus, it is possible that production of IL-17A by Th17 cells during a UTI may alter AMP expression. It was, therefore, of interest to challenge the cells with IL-17A, with and without estrogen pretreatment and flagellin, to investigate the combined effect of these treatments on the expression of AMPs in the urogenital tract.

It is well established in the literature that IL-17A exerts its actions by binding to the IL-17 receptor, both subunits of which (IL-17RA and IL-17RC) are required for IL-17A signalling[351]. Thus, end-point PCR was used to confirm that VK2 cells do indeed express both the IL-17RA and RC subunits (Figure 6.2). Previous studies have used transgenic mice lacking the IL-17RA gene to study vaginal infections, however IL-17RA expression in the vagina was not explicitly shown as part of these studies[352,353]. Furthermore, tissue expression of IL-17RC was extensively analysed by Ge and You (2008) and was found to be expressed in numerous tissues throughout the body, including many epithelial cells[335]. However, vaginal expression was not investigated by

Ge and You, suggesting that the discovery of IL-17RA and IL-17RC expression in vaginal epithelial cells is novel.

The VK2 cells were challenged with a range IL-17A concentrations, from 0.01ng/ml to 100ng/ml, and qPCR was performed to determine the effect of increasing IL-17A concentrations on AMP expression. The literature is conflicting with regards to physiological IL-17A concentrations, with reported serum values for healthy patients varying 1000-fold, ranging from 4.4pg/ml to 2.88ng/ml[283,354,355]. The average urine IL-17A concentration in patients with greater than $5x10^5$ CFU *E. coli* (the number of *E. coli* required to clinically diagnose a UTI) was 5.05pg/ml (Lauren Drage, PhD thesis in preparation). However, as this was IL-17A measured in the urine the concentration is likely to be much more dilute than that which is present at the surface of the bladder epithelium. It can be argued therefore, that dilution of IL-17A would not occur to the same extent in the vaginal fluids as there is a much smaller volume of liquid in the vaginal lumen than the volume of urine in the bladder, thus the concentration of IL-17A in the vaginal lumen during infection may be higher than that of the bladder. However, to quantify vaginal IL-17A concentrations a vaginal douche or brush sample would be needed, and both of these methods result in sample dilution in the collection fluid. Indeed, measurement of IL-17 concentration in cervicovaginal lavages of women with chlamydia reported an average concentration of approximately 3pg/ml, however, the samples were diluted in 10mls of sterile saline solution, once again making the concentration at the epithelial surface difficult to determine[356]. This result, however, suggests that vaginal concentrations of IL-17A are greater than 3pg/ml during infection. Furthermore, to accurately determine IL-17A concentrations in response to UPEC colonisation the sample would have to be taken during an infection, or alternatively an *in vivo* model, using mice for example, would need to be employed. Thus, in the future it would be of interest to determine the concentration of IL-17A in the vaginal epithelium of both healthy patients and patients during an active UTI. Other researchers have employed IL-17A concentrations ranging from 20-200ng/ml to study the effects of IL-17A on epithelial cells and thus, for the dose response experiments VK2 cells were initially treated with 0.1ng-100ng/ml IL-17A for 24 hours to observe the effect on AMP expression[317,327,357]. The trend seen with each AMP was that expression was IL-17A dose dependent, with 100ng/ml IL-17A resulting in the highest level of gene expression for each AMP (Figure 6.3). hBD3 was the only AMP which was not significantly upregulated by IL-17A, however, a recent paper by Burgey *et al.* (2016), showed that IL-17 did not induce hBD3 expression in immortalised human keratinocytes and nasal epithelial cells, but was able to induce hBD3 expression in primary human nasal epithelial cells[358]. Thus, it will be important to repeat this work using primary vaginal epithelial cells.

To investigate whether IL-17A and estrogen work synergistically on AMP expression, VK2 cells were pretreated with estrogen for seven days and then challenged with IL-17A and/or flagellin. This modelled IL-17 production in the vagina during an infection, with and without estrogen, to determine which conditions best promote AMP expression. An IL-17A concentration of 100ng/ml was selected as this was the most potent inducer of AMP expression. Thus, without knowing the true epithelial concentration of IL-17A, initial investigations examined whether estrogen pretreatment potentiated AMP expression above that seen with 100ng/ml IL-17A, or whether high concentrations of the proinflammatory cytokine IL-17A negated the beneficial effects of estrogen pretreatment on AMP expression. The results showed that the expression of hBD2, hBD3 and S100A7 was significantly increased when IL-17A and flagellin were given following estrogen pretreatment, compared to the same treatment without estrogen (Figure 6.4). hBD2 expression exhibited the most dramatic induction, with a 2307-fold change in gene expression following IL-17A plus flagellin treatment, increasing to a 3711-fold change after the same challenge with estrogen pretreatment. S100A7 and hBD3 displayed more modest fold changes of 4.9 and 7.9, respectively, following IL-17A plus flagellin challenge. The expression of S100A7 and hBD3 increased to 7.5- and 11-fold change, respectively, following estrogen pretreatment, IL-17A plus flagellin challenge. The same trend was also seen for LCN2 and RNase 7, with increased expression following estrogen pretreatment, IL-17A plus flagellin challenge compared to IL-17A plus flagellin challenge, however, these data were not statistically significant. These data are important as they indicate that even following proinflammatory cytokine production during an infection, which substantially increases AMP expression, the presence of estrogen results in further upregulation of gene expression. Thus, if estrogen potentiates AMP gene expression at high concentrations of IL-17A, it can be speculated that even if the physiological concentration of IL-17A is lower than 100ng/ml, estrogen is important for AMP gene expression. Hence, it can be argued that the production of proinflammatory cytokines, such as IL-17A, during an infection in postmenopausal women does not result in the same level of AMP expression as that in premenopausal women.

Peptide quantification by ELISA was also performed for hBD2, hBD3 and LCN2 (Figure 6.5, Figure 6.6, and Figure 6.7). The results for the hBD2 ELISA showed a significant increase in hBD2 concentration in the cell culture media following estrogen pretreatment with IL-17A plus flagellin, compared to IL-17A plus flagellin without estrogen pretreatment. However, there was variability in the results seen with each repeat experiment. As discussed previously, the hBD2 ELISA standard curve also suggested that the commercial assay is not particularly sensitive,

despite the kit stating the lower limits of detection as 8pg/ml and thus, these data should be interpreted with caution. Further work is needed to firmly establish the effect of these treatments on hBD2 secretion. In agreement with data shown in Chapter 3, the hBD3 ELISA showed no significant increase in hBD3 protein secretion with any of the treatments. This does not fit with the mRNA data which showed an approximate 11-fold increase in gene expression following estrogen pretreatment, IL-17A and flagellin challenge. It is possible that the 24 hour time point was too early to detect changes in hBD3 peptide levels. In Chapter 3 hBD2 and hBD3 expression was measured at 8, 12 and 24 hours after challenge with estrogen pretreatment and/or flagellin and increases in hBD3 expression were delayed in comparison to hBD2; flagellin treatment resulted in increases in hBD2 expression by the 8 hour time point, but hBD3 expression did not increase with flagellin challenge until the 24 hour time point. Thus, it is feasible that changes in hBD3 peptide levels may not be observed until later collection time points. The LCN2 ELISA showed that IL-17A plus flagellin significantly increased LCN2 protein levels, both with and without estrogen, compared to control. However, no difference in protein concentration was seen between the estrogen positive and estrogen negative samples. The standard curve demonstrated that the LCN2 ELISA was extremely sensitive and thus provided reliable data. Previous work in our laboratory has measured LCN2 peptide concentrations in vaginal douches from postmenopausal women. These data revealed that women receiving topical estrogen treatment had a significantly higher mean vaginal LCN2 concentration (62±11ng/ml) than postmenopausal women who did not receive topical estrogen treatment (24±4ng/ml). Thus, the ELISA data presented here were not reflective of the mRNA data, or of *in vivo* data obtained by our laboratory, which suggest that estrogen does indeed increase AMP secretion from vaginal epithelial cells. Further experiments including additional time points are required to investigate this discrepancy further, and to fully establish the role of estrogen in AMP secretion in the VK2 cell model.

Overall, the data in this chapter indicated that IL-17A is an important regulator of AMP expression, and that estrogen pretreatment prior to IL-17A plus flagellin challenge upregulated expression of all AMPs measured. *In vivo* it is predicted that IL-17A would be produced by Th17 cells recruited to the site of infection by CCL20, which binds to the CCR6 receptor on Th17 cells and stimulates migration[277,278,359]. Microarray data showed that the cytokine CCL20 was expressed following flagellin and estrogen pretreatment plus flagellin challenges (Figure 6.1), indicating that vaginal UPEC colonisation results in a CCL20 concentration gradient towards which Th17 cells could migrate. Moreover, downstream effects analysis of the microarray data revealed many functions relating to immune cell migration, such as "Cell movement of leukocytes", were

upregulated by flagellin and estrogen pretreatment plus flagellin challenges, further supporting the notion that infection of the urogenital tract would result in Th17 cell migration. This premise is also supported by the literature, which reports that IL-17 has been detected in vaginal fluid from mice infected with *C. albicans*[353]. Furthermore, treatment with halofuginone, which inhibits Th17 cell differentiation, lowered vaginal IL-17 production in mice infected with *C. albicans,* demonstrating that the source of vaginal IL-17 is Th17 cells[349]. Masson *et al.* (2015) also showed that IL-17 was increased in cervicovaginal lavages of women with bacterial sexually transmitted diseases, such as chlamydia, compared to healthy controls[356]. Thus, taken together, these results support the hypothesis that Th17 cell migration and IL-17 production occurs in the vagina following infection.

IL-17 production by Th17 cells at the site of infection is important for bacterial clearance and has been shown to have multiple antimicrobial roles. Firstly, as demonstrated here and by others, IL-17 increases AMP expression[317,327,357]. Secondly, Th17 cells recruit neutrophils to the site of infection through CXCL8, a process that has been shown to be vital to the clearance of a UTI. Mice lacking the IL-17A gene were shown to have significantly fewer neutrophils in their urine following transurethral infection with *E. coli* than WT mice[350,360]. Furthermore, mice with a neutrophil migration deficiency that were infected transurethrally with *E. coli* were unable to clear the infection and the bacteria persisted longer in the urinary tract than in neutrophil migration competent mice[79]. Thus, migration of neutrophils to the urogenital tract during a UTI is crucial for bacterial clearance and is linked to IL-17A production. In addition, estrogen pretreatment plus flagellin resulted in greater expression of S100A8 and S100A9 than flagellin challenge alone, according to the microarray data. These proteins have been reported to be important chemotactic factors for neutrophil migration[240]. Upregulation of these genes by estrogen is suggestive of a role for estrogen in increasing neutrophil migration to the site of infection, and thus, enhancing bacterial clearance. Finally, IL-17A null mice have also been shown to have significantly reduced IL-4 expression in the bladder, in response to UPEC stimulation, than wild type mice[350]. As IL-4 has a role in B cell activation, this suggests IL-17 may also be an important link between innate and adaptive immunity[361]. Therefore, despite the name, activation of the 'Role of IL-17A in Psoriasis' pathway, highlighted by microarray analysis, is likely to be important for antimicrobial responses in other tissues and conditions besides psoriasis, for example in protection against UTIs.

The role of IL-17A in UTIs is a relatively novel area, and the initial findings are encouraging. However, further work is clearly needed to expand upon this hypothesis and further elucidate the

interplay between estrogen and IL-17 in protection against UTIs. Further work should involve measurement of IL-17A in the vagina during a UTI. This would not only show that Th17 cells are recruited to the vagina during a UTI and secrete IL-17 in the area, but would also determine the concentration of IL-17 in the vagina during UPEC colonisation. It would also be of great interest to investigate whether there is an effect of estrogen on Th17 cell migration and IL-17 production in the vagina in response to colonisation, to determine whether estrogen also acts to promote IL-17 mediated responses. Such work could not be achieved within the timeframe of this thesis and would either require the use of human vaginal tissue from women with an infection at time of collection or mouse models. The interplay between estrogen and Th17 cells has been studied somewhat in the context of rheumatoid arthritis (RA). Th17 cell migration to the synovial fluid of joints has been shown to exacerbate RA, and IL-17 has been identified as a key molecule in driving inflammation and the destruction of joints in RA[360,362,363]. Similarly to UTIs, RA worsens following the menopause, which brought about the idea of hormonal regulation of RA and the hypothesis that the reduction in estrogen after the menopause promotes increased Th17 cell migration to joints, driving inflammation. This suggests that estrogen and IL-17 have an inverse correlation. However, evaluation of the literature in this area shows that estrogen actually increases the expression of CCL20 (the chemokine responsible for Th17 cell migration), but that this increase occurs within lymph nodes and thus prevents migration of Th17 cells to the site of inflammation[364]. Loss of estrogen following the menopause, therefore, results in reduced CCL20 expression in the lymph node and consequently, Th17 cell migration to the joints. Murine models of arthritis employ systemic estrogen treatment of ovariectomised mice to simulate the premenopausal state, whereas topical estrogen treatment would be employed for treatment of UTIs after the menopause. Therefore, it would be of interest to investigate whether localised application of estrogen increases Th17 cell migration to the site of topical treatment, or whether estrogen interferes with Th17 cell migration as shown for systemic estrogen in RA. Indeed, the microarray data showed that estrogen pretreatment plus flagellin upregulated CCL20 expression in VK2 cells, suggesting that topical estrogen treatment may stimulate Th17 cell migration to the vagina during UPEC colonisation. Furthermore, a recent paper published in 2016 reported that estrogen treated mice showed a higher proportion of IL-17$^+$ T cells in the vagina following herpes simplex virus infection than infected mice given placebo treatment, despite the estrogen treatment being systemic[365]. Altogether these data suggest that estrogen treatment not only increases the antimicrobial response to UTIs by potentiating AMP expression, but may also promote Th17 cell migration to the vagina during colonisation with UPEC, which in turn increases vaginal IL-17A production and AMP expression.

To summarise, this chapter has presented preliminary findings on the role of IL-17A in AMP expression from vaginal epithelial cells and demonstrated synergistic effects between IL-17A and estrogen on AMP expression. A model is proposed whereby upon infection of the vagina with *E. coli* from the bowel, AMP expression is induced resulting in bacterial killing (Figure 6.9A). The addition of estrogen treatment to the vagina primes the epithelium so that during infection AMP expression is increased, and therefore augments bacterial killing (Figure 6.9C). This prevents bacterial migration to the urethra where it may ascend to the bladder causing cystitis. Furthermore, infection stimulates CCL20 expression from epithelial cells which recruits Th17 cells to the site of infection, resulting in production of IL-17A in the vagina which further increases AMP expression (Figure 6.9B). Th17 cells also act to recruit neutrophils through the cytokine CXCL8, which aid in bacterial killing, thus expediting bacterial clearance. Estrogen treatment of vaginal cells further potentiates the AMP expression induced by IL-17 and flagellin, thus further increasing bacterial killing (Figure 6.9D). This theoretical model therefore demonstrates how estrogen pretreatment and IL-17 production during infection may both contribute to effective clearance of *E. coli* from the vaginal reservoir, and hence prevent progression to UTI.

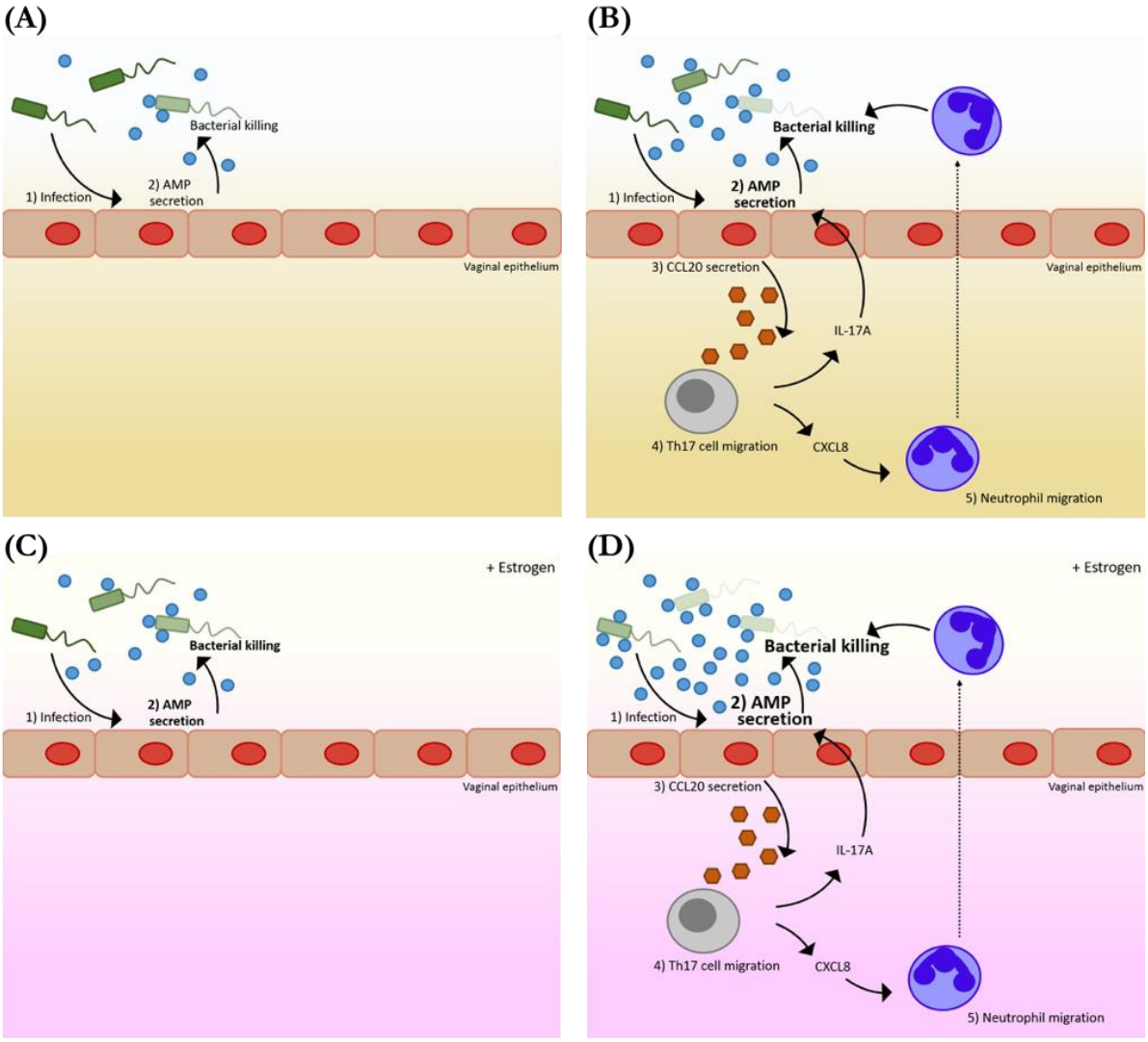

Figure 6.9: Model showing the role of estrogen and IL-17A in bacterial clearance from the vagina. (A) infection with *E. coli* stimulate antimicrobial peptide (AMP) production from vaginal epithelial cells causing bacterial killing. (B) Infection also induces CCL20 secretion from vaginal epithelial cells which causes Th17 cell migration. Th17 cells produce IL-17A, which upregulates AMP expression, and CXCL8, which causes neutrophil migration to the site of infection. Increased AMP expression and neutrophil migration increase bacterial killing. (C) The addition of estrogen to the vaginal epithelium increases AMP expression upon infection with *E. coli*, increasing bacterial killing. (D) AMP expression induced by IL-17A is increased further still by the addition of estrogen to the vaginal epithelium, increasing bacterial killing and clearance from the vagina.

7 Final discussion

Work presented in this thesis has shown that estrogen acts to upregulate AMP expression in the urogenital tract in response to UPEC colonisation. Data obtained by qPCR and microarray experiments indicated that pretreatment of vaginal epithelial cells with a physiological concentration of estrogen for seven days prior to flagellin challenge significantly upregulated several AMPs including hBD2, hBD3, LCN2 and S100A7. AMPs are a vital component of the innate immune defence to UTI, so upregulation of multiple AMPs by estrogen indicates a role for estrogen in enhancing the epithelial defence against infection.

In addition to enhancing the antimicrobial defences of vaginal epithelial cells, the microarray data also indicated that estrogen upregulated genes involved in keratinisation and inflammation. Thus, estrogen may induce multiple responses in vaginal epithelial cells that help protect against UTIs. Genes involved in keratinisation, such as keratins, small proline rich protein (SPRR) genes and late cornified envelope (LCE) genes, were upregulated by estrogen pretreatment. Increased keratinisation protects against infection by strengthening the physical barrier against microbial invasion. Topical estrogen treatment of the male foreskin has been reported to improve keratinisation of the foreskin epithelia and protect against HIV infection[233]. Thus, enhancement of the vaginal epithelial barrier may be an important mechanism by which estrogen protects against UTIs. Furthermore, work by Tam *et al.* (2012) showed that keratin fragments in the cornea have antimicrobial properties[234]. Thus, upregulation of genes involved in keratinisation by estrogen may not only improve the physical barrier to infection, but may also improve the innate antimicrobial barrier to vaginal UPEC colonisation.

Inflammatory genes such as IL-36G, SERPINB4 and S100A8/9 were also highlighted by the microarray as being upregulated by estrogen pretreatment. IL-36G and S100A8/9 have roles in recruiting immune cells, such as Th17 cells and neutrophils, to the site of infection. Neutrophils are vital to the clearance of UPEC from the urogenital tract; mouse models of UTI with mice deficient in neutrophil migration show prolonged bacterial persistence in the bladder than mice that were neutrophil migration competent[79]. Th17 cells secrete the proinflammatory cytokine IL-17A, which was shown in this thesis to have an important role in upregulation of AMP expression. Furthermore, IL-17A has also been demonstrated to be important for neutrophil migration to the bladder during UPEC infection[350,360]. Thus, upregulation of IL-36G, S100A8 and S100A9 by estrogen pretreatment may indicate a role for estrogen in enhancing migration of important immune cells to the vagina during UPEC colonisation and promoting bacterial

clearance from the vaginal reservoir.

Taken together, data from this thesis and the literature indicate that estrogen has several potential mechanisms by which it confers protection against UPEC invasion. Firstly, estrogen promotes the growth of lactobacilli in the vagina, which lower the vaginal pH through production of lactic acid and inhibit the growth of uropathogens. Secondly, estrogen increases the keratinisation of the vaginal epithelium to prevent bacterial invasion. Thirdly, estrogen potentiates AMP expression to facilitate rapid bacterial killing and clearance from the urogenital tract. Finally, estrogen may also improve immune cell migration to the site of infection, further aiding in bacterial clearance. These diverse actions of estrogen likely all contribute to effective protection against UTIs in premenopausal women.

7.1 Moving forward: informing the development of alternative treatments

The *in vitro* findings of this thesis are supported by clinical trials that have shown that topical vaginal estrogen treatment reduces the incidence of UTIs in postmenopausal women[190,194]. However, although the data relating to estrogen as a treatment for UTIs in postmenopausal women appears promising, there are safety concerns about the use of hormonal treatments. Postmenopausal women may be prescribed hormone replacement therapy (HRT) to alleviate symptoms of the menopause, however, studies have shown that estrogen HRT increases the risk of endometrial cancer. To combat this, estrogen and progestin are given together to reduce the risk of endometrial cancer, but nevertheless, estrogen-progestin HRT is still associated with an increased risk of breast cancer and cardiovascular events, such as coronary heart disease and stroke[366,367]. A recent study by Jones *et al.* (2016) found that postmenopausal women receiving estrogen-progestin HRT were 2.74 times more likely to develop breast cancer than postmenopausal women with no previous use of HRT[368]. In terms of UTIs, clinical trials have shown that topical vaginal estrogen treatment is more effective in reducing the incidence of UTIs than systemic estrogen treatment[190,194]. However, localised vaginal estrogen treatment still results in raised serum estrogen concentrations, which increases the risk of breast cancer[284,285]. In fact, vaginal estrogen treatment is contraindicated for women who have previously had breast cancer. Thus, a non-hormonal alternative therapeutic with a similar mechanism of action to estrogen would be beneficial to postmenopausal women with rUTIs.

The data presented in this thesis sheds light on the mechanism of action of estrogen and can be used to inform the development of novel therapeutics for UTIs. For example, the data in this

thesis has revealed that estrogen upregulates the expression of AMPs that are vital to bacterial clearance from the urogenital tract. Thus, the effect of new UTI therapeutics on AMP expression should be considered during development, as this is an important factor of vaginal defence against UTIs. Development of therapeutics that upregulate the vaginal AMP expression may provide an effective alternative to antibiotics, as well as hormonal treatments. Alternative UTI treatments to estrogen will now be discussed with regards to their mechanism of action and how the new information about the mechanism of action of estrogen from this thesis may inform their development.

7.1.1 Natural agents from diet

7.1.1.1 Phytoestrogens

The most obvious alternatives to estrogen are phytoestrogens, which are plant-derived xeno-estrogens with estrogenic properties. Resveratrol and genistein are two common phytoestrogens found in the diet. Resveratrol is found in foods such as grapes, red wine and peanuts, whereas genistein is mainly found in soy. In 2011, Lee *et al.* showed that 25μM resveratrol treatment for 2 hours followed by exposure to LPS and heat stress increased hBD2 expression in primary human dental pulp cells, compared to cells exposed to LPS and heat stress without resveratrol treatment[369]. This finding was supported by work by Lin *et al.* (2014); these authors demonstrated that resveratrol increased hBD2 expression in response to *Streptococcus pneumoniae* infection of an alveolar epithelial cell line[370]. Thus, these data suggest that the phytoestrogen resveratrol induces hBD2 expression during infection. However, previous data from our laboratory showed that resveratrol plus flagellin challenge significantly reduced hBD2 expression in VK2 cells, compared to flagellin challenge alone[106]. Thus, the effects of resveratrol on AMP expression require further research. Resveratrol has also been reported to have anti-cancer properties and thus, unlike estrogen treatment, would not pose a cancer risk[371]. However, resveratrol confers its anti-cancer properties through inhibition of cell proliferation and promotion of apoptosis. Accordingly, resveratrol has been reported to induce cell cycle arrest in keratinocytes and thus, may exacerbate vaginal atrophy in postmenopausal women[372]. As keratinisation is thought to be protective against infection, thinning of the vaginal epithelial by resveratrol may increase susceptibility to UTIs. Indeed, topical application of resveratrol to the skin is not advised due to its anti-proliferative effects on keratinocytes[372]. Nevertheless, Docherty *et al.* (2005) showed that topical vaginal application of resveratrol protected mice from herpes simplex virus infection[373]. However, Docherty *et al.* did not study the effects of resveratrol on the vaginal epithelium. Previous work from our laboratory revealed cytotoxic effects of resveratrol on an immortalised bladder epithelial

cell line[106]. Taken together these data suggest that resveratrol may be protective against vaginal infections, however, further research is needed to fully determine the effects of resveratrol on AMP expression and the vaginal epithelial barrier. The efficacy of resveratrol in specifically protecting against UTIs has not been studied and thus this is a potential area for both *in vitro* and *in vivo* studies.

The phytoestrogen genistein has been investigated as a potential alternative to HRT in postmenopausal women. Consumption of genistein as part of the diet has been shown to increase the thickness of the vaginal epithelium in rats[374]. However, unlike estrogen, genistein did not increase the keratinisation of the vaginal epithelium. Research into the effects of genistein on AMP expression is limited; however, in 2006 Ouhara *et al.* demonstrated that induction of hBD2 expression by *Actinobacillus actinomycetemcomitans* in human gingival epithelial cells was inhibited by genistein[375]. Thus, although genistein shows some estrogenic properties, it does not fully replicate the protective effects of estrogen and is unlikely to be a suitable candidate for a therapeutic for UTIs.

7.1.1.2 Vitamin D

As discussed in the introduction to this thesis, an initial study examining patients with type 2 diabetes mellitus found that supplementation with vitamin D reduced the incidence of UTIs compared to patients receiving placebo treatment[160]. However, a clinical trial examining the efficacy of vitamin D in pre- and postmenopausal women who suffer from rUTIs has not been conducted. Interestingly, a correlation has been reported between serum vitamin D levels and hBD2 expression *in vivo*[376]. Furthermore, an *in vitro* study using a human primary keratinocytes showed induction of hBD2 by vitamin D[377]. Several studies have also shown upregulation of the AMP LL-37 by vitamin D in epithelial and keratinocyte cell lines[378–380]. LL-37 was not identified by the microarray analysis as being upregulated by estrogen and as LL-37 has been shown to be important in bacterial clearance during a UTI, these data suggest vitamin D may enhance expression of additional AMPs that estrogen does not[268]. Conversely, Hegyi *et al.* (2012) reported that vitamin D suppressed expression of S100A7; however, this research was conducted in psoriatic skin lesions and thus different results may be observed in the context of infection[381]. Nonetheless, the effects of vitamin D on AMP expression in the vagina in response to infection is an interesting area for future research. In addition to upregulating AMP expression, vitamin D has been reported to reduce vaginal pH and prevent vaginal atrophy[382,383]. Unpublished findings by our research group have also shown that vitamin D significantly reduced bacterial invasion of

vaginal epithelial cells, compared to untreated controls. These findings indicate that vitamin D may work in a similar manner to estrogen. Furthermore, adverse reactions are rarely reported in vitamin D supplementation, indicating that vitamin D is potentially a safe alternative to antibiotic and hormonal treatment of UTIs. Future work to investigate the potential for vitamin D to protect against UTIs should investigate the effects of vitamin D on AMP expression in vaginal epithelial cells both *in vitro* and *in vivo*. Furthermore, a clinical trial examining the effects of vitamin D on UTI incidence in pre- and postmenopausal women would further elucidate the clinical effectiveness of vitamin D.

7.1.1.3 Other natural agents from the diet

Other naturally occurring dietary compounds, such as cranberry extracts and vitamin C have also been proposed to reduce the incidence of UTIs. However, the protective nature of cranberry juice against UTIs has not been definitively shown[156]. Cranberry extracts are thought to prevent bacterial adhesion to epithelial cells, preventing penetration of the epithelial barrier[384,385]. To the best of my knowledge, the effects of cranberry extracts on vaginal pH, AMP expression, and keratinisation has not been studied. Similarly, vitamin C has been shown to acidify the urine and inhibit bacterial replication, however, the effects of vitamin C on vaginal acidity, AMP expression or keratinisation has not been investigated. Thus, further investigations into the effects of cranberry products and vitamin C on vaginal lactobacilli growth, AMP expression, and keratinisation will determine whether these may provide an alternative treatment option to estrogen. The effect of these compounds, and the previously mentioned vitamin D, on vaginal AMP production could initially be determined *in vitro* using the VK2 cell model established in this thesis. This would provide direct comparison of AMP induction following treatment with these agents to the AMP induction observed with estrogen pretreatment.

7.1.2 Hyaluronic acid

Hyaluronic acid is a promising therapeutic candidate for UTI treatment. Hyaluronic acid is currently marketed as a vaginal moisturiser for treatment of vaginal atrophy in postmenopausal women. A clinical trial comparing the efficacy of vaginal hyaluronic acid gel to estrogen cream for treating vaginal dryness found that although hyaluronic acid improved the symptoms of vaginal atrophy it did not reduce vaginal pH, whereas the estrogen cream did[386]. However, several trials have shown that hyaluronic acid treatment significantly reduced UTI incidence. Constantinides *et al.* (2004) demonstrated that premenopausal women with a history of rUTI had significantly fewer UTIs following bladder instillation of hyaluronic acid than before treatment[387].

In the pretreatment phase (15.8 months) the 40 patients suffered 208 UTIs, however, post-treatment (12.4 months) only 12 of these patients had 16 UTIs. This represented significantly fewer UTIs following treatment with hyaluronic acid than before treatment. Lipovac *et al.* (2007) conducted a similar study of UTI incidence in premenopausal women before and after bladder instillation with hyaluronic acid and also found that hyaluronic acid instillation significantly reduced UTI incidence[388]. A clinical trial comparing bladder instillation of hyaluronic acid plus chondroitin sulfate to placebo was conducted in premenopausal women in 2011[389]. In the 12 month follow-up period after instillation the 29 women in the placebo group had 122 UTIs, whilst the 28 patients in the hyaluronic acid plus chondroitin sulfate group had only 17. Although these trials report promising effects with hyaluronic acid, none of the trials investigated the mechanism of action of hyaluronic acid. *In vitro* investigations by our laboratory group have shown that hyaluronic acid increased expression of hBD2, hBD3 and LCN2 in VK2 cells (Catherine Mowbray, unpublished data). In addition, these data showed that hyaluronic acid significantly reduced bacterial invasion of VK2 cells and formed a protective barrier, which reduced the leakage of mannitol through tight junctions between bladder epithelial cells. Thus, similarly to estrogen, hyaluronic acid may protect against UTIs by increasing innate immune defences and augmenting the epithelial barrier to UPEC invasion. Furthermore, our data suggests that hyaluronic acid is protective in the vagina, thus, vaginal application of hyaluronic acid should be explored as a UTI treatment as this may provide a more convenient alternative to bladder instillation. Thus, a clinical trial into the efficacy of topical vaginal hyaluronic acid treatment in protecting postmenopausal women from rUTI is warranted as hyaluronic acid is a promising alternative non-hormonal treatment for UTIs.

7.1.3 Exogenous AMPs

There is considerable effort within the AMP field to develop therapeutic synthetic AMPs. However, despite *in vitro* screening of hundreds of thousands of synthetic peptides, only a handful have ever made it to clinical trials. Notably, Pexiganan, developed as a treatment for diabetic foot ulcers, made it to phase 3 clinical trials, but was denied approval by the Food and Drug Administration (FDA) and development was halted. Pexiganan has now been renamed Locilex (Dipexium Pharmaceuticals) and has reentered phase 3 clinical trials[390]. However, the FDA is yet to approve a synthetic AMP for therapeutic use of any infection. Thus, the development of synthetic AMPs for clinical use is still in its infancy. Furthermore, development of potential targets is difficult as although many synthetic AMPs show activity *in vitro*, they only show activity *in vivo* at very high doses. These high doses are close to the toxic range of the

synthetic AMPs, and thus are often deemed unsafe. No synthetic AMPs are currently being developed specifically for treatment of UTIs. However, research into synthetic chimeric peptides of hBD1/hBD3 and hBD2/hBD3 have shown high *in vitro* antimicrobial activity against *E. coli* and low toxicity to erythrocytes and epithelial cells[216,391]. Thus, these synthetic peptides show promise for development for clinical use. However, clinical use of synthetic antimicrobial peptides should be approached with caution, as there is concern that therapeutic use of synthetic AMPs will induce the evolution of bacterial resistance in the same manner as bacterial antibiotic resistance emerged following clinical use of antibiotics[392]. Indeed, Perron *et al.* (2006) were able to experimentally induce Pexiganan resistance in *E. coli* through long-term exposure of the bacteria to the AMP[393]. Thus, enhancement of the host's natural AMP response may be a more responsible long-term treatment option.

In summary, there are a few promising therapeutic candidates (summarised in Table 7.1) that may have a similar mechanism of action to estrogen and that are safe to use. In particular, the results for vitamin D and hyaluronic acid are exciting as these agents have both demonstrated AMP induction and improved barrier function in epithelial cells. Nevertheless, further analysis of other less well studied agents, such as vitamin C, may also return promising results. In addition, these treatments may be used in combination to achieve maximal protection against UTIs. For example, combined vitamin C and D therapy may acidify the urine to prevent bacterial growth, whilst simultaneously enhancing the physical and antimicrobial barrier to infection in the vagina. Importantly, the molecular analyses performed in this thesis have identified mechanisms by which estrogen protects against UTIs. As topical estrogen treatment has been shown to significantly reduce the incidence of UTIs in postmenopausal women, the knowledge of how estrogen brings about this protection can be used to inform the identification and development of non-hormonal alternatives.

Table 7.1: Summary of protective mechanisms of potential UTI therapeutics.

	Reduces vaginal pH	Increases AMP expression	Increases epithelial barrier	Safe to use
Estrogen	✓	✓	✓	
Resveratrol		?		
Genistein			✓	
Vitamin D	✓	✓	✓	✓
Vitamin C				✓
Cranberry products				✓
Hyaluronic acid		✓	✓	✓

7.2 Future work

The future work stemming from this project should cover two main areas. Firstly, continuing from the work presented in this thesis, further work should be conducted to further inform the mechanism of estrogen action. Secondly, experiments should be performed to begin to investigate the effects of estrogen alternatives on innate vaginal epithelial defences.

With regards to further investigating the mechanism of estrogen action, several areas may be explored. To continue to investigate the roles of the estrogen receptors in AMP gene expression, ER-α and –β inhibitors that do not have agonistic effects on GPER could be employed. It is thought that the use of fulvestrant in Chapter 5 inhibited ER-α and ER-β and simultaneously caused GPER desensitisation, making it difficult to attribute the observed effects on AMP expression to a specific estrogen receptor. MPP dihydrocholride and PHTPP are selective antagonists for ER-α and ER-β, respectively, with no effect on GPER. Thus, the use of these separately, or in combination, should rule out the effects of potential GPER desensitisation on AMP expression. Such data may clearly indicate the role of the estrogen receptors in the expression of each of the AMPs.

One limitation of this project was the difficulty in obtaining accurate protein secretion data for the AMPs. The hBD2 ELISA did not accurately detect peptide concentrations for the standards or for the VK2 cell samples. This area should be investigated further, and ELISAs optimised, in order to quantify AMP secretion in the VK2 cell model. Optimisation of the hBD2 protocol by increasing the concentration of detection antibody, for example, may improve results. The hBD3 ELISA did not detect any increases in peptide concentration for any treatments. However, the increase in hBD3 mRNA following flagellin challenge was more delayed than the hBD2 response, thus, measurement of hBD3 peptide levels at later time points should be considered for future experiments.

A further limitation of the project was the measurement of AMP expression in PVECs. Culturing the PVECs proved difficult and although initial results were promising, changing the culture medium to DMEM with FCS to facilitate better PVEC growth appeared to abolish the effects of estrogen pretreatment on AMP expression. This may be due to the presence of phenol red in the DMEM and other estrogenic compounds in the FCS negating the effects of the 4nM estrogen supplementation. Thus, it would be beneficial to optimise the growth of the PVECs in medium that does not contain phenol red and FCS to more accurately study the effects of estrogen supplementation on AMP expression in vaginal epithelial cells.

The work presented in this thesis highlighted a role for estrogen in the keratinisation and inflammatory response of the vaginal epithelium, which was not further studied as part of this project. These provide exciting areas for further research into the effects of estrogen on the innate epithelial immune response to UPEC colonisation. The keratinisation response is particularly intriguing as in addition to strengthening the epithelial barrier to infection, Tam *et al.* (2012) have shown that keratin-derived fragments in the cornea have antimicrobial properties[234]. Thus, it would be of interest to determine whether increased keratinisation of the vaginal epithelium in response to estrogen pretreatment leads to production of keratin-derived AMPs (KDAMPs). To identify KDAMPs in the cornea, Tam *et al.* lysed corneal epithelial cells and fractionated the lysate by molecular mass. The fractions were tested for antimicrobial activity and mass spectrometry was utilised to identify potential KDAMPs. This process could, therefore, be used to investigate the production of KDAMPs in the vaginal epithelium in response to estrogen pretreatment. The microarray data also indicated that estrogen may increase the inflammatory response to infection; genes such as S100A8 and S100A9 were upregulated by estrogen pretreatment and have been reported to have roles in neutrophil migration to the site of infection. Furthermore, IPA analysis indicated that 'The Role of IL-17A in Psoriasis' pathway was activated by estrogen pretreatment plus flagellin. Utilising qPCR it was demonstrated that exogenous IL-17A upregulated the expression of AMPs, and that combined estrogen pretreatment, IL-17A and flagellin resulted in high AMP expression. Thus, it would be of interest to examine the effects of topical estrogen treatment on immune cell migration to the vagina during infection. Mouse models would be needed to study this effectively. Utilising such models, immune cell migration to the vagina following UPEC colonisation could be studied with and without topical estrogen treatment to determine whether estrogen acts to enhance migration of neutrophils and Th17 cells.

Alongside these analyses, future work may also involve utilising the VK2 cell model to investigate the effects of novel therapeutics on vaginal AMP expression, keratinisation and inflammatory mediators. Our laboratory has used the VK2 cells to investigate the effects of hyaluronic acid and found that, similarly to estrogen, treatment of VK2 cells with hyaluronic acid improved AMP expression and barrier function. This suggests that hyaluronic acid is a promising candidate for treatment of UTIs. *In vitro* data for hyaluronic acid obtained using VK2 cell studies will be used to support an application for a clinical trial investigating the efficacy of hyaluronic acid in reducing UTI incidence in postmenopausal women. In addition to hyaluronic acid, the effects of vitamin D, vitamin C, and resveratrol could be investigated and compared with estrogen. The effects of

combined treatments could also be explored. Improved understanding of the mechanism of AMP regulation by estrogen may also result in the identification of other therapeutic candidates that could also be tested using VK2 cells.

7.3 Summary

In summary, the data presented in this thesis have highlighted a key role for estrogen in the innate epithelial defences of the urogenital tract. Previous investigations demonstrated that estrogen stimulates glycogen production in the vagina, promoting lactobacilli colonisation and lactic acid production, which results in a lower vaginal pH. However, the data within this thesis has shown that estrogen has additional roles in enhancing the vaginal innate immune response to UPEC colonisation by potentiating expression of AMPs, including hBD2, hBD3, LCN2 and S100A7. Furthermore, estrogen pretreatment was also shown to upregulate genes involved in keratinisation, inflammation and immune cell migration. Together these data suggest that estrogen protects the urogenital tract from infection in multiple ways. Firstly, stimulation of vaginal glycogen production by estrogen promotes growth of commensal bacteria, making the vagina inhospitable for uropathogens. Secondly, estrogen strengthens the physical epithelial barrier to infection to prevent pathogen invasion and finally, estrogen enhances the antimicrobial response to infection by promoting AMP production and potential immune cell migration to facilitate rapid bacterial killing and clearance from the vagina, and hence preventing progression to bladder infection. Therefore, loss of circulating estrogen following the menopause results in the loss of these protective mechanisms and results in uropathogen growth in the vaginal reservoir, facilitating infection of the urethra and bladder. Hence, these data provide scientific evidence that reveal how loss of estrogen after the menopause increases a women's susceptibility to rUTIs and help inform future therapeutic strategies.

8 Appendix

Table 8.1: List of differentially expressed genes after 12 hours challenge.

			Fold change		
Probe	**Gene symbol**	**Gene name**	**EP12**	**F12**	**EP/F12**
ILMN_1791759	CXCL10	chemokine (C-X-C motif) ligand 10		41.73	16.00
ILMN_1795359	SPRR2A	small proline-rich protein 2A	2.06	3.95	14.75
ILMN_1662358	MX1	myxovirus (influenza virus) resistance 1, interferon-inducible protein p78 (mouse)		16.02	14.34
ILMN_2231928	MX2	myxovirus (influenza virus) resistance 2 (mouse)		24.78	14.09
ILMN_2058782	IFI27	interferon, alpha-inducible protein 27		16.48	13.76
ILMN_2211018	SPRR2E	small proline-rich protein 2E		3.14	13.53
ILMN_1674367	SPRR2F	small proline-rich protein 2F	2.20	3.60	13.08
ILMN_1723912	IFI44L	interferon-induced protein 44-like		15.81	11.51
ILMN_1701239	SPRR2E	small proline-rich protein 2E		2.46	10.84
ILMN_1805410	C15orf48	chromosome 15 open reading frame 48		14.52	10.46
ILMN_2410826	OAS1	2'-5'-oligoadenylate synthetase 1, 40/46kDa		17.19	10.41
ILMN_1674063	OAS2	2'-5'-oligoadenylate synthetase 2, 69/71kDa		14.99	10.38
ILMN_1692223	LCN2	lipocalin 2	2.18	6.38	9.47
ILMN_2347798	IFI6	interferon, alpha-inducible protein 6		14.36	9.43
ILMN_1675640	OAS1	2'-5'-oligoadenylate synthetase 1, 40/46kDa		16.92	9.09
ILMN_1788874	SERPINA3	serpin peptidase inhibitor, clade A (alpha-1 antiproteinase, antitrypsin), member 3		8.67	8.92
ILMN_1735712	KRT1	keratin 1			8.82
ILMN_1801246	IFITM1	interferon induced transmembrane protein 1		14.01	8.44
ILMN_1658247	OAS1	2'-5'-oligoadenylate synthetase 1, 40/46kDa		12.66	8.16
ILMN_1691364	STAT1	signal transducer and activator of transcription 1, 91kDa		10.53	7.90
ILMN_1690105	STAT1	signal transducer and activator of transcription 1, 91kDa		11.48	7.67
ILMN_1702127	SPRR2G	small proline-rich protein 2G			7.27
ILMN_1782716	SERPINB4	serpin peptidase inhibitor, clade B (ovalbumin), member 4		2.92	6.48
ILMN_1787509	HELZ2	helicase with zinc finger 2, transcriptional coactivator		10.48	6.45
ILMN_2415144	SP110	SP110 nuclear body protein		8.78	6.02
ILMN_2336781	SOD2	superoxide dismutase 2, mitochondrial		8.06	6.01
ILMN_1803838	CNFN	cornifelin	2.04		5.90
ILMN_1750974	S100A9	S100 calcium binding protein A9	2.13	2.53	5.86
ILMN_2197577	SPRR2C	small proline-rich protein 2C (pseudogene)			5.77
ILMN_1718395	LCE3D	late cornified envelope 3D	2.11		5.76
ILMN_2191967	SPRR2D	small proline-rich protein 2D		2.09	5.73
ILMN_1731418	SP110	SP110 nuclear body protein		7.79	5.68
ILMN_1777325	STAT1	signal transducer and activator of transcription 1, 91kDa		7.24	5.65
ILMN_2239754	IFIT3	interferon-induced protein with tetratricopeptide repeats 3		13.46	5.63
ILMN_1779252	TRIM22	tripartite motif containing 22		8.78	5.61
ILMN_1798181	IRF7	interferon regulatory factor 7		7.41	5.47
ILMN_1731224	PARP9	poly (ADP-ribose) polymerase family, member 9		7.91	5.12
ILMN_2048043	DEFB4A	defensin, beta 4A		2.35	5.11
ILMN_1757351	S100A7	S100 calcium binding protein A7			5.07
ILMN_2170814	LAMP3	lysosomal-associated membrane protein 3		7.48	5.03
ILMN_1745374	IFI35	interferon-induced protein 35		6.85	4.98
ILMN_1745397	OAS3	2'-5'-oligoadenylate synthetase 3, 100kDa		5.85	4.92
ILMN_2406501	SOD2	superoxide dismutase 2, mitochondrial		7.63	4.83
ILMN_1701789	IFIT3	interferon-induced protein with tetratricopeptide repeats 3		12.51	4.82
ILMN_2388547	EPSTI1	epithelial stromal interaction 1 (breast)		6.16	4.61
ILMN_2098126	CCL5	chemokine (C-C motif) ligand 5		9.60	4.56
ILMN_1796316	MMP9	matrix metallopeptidase 9 (gelatinase B, 92kDa gelatinase, 92kDa type IV collagenase)		3.72	4.50
ILMN_2349061	IRF7	interferon regulatory factor 7		6.23	4.44
ILMN_1712759	SBSN	suprabasin	2.06		4.44
ILMN_2158713	IL36G	interleukin 36, gamma		2.70	4.34
ILMN_1745242	PLSCR1	phospholipid scramblase 1		5.28	4.26
ILMN_1774287	CFB	complement factor B		7.62	4.21
ILMN_2148785	GBP1	guanylate binding protein 1, interferon-inducible		8.84	4.15
ILMN_1657871	RSAD2	radical S-adenosyl methionine domain containing 2		8.71	4.08
ILMN_2109708	TYMP	thymidine phosphorylase		5.26	4.00
ILMN_2184373	IL8	interleukin 8		3.59	3.99
ILMN_2376205	LTB	lymphotoxin beta (TNF superfamily, member 3)		10.91	3.88
ILMN_1794662	DSG1	desmoglein 1			3.70
ILMN_1703855	SERPINB3	serpin peptidase inhibitor, clade B (ovalbumin), member 3			3.68
ILMN_1801216	S100P	S100 calcium binding protein P			3.66
ILMN_1742618	XAF1	XIAP associated factor 1		6.19	3.66
ILMN_1723035	OLR1	oxidized low density lipoprotein (lectin-like) receptor 1		7.67	3.58
ILMN_1672661	SP110	SP110 nuclear body protein		5.17	3.54
ILMN_1691731	PARP14	poly (ADP-ribose) polymerase family, member 14		5.69	3.51
ILMN_1751079	TAP1	transporter 1, ATP-binding cassette, sub-family B (MDR/TAP)		5.37	3.48
ILMN_1770922	TMEM45A	transmembrane protein 45A			3.46
ILMN_2054019	ISG15	ISG15 ubiquitin-like modifier		4.89	3.40
ILMN_1729801	S100A8	S100 calcium binding protein A8	2.03	2.24	3.39
ILMN_1730284	DSC1	desmocollin 1			3.34
ILMN_2085862	SLC15A3	solute carrier family 15 (oligopeptide transporter), member 3		5.56	3.34
ILMN_1690921	STAT2	signal transducer and activator of transcription 2, 113kDa		4.81	3.31
ILMN_2402640	DSC1	desmocollin 1			3.28
ILMN_2148913	TMEM45A	transmembrane protein 45A			3.26
ILMN_1736729	OAS2	2'-5'-oligoadenylate synthetase 2, 69/71kDa		4.67	3.24
ILMN_1814305	SAMD9	sterile alpha motif domain containing 9		4.16	3.22
ILMN_1713397	NCCRP1	non-specific cytotoxic cell receptor protein 1 homolog (zebrafish)			3.20
ILMN_1781373	IFIH1	interferon induced with helicase C domain 1		5.09	3.20
ILMN_3240420	USP18	ubiquitin specific peptidase 18		5.43	3.17
ILMN_2079042	WFDC5	WAP four-disulfide core domain 5			3.17

			Fold change		
Probe	Gene symbol	Gene name	EP12	F12	EP/F12
ILMN_1704972	TRIM5	tripartite motif containing 5		5.72	3.16
ILMN_2114720	SLPI	secretory leukocyte peptidase inhibitor	2.16		3.16
ILMN_1773352	CCL5	chemokine (C-C motif) ligand 5		6.30	3.12
ILMN_1760062	IFI44	interferon-induced protein 44		4.03	3.08
ILMN_1778401	HLA-B	major histocompatibility complex, class I, B		4.16	3.04
ILMN_2053527	PARP9	poly (ADP-ribose) polymerase family, member 9		4.72	3.04
ILMN_1743950	IGFL1	IGF-like family member 1		2.29	3.01
ILMN_1707695	IFIT1	interferon-induced protein with tetratricopeptide repeats 1		5.47	2.98
ILMN_1693192	PI3	peptidase inhibitor 3, skin-derived		2.05	2.96
ILMN_1754576	KRT6C	keratin 6C			2.95
ILMN_1718558	PARP12	poly (ADP-ribose) polymerase family, member 12		3.91	2.93
ILMN_1752548	KRTDAP	keratinocyte differentiation-associated protein			2.92
ILMN_1708303	CYP4F22	cytochrome P450, family 4, subfamily F, polypeptide 22			2.89
ILMN_1745471	IRF9	interferon regulatory factor 9		3.21	2.89
ILMN_3223126	TYMP	thymidine phosphorylase		3.97	2.86
ILMN_1769520	UBE2L6	ubiquitin-conjugating enzyme E2L 6		3.80	2.86
ILMN_1654639	HERC6	HECT and RLD domain containing E3 ubiquitin protein ligase family member 6		3.13	2.77
ILMN_1805750	IFITM3	interferon induced transmembrane protein 3		3.50	2.74
ILMN_1692332	ALOX12B	arachidonate 12-lipoxygenase, 12R type			2.73
ILMN_1700583	ZNF750	zinc finger protein 750			2.71
ILMN_1835092	IFI44L	interferon-induced protein 44-like		3.47	2.71
ILMN_1665832	ID1	inhibitor of DNA binding 1, dominant negative helix-loop-helix protein			2.70
ILMN_3243928	DDX60L	DEAD (Asp-Glu-Ala-Asp) box polypeptide 60-like		4.39	2.70
ILMN_1806059	SPRR2B	small proline-rich protein 2B			2.70
ILMN_1845037	TRIM69	tripartite motif containing 69		3.32	2.69
ILMN_1716591	SPRR1A	small proline-rich protein 1A			2.69
ILMN_1748915	S100A12	S100 calcium binding protein A12			2.69
ILMN_1797001	DDX58	DEAD (Asp-Glu-Ala-Asp) box polypeptide 58		4.65	2.67
ILMN_1773006	FABP4	fatty acid binding protein 4, adipocyte			2.66
ILMN_2262044	PARP10	poly (ADP-ribose) polymerase family, member 10		4.13	2.65
ILMN_3297126	TYMP	thymidine phosphorylase		3.79	2.65
ILMN_1701114	GBP1	guanylate binding protein 1, interferon-inducible		4.97	2.63
ILMN_1763666	ALDH3B2	aldehyde dehydrogenase 3 family, member B2			2.61
ILMN_1699331	IFIT1	interferon-induced protein with tetratricopeptide repeats 1		7.00	2.60
ILMN_1718387	LOR	loricrin			2.59
ILMN_1705814	KRT80	keratin 80			2.57
ILMN_1703108	UBE2L6	ubiquitin-conjugating enzyme E2L 6		3.39	2.55
ILMN_1784364	STARD5	StAR-related lipid transfer (START) domain containing 5		4.76	2.54
ILMN_1657234	CCL20	chemokine (C-C motif) ligand 20		2.68	2.54
ILMN_1746085	IGFBP3	insulin-like growth factor binding protein 3			2.52
ILMN_1723480	BST2	bone marrow stromal cell antigen 2		2.66	2.50
ILMN_2150856	SERPINB2	serpin peptidase inhibitor, clade B (ovalbumin), member 2		2.73	2.49
ILMN_1750400	C19orf66	chromosome 19 open reading frame 66		3.61	2.49
ILMN_1706502	EIF2AK2	eukaryotic translation initiation factor 2-alpha kinase 2		3.11	2.49
ILMN_1681526	SLC5A1	solute carrier family 5 (sodium/glucose cotransporter), member 1			2.47
ILMN_1695924	KLK11	kallikrein-related peptidase 11			2.47
ILMN_1673352	IFITM2	interferon induced transmembrane protein 2		3.19	2.46
ILMN_1748323	CXCL14	chemokine (C-X-C motif) ligand 14			2.45
ILMN_2390586	SP100	SP100 nuclear antigen		2.44	2.45
ILMN_2150851	SERPINB2	serpin peptidase inhibitor, clade B (ovalbumin), member 2		2.80	2.44
ILMN_1771385	GBP4	guanylate binding protein 4		4.03	2.44
ILMN_1724686	CLDN1	claudin 1			2.42
ILMN_1784380	DTX3L	deltex 3-like (Drosophila)		3.33	2.41
ILMN_1690939	TYMP	thymidine phosphorylase		3.04	2.40
ILMN_1711174	SPRR1B	small proline-rich protein 1B			2.38
ILMN_2284998	SP100	SP100 nuclear antigen		2.70	2.35
ILMN_2390162	PHF11	PHD finger protein 11		3.21	2.34
ILMN_2170813	LAMP3	lysosomal-associated membrane protein 3		3.17	2.34
ILMN_2396875	IGFBP3	insulin-like growth factor binding protein 3			2.32
ILMN_1774874	IL1RN	interleukin 1 receptor antagonist		2.66	2.32
ILMN_1705241	TDRD7	tudor domain containing 7		3.55	2.32
ILMN_1776723	PHF11	PHD finger protein 11		3.02	2.31
ILMN_1716093	KRT10	keratin 10			2.29
ILMN_1762899	EGR1	early growth response 1			2.29
ILMN_2368530	IL32	interleukin 32		2.39	2.27
ILMN_1767006	PSMB8	proteasome (prosome, macropain) subunit, beta type, 8		3.43	2.26
ILMN_2304512	SAA1	serum amyloid A1		3.65	2.25
ILMN_2320964	ADAR	adenosine deaminase, RNA-specific		2.84	2.24
ILMN_1788017	HSH2D	hematopoietic SH2 domain containing		4.42	2.24
ILMN_1797009	F3	coagulation factor III (thromboplastin, tissue factor)	2.06		2.23
ILMN_1799467	SAMD9L	sterile alpha motif domain containing 9-like		3.54	2.21
ILMN_1743412	SIAE	sialic acid acetylesterase			2.21
ILMN_1686116	THBS1	thrombospondin 1			2.20
ILMN_1764709	MAFB	v-maf avian musculoaponeurotic fibrosarcoma oncogene homolog B			2.20
ILMN_1795181	DDX60	DEAD (Asp-Glu-Ala-Asp) box polypeptide 60		2.87	2.20
ILMN_1678054	TRIM21	tripartite motif containing 21		3.62	2.19
ILMN_1725912	KLK12	kallikrein-related peptidase 12			2.18
ILMN_2412336	AKR1C2	aldo-keto reductase family 1, member C2		3.18	2.18
ILMN_1684308	DEFB103A	defensin, beta 103A			2.17
ILMN_1727589	SULT2B1	sulfotransferase family, cytosolic, 2B, member 1			2.16
ILMN_2404665	TRIM5	tripartite motif containing 5		4.22	2.16
ILMN_1762861	HLA-F	major histocompatibility complex, class I, F		3.22	2.16
ILMN_1710937	IFI16	interferon, gamma-inducible protein 16		2.71	2.15
ILMN_1683792	LAP3	leucine aminopeptidase 3		2.78	2.14
ILMN_2136495	A2ML1	alpha-2-macroglobulin-like 1			2.13
ILMN_1776777	ADAR	adenosine deaminase, RNA-specific		2.46	2.12
ILMN_1672295	ZC3H12A	zinc finger CCCH-type containing 12A			2.12
ILMN_1803452	CRCT1	cysteine-rich C-terminal 1			2.11

			Fold change		
Probe	Gene symbol	Gene name	EP12	F12	EP/F12
ILMN_1758731	CYP2J2	cytochrome P450, family 2, subfamily J, polypeptide 2		2.82	2.11
ILMN_1810835	SPRR3	small proline-rich protein 3			2.11
ILMN_1703650	TNIP1	TNFAIP3 interacting protein 1		3.56	2.10
ILMN_1759598	DLX5	distal-less homeobox 5			2.09
ILMN_2390299	PSMB8	proteasome (prosome, macropain) subunit, beta type, 8		3.01	2.08
ILMN_1721134	TGM1	transglutaminase 1			2.08
ILMN_1666733	IL8	interleukin 8		2.01	2.08
ILMN_1769388	GJB2	gap junction protein, beta 2, 26kDa			2.06
ILMN_2316236	HOPX	HOP homeobox			2.04
ILMN_1674811	OASL	2'-5'-oligoadenylate synthetase-like		4.47	2.04
ILMN_2129572	F3	coagulation factor III (thromboplastin, tissue factor)			2.04
ILMN_1688892	LAMA3	laminin, alpha 3		3.08	2.03
ILMN_1745570	KLK7	kallikrein-related peptidase 7			2.02
ILMN_2376108	PSMB9	proteasome (prosome, macropain) subunit, beta type, 9		2.72	2.02
ILMN_1709333	OAS2	2'-5'-oligoadenylate synthetase 2, 69/71kDa		3.00	2.01
ILMN_2406035	LAMA3	laminin, alpha 3		2.57	2.01
ILMN_1739428	IFIT2	interferon-induced protein with tetratricopeptide repeats 2		5.34	2.01
ILMN_1763520	SULT2B1	sulfotransferase family, cytosolic, 2B, member 1			2.01
ILMN_2326512	CASP1	caspase 1, apoptosis-related cysteine peptidase		2.30	2.01
ILMN_2376403	TSC22D3	TSC22 domain family, member 3			0.45
ILMN_2276952	TSC22D3	TSC22 domain family, member 3			0.45
ILMN_1681721	OASL	2'-5'-oligoadenylate synthetase-like		4.79	
ILMN_3253787	LOC100128274	putative p150		4.26	
ILMN_1801307	TNFSF10	tumor necrosis factor (ligand) superfamily, member 10		3.98	
ILMN_1815086	NINJ1	ninjurin 1		3.47	
ILMN_1714433	MARCKSL1	MARCKS-like 1		3.47	
ILMN_1664543	IFIT3	interferon-induced protein with tetratricopeptide repeats 3		3.47	
ILMN_1659913	ISG20	interferon stimulated exonuclease gene 20kDa		3.40	
ILMN_1653466	HES4	hairy and enhancer of split 4 (Drosophila)		3.25	
ILMN_1678422	DHX58	DEXH (Asp-Glu-X-His) box polypeptide 58		3.00	
ILMN_1701621	SCO2	SCO2 cytochrome c oxidase assembly protein		2.98	
ILMN_1755173	PLEKHA4	pleckstrin homology domain containing, family A (phosphoinositide binding specific) member 4		2.90	
ILMN_1747195	PSMB8	proteasome (prosome, macropain) subunit, beta type, 8		2.84	
ILMN_1776181	BIRC3	baculoviral IAP repeat containing 3		2.77	
ILMN_2376204	LTB	lymphotoxin beta (TNF superfamily, member 3)		2.72	
ILMN_1728224	OGFR	opioid growth factor receptor		2.59	
ILMN_1667068	ZC3HAV1	zinc finger CCCH-type, antiviral 1		2.56	
ILMN_1769550	SLFN5	schlafen family member 5		2.56	
ILMN_1727689	TNFAIP2	tumor necrosis factor, alpha-induced protein 2		2.55	
ILMN_1679133	SERPINB1	serpin peptidase inhibitor, clade B (ovalbumin), member 1		2.51	
ILMN_1727271	WARS	tryptophanyl-tRNA synthetase		2.49	
ILMN_1778321	SLC2A6	solute carrier family 2 (facilitated glucose transporter), member 6		2.42	
ILMN_1812226	ICAM1	intercellular adhesion molecule 1		2.41	
ILMN_1719759	TNC	tenascin C		2.41	
ILMN_1691717	RHBDF2	rhomboid 5 homolog 2 (Drosophila)		2.39	
ILMN_2337655	WARS	tryptophanyl-tRNA synthetase		2.38	
ILMN_1745148	ZNFX1	zinc finger, NFX1-type containing 1		2.37	
ILMN_1783621	CMPK2	cytidine monophosphate (UMP-CMP) kinase 2, mitochondrial		2.35	
ILMN_1663042	SDC4	syndecan 4		2.34	
ILMN_1696654	IFIT5	interferon-induced protein with tetratricopeptide repeats 5		2.34	
ILMN_1682336	MASTL	microtubule associated serine/threonine kinase-like		2.33	
ILMN_1740418	CYP27B1	cytochrome P450, family 27, subfamily B, polypeptide 1		2.33	
ILMN_2067890	CXCL11	chemokine (C-X-C motif) ligand 11		2.32	
ILMN_1751886	REC8	REC8 meiotic recombination protein		2.31	
ILMN_1714861	CD68	CD68 molecule		2.30	
ILMN_1655595	SERPINE2	serpin peptidase inhibitor, clade E (nexin, plasminogen activator inhibitor type 1), member 2		2.28	
ILMN_1681644	BIRC3	baculoviral IAP repeat containing 3		2.27	
ILMN_1715684	LAMB3	laminin, beta 3		2.26	
ILMN_1687768	NCOA7	nuclear receptor coactivator 7		2.25	
ILMN_1690365	USP41	ubiquitin specific peptidase 41		2.24	
ILMN_1729749	HERC5	HECT and RLD domain containing E3 ubiquitin protein ligase 5		2.24	
ILMN_1785732	TNFAIP6	tumor necrosis factor, alpha-induced protein 6		2.24	
ILMN_1683026	PSMB10	proteasome (prosome, macropain) subunit, beta type, 10		2.23	
ILMN_1813625	TRIM25	tripartite motif containing 25		2.22	
ILMN_1810608	PNPT1	polyribonucleotide nucleotidyltransferase 1		2.20	
ILMN_1790472	SLC25A28	solute carrier family 25 (mitochondrial iron transporter), member 28		2.20	
ILMN_1737599	TRIM5	tripartite motif containing 5		2.19	
ILMN_1687757	AKR1C4	aldo-keto reductase family 1, member C4		2.18	
ILMN_1800078	LMO2	LIM domain only 2 (rhombotin-like 1)		2.18	
ILMN_1708375	IRF1	interferon regulatory factor 1		2.17	
ILMN_2248970	OAS2	2'-5'-oligoadenylate synthetase 2, 69/71kDa		2.17	
ILMN_1792455	TMEM158	transmembrane protein 158 (gene/pseudogene)		2.16	
ILMN_1701204	VEGFC	vascular endothelial growth factor C		2.14	
ILMN_1769734	NT5C3A	5'-nucleotidase, cytosolic IIIA		2.14	
ILMN_2326509	CASP1	caspase 1, apoptosis-related cysteine peptidase		2.14	
ILMN_2145670	TNC	tenascin C		2.13	
ILMN_1720083	EHD4	EH-domain containing 4		2.13	
ILMN_1659688	LGALS3BP	lectin, galactoside-binding, soluble, 3 binding protein		2.13	
ILMN_2370573	XAF1	XIAP associated factor 1		2.12	
ILMN_1858599	RBM43	RNA binding motif protein 43		2.10	
ILMN_1786612	PSME2	proteasome (prosome, macropain) activator subunit 2 (PA28 beta)		2.09	
ILMN_1808501	SH3KBP1	SH3-domain kinase binding protein 1		2.09	
ILMN_1807439	ALDH1A3	aldehyde dehydrogenase 1 family, member A3		2.08	
ILMN_1716815	CEACAM1	carcinoembryonic antigen-related cell adhesion molecule 1 (biliary glycoprotein)		2.07	
ILMN_1753111	NAMPT	nicotinamide phosphoribosyltransferase		2.07	
ILMN_1654696	C15orf48	chromosome 15 open reading frame 48		2.06	
ILMN_2130441	HLA-H	major histocompatibility complex, class I, H (pseudogene)		2.06	
ILMN_1729095	PDZD2	PDZ domain containing 2		2.06	

			Fold change		
Probe	**Gene symbol**	**Gene name**	**EP12**	**F12**	**EP/F12**
ILMN_2352121	NT5C3A	5'-nucleotidase, cytosolic IIIA		2.06	
ILMN_1724837	ZC3HAV1	zinc finger CCCH-type, antiviral 1		2.05	
ILMN_1678454	CASP4	caspase 4, apoptosis-related cysteine peptidase		2.04	
ILMN_1796537	FYB	FYN binding protein		2.04	
ILMN_1736863	TMEM140	transmembrane protein 140		2.03	
ILMN_2373062	RHBDF2	rhomboid 5 homolog 2 (Drosophila)		2.01	
ILMN_2082209	TOX2	TOX high mobility group box family member 2		0.46	
ILMN_1661708	LGALS7	lectin, galactoside-binding, soluble, 7	0.38	0.42	
ILMN_2064860	LGALS7B	lectin, galactoside-binding, soluble, 7B	0.38	0.39	
ILMN_3243690	LGALS7B	lectin, galactoside-binding, soluble, 7B	0.38	0.39	
ILMN_2396444	CD14	CD14 molecule	0.46		
ILMN_1770612	KRT15	keratin 15	0.39		
ILMN_1712112	RCAN1	regulator of calcineurin 1	0.46		
ILMN_1693912	SLC47A2	solute carrier family 47 (multidrug and toxin extrusion), member 2	0.49		
ILMN_1674243	TFRC	transferrin receptor (p90, CD71)	0.41		

Table 8.2: Differentially expressed genes after 24 hour challenge.

			Fold change		
Probe	**Gene symbol**	**Gene name**	**EP24**	**F24**	**EP/F24**
ILMN_1702127	SPRR2G	small proline-rich protein 2G		3.25	22.46
ILMN_2058782	IFI27	interferon, alpha-inducible protein 27		23.86	21.18
ILMN_2197577	SPRR2C	small proline-rich protein 2C (pseudogene)		2.77	19.52
ILMN_1795359	SPRR2A	small proline-rich protein 2A	3.13	3.60	17.04
ILMN_1801246	IFITM1	interferon induced transmembrane protein 1		20.20	13.40
ILMN_1674367	SPRR2F	small proline-rich protein 2F	2.68	2.79	12.32
ILMN_1806059	SPRR2B	small proline-rich protein 2B			11.96
ILMN_2347798	IFI6	interferon, alpha-inducible protein 6		13.69	11.75
ILMN_1701239	SPRR2E	small proline-rich protein 2E		2.43	11.50
ILMN_1757351	S100A7	S100 calcium binding protein A7	2.53	2.50	10.66
ILMN_1723912	IFI44L	interferon-induced protein 44-like		9.32	10.42
ILMN_1718395	LCE3D	late cornified envelope 3D	2.28	2.64	10.37
ILMN_1692223	LCN2	lipocalin 2	2.66	4.89	9.87
ILMN_2211018	SPRR2E	small proline-rich protein 2E		2.59	9.65
ILMN_1690105	STAT1	signal transducer and activator of transcription 1, 91kDa		10.50	9.53
ILMN_2231928	MX2	myxovirus (influenza virus) resistance 2 (mouse)		7.86	9.51
ILMN_1691364	STAT1	signal transducer and activator of transcription 1, 91kDa		9.53	9.07
ILMN_2048043	DEFB4A	defensin, beta 4A		2.94	8.43
ILMN_1662358	MX1	myxovirus (influenza virus) resistance 1, interferon-inducible protein p78 (mouse)		8.19	8.32
ILMN_1684308	DEFB103A	defensin, beta 103A		2.02	7.00
ILMN_1803452	CRCT1	cysteine-rich C-terminal 1			6.80
ILMN_1674063	OAS2	2'-5'-oligoadenylate synthetase 2, 69/71kDa		6.28	6.76
ILMN_1803838	CNFN	cornifelin			6.50
ILMN_1791759	CXCL10	chemokine (C-X-C motif) ligand 10		9.82	6.46
ILMN_3238649	LCE6A	late cornified envelope 6A			6.43
ILMN_1808220	LCE3E	late cornified envelope 3E			5.96
ILMN_1780649	KPRP	keratinocyte proline-rich protein			5.59
ILMN_1728632	LCE3C	late cornified envelope 3C			5.55
ILMN_1777325	STAT1	signal transducer and activator of transcription 1, 91kDa		6.89	5.45
ILMN_1712849	RNASE7	ribonuclease, RNase A family, 7		2.08	5.41
ILMN_1712759	SBSN	suprabasin			5.25
ILMN_1748915	S100A12	S100 calcium binding protein A12			5.23
ILMN_1731418	SP110	SP110 nuclear body protein		4.41	5.19
ILMN_1714587	DEFB103A	defensin, beta 103A			5.17
ILMN_1735712	KRT1	keratin 1			5.13
ILMN_1829555	LCE6A	late cornified envelope 6A			5.05
ILMN_1762284	ASPRV1	aspartic peptidase, retroviral-like 1			5.00
ILMN_2410826	OAS1	2'-5'-oligoadenylate synthetase 1, 40/46kDa		5.85	4.84
ILMN_2349061	IRF7	interferon regulatory factor 7		5.64	4.69
ILMN_1745374	IFI35	interferon-induced protein 35		5.17	4.67
ILMN_2158713	IL36G	interleukin 36, gamma		2.08	4.65
ILMN_1779252	TRIM22	tripartite motif containing 22		5.64	4.62
ILMN_2402640	DSC1	desmocollin 1			4.57
ILMN_2415144	SP110	SP110 nuclear body protein		4.43	4.57
ILMN_1718387	LOR	loricrin			4.56
ILMN_1730284	DSC1	desmocollin 1			4.55
ILMN_1727880	CDSN	corneodesmosin			4.45
ILMN_1794662	DSG1	desmoglein 1			4.43
ILMN_1798181	IRF7	interferon regulatory factor 7		5.87	4.41
ILMN_3223126	TYMP	thymidine phosphorylase		4.90	4.38
ILMN_1788874	SERPINA3	serpin peptidase inhibitor, clade A (alpha-1 antiproteinase, antitrypsin), member 3		5.14	4.13
ILMN_2388547	EPSTI1	epithelial stromal interaction 1 (breast)		3.73	4.13
ILMN_1805410	C15orf48	chromosome 15 open reading frame 48		6.78	4.12
ILMN_2191967	SPRR2D	small proline-rich protein 2D			4.10
ILMN_1658247	OAS1	2'-5'-oligoadenylate synthetase 1, 40/46kDa		4.92	4.06
ILMN_1774287	CFB	complement factor B		5.09	3.97
ILMN_1675640	OAS1	2'-5'-oligoadenylate synthetase 1, 40/46kDa		4.81	3.95
ILMN_1750974	S100A9	S100 calcium binding protein A9		2.25	3.79
ILMN_1787509	HELZ2	helicase with zinc finger 2, transcriptional coactivator		3.56	3.78
ILMN_2170814	LAMP3	lysosomal-associated membrane protein 3		4.65	3.75
ILMN_2109708	TYMP	thymidine phosphorylase		4.68	3.74
ILMN_2316236	HOPX	HOP homeobox			3.74
ILMN_1745397	OAS3	2'-5'-oligoadenylate synthetase 3, 100kDa		4.45	3.65
ILMN_1796316	MMP9	matrix metallopeptidase 9 (gelatinase B, 92kDa gelatinase, 92kDa type IV collagenase)		3.18	3.61
ILMN_1686116	THBS1	thrombospondin 1		3.51	3.53
ILMN_1782716	SERPINB4	serpin peptidase inhibitor, clade B (ovalbumin), member 4			3.42
ILMN_1656706	LCE2D	late cornified envelope 2D			3.40
ILMN_3297126	TYMP	thymidine phosphorylase		3.55	3.33
ILMN_1708303	CYP4F22	cytochrome P450, family 4, subfamily F, polypeptide 22			3.31
ILMN_1745242	PLSCR1	phospholipid scramblase 1		3.36	3.31
ILMN_1713397	NCCRP1	non-specific cytotoxic cell receptor protein 1 homolog (zebrafish)			3.31
ILMN_2150851	SERPINB2	serpin peptidase inhibitor, clade B (ovalbumin), member 2		2.72	3.27
ILMN_2148913	TMEM45A	transmembrane protein 45A			3.25
ILMN_1805750	IFITM3	interferon induced transmembrane protein 3		3.64	3.23
ILMN_1778401	HLA-B	major histocompatibility complex, class I, B		3.64	3.22
ILMN_1709708	LCE2C	late cornified envelope 2C			3.14
ILMN_1692332	ALOX12B	arachidonate 12-lipoxygenase, 12R type			3.11
ILMN_2304512	SAA1	serum amyloid A1		4.30	3.08
ILMN_2098126	CCL5	chemokine (C-C motif) ligand 5		4.22	3.04
ILMN_1795181	DDX60	DEAD (Asp-Glu-Ala-Asp) box polypeptide 60		2.37	2.99
ILMN_1770922	TMEM45A	transmembrane protein 45A			2.97
ILMN_2150856	SERPINB2	serpin peptidase inhibitor, clade B (ovalbumin), member 2		2.57	2.94
ILMN_2079042	WFDC5	WAP four-disulfide core domain 5			2.94
ILMN_1786847	TGM3	transglutaminase 3			2.92
ILMN_1723480	BST2	bone marrow stromal cell antigen 2		2.92	2.87
ILMN_1731224	PARP9	poly (ADP-ribose) polymerase family, member 9		2.87	2.87
ILMN_1776181	BIRC3	baculoviral IAP repeat containing 3		2.46	2.86
ILMN_1736729	OAS2	2'-5'-oligoadenylate synthetase 2, 69/71kDa		2.68	2.85

			Fold change		
Probe	Gene symbol	Gene name	EP24	F24	EP/F24
ILMN_1743412	SIAE	sialic acid acetylesterase			2.83
ILMN_1735570	HOPX	HOP homeobox			2.81
ILMN_2114720	SLPI	secretory leukocyte peptidase inhibitor			2.79
ILMN_2239754	IFIT3	interferon-induced protein with tetratricopeptide repeats 3			2.78
ILMN_1760062	IFI44	interferon-induced protein 44			2.77
ILMN_1690939	TYMP	thymidine phosphorylase		2.89	2.75
ILMN_1655077	PRDM1	PR domain containing 1, with ZNF domain			2.74
ILMN_1673352	IFITM2	interferon induced transmembrane protein 2		3.37	2.73
ILMN_1725912	KLK12	kallikrein-related peptidase 12			2.72
ILMN_1672661	SP110	SP110 nuclear body protein		2.43	2.70
ILMN_1791545	KRT23	keratin 23 (histone deacetylase inducible)			2.70
ILMN_1769520	UBE2L6	ubiquitin-conjugating enzyme E2L 6		3.62	2.69
ILMN_1742618	XAF1	XIAP associated factor 1		2.69	2.69
ILMN_1695924	KLK11	kallikrein-related peptidase 11			2.69
ILMN_1703108	UBE2L6	ubiquitin-conjugating enzyme E2L 6		3.63	2.68
ILMN_1762861	HLA-F	major histocompatibility complex, class I, F		2.96	2.66
ILMN_2262044	PARP10	poly (ADP-ribose) polymerase family, member 10		2.83	2.65
ILMN_1679960	LCE1A	late cornified envelope 1A			2.63
ILMN_3243928	DDX60L	DEAD (Asp-Glu-Ala-Asp) box polypeptide 60-like		2.54	2.61
ILMN_2336781	SOD2	superoxide dismutase 2, mitochondrial		3.99	2.60
ILMN_3249101	SDR9C7	short chain dehydrogenase/reductase family 9C, member 7			2.59
ILMN_1700081	FST	follistatin		2.07	2.58
ILMN_1724686	CLDN1	claudin 1			2.58
ILMN_1698666	CST6	cystatin E/M			2.57
ILMN_2085862	SLC15A3	solute carrier family 15 (oligopeptide transporter), member 3		4.05	2.55
ILMN_1703855	SERPINB3	serpin peptidase inhibitor, clade B (ovalbumin), member 3			2.53
ILMN_1705814	KRT80	keratin 80			2.52
ILMN_1690921	STAT2	signal transducer and activator of transcription 2, 113kDa			2.51
ILMN_1814106	C9orf169	chromosome 9 open reading frame 169			2.50
ILMN_1754576	KRT6C	keratin 6C			2.50
ILMN_1812281	ARG1	arginase 1			2.49
ILMN_1665832	ID1	inhibitor of DNA binding 1, dominant negative helix-loop-helix protein			2.49
ILMN_1701789	IFIT3	interferon-induced protein with tetratricopeptide repeats 3			2.48
ILMN_1654639	HERC6	HECT and RLD domain containing E3 ubiquitin protein ligase family member 6		2.77	2.47
ILMN_1835092	IFI44L	interferon-induced protein 44-like		2.40	2.46
ILMN_1773352	CCL5	chemokine (C-C motif) ligand 5		3.23	2.46
ILMN_1709725	PAPL	iron/zinc purple acid phosphatase-like protein			2.45
ILMN_1718558	PARP12	poly (ADP-ribose) polymerase family, member 12		2.07	2.44
ILMN_1719695	NFKBIZ	nuclear factor of kappa light polypeptide gene enhancer in B-cells inhibitor, zeta			2.42
ILMN_1729801	S100A8	S100 calcium binding protein A8		2.10	2.41
ILMN_1706502	EIF2AK2	eukaryotic translation initiation factor 2-alpha kinase 2		2.81	2.41
ILMN_1657234	CCL20	chemokine (C-C motif) ligand 20		2.61	2.40
ILMN_2134130	FLG	filaggrin			2.39
ILMN_1697629	JMJD7-PLA2G4B	JMJD7-PLA2G4B readthrough			2.38
ILMN_1745471	IRF9	interferon regulatory factor 9		2.27	2.38
ILMN_2170813	LAMP3	lysosomal-associated membrane protein 3		2.79	2.38
ILMN_2054019	ISG15	ISG15 ubiquitin-like modifier		2.24	2.36
ILMN_1773006	FABP4	fatty acid binding protein 4, adipocyte			2.35
ILMN_1699989	BNIPL	BCL2/adenovirus E1B 19kD interacting protein like			2.34
ILMN_1776723	PHF11	PHD finger protein 11		2.34	2.34
ILMN_2390162	PHF11	PHD finger protein 11		2.44	2.34
ILMN_1795711	LCE2B	late cornified envelope 2B			2.33
ILMN_2381257	DSC2	desmocollin 2			2.31
ILMN_1784294	CPA4	carboxypeptidase A4			2.30
ILMN_1687384	IFI6	interferon, alpha-inducible protein 6		2.51	2.30
ILMN_1814305	SAMD9	sterile alpha motif domain containing 9			2.30
ILMN_1744923	WFDC5	WAP four-disulfide core domain 5			2.29
ILMN_1764709	MAFB	v-maf avian musculoaponeurotic fibrosarcoma oncogene homolog B			2.29
ILMN_2376108	PSMB9	proteasome (prosome, macropain) subunit, beta type, 9		2.62	2.26
ILMN_1657871	RSAD2	radical S-adenosyl methionine domain containing 2		2.20	2.25
ILMN_2053527	PARP9	poly (ADP-ribose) polymerase family, member 9		2.10	2.24
ILMN_3240420	USP18	ubiquitin specific peptidase 18		2.14	2.24
ILMN_1681644	BIRC3	baculoviral IAP repeat containing 3			2.24
ILMN_1659688	LGALS3BP	lectin, galactoside-binding, soluble, 3 binding protein		2.44	2.23
ILMN_1749118	CALML5	calmodulin-like 5			2.23
ILMN_1801216	S100P	S100 calcium binding protein P			2.22
ILMN_1763666	ALDH3B2	aldehyde dehydrogenase 3 family, member B2			2.21
ILMN_1711174	SPRR1B	small proline-rich protein 1B			2.20
ILMN_1700583	ZNF750	zinc finger protein 750			2.19
ILMN_1721134	TGM1	transglutaminase 1			2.18
ILMN_1845037	TRIM69	tripartite motif containing 69			2.18
ILMN_1745964	IRAK2	interleukin-1 receptor-associated kinase 2			2.18
ILMN_3248032	NCCRP1	non-specific cytotoxic cell receptor protein 1 homolog (zebrafish)			2.17
ILMN_1788017	HSH2D	hematopoietic SH2 domain containing			2.17
ILMN_1723035	OLR1	oxidized low density lipoprotein (lectin-like) receptor 1			2.17
ILMN_1745570	KLK7	kallikrein-related peptidase 7			2.15
ILMN_1746085	IGFBP3	insulin-like growth factor binding protein 3			2.15
ILMN_1704972	TRIM5	tripartite motif containing 5			2.15
ILMN_1739882	SDR9C7	short chain dehydrogenase/reductase family 9C, member 7			2.13
ILMN_1663119	DSC2	desmocollin 2			2.12
ILMN_1701621	SCO2	SCO2 cytochrome c oxidase assembly protein			2.11
ILMN_1784364	STARD5	StAR-related lipid transfer (START) domain containing 5			2.11
ILMN_1682636	CXCL2	chemokine (C-X-C motif) ligand 2			2.08
ILMN_1751079	TAP1	transporter 1, ATP-binding cassette, sub-family B (MDR/TAP)		2.31	2.08
ILMN_2396875	IGFBP3	insulin-like growth factor binding protein 3			2.07
ILMN_1727589	SULT2B1	sulfotransferase family, cytosolic, 2B, member 1			2.07
ILMN_1770338	TM4SF1	transmembrane 4 L six family member 1			2.06
ILMN_1693192	PI3	peptidase inhibitor 3, skin-derived			2.06

			Fold change		
Probe	Gene symbol	Gene name	EP24	F24	EP/F24
ILMN_1718033	LYPD5	LY6/PLAUR domain containing 5			2.06
ILMN_2390586	SP100	SP100 nuclear antigen		2.07	2.06
ILMN_1793537	MUC15	mucin 15, cell surface associated			2.06
ILMN_1683792	LAP3	leucine aminopeptidase 3		2.36	2.05
ILMN_1810835	SPRR3	small proline-rich protein 3			2.05
ILMN_1741014	SLC28A3	solute carrier family 28 (concentrative nucleoside transporter), member 3			2.04
ILMN_2406501	SOD2	superoxide dismutase 2, mitochondrial		2.76	2.04
ILMN_2133090	SDR9C7	short chain dehydrogenase/reductase family 9C, member 7			2.03
ILMN_1737308	GLRX	glutaredoxin (thioltransferase)			2.03
ILMN_1774901	GDPD3	glycerophosphodiester phosphodiesterase domain containing 3			2.02
ILMN_1758731	CYP2J2	cytochrome P450, family 2, subfamily J, polypeptide 2		2.19	2.01
ILMN_1697220	NT5E	5'-nucleotidase, ecto (CD73)		2.14	2.01
ILMN_2366445	KRT80	keratin 80			2.00
ILMN_1687757	AKR1C4	aldo-keto reductase family 1, member C4			0.45
ILMN_1677511	PTGS2	prostaglandin-endoperoxide synthase 2 (prostaglandin G/H synthase and cyclooxygenase)		2.35	
ILMN_1714861	CD68	CD68 molecule		2.31	
ILMN_2054297	PTGS2	prostaglandin-endoperoxide synthase 2 (prostaglandin G/H synthase and cyclooxygenase)		2.28	
ILMN_2368530	IL32	interleukin 32		2.25	
ILMN_2184373	IL8	interleukin 8		2.23	
ILMN_2139100	SHISA5	shisa family member 5		2.23	
ILMN_2376205	LTB	lymphotoxin beta (TNF superfamily, member 3)		2.21	
ILMN_1781966	OSBP2	oxysterol binding protein 2	2.03	2.18	
ILMN_1710937	IFI16	interferon, gamma-inducible protein 16		2.07	
ILMN_1755173	PLEKHA4	pleckstrin homology domain containing, family A (phosphoinositide binding specific) member 4		2.04	
ILMN_1785732	TNFAIP6	tumor necrosis factor, alpha-induced protein 6		2.01	
ILMN_1764109	C1R	complement component 1, r subcomponent		2.00	
ILMN_1783753	TXNDC12	thioredoxin domain containing 12 (endoplasmic reticulum)		0.48	
ILMN_1750800	ACO1	aconitase 1, soluble		0.48	
ILMN_1790211	C7orf57	chromosome 7 open reading frame 57	2.31		
ILMN_1697448	TXNIP	thioredoxin interacting protein	2.12		
ILMN_1661708	LGALS7	lectin, galactoside-binding, soluble, 7	0.49		
ILMN_2064860	LGALS7B	lectin, galactoside-binding, soluble, 7B	0.48		
ILMN_1713124	AKR1C3	aldo-keto reductase family 1, member C3	0.45		
ILMN_2412336	AKR1C2	aldo-keto reductase family 1, member C2	0.41		
ILMN_1684306	S100A4	S100 calcium binding protein A4	0.40		
ILMN_2396444	CD14	CD14 molecule	0.40		
ILMN_2367239	RCAN1	regulator of calcineurin 1	0.38		
ILMN_1712112	RCAN1	regulator of calcineurin 1	0.31		

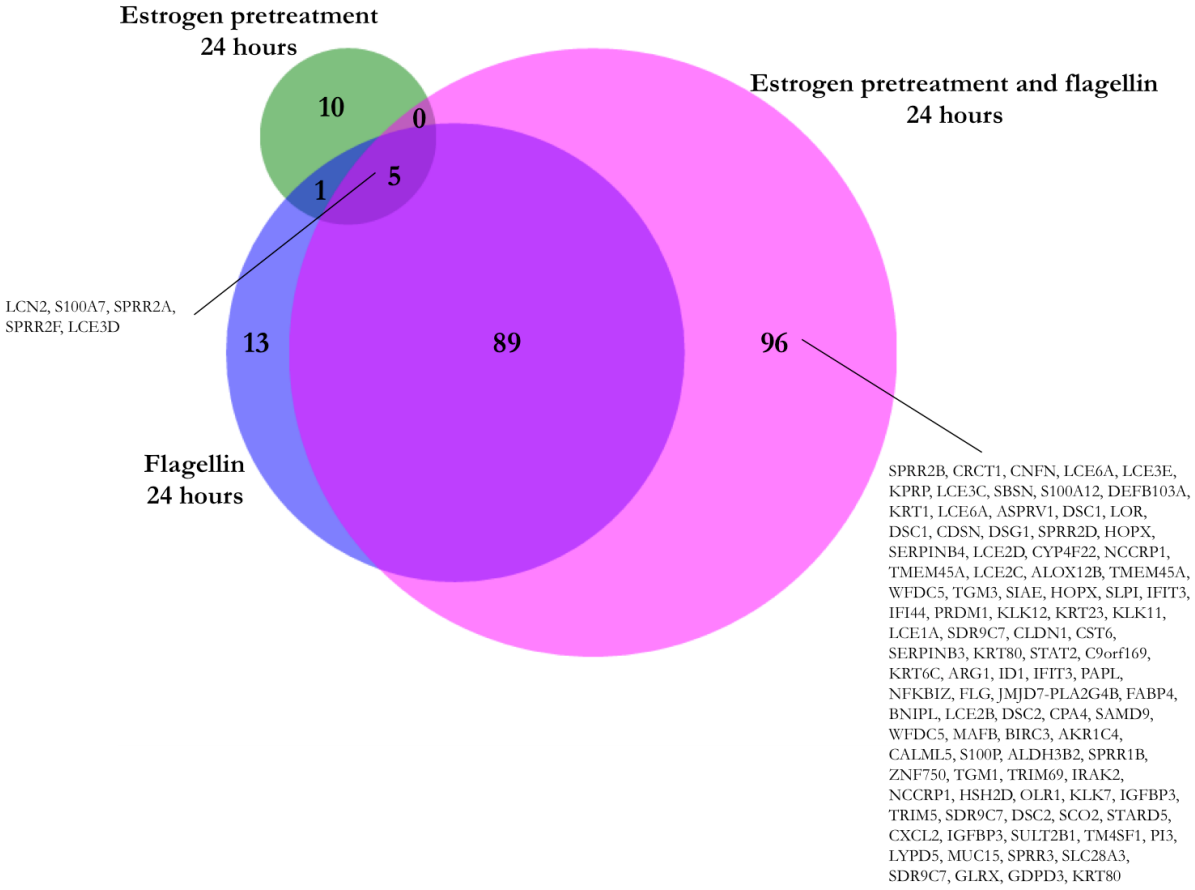

Figure 8.1: Venn diagram of differentially expressed genes after 24 hours.

References

1 Nielubowicz G.R. & Mobley H.L.T. (2010) Host-pathogen interactions in urinary tract infection. *Nature Reviews Urology* **7**, 430–441.

2 Gruneberg R.N. (1969) Relationship of infecting urinary organism to the faecal flora in patients with symptomatic urinary infection. *The Lancet* **2**, 766–768.

3 Rosen D.A., Hooton T.M., *et al.* (2007) Detection of intracellular bacterial communities in human urinary tract infection. *PLoS Medicine* **4**, e329.

4 Ramakrishnan K. & Scheid D.C. (2005) Diagnosis and management of acute pyelonephritis in adults. *American Family Physician* **71**, 933–942.

5 Urinary tract infections in women *[Accessed 02.08.2016] http://www.fairviewebenezer.org/HealthLibrary/Article/83049*.

6 Foxman B. (1990) Recurring urinary tract infection: incidence and risk factors. *American Journal of Public Health* **80**, 331–333.

7 Perrotta C., Aznar M., *et al.* (2008) Oestrogens for preventing recurrent urinary tract infection in postmenopausal women. *Cochrane Database of Systematic Reviews*, CD005131.

8 Russo T.A., Stapleton A., *et al.* (1995) Chromosomal restriction fragment length polymorphism analysis of *Escherichia coli* strains causing recurrent urinary tract infections in young women. *The Journal of Infectious Diseases* **172**, 440–445.

9 Kucheria R., Dasgupta P., *et al.* (2005) Urinary tract infections: new insights into a common problem. *Postgraduate Medical Journal* **81**, 83–86.

10 Foxman B. (2002) Epidemiology of urinary tract infections: incidence, morbidity, and economic costs. *The American Journal of Medicine* **113**, 5S–13S.

11 Plowman R., Graves N., *et al.* (2001) The rate and cost of hospital-acquired infections occurring in patients admitted to selected specialties of a district general hospital in England and the national burden imposed. *Journal of Hospital Infection* **47**, 198–209.

12 Turner D., Little P., *et al.* (2010) Cost effectiveness of management strategies for urinary tract infections: results from randomised controlled trial. *BMJ* **340**, c346.

13 Ikäheimo R., Siitonen A., *et al.* (1996) Recurrence of urinary tract infection in a primary care setting: analysis of a 1-year follow-up of 179 women. *Clinical Infectious Diseases* **22**, 91–99.

14 Raz R., Gennesin Y., *et al.* (2000) Recurrent urinary tract infections in postmenopausal women. *Clinical Infectious Diseases* **30**, 152–6.

15 Paduch D.A. (2007) Viral lower urinary tract infections. *Current Urology Reports* **8**, 324–335.

16 Sobel J.D., Fisher J.F., *et al.* (2011) *Candida* urinary tract infections - epidemiology. *Clinical Infectious Diseases* **52**, 433–436.

17 Hooton T.M. (2012) Uncomplicated urinary tract infection. *New England Journal of Medicine* **366**, 1028–1037.

18 Kline K. & Lewis A. (2016) Gram-positive uropathogens, polymicrobial urinary tract infection, and the emerging microbiota of the urinary tract. *Microbiology Spectrum* **4**, doi: 10.1128/microbiolspec.UTI–0012–2012.

19 Spurbeck R.R., Stapleton A.E., *et al.* (2011) Fimbrial profiles predict virulence of uropathogenic *Escherichia coli* strains: contribution of Ygi and Yad fimbriae. *Infection and Immunity* **79**, 4753–4763.

20 Connell I., Agace W., *et al.* (1996) Type 1 fimbrial expression enhances *Escherichia coli* virulence for the urinary tract. *Proceeding of the National Academy of Sciences of the United States of America* **93**, 9827–9832.

21 Bahrani-Mougeot F.K., Buckles E.L., *et al.* (2002) Type 1 fimbriae and extracellular polysaccharides are preeminent uropathogenic *Escherichia coli* virulence determinants in the murine urinary tract. *Molecular Microbiology* **45**, 1079–1093.

22 Martinez J.J., Mulvey M.A., *et al.* (2000) Type 1 pilus-mediated bacterial invasion of

bladder epithelial cells. *The EMBO Journal* **19**, 2803–2812.
23 Zhou G., Mo W.-J., *et al.* (2001) Uroplakin Ia is the urothelial receptor for uropathogenic *Escherichia coli*: evidence from in vitro FimH binding. *Journal of Cell Science* **114**, 4095–4103.
24 Wright K.J., Seed P.C. & Hultgren S.J. (2007) Development of intracellular bacterial communities of uropathogenic *Escherichia coli* depends on type 1 pili. *Cellular Microbiology* **9**, 2230–2241.
25 Lane M.C. & Mobley H.L.T. (2007) Role of P-fimbrial-mediated adherence in pyelonephritis and persistence of uropathogenic *Escherichia coli* (UPEC) in the mammalian kidney. *Kidney International* **72**, 19–25.
26 Lund B., Lindberg F., *et al.* (1987) The PapG protein is the alpha-D-galactopyranosyl-(1,4)-beta-D-galactopyranose-binding adhesin of uropathogenic *Escherichia coli*. *Proceedings of the National Academy of Sciences of the United States of America* **84**, 5898–5902.
27 O'Hanley P., Lark D., *et al.* (1985) Molecular basis of *Escherichia coli* colonization of the upper urinary tract in BALB/c mice. *Journal of Clinical Investigation* **75**, 347–360.
28 Lane M.C., Alteri C.J., *et al.* (2007) Expression of flagella is coincident with uropathogenic *Escherichia coli* ascension to the upper urinary tract. *Proceedings of the National Academy of Sciences of the United States of America* **104**, 16669–16674.
29 Lane M.C., Simms A.N. & Mobley H.L.T. (2007) Complex interplay between type 1 fimbrial expression and flagellum-mediated motility of uropathogenic *Escherichia coli*. *Journal of Bacteriology* **189**, 5523–5533.
30 Zhang L. & Foxman B. (2003) Molecular epidemiology of *Escherichia coli* mediated urinary tract infections. *Frontiers in Bioscience* **8**, 235–244.
31 Hannan T.J., Mysorekar I.U., *et al.* (2008) LeuX tRNA-dependent and -independent mechanisms of *Escherichia coli* pathogenesis in acute cystitis. *Molecular Microbiology* **67**, 116–128.
32 Smith Y.C., Rasmussen S.B., *et al.* (2008) Hemolysin of uropathogenic *Escherichia coli* evokes extensive shedding of the uroepithelium and hemorrhage in bladder tissue within the first 24 hours after intraurethral inoculation of mice. *Infection and Immunity* **76**, 2978–2990.
33 Nagamatsu K., Hannan T.J., *et al.* (2015) Dysregulation of *Escherichia coli* α-hemolysin expression alters the course of acute and persistent urinary tract infection. *Proceedings of the National Academy of Sciences of the United States of America* **112**, E871–880.
34 Ding X., Boney-montoya J., *et al.* (2013) The UPEC pore forming toxin alpha-hemolysin triggers proteolysis of host proteins to disrupt cell adhesion, inflammatory and survival pathways. *Cell Host and Microbe* **16**, 387–393.
35 Doye A., Mettouchi A., *et al.* (2002) CNF1 exploits the ubiquitin-proteasome machinery to restrict Rho GTPase activation for bacterial host cell invasion. *Cell* **111**, 553–564.
36 Mills M., Meysick K.C. & O'Brien A.D. (2000) Cytotoxic necrotizing factor type 1 of uropathogenic *Escherichia coli* kills cultured human uroepithelial 5637 cells by an apoptotic mechanism. *Infection and Immunity* **68**, 5869–5880.
37 Rippere-Lampe K.E., O'Brien A.D., *et al.* (2001) Mutation of the gene encoding cytotoxic necrotizing factor type 1 (cnf1) attenuates the virulence of uropathogenic *Escherichia coli*. *Infection and Immunity* **69**, 3954–3964.
38 Henderson J.P., Crowley J.R., *et al.* (2009) Quantitative metabolomics reveals an epigenetic blueprint for iron acquisition in uropathogenic *Escherichia coli*. *PLoS Pathogens* **5**, e1000305.
39 Garcia E.C., Brumbaugh A.R. & Mobley H.L.T. (2011) Redundancy and specificity of *Escherichia coli* iron acquisition systems during urinary tract infection. *Infection and Immunity* **79**, 1225–1235.
40 Govindaraj R.G., Manavalan B., *et al.* (2010) Molecular modeling-based evaluation of hTLR10 and identification of potential ligands in Toll-like receptor signaling. *PLoS ONE* **5**, e12713.
41 Oosting M., Cheng S.-C., *et al.* (2014) Human TLR10 is an anti-inflammatory pattern-

recognition receptor. *Proceedings of the National Academy of Sciences of the United States of America* **111**, E4478–4484.
42 Bussey C., Flavell R.A. & Ghosh S. (2004) A Toll-like receptor that prevents infection by uropathogenic bacteria. *Science* **303**, 1522–1527.
43 Poltorak A., He X., *et al.* (1998) Defective LPS signaling in C3H / HeJ and C57BL / 10ScCr mice: mutations in Tlr4 gene. *Science* **282**, 2085–2089.
44 Hemmi H., Takeuchi O., *et al.* (2000) A Toll-like receptor recognizes bacterial DNA. *Nature* **408**, 740–745.
45 Alexopoulou L., Czopik Holt A., *et al.* (2001) Recognition of double-stranded RNA and activation of NF-kappaB by Toll-like receptor 3. *Nature* **413**, 732–738.
46 Takeuchi O., Kawai T., *et al.* (2001) Discrimination of bacterial lipoproteins by Toll-like receptor 6. *International Immunology* **13**, 933–940.
47 Takeuchi O., Sato S., *et al.* (2002) Cutting edge: role of Toll-like receptor 1 in mediating immune response to microbial lipoproteins. *Journal of Immunology* **169**, 10–14.
48 Hayashi F., Smith K.D., *et al.* (2001) The innate immune response to bacterial flagellin is mediated by Toll-like receptor 5. *Nature* **410**, 1099–1103.
49 Heil F., Hemmi H., *et al.* (2004) Species-specific recognition of single-stranded RNA via Toll-like receptor 7 and 8. *Science* **303**, 1526–1529.
50 Medzhitov R., Preston-Hurlburt P., *et al.* (1998) MyD88 is an adaptor protein in the hToll/IL-1 receptor family signaling pathways. *Molecular Cell* **2**, 253–258.
51 Takeuchi O., Takeda K., *et al.* (2000) Cellular responses to bacterial cell wall components are mediated through MyD88-dependent signaling cascades. *International Immunology* **12**, 113–117.
52 Zhong J. & Kyriakis J.M. (2007) Dissection of a signaling pathway by which pathogen-associated molecular patterns recruit the JNK and p38 MAPKs and trigger cytokine release. *Journal of Biological Chemistry* **282**, 24246–24254.
53 Flannery S. & Bowie A.G. (2010) The interleukin-1 receptor-associated kinases: critical regulators of innate immune signalling. *Biochemical Pharmacology* **80**, 1981–1991.
54 Kawai T., Takeuchi O., *et al.* (2001) Lipopolysaccharide stimulates the MyD88-independent pathway and results in activation of IFN-regulatory factor 3 and the expression of a subset of lipopolysaccharide-inducible genes. *The Journal of Immunology* **167**, 5887–5894.
55 Yamamoto M., Sato S., *et al.* (2003) Role of adaptor TRIF in the MyD88-independent Toll-Like receptor signaling pathway. *Science* **301**, 640–643.
56 Fitzgerald K.A., Rowe D.C., *et al.* (2003) LPS-TLR4 signaling to IRF-3/7 and NF-kappaB involves the toll adapters TRAM and TRIF. *The Journal of Experimental Medicine* **198**, 1043–1055.
57 Tabel Y., Berdeli A. & Mir S. (2007) Association of TLR2 gene Arg753Gln polymorphism with urinary tract infection in children. *International Journal of Immunogenetics* **34**, 399–405.
58 Hawn T.R., Scholes D., *et al.* (2009) Toll-like receptor polymorphisms and susceptibility to urinary tract infections in adult women. *PLoS ONE* **4**, e5990.
59 Yin X., Hou T., *et al.* (2010) Association of Toll-like receptor 4 gene polymorphism and expression with urinary tract infection types in adults. *PLoS ONE* **5**, e14223.
60 Ali A.S.M. (2013) Are beta defensin 1 and beta defensin 2 key innate immune effector peptides against urinary tract infection in women? *PhD Thesis*, Newcastle University.
61 Andersen-Nissen E., Hawn T.R., *et al.* (2007) Cutting edge: Tlr5 − / − mice are more susceptible to *Escherichia coli* urinary tract infection. *Journal of immunology* **178**, 4717–4720.
62 Chamaillard M., Hashimoto M., *et al.* (2003) An essential role for NOD1 in host recognition of bacterial peptidoglycan containing diaminopimelic acid. *Nature Immunology* **4**, 702–707.
63 Inohara N., Ogura Y., *et al.* (2003) Host recognition of bacterial muramyl dipeptide mediated through NOD2: implications for Crohn's disease. *Journal of Biological Chemistry*

278, 5509–5512.
64 Kobayashi K., Inohara N., *et al.* (2002) RICK/Rip2/CARDIAK mediates signalling for receptors of the innate and adaptive immune systems. *Nature* **416**, 194–199.
65 Kobayashi K.S., Chamaillard M., *et al.* (2005) Nod2-dependent regulation of innate and adaptive immunity in the intestinal tract. *Science* **307**, 731–734.
66 Park J., Kim Y., *et al.* (2007) RICK/RIP2 mediates innate immune responses induced through Nod1 and Nod2 but not TLRs. *The Journal of Immunology* **178**, 2380–2386.
67 Bens M., Goujon J., *et al.* (2013) Cyclosporine A impairs nucleotide binding oligomerization domain (Nod1)-mediated innate antibacterial renal defenses in mice and human transplant recipients. *PLoS Pathogens* **9**, e1003152.
68 Wang C., Yuan X., *et al.* (2014) NOD2 is dispensable for ATG16L1 deficiency-mediated resistance to urinary tract infection. *Autophagy* **10**, 331–338.
69 Kang D., Gopalkrishnan R. V, *et al.* (2002) mda-5: An interferon-inducible putative RNA helicase with double-stranded RNA-dependent ATPase activity and melanoma growth-suppressive properties. *Proceedings of the National Academy of Sciences of the United States of America* **99**, 637–642.
70 Yoneyama M., Kikuchi M., *et al.* (2004) The RNA helicase RIG-I has an essential function in double-stranded RNA-induced innate antiviral responses. *Nature Immunology* **5**, 730–737.
71 Rothenfusser S., Goutagny N., *et al.* (2005) The RNA helicase LGP2 inhibits TLR-independent sensing of viral replication by retinoic acid-inducible gene-I. *Journal of Immunology* **175**, 5260–5268.
72 Takeuchi O. & Akira S. (2010) Pattern recognition receptors and inflammation. *Cell* **140**, 805–820.
73 Geijtenbeek T.B.H. & Gringhuis S.I. (2009) Signalling through C-type lectin receptors: shaping immune responses. *Nature Reviews Immunology* **9**, 465–479.
74 Saijo S., Ikeda S., *et al.* (2010) Dectin-2 recognition of α-mannans and induction of Th17 cell differentiation is essential for host defense against *Candida albicans*. *Immunity* **32**, 681–691.
75 Ko Y.C., Mukaida N., *et al.* (1993) Elevated interleukin-8 levels in the urine of patients with urinary tract infections. *Infection and Immunity* **61**, 1307–1314.
76 Hedges S., Agace W., *et al.* (1994) Uroepithelial cells are part of a mucosal cytokine network. *Infection and Immunity* **62**, 2315–2321.
77 Agace W.W. (1996) The role of the epithelial cell in *Escherichia coli* induced neutrophil migration into the urinary tract. *European Respiratory Journal* **9**, 1713–1728.
78 Hang L., Haraoka M., *et al.* (1999) Macrophage inflammatory protein-2 is required for neutrophil passage across the epithelial barrier of the infected urinary tract. *Journal of Immunology* **162**, 3037–3044.
79 Haraoka M., Hang L., *et al.* (1999) Neutrophil recruitment and resistance to urinary tract infection. *Journal of Infectious Diseases* **180**, 1220–1229.
80 Frendéus B., Godaly G., *et al.* (2000) Interleukin 8 receptor deficiency confers susceptibility to acute experimental pyelonephritis and may have a human counterpart. *The Journal of Experimental Medicine* **192**, 881–890.
81 Abraham S., Shin J. & Malaviya R. (2001) Type 1 fimbriated *Escherichia coli*-mast cell interactions in cystitis. *Journal of Infectious Diseases* **183**, S51–55.
82 Gur C., Coppenhagen-Glazer S., *et al.* (2013) Natural killer cell-mediated host defense against uropathogenic *E. coli* is counteracted by bacterial hemolysinA-dependent killing of NK cells. *Cell Host and Microbe* **14**, 664–674.
83 Engel D., Dobrindt U., *et al.* (2006) Tumor necrosis factor alpha- and inducible nitric oxide synthase-producing dendritic cells are rapidly recruited to the bladder in urinary tract infection but are dispensable for bacterial clearance. *Infection and Immunity* **74**, 6100–6107.
84 Wang G., Li X. & Wang Z. (2016) APD3: the antimicrobial peptide database as a tool for research and education. *Nucleic Acids Research* **44**, D1087–D1093.

85 Wimley W.C. (2010) Describing the mechanism of antimicrobial peptide action wih the interfacial activity model. *ACS Chemical Biology* **5**, 905–917.
86 Matsuzaki K., Sugishita K., *et al.* (1995) Molecular basis for membrane selectivity of an antimicrobial peptide, magainin 2. *Biochemistry* **34**, 3423–3429.
87 Verly R.M., Rodrigues M.A., *et al.* (2008) Effect of cholesterol on the interaction of the amphibian antimicrobial peptide DD K with liposomes. *Peptides* **29**, 15–24.
88 Cullen T.W., Schofield W., *et al.* (2015) Antimicrobial peptide resistance mediates resilience of prominent gut commensals during inflammation. *Science* **347**, 170–175.
89 Di Luca M., Maccari G. & Nifosi R. (2014) Treatment of microbial biofilms in the post-antibiotic era: prophylactic and therapeutic use of antimicrobial peptides and their design by bioinformatics tools. *Pathogens and Disease* **70**, 257–270.
90 Zasloff M. (2002) Antimicrobial peptides of multicellular organisms. *Nature* **415**, 389–395.
91 Ganz T., Selsted M.E. & Lehrer R.I. (1990) Defensins. *European Journal of Haematology* **44**, 1–8.
92 Ganz T., Selsted M.E., *et al.* (1985) Defensins, natural peptide antibiotics of human neutrophils. *The Journal of Clinical Investigation* **76**, 1427–1435.
93 Ayabe T., Satchell D.P., *et al.* (2000) Secretion of microbicidal alpha-defensins by intestinal Paneth cells in response to bacteria. *Nature Immunology* **1**, 113–118.
94 Quayle A.J., Porter E.M., *et al.* (1998) Gene expression, immunolocalization, and secretion of human defensin-5 in human female reproductive tract. *American Journal of Pathology* **152**, 1247–1258.
95 Frye M., Bargon J., *et al.* (2000) Expression of human alpha-defensin 5 (HD5) mRNA in nasal and bronchial epithelial cells. *Journal of Clinical Pathology* **53**, 770–773.
96 Spencer J.D., Hains D.S., *et al.* (2012) Human alpha defensin 5 expression in the human kidney and urinary tract. *PLoS ONE* **7**, e31712.
97 Tang Y. (1999) A cyclic antimicrobial peptide produced in primate leukocytes by the ligation of two truncated alpha-defensins. *Science* **286**, 498–502.
98 Schutte B.C., Mitros J.P., *et al.* (2002) Discovery of five conserved beta-defensin gene clusters using a computational search strategy. *Proceedings of the National Academy of Sciences of the United States of America* **99**, 2129–2133.
99 Zhou Y.S., Webb S., *et al.* (2013) Partial deletion of chromosome 8 beta-defensin cluster confers sperm dysfunction and infertility in male mice. *PLoS Genetics* **9**, e1003826.
100 Zhao C., Wang I. & Lehrer R.I. (1996) Widespread expression of beta-defensin hBD-1 in human secretory glands and epithelial cells. *FEBS Letters* **396**, 319–322.
101 Goldman M.J., Anderson G.M., *et al.* (1997) Human beta-defensin-1 is a salt-sensitive antibiotic in lung that is inactivated in cystic fibrosis. *Cell* **88**, 553–560.
102 Harder J., Bartels J., *et al.* (1997) A peptide antibiotic from human skin. *Nature* **387**, 861.
103 Harder J., Bartels J., *et al.* (2001) Isolation and characterization of human β-defensin-3, a novel human inducible peptide antibiotic. *Journal of Biological Chemistry* **276**, 5707–5713.
104 MacRedmond R., Greene C., *et al.* (2005) Respiratory epithelial cells require Toll-like receptor 4 for induction of human beta-defensin 2 by lipopolysaccharide. *Respiratory Research* **6**, doi:10.1186/1465–9921–6–116.
105 Gao N., Kumar A., *et al.* (2010) Flagellin-induced corneal antimicrobial peptide production and wound repair involve a novel NF-kappaB-independent and EGFR-dependent pathway. *PLoS ONE* **5**, e9351.
106 Lanz M. (2013) Investigations of the innate immune defences in the urogenital tract. *PhD Thesis.*, Newcastle University.
107 García J.R., Krause A., *et al.* (2001) Human beta-defensin 4: a novel inducible peptide with a specific salt-sensitive spectrum of antimicrobial activity. *FASEB Journal* **15**, 1819–1821.
108 Harder J., Meyer-Hoffert U., *et al.* (2004) Differential gene induction of human beta-defensins (hBD-1, -2, -3, and -4) in keratinocytes is inhibited by retinoic acid. *The Journal of Investigative Dermatology* **123**, 522–529.

109 Scocchi M., Wang S. & Zanetti M. (1997) Structural organization of the bovine cathelicidin gene family and identification of a novel member. *FEBS Letters* **417**, 311–315.
110 Gudmundsson G.H., Agerberth B., *et al.* (1996) The human gene FALL39 and processing of the cathelin precursor to the antibacterial peptide LL-37 in granulocytes. *European Journal of Biochemistry* **238**, 325–332.
111 Sørensen O., Arnljots K., *et al.* (1997) The human antibacterial cathelicidin, hCAP-18, is synthesized in myelocytes and metamyelocytes and localized to specific granules in neutrophils. *Blood* **90**, 2796–2803.
112 Bals R., Wang X., *et al.* (1998) The peptide antibiotic LL-37/hCAP-18 is expressed in epithelia of the human lung where it has broad antimicrobial activity at the airway surface. *Proceeding of the National Academy of Sciences of the United States of America* **95**, 9541–9546.
113 Turner J., Cho Y., *et al.* (1998) Activities of LL-37, a cathelin-associated antimicrobial peptide of human neutrophils. *Antimicrobial Agents and Chemotherapy* **42**, 2206–2214.
114 Nell M.J., Sandra Tjabringa G., *et al.* (2004) Bacterial products increase expression of the human cathelicidin hCAP-18/LL-37 in cultured human sinus epithelial cells. *FEMS Immunology and Medical Microbiology* **42**, 225–231.
115 Barnard E. (1969) Biological function of pancreatic ribonuclease. *Nature* **221**, 340–344.
116 Hamann K.J., Gleich G.J., *et al.* (1990) In vitro killing of microfilariae of *Brugia pahangi* and *Brugia malayi* by eosinophil granule proteins. *Journal of Immunology* **144**, 3166–3173.
117 Domachowske J.B., Bonville C.A., *et al.* (1998) Evolution of antiviral activity in the ribonuclease A gene superfamily: evidence for a specific interaction between eosinophil-derived neurotoxin (EDN/RNase 2) and respiratory syncytial virus. *Nucleic Acids Research* **26**, 5327–32.
118 Pulido D., Torrent M., *et al.* (2013) Two human host defense ribonucleases against mycobacteria, the eosinophil cationic protein (RNase 3) and RNase 7. *Antimicrobial Agents and Chemotherapy* **57**, 3797–3805.
119 Hooper L. V, Stappenbeck T.S., *et al.* (2003) Angiogenins: a new class of microbicidal proteins involved in innate immunity. *Nature Immunology* **4**, 269–273.
120 Avdeeva S. V., Chernukha M.U., *et al.* (2006) Human angiogenin lacks specific antimicrobial activity. *Current Microbiology* **53**, 477–478.
121 Harder J. & Schröder J.-M. (2002) RNase 7, a novel innate immune defense antimicrobial protein of healthy human skin. *Journal of Biological Chemistry* **277**, 46779–46784.
122 Rudolph B., Podschun R., *et al.* (2006) Identification of RNase 8 as a novel human antimicrobial protein. *Antimicrobial Agents and Chemotherapy* **50**, 3194–3196.
123 Kline J., Eichler T., *et al.* (2013) Ribonuclease 7, an antimicrobial peptide up-regulated during infection, contributes to microbial defense of the human urinary tract. *Kidney International* **83**, 615–625.
124 Martinsson H., Yhr M. & Enerbäck C. (2005) Expression patterns of S100A7 (psoriasin) and S100A9 (calgranulin-B) in keratinocyte differentiation. *Experimental Dermatology* **14**, 161–168.
125 Deol Y.S., Nasser M.W., *et al.* (2011) Tumor-suppressive effects of psoriasin (S100A7) are mediated through the β-catenin/T cell factor 4 protein pathway in estrogen receptor-positive breast cancer cells. *Journal of Biological Chemistry* **286**, 44845–44854.
126 Donato R., Cannon B.R., *et al.* (2013) Functions of S100 proteins. *Current Molecular Medicine* **13**, 24–57.
127 Cole A.M., Kim Y.H., *et al.* (2001) Calcitermin, a novel antimicrobial peptide isolated from human airway secretions. *FEBS letters* **504**, 5–10.
128 Büchau A.S., Hassan M., *et al.* (2007) S100A15, an antimicrobial protein of the skin: regulation by *E. coli* through Toll-like receptor 4. *The Journal of Investigative Dermatology* **127**, 2596–2604.
129 Mildner M., Stichenwirth M., *et al.* (2010) Psoriasin (S100A7) is a major *Escherichia coli*-cidal factor of the female genital tract. *Mucosal Immunology* **3**, 602–609.

130 Bullen J.J., Rogers H.J. & Leigh L. (1972) Iron-binding proteins in milk and resistance to *Escherichia coli* infection in infants. *British Medical Journal* **1**, 69–75.
131 Arnold R., Cole M. & McGhee J. (1977) A bactericidal effect for human lactoferrin. *Science* **197**, 263–265.
132 Ekins A., Khan A.G., *et al.* (2004) Lactoferrin receptors in Gram-negative bacteria: Insights into the iron acquisition process. *BioMetals* **17**, 235–243.
133 Flo T.H., Smith K.D., *et al.* (2004) Lipocalin 2 mediates an innate immune response to bacterial infection by sequestrating iron. *Nature* **432**, 917–921.
134 Luthje P., Brauner H., *et al.* (2013) Estrogen supports urothelial defense mechanisms. *Science Translational Medicine* **5**, 190ra80.
135 Becknell B., Schwaderer A., *et al.* (2015) Amplifying renal immunity: the role of antimicrobial peptides in pyelonephritis. *Nature Reviews Nephrology* **11**, 642–655.
136 Chan C., John A. & Abraham S. (2013) Mast cell interleukin-10 drives localized tolerance in chronic bladder infection. *Immunity* **38**, 349–359.
137 Duell B.L., Carey A.J., *et al.* (2012) Innate transcriptional networks activated in bladder in response to uropathogenic *Escherichia coli* drive diverse biological pathways and rapid synthesis of IL-10 for defense against bacterial urinary tract infection. *The Journal of Immunology* **188**, 781–792.
138 Mora-Bau G., Platt A.M., *et al.* (2015) Macrophages subvert adaptive immunity to urinary tract infection. *PLoS Pathogens* **11**, e1005044.
139 Gupta K., Hooton T.M. & Stamm W.E. (2001) Increasing antimicrobial resistance and the management of uncomplicated community-acquired urinary tract infections. *Annals of Internal Medicine* **135**, 41–50.
140 Milo G., Katchman E., *et al.* (2005) Duration of antibacterial treatment for uncomplicated urinary tract infection in women. *Cochrane Database of Systematic Reviews*, CD004682.
141 Albert X., Huertas I., *et al.* (2008) Antibiotics for preventing recurrent urinary tract infection in non-pregnant women. *Cochrane Database of Systematic Reviews*, CD001209.
142 Waseem M., Cheng J., *et al.* (2014) Can a simple urinalysis predict the causative agent and the antibiotic sensitivities? *Pediatric Emergency Care* **30**, 244–247.
143 Sahm D.F., Thornsberry C., *et al.* (2001) Multidrug-resistant urinary tract isolates of *Escherichia coli*: prevalence and patient demographics in the United States in 2000. *Antimicrobial Agents and Chemotherapy* **45**, 1402–1406.
144 Langermann S., Palaszynski S., *et al.* (1997) Prevention of mucosal *Escherichia coli* infection by FimH-adhesin-based systemic vaccination. *Science* **276**, 607–611.
145 Russo T.A., Mcfadden C.D., *et al.* (2003) The siderophore receptor IroN of extraintestinal pathogenic Escherichia coli is a potential vaccine candidate. *Infection and Immunity* **71**, 7164–7169.
146 Durant L., Metais A., *et al.* (2007) Identification of candidates for a subunit vaccine against extraintestinal pathogenic *Escherichia coli*. *Infection and Immunity* **75**, 1916–1925.
147 Alteri C.J., Hagan E.C., *et al.* (2009) Mucosal immunization with iron receptor antigens protects against urinary tract infection. *PLoS Pathogens* **5**, e:1000586.
148 Karam M.R.A., Oloomi M., *et al.* (2013) Assessment of immune responses of the flagellin (FliC) fused to FimH adhesin of uropathogenic *Escherichia coli*. *Molecular Immunology* **54**, 32–39.
149 Karam M.R.A., Oloomi M., *et al.* (2013) Vaccination with recombinant FimH fused with flagellin enhances cellular and humoral immunity against urinary tract infection in mice. *Vaccine* **31**, 1210–1216.
150 Langermann S., Möllby R., *et al.* (2000) Vaccination with FimH adhesin protects cynomolgus monkeys from colonization and infection by uropathogenic *Escherichia coli*. *The Journal of Infectious Diseases* **181**, 774–778.
151 Bauer H.W., Alloussi S., *et al.* (2005) A long-term, multicenter, double-blind study of an Escherichia coli extract (OM-89) in female patients with recurrent urinary tract infections.

European Urology **47**, 542–548.
152 Hopkins W.J., Elkahwaji J., *et al.* (2007) Vaginal mucosal vaccine for recurrent urinary tract infections in women: results of a phase 2 clinical trial. *The Journal of Urology* **177**, 1349–1353.
153 Moriel D.G. & Schembri M.A. (2013) Vaccination approaches for the prevention of urinary tract infection. *Current Pharmaceutical Biotechnology* **14**, 967–974.
154 Zafriri D., Ofek I., *et al.* (1989) Inhibitory activity of cranberry juice on adherence of type 1 and type P fimbriated *Escherichia coli* to eucaryotic cells. *Antimicrobial Agents and Chemotherapy* **33**, 92–98.
155 Howell A.B., Reed J.D., *et al.* (2005) A-type cranberry proanthocyanidins and uropathogenic bacterial anti-adhesion activity. *Phytochemistry* **66**, 2281–2291.
156 Jepson R., Williams G. & Craig J. (2012) Cranberries for preventing urinary tract infections. *Cochrane Database of Systematic Reviews*, CD001321.
157 Carlsson S., Wiklund N., *et al.* (2001) Effects of pH, nitrite, and ascorbic acid on nonenzymatic nitric oxide generation and bacterial growth in urine. *Nitric Oxide : Biology and Chemistry* **5**, 580–586.
158 Ochoa-Brust G.J., Fernández A.R., *et al.* (2007) Daily intake of 100 mg ascorbic acid as urinary tract infection prophylactic agent during pregnancy. *Acta Obstetricia et Gynecologica* **86**, 783–787.
159 Nseir W., Taha M., *et al.* (2013) The association between serum levels of vitamin D and recurrent urinary tract infections in premenopausal women. *International Journal of Infectious Diseases* **17**, e1121–e1124.
160 Jorde R., Sollid S.T., *et al.* (2016) Prevention of urinary tract infections with vitamin D supplementation 20,000 IU per week for five years. Results from an RCT including 511 subjects. *Infectious Diseases* **4235**, DOI: 10.1080/23744235.2016.1201853.
161 Ascenzi P., Bocedi A. & Marino M. (2006) Structure-function relationship of estrogen receptor alpha and beta: impact on human health. *Molecular Aspects of Medicine* **27**, 299–402.
162 Oestradiol reference range *GP Notebook [Accessed 30.07.2016]*, http://www.gpnotebook.co.uk/simplepage.cfm?ID=5708.
163 Linstedt A., West N. & RM B. (1986) Analysis of monomeric-dimeric states of the estrogen receptor with monoclonal antiestrophilins. *Journal of Steroid Biochemistry* **24**, 677–686.
164 Cowley S.M. (1997) Estrogen receptors alpha and beta form heterodimers on DNA. *Journal of Biological Chemistry* **272**, 19858–19862.
165 Klein-Hitpass L., Schorpp M., *et al.* (1986) An estrogen-responsive element derived from the 5' flanking region of the Xenopus vitellogenin A2 gene functions in transfected human cells. *Cell* **46**, 1053–1061.
166 Katzenellenbogen B.S. & Katzenellenbogen J.A. (2000) Estrogen receptor transcription and transactivation: estrogen receptor alpha and estrogen receptor beta - regulation by selective estrogen receptor modulators and importance in breast cancer. *Breast Cancer Research* **2**, 335–344.
167 Kuiper G.G.J.M., Carlsson B., *et al.* (1997) Comparison of the ligand binding specificty and transcript tissue distribution of estrogen receptors α and β. *Endocrinology* **138**, 863–870.
168 Hall J. & McDonnell D. (1999) The estrogen receptor β-isoform (ERβ) of the human estrogen receptor modulates ERα transcriptional activity and is a key regulator of the cellular response to estrogens and antiestrogens. *Endocrinology* **140**, 5566–5578.
169 Jordan V.C. (2003) Tamoxifen: a most unlikely pioneering medicine. *Nature Reviews. Drug Discovery* **2**, 205–213.
170 Couse J.F. & Korach K.S. (1999) Estrogen receptor null mice: what have we learned and where will they lead us? *Endocrine Reviews* **20**, 358–417.
171 Soulez M. & Parker M.G. (2001) Identification of novel oestrogen receptor target genes in human ZR75-1 breast cancer cells by expression profiling. *Journal of Molecular Endocrinology* **27**, 259–274.

172 Inoue A., Yoshida N., *et al.* (2002) Development of cDNA microarray for expression profiling of estrogen-responsive genes. *Journal of Molecular Endocrinology* **29**, 175–192.
173 Gu Q. & Moss L. (1996) 17beta-estradiol potentiates kainate-induced currents via activation of the cAMP cascade. *The Journal of Neuroscience* **16**, 3620–3629.
174 Zhou Y., Watters J.J. & Dorsa D.M. (1996) Estrogen rapidly induces the phosphorylation of the cAMP response element binding protein in rat brain. *Endocrinology* **137**, 2163–2166.
175 Maggiolini M. & Picard D. (2010) The unfolding stories of GPR30, a new membrane-bound estrogen receptor. *The Journal of Endocrinology* **204**, 105–114.
176 Revankar C.M., Cimino D.F., *et al.* (2005) A transmembrane intracellular estrogen receptor mediates rapid cell signaling. *Science* **307**, 1625–1630.
177 Funakoshi T., Yanai A., *et al.* (2006) G protein-coupled receptor 30 is an estrogen receptor in the plasma membrane. *Biochemical and Biophysical Research Communications* **346**, 904–910.
178 Cheng S.-B., Graeber C.T., *et al.* (2011) Retrograde transport of the transmembrane estrogen receptor, G-protein-coupled-receptor-30 (GPR30/GPER) from the plasma membrane towards the nucleus. *Steroids* **76**, 892–896.
179 Samartzis E.P., Noske A., *et al.* (2014) The G protein-coupled estrogen receptor (GPER) is expressed in two different subcellular localizations reflecting distinct tumor properties in breast cancer. *PloS ONE* **9**, e83296.
180 Don Santos E., Dieudonne M., *et al.* (2002) Rapid nongenomic E2 effects on p42/p44 MAPK, activator protein-1, and cAMP response element binding protein in rat white adipocytes. *Endocrinology* **143**, 930–940.
181 Kousteni S., Han L., *et al.* (2003) Kinase-mediated regulation of common transcription factors accounts for the bone-protective effects of sex steroids. *The Journal of Clinical Investigation* **111**, 1651–1664.
182 Björnström L. & Sjöberg M. (2005) Mechanisms of estrogen receptor signaling: convergence of genomic and nongenomic actions on target genes. *Molecular Endocrinology* **19**, 833–842.
183 Bitman J. & Cecil H.C. (1967) Mechanism of estrogen in glycogen. *Archives of Biochemistry and Biophysics* **118**, 424–427.
184 Boskey E.R., Cone R.A., *et al.* (2001) Origins of vaginal acidity: high D/L lactate ratio is consistent with bacteria being the primary source. *Human Reproduction* **16**, 1809–1813.
185 Klebanoff S.J., Hillier S.L., *et al.* (1991) Control of the microbial flora of the vagina by H2O2-generating Lactobacilli. *The Journal of Infectious Diseases* **164**, 94–100.
186 Eschenbach D.A., Davick P.R., *et al.* (1989) Prevalence of hydrogen peroxide-producing *Lactobacillus* species in normal women and women with bacterial vaginosis. *Journal of Clinical Microbiology* **27**, 251–256.
187 Lucas F. V, Neufeld H.A., *et al.* (1955) The effect of estrogen on the production of a peroxide in the rat uterus. *The Journal of Biological Chemistry* **214**, 775–780.
188 Tsibris J., Virgin S., *et al.* (1986) Cervicovaginal peroxidases: Markers of the fertile period. *Obstetrics and Gynecology* **67**, 316–320.
189 Chan R.C., Reid G., *et al.* (1985) Competitive exclusion of uropathogens from human uroepithelial cells by *Lactobacillus* whole cells and cell wall fragments. *Infection and Immunity* **47**, 84–89.
190 Raz R. & Stamm W. (1993) A controlled trial of intravaginal estriol in postmenopausal women with recurrent urinary tract infections. *The New England Journal of Medicine* **329**, 753–756.
191 Cardozo L., Benness C. & Abbott D. (1998) Low dose oestrogen prophylaxis for recurrent urinary tract infections in elderly women. *British Journal of Obstetrics and Gynaecology* **105**, 403–407.
192 Brown J.S., Vittinghoff E., *et al.* (2001) Urinary tract infections in postmenopausal women: effect of hormone therapy and risk factors. *Obstetrics and Gynecology* **98**, 1045–1052.
193 Ouslander J.G., Greendale G.A., *et al.* (2001) Effects of oral estrogen and progestin on the

lower urinary tract among female nursing home residents. *Journal of the American Geriatrics Society* **49**, 803–807.
194 Xu R., Wu Y. & Hu Y. (2001) Prevention and treatment of recurrent urinary system infection with oestrogen cream in postmenopausal women. *Chinese Journal of Obstetrics and Gynecology* **36**, 531–533.
195 Raz R., Colodner R., *et al.* (2003) Effectiveness of estriol-containing vaginal pessaries and nitrofurantoin macrocrystal therapy in the prevention of recurrent urinary tract infection in postmenopausal women. *Clinical Infectious Diseases* **36**, 1362–1368.
196 Eriksen B. (1999) A randomized, open, parallel-group study on the preventive effect of an estradiol-releasing vaginal ring (Estring) on recurrent urinary tract infections in postmenopausal women. *American Journal of Obstetrics and Gynecology* **180**, 1072–1079.
197 Curran E.M., Tassell A.H.-V., *et al.* (2007) Estrogen increases menopausal host susceptibility to experimental ascending urinary-tract infection. *The Journal of Infectious Diseases* **195**, 680–683.
198 Wang C., Symington J.W., *et al.* (2013) Estrogenic modulation of uropathogenic *Escherichia coli* infection pathogenesis in a murine menopause model. *Infection and Immunity* **81**, 733–739.
199 Han J.H., Kim M.S., *et al.* (2010) Modulation of human beta-defensin-2 expression by 17beta-estradiol and progesterone in vaginal epithelial cells. *Cytokine* **49**, 209–214.
200 DNA Microarray *[Accessed 23.01.2016] http://learn.genetics.utah.edu/content/labs/microarray/*.
201 Hulsen T., de Vlieg J. & Alkema W. (2008) BioVenn - a web application for the comparison and visualization of biological lists using area-proportional Venn diagrams. *BMC Genomics* **9**.
202 Shetty S. & Gokul S. (2012) Keratinization and its disorders. *Oman Medical Journal* **27**, 348–357.
203 Anderson D.J., Marathe J. & Pudney J. (2014) The structure of the human vaginal stratum corneum and its role in immune defense. *American Journal of Reproductive Immunology* **71**, 618–623.
204 Veazey R.S. (2008) Microbicide safety/efficacy studies in animals- macaques and small animal models. *Current Opinion in HIV and AIDS* **3**, 567–573.
205 Huseby R.A., Maloney T.M. & Mcgrath C.M. (1984) Evidence for a direct growth-stimulating effect of estradiol of human MCF-7 cells *in vivo*. *Cancer Research* **44**, 2654–2659.
206 Soto A.M. & Sonnenschein C. (1987) Cell proliferation of estrogen-sensitive cells: the case for negative control. *Endocrine Reviews* **8**, 44–52.
207 Butt A.J., McNeil C.M., *et al.* (2005) Downstream targets of growth factor and oestrogen signalling and endocrine resistance: the potential roles of c-Myc, cyclin D1 and cyclin E. *Endocrine-Related Cancer* **12**, S47–S59.
208 Liang J. & Shang Y. (2013) Estrogen and cancer. *Annual Review of Physiology* **75**, 225–40.
209 Gimenez-Conti I.B., Lynch M., *et al.* (1994) Expression of keratins in mouse vaginal epithelium. *Differentiation* **56**, 143–151.
210 Moll R., Divo M. & Langbein L. (2008) The human keratins: biology and pathology. *Histochemistry and Cell Biology* **129**, 705–733.
211 Singh P., Jia H., *et al.* (1998) Production of beta-defensins by human airway epithelia. *Proceeding of the National Academy of Sciences of the United States of America* **95**, 14961–14966.
212 Bals R., Wang X., *et al.* (1998) Human beta-defensin 2 is a salt-sensitive peptide antibiotic expressed in human lung. *Journal of Clinical Investigation* **102**, 874–880.
213 Zhao J., Wang Z., *et al.* (2011) Effects of intravesical liposome-mediated human beta-defensin-2 gene transfection in a mouse urinary tract infection model. *Microbiology and Immunology* **55**, 217–223.
214 Starner T.D., Agerberth B., *et al.* (2005) Expression and activity of beta-defensins and LL-37 in the developing human lung. *Journal of Immunology* **174**, 1608–1615.
215 Scudiero O., Galdiero S., *et al.* (2010) Novel synthetic, salt-resistant analogs of human

beta-defensins 1 and 3 endowed with enhanced antimicrobial activity. *Antimicrobial Agents and Chemotherapy* **54**, 2312–2322.
216 Jung S., Mysliwy J., *et al.* (2011) Human beta-defensin 2 and beta-defensin 3 chimeric peptides reveal the structural basis of the pathogen specificity of their parent molecules. *Antimicrobial Agents and Chemotherapy* **55**, 954–960.
217 Wagner G. & Levin R. (1980) Electrolytes of coitally active and inactive cycle. *Journal of Reproduction and Fertility* **60**, 17–27.
218 Owen D.H. & Katz D.F. (1999) A vaginal fluid simulant. *Contraception* **59**, 91–95.
219 Venkataraman N., Cole A., *et al.* (2002) Cationic polypeptides are required for antibacterial activity of human airway fluid. *The Journal of Immunology* **169**, 6985–6991.
220 Patel M. V, Fahey J. V, *et al.* (2013) Innate immunity in the vagina (part I): estradiol inhibits hBD2 and elafin secretion by human vaginal epithelial cells. *American Journal of Reproductive Immunology* **69**, 463–474.
221 Spencer J., Schawaderer A., *et al.* (2014) The innate immune response during urinary tract infection and pyelonephritis. *Pediatric Nephrology* **29**, 1139–1149.
222 Choi H. & Abraham S. (2016) Why serological responses during cystitis are limited. *Pathogens* **5**, 19.
223 Du P., Kibbe W.A. & Lin S.M. (2008) lumi: A pipeline for processing Illumina microarray. *Bioinformatics* **24**, 1547–1548.
224 Ritchie M.E., Phipson B., *et al.* (2015) Limma powers differential expression analyses for RNA-sequencing and microarray studies. *Nucleic Acids Research* **43**, e47.
225 Cabral A. (2001) Structural organization and regulation of the small proline-rich family of cornified envelope precursors suggest a role in adaptive barrier function. *Journal of Biological Chemistry* **276**, 19231–19237.
226 Hong S.H., Nah H.Y., *et al.* (2004) Estrogen regulates the expression of the small proline-rich 2 gene family in the mouse uterus. *Molecules and Cells* **17**, 477–484.
227 Sobiak B., Graczyk-Jarzynka A. & Leśniak W. (2015) Comparison of DNA methylation and expression pattern of S100 and other epidermal differentiation complex genes in differentiating keratinocytes. *Journal of Cellular Biochemistry* **9999**, 1–7.
228 Hattori F., Kiatsurayanon C., *et al.* (2014) The antimicrobial protein S100A7/psoriasin enhances expression of keratinocyte differentiation markers and strengthens the skin's tight junction barrier. *British Journal of Dermatology* **171**, 742–753.
229 Voss A., Bode G., *et al.* (2011) Expression of S100A8/A9 in HaCaT keratinocytes alters the rate of cell proliferation and differentiation. *FEBS Letters* **585**, 440–446.
230 Marshall D., Hardman M.J., *et al.* (2001) Differentially expressed late constituents of the epidermal cornified envelope. *Proceedings of the National Academy of Sciences of the United States of America* **98**, 13031–13036.
231 Niehues H., van Vlijmen-Willems I.M.J.., *et al.* (2015) Late cornified envelope (LCE) proteins: Distinct expression patterns of LCE2 and LCE3 members suggest non-redundant roles in human epidermis and other epithelia. *British Journal of Dermatology*, DOI 10.1111/bjd.14284.
232 Jackson B., Tilli C.M.L.J., *et al.* (2005) Late cornified envelope family in differentiating epithelia - Response to calcium and ultraviolet irradiation. *Journal of Investigative Dermatology* **124**, 1062–1070.
233 Pask A.J., McInnes K.J., *et al.* (2008) Topical oestrogen keratinises the human foreskin and may help prevent HIV infection. *PloS One* **3**, e2308.
234 Tam C., Mun J.J., *et al.* (2012) Cytokeratins mediate epithelial innate defense through their antimicrobial properties. *The Journal of Clinical Investigation* **122**, 3665–3677.
235 Debets R., Timans J.C., *et al.* (2001) Two novel IL-1 family members, IL-1delta and IL-1epsilon, function as an antagonist and agonist of NF-kappaB activation through the orphan IL-1 receptor-related protein 2. *Journal of Immunology* **167**, 1440–1446.
236 Towne J.E., Garka K.E., *et al.* (2004) Interleukin (IL)-1F6, IL-1F8, and IL-1F9 signal

through IL-1Rrp2 and IL-1RAcP to activate the pathway leading to NF-kappaB and MAPKs. *Journal of Biological Chemistry* **279**, 13677–13688.
237 Vigne S., Palmer G., *et al.* (2011) IL-36R ligands are potent regulators of dendritic and T cells. *Blood* **118**, 5813–5823.
238 D'Erme A.M., Wilsmann-Theis D., *et al.* (2015) IL-36γ (IL-1F9) is a biomarker for psoriasis skin lesions. *Journal of Investigative Dermatology* **135**, 1025–1032.
239 Zheng Y., Niyonsaba F., *et al.* (2008) Microbicidal protein psoriasin is a multifunctional modulator of neutrophil activation. *Immunology* **124**, 357–367.
240 Ryckman C., Vandal K., *et al.* (2003) Proinflammatory activities of S100: proteins S100A8, S100A9, and S100A8/A9 induce neutrophil chemotaxis and adhesion. *Journal of Immunology* **170**, 3233–3242.
241 Yang Z., Tao T., *et al.* (2001) Proinflammatory properties of the human S100 protein S100A12. *Journal of Leukocyte Biology* **69**, 986–994.
242 Yan W.X., Armishaw C., *et al.* (2008) Mast cell and monocyte recruitment by S100A12 and its hinge domain. *Journal of Biological Chemistry* **283**, 13035–13043.
243 Hofmann M.A., Drury S., *et al.* (1999) RAGE mediates a novel proinflammatory axis: A central cell surface receptor for S100/calgranulin polypeptides. *Cell* **97**, 889–901.
244 Yang Z., Yan W.X., *et al.* (2007) S100A12 provokes mast cell activation: a potential amplification pathway in asthma and innate immunity. *The Journal of Allergy and Clinical Immunology* **119**, 106–114.
245 Ikemoto M., Murayama H., *et al.* (2007) Intrinsic function of S100A8/A9 complex as an anti-inflammatory protein in liver injury induced by lipopolysaccharide in rats. *Clinica Chimica Acta* **376**, 197–204.
246 Goetz D.H., Holmes M. a., *et al.* (2002) The neutrophil lipocalin NGAL is a bacteriostatic agent that interferes with siderophore-mediated iron acquisition. *Molecular Cell* **10**, 1033–1043.
247 Steigedal M., Marstad A., *et al.* (2014) Lipocalin 2 imparts selective pressure on bacterial growth in the bladder and is elevated in women with urinary tract infection. *The Journal of Immunology* **193**, 6081–6089.
248 Spencer J.D., Schwaderer A.L., *et al.* (2011) Ribonuclease 7 is a potent antimicrobial peptide within the human urinary tract. *Kidney International* **80**, 174–180.
249 Erhart W., Alkasi Ö., *et al.* (2011) Induction of human β-defensins and psoriasin in vulvovaginal human papillomavirus-associated lesions. *The Journal of Infectious Diseases* **204**, 391–399.
250 Sohnle P.G., Hunter M.J., *et al.* (2000) Zinc-reversible antimicrobial activity of recombinant calprotectin (migration inhibitory factor-related proteins 8 and 14). *The Journal of Infectious Diseases* **182**, 1272–1275.
251 Gläser R., Harder J., *et al.* (2005) Antimicrobial psoriasin (S100A7) protects human skin from Escherichia coli infection. *Nature Immunology* **6**, 57–64.
252 Corbin B.D., Seeley E.H., *et al.* (2008) Metal chelation and inhibition of bacterial growth in tissue abscesses. *Science* **319**, 962–966.
253 Hashemi F.B., Mollenhauer J., *et al.* (2001) Myeloid-related protein (MRP)-8 from cervico-vaginal secretions activates HIV replication. *AIDS* **15**, 441–449.
254 Yano J., Lilly E., *et al.* (2010) Epithelial cell-derived S100 calcium-binding proteins as key mediators in the hallmark acute neutrophil response during Candida vaginitis. *Infection and Immunity* **78**, 5126–5137.
255 Abtin A., Eckhart L., *et al.* (2008) Flagellin is the principal inducer of the antimicrobial peptide S100A7c (psoriasin) in human epidermal keratinocytes exposed to *Escherichia coli*. *The FASEB Journal* **22**, 2168–2176.
256 Abtin A., Eckhart L., *et al.* (2010) The antimicrobial heterodimer S100A8/S100A9 (calprotectin) is upregulated by bacterial flagellin in human epidermal keratinocytes. *The Journal of Investigative Dermatology* **130**, 2423–2430.

257 Hiemstra P., Maassen R., *et al.* (1996) Antibacterial activity of antileukoprotease. *Infection and Immunity* **64**, 4520–4524.
258 Wiedow O., Harder J., *et al.* (1998) Antileukoprotease in human skin: an antibiotic peptide constitutively produced by keratinocytes. *Biochemical and Biophysical Research Communications* **248**, 904–909.
259 Gomez S.A., Arguelles C.L., *et al.* (2009) Secretory leukocyte protease inhibitor: a secreted pattern recognition receptor for mycobacteria. *American Journal of Respiratory and Critical Care Medicine* **179**, 247–253.
260 Cooper M., Roberts M., *et al.* (2012) Secretory leukocyte protease inhibitor binds to *Neisseria gonorrhoeae* outer membrane opacity protein and is bactericidal. *American Journal of Reproductive Immunology* **68**, 116–127.
261 Chaudhry R., Madden-Fuentes R.J., *et al.* (2014) Inflammatory response to *Escherichia coli* urinary tract infection in the neurogenic bladder of the spinal cord injured host. *Journal of Urology* **191**, 1454–1461.
262 Ohlsson S., Ljungkrantz I., *et al.* (2001) Novel distribution of the secretory leucocyte proteinase inhibitor in kidney. *Mediators of Inflammation* **10**, 347–350.
263 Valore E. V., Park C.H., *et al.* (2002) Antimicrobial components of vaginal fluid. *American Journal of Obstetrics and Gynecology* **187**, 561–568.
264 Yarbrough V.L., Winkle S. & Herbst-Kralovetz M.M. (2014) Antimicrobial peptides in the female reproductive tract: a critical component of the mucosal immune barrier with physiological and clinical implications. *Human Reproduction Update* **0**, 1–25.
265 Fahey J. V & Wira C.R. (2002) Effect of menstrual status on antibacterial activity and secretory leukocyte protease inhibitor production by human uterine epithelial cells in culture. *The Journal of Infectious Diseases* **185**, 1606–1613.
266 Nilsson M.F., Sandstedt B., *et al.* (1999) The human cationic antimicrobial protein (hCAP18), a peptide antibiotic, is widely expressed in human squamous epithelia and colocalizes with interleukin-6. *Infection and Immunity* **67**, 2561–2566.
267 Chromek M., Slamová Z., *et al.* (2006) The antimicrobial peptide cathelicidin protects the urinary tract against invasive bacterial infection. *Nature Medicine* **12**, 636–641.
268 Nielsen K.L., Dynesen P., *et al.* (2014) Role of urinary cathelicidin LL-37 and human β-defensin 1 in uncomplicated *Escherichia coli* urinary tract infections. *Infection and Immunity* **82**, 1572–1578.
269 Arao S., Matsuura S., *et al.* (1999) Measurement of urinary lactoferrin as a marker of urinary tract infection. *Journal of Clinical Microbiology* **37**, 553–557.
270 Håversen L.A., Engberg I., *et al.* (2000) Human lactoferrin and peptides derived from a surface-exposed helical region reduce experimental *Escherichia coli* urinary tract infection in mice. *Infection and Immunity* **68**, 5816–5823.
271 Chen H.Y., Weng I.C., *et al.* (2014) Galectins as bacterial sensors in the host innate response. *Current Opinion in Microbiology* **17**, 75–81.
272 Hossain M.S., Jaye D.L., *et al.* (2011) Flagellin, a TLR5 agonist, reduces graft-versus-host disease in allogeneic hematopoietic stem cell transplantation recipients while enhancing antiviral immunity. *The Journal of Immunology* **187**, 5130–5140.
273 Yoon G.S., Dong C., *et al.* (2013) Interferon regulatory factor-1 in flagellin-induced reprogramming: Potential protective role of CXCL10 in cornea innate defense against *Pseudomonas aeruginosa* infection. *Investigative Ophthalmology and Visual Science* **54**, 7510–7521.
274 Rajeevan M.S., Ranamukhaarachchi D.G., *et al.* (2001) Use of real-time quantitative PCR to validate the results of cDNA array and differential display PCR technologies. *Methods* **25**, 443–451.
275 Svaren J., Ehrig T., *et al.* (2000) EGR1 target genes in prostate carcinoma cells identified by microarray analysis. *Journal of Biological Chemistry* **275**, 38524–38531.
276 Ingenuity Systems (2011) Ingenuity Downstream Effects Analysis in IPA. , 1–5.
277 Hirota K., Yoshitomi H., *et al.* (2007) Preferential recruitment of CCR6-expressing Th17

cells to inflamed joints via CCL20 in rheumatoid arthritis and its animal model. *The Journal of Experimental Medicine* **204**, 2803–2812.
278 Yu Q., Lou X. & He Y. (2015) Preferential recruitment of Th17 cells to cervical cancer via CCR6-CCL20 pathway. *PLoS One* **10**, e0120855.
279 Hollenhorst P.C., McIntosh L.P. & Graves B.J. (2011) Genomic and biochemical insights into the specificity of ETS transcription factors. *Annual Review of Biochemistry* **80**, 437–471.
280 Stephens D.N., Klein R.H., *et al.* (2013) The Ets transcription factor EHF as a regulator of cornea epithelial cell identity. *Journal of Biological Chemistry* **288**, 34304–34324.
281 Fossum S.L., Mutolo M.J., *et al.* (2014) Ets homologous factor regulates pathways controlling response to injury in airway epithelial cells. *Nucleic Acids Research* **42**, 13588–13598.
282 Fenne I.S., Hoang T., *et al.* (2008) Recruitment of coactivator glucocorticoid receptor interacting protein 1 to an estrogen receptor transcription complex is regulated by the 3',5'-cyclic adenosine 5'-monophosphate-dependent protein kinase. *Endocrinology* **149**, 4336–4345.
283 Molnár I., Bohaty I. & Somogyiné-Vári É. (2014) High prevalence of increased interleukin-17A serum levels in postmenopausal estrogen deficiency. *Menopause* **21**, 749–752.
284 Cummings S.R., Duong T., *et al.* (2002) Serum estradiol level and risk of breast cancer during treatment with raloxifene. *Journal of the American Medical Association* **287**, 216–220.
285 Wills S., Ravipati A., *et al.* (2012) Effects of vaginal estrogens on serum estradiol levels in postmenopausal breast cancer survivors and women at risk of breast cancer taking an aromatase inhibitor or a selective estrogen receptor modulator. *Journal of Oncology Practice* **8**, 144–148.
286 Thomas P., Pang Y., *et al.* (2005) Identity of an estrogen membrane receptor coupled to a G protein in human breast cancer cells. *Endocrinology* **146**, 624–632.
287 Wang C., Uray I.P., *et al.* (2012) SLC22A5/OCTN2 expression in breast cancer is induced by estrogen via a novel intronic estrogen-response element (ERE). *Breast Cancer Research and Treatment* **134**, 101–115.
288 Zhang Y., Xiao X., *et al.* (2012) Estrogen facilitates spinal cord synaptic transmission via membrane-bound estrogen receptors: implications for pain hypersensitivity. *The Journal of Biological Chemistry* **287**, 33268–33281.
289 Klinge C.M. (2001) Estrogen receptor interaction with estrogen response elements. *Nucleic Acids Research* **29**, 2905–2919.
290 Kato S., Tora L., *et al.* (1992) A far upstream estrogen response element of the ovalbumin gene contains several half-palindromic 5'-TGACC-3' motifs acting synergistically. *Cell* **68**, 731–742.
291 Yang Q., Jian J., *et al.* (2012) 17beta-estradiol inhibits iron hormone hepcidin through an estrogen responsive element half-site. *Endocrinology* **153**, 3170–3178.
292 Messeguer X., Escudero R., *et al.* (2002) PROMO: detection of known transcription regulatory elements using species-tailored searches. *Bioinformatics* **18**, 333–334.
293 Farre D., Roset R., *et al.* (2003) Identification of patterns in biological sequences at the ALGGEN server: PROMO and MALGEN. *Nucleic Acids Research* **31**, 3651–3653.
294 Albanito L., Madeo A., *et al.* (2007) G protein-coupled receptor 30 (GPR30) mediates gene expression changes and growth response to 17beta-estradiol and selective GPR30 ligand G-1 in ovarian cancer cells. *Cancer Research* **67**, 1859–1866.
295 Wakeling A.E., Dukes M. & Bowler J. (1991) A potent specific pure antiestrogen with clinical potential. *Cancer Research* **51**, 3867–3873.
296 Annex I: Summary of product characteristics (2006) *European Medicines Agency*, 107–123.
297 Wada A., Ogushi K., *et al.* (2001) *Helicobacter pylori*-mediated transcriptional regulation of the human beta-defensin 2 gene requires NF-kappaB. *Cellular Microbiology* **3**, 115–123.
298 Tsutsumi-Ishii Y. & Nagaoka I. (2002) NF-kappaB-mediated transcriptional regulation of

human beta-defensin-2 gene following lipopolysaccharide stimulation. *Journal of Leukocyte Biology* **71**, 154–62.

299 McDermott A.M., Redfern R.L., *et al.* (2003) Defensin expression by the cornea: multiple signalling pathways mediate IL-1beta stimulation of hBD-2 expression by human corneal epithelial cells. *Investigative Ophthalmology and Visual Science* **44**, 1859–1865.

300 Steubesand N., Kiehne K., *et al.* (2009) The expression of the beta-defensins hBD-2 and hBD-3 is differentially regulated by NF-kappaB and MAPK/AP-1 pathways in an in vitro model of *Candida* esophagitis. *BMC Immunology* **10**, doi:10.1186/1471–2172–10–36.

301 Weisz A. & Rosales R. (1990) Identification of an estrogen response element upstream of the human c-fos gene that binds the estrogen receptor and the AP-1 transcription factor. *Nucleic Acids Research* **18**, 5097–106.

302 Teng C.T., Liu Y., *et al.* (1992) Differential molecular mechanism of the estrogen action that regulates lactoferrin gene in human and mouse. *Molecular Endocrinology* **6**, 1969–1981.

303 Driscoll M.D., Sathya G., *et al.* (1998) Sequence requirements for estrogen receptor binding to estrogen response elements. *Journal of Biological Chemistry* **273**, 29321–29330.

304 Cheng S. Bin, Quinn J.A., *et al.* (2011) Down-modulation of the G-protein-coupled estrogen receptor, GPER, from the cell surface occurs via a trans-golgi-proteasome pathway. *Journal of Biological Chemistry* **286**, 22441–22455.

305 Pahl R., Brunke G., *et al.* (2011) IL-1β and ADAM17 are central regulators of β-defensin expression in *Candida* esophagitis. *American Journal of Physiology: Gastrointestinal and Liver Physiology* **300**, G547–G553.

306 Filardo E.J., Quinn J.A., *et al.* (2000) Estrogen-induced activation of Erk-1 and Erk-2 requires the G protein-coupled receptor homolog, GPR30, and occurs via trans-activation of the epidermal growth factor receptor through release of HB-EGF. *Molecular Endocrinology* **14**, 1649–1660.

307 Cowland J.B., Sorensen O.E., *et al.* (2003) Neutrophil gelatinase-associated lipocalin is up-regulated in human epithelial cells by IL-1beta, but not by TNF-alpha. *Journal of Immunology* **171**, 6630–6639.

308 Conde J., Otero M., *et al.* (2016) E74-like factor (ELF3) and NFkB regulate lipocalin-2 expression in chondrocytes. *Journal of Physiology*, doi: 10.1113/JP272240.

309 Sun L. & Carpenter G. (1998) Epidermal growth factor activation of NF-kB is mediated through IkBa degradation and intracellular free calcium. *Oncogene* **16**, 2095–2102.

310 Galien R. & Garcia T. (1997) Estrogen receptor impairs interleukin-6 expression by preventing protein binding on the NF-ϰB site. *Nucleic Acids Research* **25**, 2424–2429.

311 Ghisletti S., Meda C., *et al.* (2005) 17beta-estradiol inhibits inflammatory gene expression by controlling NF- ϰB intracellular localization. *Molecular and Cellular Biology* **25**, 2957–2968.

312 Borras C., Gambini J., *et al.* (2005) 17beta-oestradiol up-regulates longevity-related, antioxidant enzyme expression via the ERK1 and ERK2[MAPK]/NF-kappaB cascade. *Aging Cell* **4**, 113–118.

313 Viña J., Borrás C., *et al.* (2005) Why females live longer than males? Importance of the upregulation of longevity-associated genes by oestrogenic compounds. *FEBS Letters* **579**, 2541–2545.

314 King A., Collins F., *et al.* (2010) An additive interaction between the NFkappaB and estrogen receptor signalling pathways in human endometrial epithelial cells. *Human Reproduction* **25**, 510–518.

315 Baldwin B.R., Timchenko N.A. & Zahnow C.A. (2004) Epidermal growth factor receptor stimulation activates the RNA binding protein CUG-BP1 and increases expression of C/EBPbeta-LIP in mammary epithelial cells. *Molecular and Cellular Biology* **24**, 3682–3691.

316 Mohammed I., Yeung A., *et al.* (2011) Signalling pathways involved in ribonuclease-7 expression. *Cellular and Molecular Life Sciences* **68**, 1941–1952.

317 Simanski M., Rademacher F., *et al.* (2013) IL-17A and IFN-gamma synergistically induce RNase 7 expression via STAT3 in primary keratinocytes. *PLoS ONE* **8**, e59531.

318 Tokumaru S., Sayama K., *et al.* (2005) Induction of keratinocyte migration via transactivation of the epidermal growth factor receptor by the antimicrobial peptide LL-37. *Journal of Immunology* **175**, 4662–4668.
319 Garreis F., Gottschalt M., *et al.* (2011) Expression and regulation of antimicrobial peptide psoriasin (S100A7) at the ocular surface and in the lacrimal apparatus. *Investigative Ophthalmology and Visual Science* **52**, 4914–4922.
320 Skliris G.P., Lewis A., *et al.* (2007) Estrogen receptor-beta regulates psoriasin (S100A7) in human breast cancer. *Breast Cancer Research and Treatment* **104**, 75–85.
321 Bachmann M., Scheiermann P., *et al.* (2012) IL-36γ/IL-1F9, an innate T-bet target in myeloid cells. *Journal of Biological Chemistry* **287**, 41684–41696.
322 Rouvier E., Luciani M.F., *et al.* (1993) CTLA-8, cloned from an activated T cell, bearing AU-rich messenger RNA instability sequences, and homologous to a herpesvirus saimiri gene. *Journal of Immunology* **150**, 5445–5456.
323 Fossiez F., Djossou O., *et al.* (1996) T cell interleukin-17 induces stromal cells to produce proinflammatory and hematopoietic cytokines. *The Journal of Experimental Medicine* **183**, 2593–2603.
324 Sutton C.E., Lalor S.J., *et al.* (2009) Interleukin-1 and IL-23 induce innate IL-17 production from gamma delta T Cells, amplifying Th17 responses and autoimmunity. *Immunity* **31**, 331–341.
325 Hueber A., Asquith D., *et al.* (2010) Cutting Edge: Mast cells express IL-17A in rheumatoid arthritis synovium. *The Journal of Immunology* **184**, 3336–3340.
326 Mosmann T.R. & Coffman R.L. (1989) Th1 and Th2 cells: different patterns of lymphokine secretion lead to different functional properties. *Annual Review of Immunology* **7**, 145–173.
327 Liang S.C., Tan X.-Y., *et al.* (2006) Interleukin (IL)-22 and IL-17 are coexpressed by Th17 cells and cooperatively enhance expression of antimicrobial peptides. *The Journal of Experimental Medicine* **203**, 2271–2279.
328 Guglani L. & Khader S.A. (2010) Th17 cytokines in mucosal immunity and inflammation. *Current Opinion in HIV and AIDS* **5**, 120–127.
329 Akimzhanov A.M., Yang X.O. & Dong C. (2007) Chromatin remodeling of interleukin-17 (IL-17)-IL-17F cytokine gene locus during inflammatory helper T cell differentiation. *Journal of Biological Chemistry* **282**, 5969–5972.
330 Wright J.F., Guo Y., *et al.* (2007) Identification of an interleukin 17F/17A heterodimer in activated human CD4+ T cells. *Journal of Biological Chemistry* **282**, 13447–13455.
331 Im E., Jung J. & Rhee S.H. (2012) Toll-like receptor 5 engagement induces interleukin-17C expression in intestinal epithelial cells. *Journal of Interferon and Cytokine Research* **32**, 583–591.
332 Johnston A., Fritz Y., *et al.* (2013) Keratinocyte overexpression of IL-17C promotes psoriasiform skin inflammation. *The Journal of Immunology* **190**, 2252–2262.
333 Hurst S.D., Muchamuel T., *et al.* (2002) New IL-17 family members promote Th1 or Th2 responses in the lung: in vivo function of the novel cytokine IL-25. *The Journal of Immunology* **169**, 443–453.
334 Toy D., Kugler D., *et al.* (2006) Cutting edge: Interleukin 17 signals through a heteromeric receptor complex. *The Journal of Immunology* **177**, 36–39.
335 Ge D. & You Z. (2008) Expression of interleukin-17RC protein in normal human tissues. *International Archives of Medicine* **1**, doi: 10.1186/1755–7682–1–19.
336 Parajuli P., Anand R., *et al.* (2015) Preferential expression of functional IL-17R in glioma stem cells : potential role in self-renewal. *Oncotarget* **7**, 6121–6135.
337 Maxwell J.R., Zhang Y., *et al.* (2015) Differential roles for Interleukin-23 and Interleukin-17 in intestinal immunoregulation. *Immunity* **43**, 739–750.
338 Giles D.A., Moreno-Fernandez M.E., *et al.* (2016) Regulation of inflammation by IL-17A and IL-17F modulates non-alcoholic fatty liver disease pathogenesis. *PLoS ONE* **11**,

e0149783.
339 Wright J.F., Bennett F., *et al.* (2008) The human IL-17F/IL-17A heterodimeric cytokine signals through the IL-17RA/IL-17RC receptor complex. *Journal of Immunology* **181**, 2799–2805.
340 Yao Z., Fanslow W.C., *et al.* (1995) Herpesvirus Saimiri encodes a new cytokine, IL-17, which binds to a novel cytokine receptor. *Immunity* **3**, 811–821.
341 Hata K., Andoh A., *et al.* (2002) IL-17 stimulates inflammatory responses via NF-κB and MAP kinase pathways in human colonic myofibroblasts. *American Journal of Physiology - Gastrointestinal and Liver Physiology* **282**, G1035–G1044.
342 Ruddy M.J., Wong G.C., *et al.* (2004) Functional cooperation between interleukin-17 and tumor necrosis factor-alpha is mediated by CCAAT/enhancer-binding protein family members. *The Journal of Biological Chemistry* **279**, 2559–2567.
343 Henness S., Johnson C.K., *et al.* (2004) IL-17A augments TNF-α-induced IL-6 expression in airway smooth muscle by enhancing mRNA stability. *Journal of Allergy and Clinical Immunology* **114**, 958–964.
344 Henness S., van Thoor E., *et al.* (2006) IL-17A acts via p38 MAPK to increase stability of TNF-α-induced IL-8 mRNA in human ASM. *American Journal of Physiology. Lung Cellular and Molecular Physiology* **290**, L1283–L1290.
345 Peul A., Cypowyj S., *et al.* (2011) Chronic mucocutaneous candidiasis in humans with inborn errors of interleukin-17 immunity. *Science* **332**, 65–68.
346 Cho J.S., Pietras E.M., *et al.* (2010) IL-17 is essential for host defense against cutaneous *Staphylococcus aureus* infection in mice. *Journal of Clinical Investigation* **120**, 1762–1773.
347 Feinen B., Jerse A.E., *et al.* (2010) Critical role of Th17 responses in a murine model of *Neisseria gonorrhoeae* genital infection. *Mucosal Immunology* **3**, 312–321.
348 Ma Q., Teter B., *et al.* (2009) Regulation of gastric B cell recruitment is dependent on IL-17 receptor A signalling in a model of chronic bacterial infection. *Journal of Immunology* **27**, 14299–14307.
349 Pietrella D., Rachini A., *et al.* (2011) TH17 cells and IL-17 in protective immunity to vaginal candidiasis. *PLoS ONE* **6**, 1–11.
350 Sivick K.E., Schaller M.A., *et al.* (2010) The innate immune response to uropathogenic *Escherichia coli* involves IL-17A in a murine model of urinary tract infection. *Journal of Immunology* **184**, 2065–2075.
351 Toy D., Kugler D., *et al.* (2006) Cutting edge: interleukin 17 signals through a heteromeric receptor complex. *Journal of Immunology* **177**, 36–39.
352 Scurlock A.M., Frazer L.C., *et al.* (2011) Interleukin-17 contributes to generation of Th1 immunity and neutrophil recruitment during *Chlamydia muridarum* genital tract infection but is not required for macrophage influx or normal resolution of infection. *Infection and Immunity* **79**, 1349–1362.
353 Yano J., Kolls J.K., *et al.* (2012) The acute neutrophil response mediated by S100 alarmins during vaginal *Candida* infections is independent of the Th17-pathway. *PLoS ONE* **7**, 1–8.
354 Yilmaz S.B., Cicek N., *et al.* (2012) Serum and tissue levels of IL-17 in different clinical subtypes of psoriasis. *Archives of Dermatological Research* **304**, 465–469.
355 Kleiner G., Marcuzzi A., *et al.* (2013) Cytokine levels in the serum of healthy subjects. *Mediators of Inflammation* **2013**, 434010.
356 Masson L., Salkinder A.L., *et al.* (2015) Relationship between female genital tract infections, mucosal interleukin-17 production and local T helper type 17 cells. *Immunology* **146**, 557–567.
357 Guttman-Yassky E., Lowes M.A., *et al.* (2008) Low expression of the IL-23/Th17 pathway in atopic dermatitis compared to psoriasis. *Journal of Immunology* **181**, 7420–7.
358 Burgey C., Kern W. V., *et al.* (2016) Differential induction of innate defense antimicrobial peptides in primary nasal epithelial cells upon stimulation with inflammatory cytokines, Th17 cytokines or bacterial conditioned medium from *Staphylococcus aureus* isolates.

Microbial Pathogenesis **90**, 69–77.
359 Liao F., Rabin R.L., *et al.* (1999) CC-chemokine receptor 6 is expressed on diverse memory subsets of T cells and determines responsiveness to macrophage inflammatory protein 3 α. *Journal of Immunology* **162**, 186–194.
360 Pelletier M., Maggi L., *et al.* (2014) Evidence for a cross-talk between human neutrophils and Th17 cells. *Blood* **115**, 335–343.
361 Hodgkin P.D., Fei Go N., *et al.* (1991) Interleukin-4 enhances anti-IgM stimulation of B cells by improving cell viability and by increasing the sensitivity of b cells to the anti-IgM signal. *Cellular Immunology* **134**, 14–30.
362 Kotake S., Udagawa N., *et al.* (1999) IL-17 in synovial fluids from patients with rheumatoid arthritis is a potent stimulator of osteoclastogenesis. *Journal of Clinical Investigation* **103**, 1345–1352.
363 Van Hamburg J.P., Asmawidjaja P.S., *et al.* (2011) Th17 cells, but not Th1 cells, from patients with early rheumatoid arthritis are potent inducers of matrix metalloproteinases and proinflammatory cytokines upon synovial fibroblast interaction, including autocrine interleukin-17A production. *Arthritis and Rheumatism* **63**, 73–83.
364 Andersson A., Stubelius A., *et al.* (2015) Estrogen regulates T helper 17 phenotype and localization in experimental autoimmune arthritis. *Arthritis Research & Therapy* **17**, 32.
365 Anipindi V.C., Bagri P., *et al.* (2016) Estradiol enhances CD4+ T-Cell anti-viral immunity by priming vaginal DCs to induce Th17 responses via an IL-1-dependent pathway. *PLoS Pathogens* **12**, e1005589.
366 Pike M., Peters R., *et al.* (1997) Estrogen-progestin replacement therapy and endometrial cancer. *Journal of the National Cancer Institute* **89**, 1110–1116.
367 Rossouw J., Anderson G., *et al.* (2002) Risks and benefits of estrogen plus progestin in healthy postmenopausal women. *The Journal of the American Medical Association* **288**, 321–333.
368 Jones M.E., Schoemaker M.J., *et al.* (2016) Menopausal hormone therapy and breast cancer: what is the true size of the increased risk? *British Journal of Cancer* **115**, 607–615.
369 Lee S.-I., Min K.-S., *et al.* (2011) Role of SIRT1 in heat stress- and lipopolysaccharide-induced immune and defense gene expression in human dental pulp cells. *Journal of Endodontics* **37**, 1525–1530.
370 Lin L., Wen S. hang, *et al.* (2014) Role of SIRT1 in *Streptococcus pneumoniae*-induced human beta-defensin-2 and interleukin-8 expression in A549 cell. *Molecular and Cellular Biochemistry* **394**, 199–208.
371 Aluyen J.K., Ton Q.N., *et al.* (2012) Resveratrol: potential as anticancer agent. *Journal of Dietary Supplements* **9**, 45–56.
372 Pastore S., Lulli D., *et al.* (2013) Resveratrol induces long-lasting IL-8 expression and peculiar EGFR activation/distribution in human keratinocytes: mechanisms and implications for skin administration. *PLoS ONE* **8**, e59632.
373 Docherty J.J., Fu M.M., *et al.* (2005) Effect of resveratrol on herpes simplex virus vaginal infection in the mouse. *Antiviral Research* **67**, 155–162.
374 Rimoldi G., Christoffel J., *et al.* (2007) Effects of chronic genistein treatment in mammary gland, uterus, and vagina. *Environmental Health Perspectives* **115**, 62–68.
375 Ouhara K., Komatsuzawa H., *et al.* (2006) *Actinobacillus actinomycetemcomitans* outer membrane protein 100 triggers innate immunity and production of beta-defensin and the 18-kilodalton cationic antimicrobial protein through the fibronectin-integrin pathway in human gingival epithelial cell. *Infection and Immunity* **74**, 5211–5220.
376 Kim S.K., Park S. & Lee E.S. (2010) Toll-Like receptors and antimicrobial peptides expressions of psoriasis: correlation with serum vitamin D level. *Journal of Korean Medical Science* **25**, 1506–1512.
377 Wang T.T., Nestel F.P., *et al.* (2004) Cutting edge: 1,25-dihydroxyvitamin D3 is a direct inducer of antimicrobial peptide gene expression. *The Journal of Immunology* **173**, 2909–2912.

378 Weber G., Heilborn J.D., *et al.* (2005) Vitamin D induces the antimicrobial protein hCAP18 in human skin. *Journal of Investigative Dermatology* **124**, 1080–1082.
379 Svensson D., Nebel D., *et al.* (2016) Vitamin D-induced up-regulation of human keratinocyte cathelicidin anti-microbial peptide expression involves retinoid X receptor α. *Cell and Tissue Research*, DOI: 10.1007/s00441–016–2449–z.
380 Ada H.T., Himizu T.S., *et al.* (2016) Vitamin D3 analog maxacalcitol (OCT) induces hCAP-18 / LL-37 production in human oral epithelial cells. *Biomedical Research* **37**, 199–205.
381 Hegyi Z., Zwicker S., *et al.* (2012) Vitamin D analog calcipotriol suppresses the Th17 cytokine–induced proinflammatory S100 "alarmins" psoriasin (S100A7) and koebnerisin (S100A15) in psoriasis. *Journal of Investigative Dermatology* **132**, 1416–1424.
382 Yildirim B., Kaleli B., *et al.* (2004) The effects of postmenopausal Vitamin D treatment on vaginal atrophy. *Maturitas* **49**, 334–337.
383 Taheri M., Baheiraei A., *et al.* (2015) Treatment of vitamin D deficiency is an effective method in the elimination of asymptomatic bacterial vaginosis: A placebo-controlled randomized clinical trial. *Indian Journal of Medical Research* **141**, 799–806.
384 Gupta K., Chou M.Y., *et al.* (2007) Cranberry products inhibit adherence of P-fimbriated *Escherichia coli* to primary cultured bladder and vaginal epithelial cells. *Journal of Urology* **177**, 2357–2360.
385 De Llano D.G., Esteban-Fernandez A., *et al.* (2015) Anti-adhesive activity of cranberry phenolic compounds and their microbial-derived metabolites against uropathogenic *Escherichia coli* in bladder epithelial cell cultures. *International Journal of Molecular Sciences* **16**, 12119–12130.
386 Chen J., Geng L., *et al.* (2013) Evaluation of the efficacy and safety of hyaluronic acid vaginal gel to ease vaginal dryness: a multicenter, randomized, controlled, open-label, parallel-group, clinical trial. *Journal of Sexual Medicine* **10**, 1575–1584.
387 Constantinides C., Manousakas T., *et al.* (2004) Prevention of recurrent bacterial cystitis by intravesical administration of hyaluronic acid: a pilot study. *BJU International* **93**, 1262–1266.
388 Lipovac M., Kurz C., *et al.* (2007) Prevention of recurrent bacterial urinary tract infections by intravesical instillation of hyaluronic acid. *International Journal of Gynaecology and Obstetrics* **96**, 192–195.
389 Damiano R., Quarto G., *et al.* (2011) Prevention of recurrent urinary tract infections by intravesical administration of hyaluronic acid and chondroitin sulphate: a placebo-controlled randomised trial. *European Urology* **59**, 645–651.
390 Locilex clinical trials *[Accessed 22.08.2016] http://www.dipexiumpharmaceuticals.com/locilex/clinical-trials*.
391 Scudiero O., Galdiero S., *et al.* (2013) Chimeric beta-defensin analogs, including the novel 3NI analog, display salt-resistant antimicrobial activity and lack toxicity in human epithelial cell lines. *Antimicrobial Agents and Chemotherapy* **57**, 1701–1708.
392 Anaya-López J.L., López-Meza J.E. & Ochoa-Zarzosa A. (2013) Bacterial resistance to cationic antimicrobial peptides. *Critical Reviews in Microbiology* **39**, 180–195.
393 Perron G.G., Zasloff M. & Bell G. (2006) Experimental evolution of resistance to an antimicrobial peptide. *Proceedings of the Royal Society of London B* **273**, 251–256.

Abstracts and prizes

Published abstracts

A. Stanton, A. S. M. Ali, R. S. Pickard & J. Hall (2015) Estrogen and hBD2 in the innate defence of the female uro-genital tract. *European Urology Supplements* **14**(2), e140

A. M. Stanton, M. Lanz, C. L. Townes, A. S. M. Ali, J. Hall & R. S. Pickard (2014) Oestrogen and the innate epithelial defences of the uro-genital tract. *British Journal of Surgery* **101**(S4), p61.

Conferences and prizes

March 2015	European Association of Urology Conference (Attended by Dr Ased Ali) Madrid, Spain Poster presentation, **Best poster in section**
March 2015	MRC Mission Training Day Newcastle upon Tyne, UK Poster presentation, **Runner up poster prize**
August 2014	Molecular UTI Conference Malmo, Sweden Poster presentation
January 2014	British Association of Urological Surgeons Conference Cambridge, UK Poster presentation, **Best poster prize**
September 2013	3rd International Meeting on Antimicrobial Peptides London, UK Poster presentation
July 2013	MRes student poster evening, Newcastle University Newcastle upon Tyne, UK Poster presentation, **Best poster prize**

Courses

Received Wellcome Trust Institutional Strategic Support Funding in April 2015 to attend the "Human and Vertebrate Genomics: Bioinformatics Tools and Resources" Wellcome Trust Open Door Workshop in Cambridge in May 2015.